



# UNIVERSITAT POLITÈCNICA DE VALÈNCIA

## *Application of Advanced Integrated Technologies (Membrane and Photo-Oxidation Processes) for the Removal of CECs contained in Urban Wastewater*

**Dennis Deemter M. Sc.**

PhD Thesis

Almería, 2023





*Application of Advanced Integrated Technologies  
(Membrane and Photo-Oxidation Processes) for the  
Removal of CECs contained in Urban Wastewater*

Memory presented for the title of Doctor:

By Roger Dennis Deemter (Emmen, The Netherlands, 19-05-1991)

Almería, 2023

**Thesis supervisors:**

**Prof. Dr. Sixto Malato Rodríguez**

Director and Senior Researcher

CIEMAT – Plataforma Solar de Almería

**Prof. Dr. Ana M. Amat**

Professor

Universitat Politècnica de València



Scientific work must not be considered from the point of view of the direct usefulness of it. It must be done for itself, for the beauty of science, and then there is always a chance that a scientific discovery may become a benefit for humanity.

- Maria Salomea (Marie) Skłodowska-Curie (1867 – 1934)



## Word of Thanks

Through this way I would like to express my words and feelings of deep appreciation and thanks to all the persons and organizations, that directly or indirectly contributed to the development of this PhD thesis.

Firstly, to Sixto Malato, my first academic supervisor, always being objective and professional, with a clear goal in sight, with the keenest eye and mind for detail, a founder and true expert in the field of (solar) water treatment. Whose true contribution and utmost dedication to the cause, I will always aim for. Available at any time, any day, and any moment of the year, a supervisor and mentor I could always trust and rely on, even in the hardest of times. Without his efforts in guiding me, this PhD thesis would not have been possible. My sincerest thanks, humble respect, and appreciation to you.

Equally to Isabel Oller, who was always there when needed, no effort too much, with the greatest efficiency, dedication, and care. A true professional, from helping me with starting the work and life in Almería, to being the head of the Solar Treatment of Water Unit, and to being the ESR coordinator within the AQUALity project from CIEMAT. For always being willing and able to perform revisions to the innumerable documents and formalities, to advise and to guide me in all of my work. My sincerest thanks, humble respect, and appreciation to you too.

You two both, were, are, and always will be, a true inspiration and aspiration to me.

My most special thanks to Ana M. Amat for being my second academic supervisor, for always being available to advise in the many formalities related to the Universitat Politècnica de València, the sharpness about the experimental work and impulses of academic and technical expertise, for the many manuscripts, papers, and documents.

Further special thanks to Paola Calza, for setting up this amazing AQUALity project, and a special thanks to Inma, for doing so much for us within the AQUALity project and for being a true and most dedicated specialist in microbiology and wastewater disinfection at the PSA.

To all that worked with me in the laboratory during my times at the Plataforma Solar de Almería, to Alba, Ana, Irene and Samira, great examples of PhD students, to Ilaria, my AQUALity ESR colleague at the Plataforma Solar, always at my side, to Azahara, Melina, Alba, and Joyce. To Alex and Sara, the inspiring water treatment post-doc power couple. To all that visited us from abroad in our laboratory during these years, to Lis, Giusy, Leonor, Elizângela, Isaac, Kasia and Gulnara. To Kuba, and although we never worked together at the Plataforma Solar, for being the greatest housemate and friend during my final months in Almería. The laboratory that would never be able to

operate as good as it does without Eli and Isa, who tirelessly supported me with all the laboratory work, and a listening ear for an indistinctive language mix. To Agustín and Panchy, always there to offer a strong, helping hand, a practical solution, or a mind clearing distraction, at the most necessary moments. To Bethel, my AQUALity ESR colleague that always checked up on me from Turkey.

To all the other employees at the Plataforma Solar de Almería, for the administrative, auxiliary, and technical services, especially at the times last-minute and most needed. Sometimes already, with requests and instructions, as early as at our bus stop, thank you Pepe. Every one of them, always with the kindest '*buenos días!*' and smiles.

To Vittorio and Mads, my supervisors, and all other personnel during my first secondment at the Aalborg University, Denmark, for opening my world to the production of high-tech polymer membranes. To Max (Xianzheng) and Federico, both great laboratory and travel companions. It was during this secondment that I got to meet my fellow ESRs of the AQUALity project for the first time and I got to work with Kate, Fabricio and Reni. Who furthermore showed me all the best of Aalborg and the University. The many international friends I made in the different laboratories, to Jens, Patrícia, Søren, Usuma, Vahid, and to my Danish and Chinese Trainer Team members, present at any time of the day.

To the team during my secondment at LiqTech, in Ballerup, Denmark. Special thanks to Victor for being my supervisor and teaching me all the *ins and outs* of the SiC and other ceramics membrane world. As well as to Karsten, Harris, Niklas, Helle, Juliet and Nanette, for offering me the freedom, inspiration, insights in, and wonderful discussions about, so many disciplines. To all the many international production colleagues, we always found a common foreign language to speak in, if not the very technology we worked with, showing me even the smallest of details. And clearly, also here with much appreciation to Esra and Fabricio, my AQUALity colleagues that received me with open arms in Copenhagen.

To all the involved members of my secondment at FACSA, with special thanks to Núria, for organizing and making me feel welcome in FACSA and Murcia, even before arriving. Special thanks to Fran, my supervisor in Alhama de Murcia, who kindly took me to work and back, and so, for the nice talks in the early mornings and in the afternoons, and for showing me all the *ins and outs* of working as a wastewater treatment plant manager. Furthermore, for the guidance at the wastewater treatment plants and experimental installations. To Cristian, for always being a kind colleague and teaching me the daily activities at a wastewater treatment plant. Finally, of course, all the operators, Dani, Gabriel, Jose, Oscar, and Pedro.



As last, to my direct and extended family, that had to miss me, once again, some extra years. My parents, to whom I think to have proven now, that it does not matter where you come from, or which path you take, with time, dedication, and perseverance, you can always achieve your goals. To my siblings, to whom I will always be an example. My Uncle Ron, for always being true and supportive. My extended family and my dearest, dearest friends, who, some of you, I was lucky enough to visit these years, even in these hard times with impossible restrictions. All others, from whom I received the most appreciated messages, video- and phone calls, from any corner of the World, at any time to either one of us.

May this PhD thesis as well be dedicated to you all!

*Dennis*

*“My promise to come back home, I will never break nor fulfill,  
as it is with all of you, but never at the same time.”*



This PhD Thesis has received funding from the European Union's Horizon 2020 research and innovation program, the AQUALity project, under the Marie Skłodowska-Curie grant agreement No 765860. Performing research work at CIEMAT – Plataforma Solar de Almería.



## Indices of Contents

## Index of Contents

Indices of Contents .....	i
Abstract.....	x
Resumen .....	xv
Resum .....	xx
Chapter I. Introduction .....	2
1. The Necessity for Water .....	3
2.1. Wastewaters .....	6
2.2. Modern concepts related with water and circular economy .....	12
2. Advanced oxidation processes .....	13
2.1. Photooxidation processes .....	13
2.2. Electrochemical oxidation processes .....	14
2.2.1. The anodic oxidation process .....	15
2.2.2. The electro-Fenton and (solar) photoelectro-Fenton processes .....	16
3. Membranes for water treatment .....	17
2.1. Membrane separation .....	18
2.2. Membrane systems .....	18
2.3. Membrane materials.....	20
2.4. Membrane fouling.....	21
2.5. Prevention of fouling.....	22
2.6. AOPs application as fouling prevention .....	23
4. Advanced integrated technologies and nutrient recovery in UWW treatment ..	23
5. Future perspectives related to the main goal of this Ph.D. ....	25
Chapter II. Objectives and Experimental Plan .....	28
1. Objectives .....	29
2. Experimental plan.....	30
5.2. Assessment of the self-cleaning capabilities of the UF membrane when using high volumes of UWW .....	32
Chapter III. Materials and Methods.....	35
1. Chemicals.....	37
2.1. Organic microcontaminants.....	37
2.2. Reagents.....	42
2.3. Water matrices.....	43

## Indices of Contents

2. Microorganisms .....	45
3. Analyses .....	46
3.1 Physicochemical parameters .....	46
3.1.1. Electrical conductivity and pH measurements .....	46
3.1.2. Turbidity measurement .....	47
3.1.3. UV-visible light spectrophotometry .....	47
3.1.4. Chemical oxygen Demand determination .....	48
3.1.5. Free Available Chlorine measurement .....	48
3.1.6. Iron concentration determination .....	49
3.1.7. Hydrogen peroxide measurement .....	50
3.1.8. Persulfate measurement .....	50
3.2 Dissolved organic carbon .....	51
3.3 Ionic chromatography .....	52
3.4 Ultra-performance liquid chromatography .....	53
3.5 Solar radiation measurement .....	54
3.6 Phytotoxicity, acute- and chronic toxicity determination .....	54
4 Experimental set-ups and methodology .....	56
4.2 Fe:EDDS complex preparation .....	56
4.3 Sand filtration system .....	57
4.4 Nanofiltration pilot plant .....	58
4.5 Solar photoelectro-Fenton pilot plant .....	60
4.6 Solar simulator .....	64
Chapter IV. Results and Discussion .....	67
1. The Effects of salinity on NF membranes .....	70
2 Solar photo-Fenton as tertiary treatment .....	74
2.2 Treatment with the conventional solar photo-Fenton process at a pH of 3	74
2.3 The application of EDDS for the solar photo-Fenton process at natural pH	75
2.4 The NF operating parameter effect on the solar photo-Fenton process as	77
tertiary treatment at a pH of 3 .....	77
2.5 The Solar photo-Fenton process as tertiary treatment .....	81
3 Applying Nanofiltration for ammonium recovery .....	84
4 Treatment of the Nanofiltration concentrate stream by the solar photo-Fenton	86
process at lab and pilot scale .....	86
5 Treatment of the concentrate stream volumes by electrooxidation .....	88

6	Determination of acute and chronic toxicity of the Nanofiltration streams .....	92
7	The fouling and self-cleaning properties of the photocatalytic membrane .....	96
8	Treatment of the membrane streams by solar photo-Fenton.....	101
9	The membrane retention of the <i>Pseudomonas Aeruginosa</i> bacterial species ..	105
	Chapter V. Conclusions .....	108
	References .....	113
	List of abbreviations.....	134
	Annex A	
	Annex B	



## Index of Figures

<b>Figure III.1:</b> Conductivity meter used in the TSA lab of the PSA. ....	46
<b>Figure III.2:</b> The mobile pH meter used in the TSA lab at the PSA. ....	46
<b>Figure III.3:</b> Turbidity meter used in the TSA lab at the PSA, of the type HACH 2100N. .....	47
<b>Figure III.4:</b> UV-vis set up used in the TSA lab at the PSA with on the right the UV-visible light spectrophotometer and on the right the computer connected to it with the compatible software. ....	48
<b>Figure III.5:</b> Vial with a sample containing free available chlorine as indicated by the faint pink color. ....	49
<b>Figure III.6:</b> Total Organic Carbon analyzer used at the TSA lab of the PSA, with on the right the analysis device and on the left the sample carousel and autosampler. ....	51
<b>Figure III.7:</b> The ionic chromatograph available at the PSA of the type Metrohm 850 Professional IC, with on the right the columns and the solvent tray, the autosampler in the middle, and the computer on the left. ....	52
<b>Figure III.8:</b> UPLC used at the TSA lab of the PSA. With 1) Diode Array Detection (DAD), 2) column compartment with temperature control, 3) autosampler, 4) mobile phase pumps, 5) degasser, and 6) mobile phase tray. ....	53
<b>Figure III.9:</b> The translucent plastic cassettes containing the black colored foam pad and the germinated seeds of the three plant species <i>Sorghum saccharatum</i> (left), <i>Sinapis alba</i> (middle), and <i>Lepidium sativum</i> (right). ....	55
<b>Figure III.10:</b> <i>Ephippia</i> of <i>Daphnia magna</i> in the hatching process by placing them on a petri dish filled with Standard Freshwater solution, and algae to feed them. ....	56
<b>Figure III.11:</b> UWWTP effluent pretreatment filtration system available at the PSA. Consisting out of a feed tank for UWWTP effluent, a sand filter (75 µm) and two cartridge filters (25 µm and 5 µm) in series, and a storage tank (1 m <sup>3</sup> ) for the filtered UWWTP effluent. The systems flow is powered by two centrifugal pumps. ....	57
<b>Figure III.12:</b> The pilot plant for NF available at the PSA. ....	58
<b>Figure III.13:</b> Screenshot of the SCADA control software of the pilot plant. ....	59
<b>Figure III.14:</b> Photo of the system wall containing four cells for EO treatment of water. .....	61
<b>Figure III.15:</b> Photo of the CPC reactor connected to the EO cell system as part of the EO pilot plant. ....	61
<b>Figure III.16:</b> The EO cell set-up, with 1) the air-inlet and pressure meter, 2) the EO cell, 3) the water-inlet and pressure meter. ....	62
<b>Figure III.17:</b> Schematic overview of the SPEF pilot plant available at the PSA, consisting out of 1) the feed tank, 2) the feed tank pump, 3) the compressor, 4) the EO cell set-up, 5) CPC-feed tank circulation pump, and 6) the CPC reactor. ....	63

<b>Figure III.18:</b> The Atlas-SunTest XLS+ available at the PSA, equipped with a xenon lamp and a daylight filter. ....	64
<b>Figure III.19:</b> The 1 L cylindrical glass container placed in the solar simulator on a magnetic stirrer plate, a tube for sampling, and on the side a solar irradiation meter. The perpendicular holes on both sides belong to the venting system that control the air temperature. ....	65
<b>Figure IV.1:</b> The concentration of the sum of MCs, and the evolution thereof, in the permeate stream and the concentrate stream (inset). The natural water matrix had 3, 5, and 7 g/L NaCl added to it. ....	72
<b>Figure IV.2:</b> Solar photo-Fenton treatment applied on concentrate volume C1, at a pH of 3. The treatment applied on permeate streams P1 and P2 are shown in the insets. ....	74
<b>Figure IV.3:</b> Evolution of dissolved iron and MC concentration decline by solar photo-Fenton treatment of concentrate volume C1, applied at a natural pH of 7, using Fe(III):EDDS at a ratio of [1:2], with the insets showing the results of the treatment applied to permeate volumes P1 and P2. ....	76
<b>Figure IV.4:</b> The solar photo-Fenton treatment applied at a pH of 3, with 0.20 mM of Fe(II) and 1.50 mM of H <sub>2</sub> O <sub>2</sub> on concentrate volume C1, showing the degrading concentrations of the MCs. When persulfate is used as an alternative oxidizing agent, the MC concentration decline is shown in the inset. ....	78
<b>Figure IV.5:</b> Dissolved iron evolution and MC concentration decline when applying the solar photo-Fenton treatment at a natural pH on concentrate volume C1, utilizing 0.20 mM of Fe(III): EDDS [1:1], and 1.50 mM of H <sub>2</sub> O <sub>2</sub> . The results when 0.10 mM of Fe(III):EDDS and the same ratio with persulfate (1.50 mM) as an alternative oxidizing agent are shown in the insets. ....	80
<b>Figure IV.6:</b> The concentration of NH <sub>4</sub> <sup>+</sup> in mg/L present in the permeate stream at different pH values and feed tank concentrations. The different experiments were performed till CF= 4 was reached. ....	85
<b>Figure IV.7:</b> The evolution of the dissolved iron and MC concentration during the treatment of concentrate volume C2 with photo-Fenton, with an initial concentration of Fe(III):EDDS of 0.10 mM [1:1], applying H <sub>2</sub> O <sub>2</sub> and persulfate at a concentration of 1.50 mM in the solar simulator at a circumneutral pH. ....	87
<b>Figure IV.8:</b> The evolution of the dissolved iron and MC concentration during the treatment of concentrate volume C2 with solar photo-Fenton at a circumneutral pH, performed in the pilot plant. ....	88
<b>Figure IV.9:</b> The evolution of the MC concentration in concentrate volume C1 (CF= 2) during the treatment with AO, SAAO, and SPEF, at its natural pH. ....	90
<b>Figure IV.10:</b> The evolution of the MC concentrations in concentrate volume C1 (CF= 2) at its natural pH during the treatment with SPEF at pilot scale, performed at low concentrations of carbonate. ....	92

**Figure IV.11:** Performed toxicity tests, acute toxicity measured at 24 and 48 hours, and chronic toxicity measured at 72 hours, applying *Daphnia magna* organisms at different dilutions in freshwater. In the front permeate volume CF= 2 is shown, followed by permeate volume CF= 4 in the middle and the freshwater control in the back. ....94

**Figure IV.16:** The evolution of the MC concentration of the permeate stream and the concentrate stream in the UWWTP effluent during solar photo-Fenton treatment and the evolution of the dissolved iron in the solar simulator, using 0.10 mM of Fe(III):EDDS and 1.50 mM of H<sub>2</sub>O<sub>2</sub>. ....102

**Figure IV.17:** The evolution of the MC concentration of the permeate and the concentrate stream, and the dissolved iron concentration during treatment with solar photo-Fenton in the solar simulator, with UWWTP effluents containing a low concentration (75 mg/L) of bicarbonates, using 0.10 mM of Fe(III):EDDS and 1.50 mM of H<sub>2</sub>O<sub>2</sub>. ....103

**Figure IV.18:** The retention by the self-cleaning membrane of *P. Aeruginosa* at an initial concentration of 1·10<sup>6</sup> CFU/mL in natural water (Tabernas, Spain). The detection limit (DL) of for the *P. Aeruginosa* was 1·10<sup>6</sup> CFU/mL. ....105

## Index of Tables

<b>Table III.1:</b> Characteristics of selected microcontaminants. ....	38
<b>Table III.2:</b> Overview of the natural water characteristics at the PSA. ....	43
<b>Table III.3:</b> Overview of the representative average secondary UWWTP effluent characteristics collected from the UWWTP EDAR 'El Bobar', Almería, Spain. ....	44
<b>Table III.4:</b> Retention time, LOQ and maximum absorption of each contaminant. ....	54
<b>Table III.5:</b> Predetermined concentrations of biocide needed for set periods of time. ....	60
<b>Table IV.1:</b> Overview of the times necessary to reach a concentration of 10 µg/L of each MC in the permeate stream, while operating with demineralized water as the matrix and an addition of 3 g/L NaCl. ....	71



## Abstract

## Abstract

The last decades, water, and then specifically sweet and potable water, turned to be one of Earth's scarcest commodities, and is increasingly growing to be so. This scarcity is induced by different reasons such as climate and environmental change, soil salination, growing use and pollution of available water sources due to an increase in human population and consumption.

Therefore, novel technologies need to be developed in order to slow down these trends. This can start with an appropriate treatment of produced urban wastewaters (UWWs) for its reuse as irrigation waters for crop irrigation in agriculture, and even for the production of potable water.

Currently, multiple technologies for UWW treatment are proven to be effective when they are applied solely. However, most often many of these proven and researched technologies are not applied in real-life applications or integrated into conventional UWW treatment methods. Resulting that their advantages being missed out on, as well as potential synergetic effects when combined with other technologies.

It is for these reasons that research into the combining and integration of these novel technologies is of the utmost importance. When thus applied, these combined technologies are also known and indicated as Advanced Integrated Technologies (AITs).

In this PhD thesis, research work was conducted on the performance of a pilot scale nanofiltration (NF) plant, based on the effects of salinity on the retention of different ions and contaminants by a commercial spiral-wound polyamide NF membrane. This membrane treatment method for UWW, which is mainly based on (physical) size exclusion, was then followed by the application of other (chemical) treatment methods, in order to treat the produced concentrate and permeate streams.

The degradation of microcontaminants (MCs) in UWW, or for example the concentrate and permeate streams produced after the application of NF membrane filtration, can be obtained by the application of Advanced Oxidation Processes (AOPs). These as the (solar) photo-Fenton process. This process makes use of the catalytic cycle of iron ( $\text{Fe}^{2+}$  and  $\text{Fe}^{3+}$ ), UV-vis light, along with an oxidizing agent, such as hydrogen peroxide ( $\text{H}_2\text{O}_2$ ), or persulfate, producing the relatively slow and selective persulfate radicals ( $\text{SO}_4^{\bullet}$ ) with the latter, and the highly reactive and non-selective hydroxyl radicals ( $\bullet\text{OH}$ ) with the former.

One of the drawbacks of this (solar) photo-Fenton process is that it must be applied at acidic pH 3, in order to prevent iron precipitation. There are a variety of ways to prevent this, such as by applying chelating agents naming Ethylenediamine-tetraacetic acid (EDTA) and Ethylenediamine-N, N'-disuccinic acid (EDDS), of which EDDS is a biodegradable and non-toxic.

A variety of target MCs were selected, based on their general presence in UWW, and their lack of degradation by conventional UWW treatment plants (UWWTPs). The

selected MCs in this research work are caffeine, which is a widely used psychoactive drug, imidacloprid and thiacloprid, two neonicotinoid pesticides commonly used in agriculture, carbamazepine, an anticonvulsant medication generally used in epilepsy and neuropathic pain, and diclofenac, an anti-inflammatory agent used both in professional healthcare and for domestic purposes.

Neither increased salinity of natural water matrices with added NaCl, nor system pressure, showed negligible effects on the permeation order of the present ions in the natural water, nor the selectivity by the polyamide NF membrane during concentration. Whereas preconcentration is an essential step before applying AOPs as tertiary treatment of UWWTP effluents, as it significantly lowers the to be treated volume, and therefore the economic costs.

Treating the concentrate stream from the NF by the solar photo-Fenton process showed to be effective for the removal of the aforementioned MCs when H<sub>2</sub>O<sub>2</sub> was used as an oxidation agent. Opposite to that, the application of persulfate and its derived radicals showed lower degradation of the selected MC.

Effective degradation of MCs in saline matrices at low concentrations, such as in the permeate streams, was also shown to be possible.

Different concentrations and ratios of iron and EDDS, and oxidizing agent were tried to find the optimum technical and economic parameters. The optimum parameters when applying the solar photo-Fenton process for the treatment of (concentrated) UWWs were set to be 0.10 mM Fe:EDDS, at a ratio of [1:2], and a concentration of 1.50 mM H<sub>2</sub>O<sub>2</sub>. Showing the highest degradation rates of the MCs, with the lowest residual amounts of iron and H<sub>2</sub>O<sub>2</sub>, both at pH 3 and circumneutral pH. For which a higher MC degradation is adhered to a directly proportional lower toxicity.

Therefore, further research work in this PhD thesis covers UWWTP effluent valorization by the recovery of ammonium, with combined MC elimination by NF and different advanced AOPs, in order to produce permeate streams for direct crop fertilization and irrigation, also called 'fertigation'. These AOP processes include the previously mentioned solar photo-Fenton, but was this time also combined with electrooxidation (EO) processes, such as anodic oxidation (AO), solar-assisted anodic oxidation (SAAO), electro-Fenton (EF), and solar photoelectro-Fenton.

Solar photo-Fenton was most effective when treating NF concentrate streams at circumneutral pH, at MC concentration lower than 1 mg/L in order to obtain rapid MC degradation. High saline and highly concentrated NF concentrate streams are ideal to be treated by EO processes, as they possess high conductivity and require longer treatment times. Significant lower electric consumption was obtained by solar assistance, whereas solar-assisted electro-Fenton showed to be ineffective for UWW treatment due to higher consumable use, as compared to AO.

MC retention efficiency by NF and toxicity after the AOP treatments was also assessed by determining the phytotoxicity of the different permeate streams when they would be applied as irrigation water for crop irrigation in agriculture. The results showed that



## Abstract

permeates used for the irrigation of crops such as *Sorghum saccharatum*, *Sinapis alba*, and *Lepidium sativum* lowered the germination of their seeds. In the contrary to that, it showed that irrigation with the produced permeates of the permeate streams generally promoted the root development, while the development of the shoots only thrived when using permeates which had concentration factors lower than concentration factor (CF),  $CF = 2$ .

Continued toxicity research of the produced permeate streams by the NF pilot plant was performed to also determine the acute and chronic toxicity using *Daphnia magna*. These studies showed that permeates coming from the produced permeate streams which are to be used for crop irrigation should first be diluted with a minimum of 50%, in order to be suitable for direct crop irrigation in agriculture.

More conducted research work included in this PhD thesis involves the assessment of a priorly developed photocatalytic  $TiO_2-ZrO_2$  ceramic ultrafiltration (UF) membrane. The goal of this previous work was to develop an UF membrane that possesses photocatalytic self-cleaning properties when irradiated by sunlight, in order to extend its operation time by the prevention and reversal of fouling.

When the novel developed ceramic UF membrane was utilized for the filtration of set volumes of UWWTP effluent in the dark, a decline in flux was observed over time. This phenomenon is something which can be assigned to the fouling of the membrane surface and the membrane pores of the ceramic UF membrane by substances present in the UWWTP effluent, such as bacteria, protozoa, and viruses as part of the microbiological load, as also the presence of other substances such as natural organic matter (NOM), and different suspended solids and colloids.

It was shown that this decline of flux can be reversed when the ceramic UF membrane was irradiated by light in a solar simulator. This proves that the ceramic UF membrane is indeed self-cleaning and photocatalytic active. However, it was thereby found that the flux reversal of the photocatalytic ceramic UF membrane was not only induced by photocatalytic activity, but as well as by another phenomenon called photo-induced super-hydrophilicity.

After spiking UWWTP effluent with the previously selected MCs, caffeine, imidacloprid, thiacloprid, carbamazepine, and diclofenac, at an initial concentration of  $100 \mu\text{g/L}$  each, the UWWTP effluent was then treated by UF membrane filtration. The resulting retentates and permeate streams were on their turn treated by the solar photo-Fenton process. The study showed that a reduction of permeate turbidity by the photocatalytic UF membrane significantly improved the efficiency of the solar photo-Fenton process, as scavenging of the  $\cdot\text{OH}$  is reduced.

Finally, the microbiological retention of the UF membrane was determined by deploying a Gram-negative bacterial strain, *Pseudomonas aeruginosa* (*P. Aeruginosa*). With the study it was not only proven that the UF membrane is self-cleaning when irradiated by sunlight, but also that it was able to consistently retain *P. Aeruginosa* till an order of magnitude of  $1 \times 10^3$ - $1 \times 10^4$  CFU/ml.

## Resumen

En las últimas décadas, el agua, y específicamente el agua dulce y potable, se ha convertido en uno de los recursos más escasos de la Tierra, e incrementándose esta escasez. Esta carestía es inducida por diferentes razones, como el cambio climático, la salinización del suelo, su uso creciente y la contaminación de las fuentes de agua disponibles, debido al aumento de la población humana y sus necesidades de consumo.

Por lo tanto, es necesario desarrollar nuevas tecnologías para frenar esta tendencia. Esto puede paliarse con un tratamiento adecuado de las aguas residuales urbanas (ARU; inglés UWW) para su reutilización como agua de riego, e incluso para la producción de agua potable.

Actualmente, múltiples tecnologías para el tratamiento de las ARUs han demostrado ser efectivas. Sin embargo, la mayoría de las veces, muchas de estas tecnologías avanzadas de eficiencia probada no se aplican en vida real ni se integran en los métodos de tratamiento convencionales de las ARUs. Como resultado, se están perdiendo sus ventajas, así como los posibles efectos sinérgicos cuando se combinan con las existentes.

Es por estas razones que la investigación sobre la combinación e integración de estas nuevas tecnologías es de máxima importancia. Cuando se aplican de este modo, también se conocen como Tecnologías Integradas Avanzadas (TIA; inglés AIT).

En esta tesis doctoral, se realizó un trabajo de investigación sobre el funcionamiento la nanofiltración (NF) a escala planta piloto, basado en los efectos de la salinidad en la retención de diferentes iones y contaminantes por una membrana de NF de poliamida comercial enrollada en espiral. Este método de tratamiento de membrana para las ARUs, que se basa principalmente en la exclusión por tamaño (físico), se combinó con otros métodos de tratamiento (químicos) en las corrientes de concentrado y permeado producidas.

La degradación de microcontaminantes (MC) en las ARUs, o en las corrientes de concentrado y permeado producidas después de la NF, se puede conseguir mediante la aplicación de procesos de oxidación avanzada (inglés AOP), como el proceso (solar) foto-Fenton. Este proceso utiliza el hierro de forma catalítica (ciclo entre  $\text{Fe}^{2+}$  y  $\text{Fe}^{3+}$ ), la luz UV-vis, junto con un agente de oxidación, como el peróxido de hidrógeno ( $\text{H}_2\text{O}_2$ ) o el persulfato. Se producen radicales sulfato ( $\text{SO}_4^{\bullet}$ ), relativamente lentos y selectivos, con el segundo agente de oxidación, y radicales hidroxilo ( $^{\bullet}\text{OH}$ ), altamente reactivos y no selectivos, con el primer agente de oxidación.

## Resumen

Una de las desventajas del proceso clásico (solar) foto-Fenton es que debe aplicarse a un pH cercano a pH 3, para evitar la precipitación del hierro. Hay una variedad de formas de prevenir esto y poder trabajar a pH circunneutro, entre ellas la aplicación de agentes quelantes como el ácido etilendiamino tetraacético (EDTA) y ácido etilendiamino-N, N'-disuccínico (EDDS), siendo el EDDS biodegradable y no tóxico.

Se seleccionó una variedad de MCs objetivo, en función de su presencia general en las ARUs y su falta de degradación en las estaciones de depuración de aguas residuales (EDAR; inglés UWWTP). Los MCs seleccionados en este trabajo de investigación han sido la cafeína, que es un fármaco psicoactivo de amplio uso; el imidacloprid y el tiacloprid, dos pesticidas neonicotinoides de uso común en la agricultura; la carbamazepina, un medicamento anticonvulsivo generalmente utilizado en la epilepsia y el dolor neuropático; y el diclofenaco, un agente antiinflamatorio.

Ni el aumento de la salinidad en las matrices de aguas naturales con NaCl añadido, ni la presión del sistema, mostraron efectos significantes sobre el orden de permeación de los iones presentes en el agua natural, ni la selectividad de la membrana de NF de poliamida. Se ha tenido en cuenta que la preconcentración del efluente es un paso imprescindible antes de aplicar los AOPs como tratamiento terciario de EDAR, ya que reduce significativamente el volumen a tratar, y por tanto los costes económicos.

El tratamiento de la corriente de concentrado de NF, mediante el proceso solar foto-Fenton, demostró ser efectivo para la eliminación de los MCs mencionados anteriormente cuando se utilizó H<sub>2</sub>O<sub>2</sub> como agente de oxidación. Por el contrario, la aplicación de persulfato mostró una menor degradación de los MCs seleccionados.

La degradación de los MCs a bajas concentraciones en matrices salinas, como en las corrientes de permeado, también se demostró posible.

Se probaron diferentes concentraciones y proporciones de hierro y EDDS, y de los agentes de oxidación para encontrar los parámetros técnicos y económicos óptimos. Estos parámetros se establecieron en 0,10 mM de Fe:EDDS, en una proporción de [1:2] y una concentración de 1,50 mM de H<sub>2</sub>O<sub>2</sub>. Así se alcanzaron las mayores tasas de degradación de los MCs, con las menores cantidades residuales de hierro y H<sub>2</sub>O<sub>2</sub> al final del tratamiento, tanto a pH 3 como a pH circunneutro.

También se estudió la valorización de efluentes de EDAR mediante la recuperación de amonio, con la eliminación combinada de MCs por NF y diferentes AOPs avanzados, con el objetivo de producir corrientes de permeado para la fertilización e irrigación directa de cultivos, también llamado 'fertirrigación'. Estos procesos AOP incluyen el anteriormente mencionado solar foto-Fenton, pero esta vez combinado con procesos como electro oxidación (EO), oxidación anódica (OA), oxidación anódica asistida por energía solar (OAAS), electro-Fenton (EF) y solar-foto electro-Fenton.

El solar foto-Fenton fue más efectivo cuando se trataron corrientes de concentrado de NF a pH circunneutro, con una concentración de MCs inferior a 1 mg/L. Las corrientes de concentrado de NF altamente salino son ideales para ser tratadas mediante procesos de EO, ya que poseen una alta conductividad y requieren tiempos de tratamiento menos prolongados. Se obtuvo un consumo eléctrico significativamente menor cuando los procesos EO se combinaron con sol, mientras que EF asistido por energía solar demostró ser ineficaz para el tratamiento de las ARUs, con un mayor uso de reactivos, en comparación con la OA.

También se evaluó la eficiencia de retención de los MCs por NF y la toxicidad después de los tratamientos con AOP mediante la determinación de la fitotoxicidad (con *Sinapis alba*, *Sorghum saccharatum* and *Lepidium sativum*) de las diferentes corrientes de permeado.

Se realizaron pruebas de fitotoxicidad a dos diferentes relaciones de concentración de permeado (CF), CF = 2 y 4, para evaluar sus efectos sobre la germinación de semillas y el crecimiento de raíces y brotes. Los permeados redujeron ligeramente la germinación de *S. saccharatum* y *S. alba*. En *S. saccharatum* y *S. alba* el permeado CF=2 promovió el desarrollo de raíces, pero *Lepidium sativum* fue severamente afectado. La longitud de los brotes de *S. saccharatum* se redujo solo con CF=4. El crecimiento de brotes de *S. alba* y *Lepidium sativum* se redujo claramente con CF = 4. Por lo tanto, la aplicación directa de permeado de CF = 2 es adecuada para el riego de cultivos.

Se llevó a cabo también una evaluación de la toxicidad de las corrientes de permeado producidas por la planta piloto de NF mediante la toxicidad aguda y crónica usando *Daphnia magna*. Estos estudios demostraron que los permeados provenientes de las corrientes de permeado deben diluirse primero al menos un 50%, para que sean adecuados para la irrigación en la agricultura.

Otros trabajos de investigación realizados e incluidos en esta tesis doctoral implicaron la evaluación de una membrana de ultrafiltración (UF) basada en una cerámica foto catalítica de TiO<sub>2</sub>-ZrO<sub>2</sub> desarrollada previamente. El objetivo de este trabajo fue desarrollar una membrana de UF que posea propiedades foto catalíticas de autolimpieza, cuando es irradiada por la luz solar, con el fin de extender su tiempo de operación, previniendo e incluso revirtiendo su ensuciamiento.

Cuando se utilizó esta nueva membrana con efluentes de EDAR en la oscuridad, se observó una disminución en el flujo de permeado con el tiempo. Esto se puede atribuir al ensuciamiento de la superficie de la membrana y de los poros por sustancias y microorganismos presentes en el efluente de EDAR, como bacterias, protozoos y virus. La presencia de otras sustancias como materia orgánica natural, y diferentes sólidos en suspensión y coloides son también responsables del ensuciamiento.

## Resumen

Se demostró que esta disminución del flujo se puede revertir cuando la membrana se irradió con luz en un simulador solar. Esto prueba que la membrana de UF cerámica es auto limpiante y foto catalíticamente activa. Sin embargo, se encontró que la recuperación del flujo de la membrana no solo fue inducida por la actividad foto catalítica, sino también por otro fenómeno llamado 'super-hidrofilia foto-inducida'.

Después de añadir los MCs previamente seleccionados, la cafeína, el imidacloprid, el tiacloprid, la carbamazepina y el diclofenaco, a una concentración inicial de 100 µg/L cada uno al efluente de EDAR, éste se trató mediante filtración por membrana de UF. Los rechazos resultantes y las corrientes de permeado se trataron mediante el proceso solar foto-Fenton. El estudio mostró que una reducción de la turbidez del permeado por parte de la membrana de UF foto catalítica, mejoró significativamente la eficiencia del proceso solar foto-Fenton, disminuyendo el consumo de  $^{\bullet}\text{OH}$ .

Finalmente, se determinó la retención microbiológica de la membrana de UF mediante una cepa bacteriana Gram negativa, *Pseudomonas aeruginosa* (*P. aeruginosa*). Con el estudio no solo se demostró que la membrana de UF es auto limpiante cuando es irradiada por la luz solar, sino que también es capaz de retener *P. Aeruginosa* de manera constante hasta un orden de magnitud de  $1 \times 10^3$ - $1 \times 10^4$  CFU/mL.

Resum



## Resum

A les darreres dècades, l'aigua, i específicament l'aigua dolça i potable, s'ha convertit en un dels recursos més escassos de la Terra, i s'ha incrementat aquesta escassetat. Aquesta carestia és induïda per diferents raons, com el canvi climàtic, la salinització del sòl, el seu ús creixent i la contaminació de les fonts d'aigua disponibles a causa de l'augment de la població humana i les necessitats de consum.

Per tant, cal desenvolupar noves tecnologies per frenar aquesta tendència. Això es pot pal·liar amb un tractament adequat de les aigües residuals urbanes (ARU; anglès UWW) per a la seva reutilització com a aigua de reg, i fins i tot per a la producció d'aigua potable.

Actualment, múltiples tecnologies per al tractament de les ARU han demostrat ser efectives. Tot i això, la majoria de vegades moltes d'aquestes tecnologies avançades d'eficiència provada no s'apliquen en vida real ni s'integren en els mètodes de tractament convencionals de les ARUs. Com a resultat, se n'estan perdent els avantatges, així com els possibles efectes sinèrgics quan es combinen amb els existents.

És per aquestes raons que la investigació sobre la combinació i la integració d'aquestes noves tecnologies és de màxima importància. Quan s'apliquen així, també es coneixen com a Tecnologies Integrades Avançades (TIA; anglès AIT).

En aquesta tesi doctoral, es va realitzar un treball de recerca sobre el funcionament de la nanofiltració (NF) a escala planta pilot, basat en els efectes de la salinitat en la retenció de diferents ions i contaminants per una membrana de NF de poliamida comercial enrotllada en espiral. Aquest mètode de tractament de membrana per a les ARUs, que es basa principalment en l'exclusió per mesura (físic), es va combinar amb altres mètodes de tractament (químics) als corrents de concentrat i permeat produïts.

La degradació de microcontaminants (MC) a les ARUs, o als corrents de concentrat i permeat produïts després de la NF, es pot aconseguir mitjançant l'aplicació de processos d'oxidació avançada (anglès AOP), com el procés (solar) foto-Fenton. Aquest procés utilitza el ferro de forma catalítica (cicle entre  $Fe^{2+}$  i  $Fe^{3+}$ ), la llum UV-vis, juntament amb un agent d'oxidació, com ara el peròxid d'hidrogen ( $H_2O_2$ ) o el persulfat. Es produeixen radicals sulfat ( $SO_4^{\bullet}$ ), relativament lents i selectius, amb el segon agent d'oxidació, i radicals hidroxil ( $\bullet OH$ ), altament reactius i no selectius, amb el primer agent d'oxidació.

Un dels desavantatges del procés clàssic (solar) foto-Fenton és que s'ha d'aplicar a un pH proper a pH 3, per evitar la precipitació del ferro. Hi ha una varietat de maneres de prevenir això i poder treballar a pH circumneutre, entre elles l'aplicació d'agents quelants com l'àcid etilendiamino tetraacètic (EDTA) i àcid etilendiamino-N, N'-disuccínic (EDDS), sent l'EDDS biodegradable i no tòxic.

Es va seleccionar una varietat de MCs objectiu, en funció de la seva presència general a les ARUs i la seva manca de degradació a les estacions de depuració d'aigües residuals (EDAR; anglès UWWTP). Els MC seleccionats en aquest treball de recerca han

estat la cafeïna, que és un fàrmac psicoactiu d'ampli ús; l'imidacloprid i el tiacloprid, dues pesticides neonicotinoides d'ús comú a l'agricultura; la carbamazepina, un medicament anticonvulsiu generalment utilitzat a l'epilèpsia i el dolor neuropàtic; i el diclofenac, un agent antiinflamatori.

Ni l'augment de la salinitat a les matrius d'aigües naturals amb NaCl afegit, ni la pressió del sistema, van mostrar efectes significants sobre l'ordre de permeació dels ions presents a l'aigua natural, ni la selectivitat de la membrana de NF de poliamida. S'ha tingut en compte que la preconcentració de l'efluent és un pas imprescindible abans d'aplicar els AOP com a tractament terciari d'EDAR, ja que redueix significativament el volum a tractar, i per tant els costos econòmics.

El tractament del corrent de concentrat de NF, mitjançant el procés solar foto-Fenton, va demostrar ser efectiu per a l'eliminació dels MCs esmentats anteriorment quan es va utilitzar H<sub>2</sub>O<sub>2</sub> com a agent d'oxidació. Per contra, l'aplicació de persulfat va mostrar una menor degradació dels MC seleccionats.

La degradació dels MCs a baixes concentracions en matrius salines, com en els corrents de permeat, també es va demostrar possible.

Es van provar diferents concentracions i proporcions de ferro i EDDS i dels agents d'oxidació per trobar els paràmetres tècnics i econòmics òptims. Aquests paràmetres es van establir en 0,10 mM de Fe:EDDS, en una proporció de [1:2] i una concentració de 1,50 mM de H<sub>2</sub>O<sub>2</sub>. Així es van assolir les majors taxes de degradació dels MCs, amb les menors quantitats residuals de ferro i H<sub>2</sub>O<sub>2</sub> al final del tractament, tant a pH 3 com a pH circumneutre.

També es va estudiar la valorització d'efluents d'EDAR mitjançant la recuperació d'amoni, amb l'eliminació combinada de MCs per NF i diferents AOPs avançats, amb l'objectiu de produir corrents de permeat per fertilització i irrigació directa de cultius, també anomenat 'fertirrigació'. Aquests processos AOP inclouen l'anteriorment esmentat solar foto-Fenton, però aquesta vegada combinat amb processos com electro-oxidació (EO), oxidació anòdica (OA), oxidació anòdica assistida per energia solar (OAAS), electro-Fenton (EF) i solar- foto electro-Fenton.

El solar foto-Fenton va ser més efectiu quan es van tractar corrents de concentrat de NF a pH circumneutre, amb una concentració de MCs inferior a 1 mg/L. Els corrents de concentrat de NF altament salí són ideals per ser tractats mitjançant processos d'EO, ja que tenen una alta conductivitat i requereixen temps de tractament menys perllongats. Es va obtenir un consum elèctric significativament menor quan els processos EO es van combinar amb sol, mentre que EF assistit per energia solar va demostrar ser ineficaç per al tractament de les ARUs, amb un ús més gran de reactius, en comparació amb l'OA.

També es va avaluar l'eficiència de retenció dels MC per NF i la toxicitat després dels tractaments amb AOP mitjançant la determinació de la fitotoxicitat (amb *Sinapis alba*, *Sorghum saccharatum* and *Lepidium sativum*) dels diferents corrents de permeat.

## Resum

Es van realitzar proves de fitotoxicitat a dues diferents relacions de concentració de permeat (CF), CF = 2 i 4, per avaluar-ne els efectes sobre la germinació de llavors i el creixement d'arrels i brots. Els permeats van reduir lleugerament la germinació de *S. saccharatum* i *S. alba*. A *S. saccharatum* i *S. alba* el permeat CF=2 va promoure el desenvolupament d'arrels, però *Lepidium sativum* va ser severament afectat. La longitud dels brots de *S. saccharatum* es va reduir només amb CF=4. El creixement de brots de *S. alba* i *Lepidium sativum* es va reduir clarament amb CF=4. Per tant, l'aplicació directa de permeat de CF=2 és adequada per al reg de cultius.

Es va dur a terme també una avaluació de la toxicitat dels corrents de permeat produïts per la planta pilot de NF mitjançant la toxicitat aguda i crònica usant *Daphnia magna*. Aquests estudis van demostrar que els permeats provinents dels corrents de permeat s'han de diluir primer almenys un 50%, perquè siguin adequats per a la irrigació a l'agricultura.

Altres treballs de recerca realitzats i inclosos en aquesta tesi doctoral van implicar l'avaluació d'una membrana d'ultrafiltració (UF) basada en una ceràmica foto catalítica de TiO<sub>2</sub>-ZrO<sub>2</sub> desenvolupada prèviament. L'objectiu d'aquest treball va ser desenvolupar una membrana d'UF que posseïssa propietats foto catalítiques d'autoneteja, quan és irradiada per la llum solar, per tal d'estendre el seu temps d'operació, prevenint i fins i tot revertint-ne l'embrutament.

Quan es va utilitzar aquesta nova membrana amb efluents d'EDAR a la foscor, es va observar una disminució en el flux de permeat amb el temps. Això es pot atribuir a l'embrutament de la superfície de la membrana i dels porus per substàncies i microorganismes presents a l'efluent d'EDAR, com bacteris, protozous i virus. La presència d'altres substàncies com a matèria orgànica natural, i diferents sòlids en suspensió i col·loïdes són també responsables de l'embrutament.

Es va demostrar que aquesta disminució del flux es pot revertir quan la membrana es va irradiar amb llum en un simulador solar. Això prova que la membrana de UF ceràmica és auto netejant i foto catalíticament activa. Tot i això, es va trobar que la recuperació del flux de la membrana no només va ser induïda per l'activitat foto catalítica, sinó també per un altre fenomen anomenat 'super-hidrofilia foto-induïda'.

Després d'afegir els MC prèviament seleccionats, la cafeïna, l'imidacloprid, el tiacloprid, la carbamazepina i el diclofenac, a una concentració inicial de 100 µg/L cadascun a l'efluent d'EDAR, aquest es va tractar mitjançant filtració per membrana d'UF. Els rebutjos resultants i els corrents de permeat es van tractar mitjançant el procés solar foto-Fenton. L'estudi va mostrar que una reducció de la terbolesa del permeat per part de la membrana d'UF foto catalítica, va millorar significativament l'eficiència del procés solar foto-Fenton, disminuint el consum d\*OH.

Finalment, es va determinar la retenció microbiològica de la membrana d'UF mitjançant un cep bacterià Gram negatiu, *Pseudomonas aeruginosa* (*P. aeruginosa*). Amb l'estudi no només es va demostrar que la membrana d'UF és auto netejant quan és irradiada per la llum solar, sinó que també és capaç de retenir *P. Aeruginosa* de manera constant fins a un ordre de magnitud de  $1 \times 10^3$ - $1 \times 10^4$  CFU /mL.







## Chapter I. Introduction



## I. Introduction

### 1. The Necessity for Water

The demand for water is growing every day to astonishing heights. In the first place, it is directly consumed by humans and all other organisms on Earth, as it is the first life necessity. Thereby, water is used for hygienic purposes, from bathing to washing dishes and clothes, and it is for these reasons that most of life on Earth can be found in and around it many forms. Second to that, water is used for a range of recreative purposes, thinking about boating and other sports, swimming pools, up to whole theme parks. And third, it is used by humans for economic purposes, from irrigation in agriculture, shipping in transport, to the most basic and advanced industrial processes. [1–3] As only three percent of Earth's water supply is sweet, this demand is not only growing locally, but also on a global level. This, especially on a local level, brings a lot of problems and conflicts to human life, resulting in an unfair distribution of the available supply, and related wealth. More and more areas are prone to soil desertification, salination and pollution, due to extensive agricultural and mining use, especially in lower developed countries, often countries with colonial pasts. The products produced in these areas are thereby oftentimes directly exported to richer countries. [2,4,5]

Other than the unfair distribution of wealth, also climate change is subject to the constant growing demand for water. A growing number of heatwaves are registered, that are not only more severe, but also registered earlier or later than their normal time of the year. Resulting in extreme droughts, forest fires, extreme winds that dry out the soil even more and spread wildfires, in oxygen free 'dead-zones' in seas and oceans, and in the creation of similar areas on earth with 100% humidity and temperatures above 40 °C, making biological cooling mechanisms, such as sweating, impossible. [6–8]

Opposite to that, shifting high and low atmospheric pressures, changes in hot and cold water and air streams, result in the sudden accumulation of atmospheric energy, water and cloud formations that burst out in destructive thunderstorms and local spring floods. Destroying age old vegetation and flooding and destroying urban areas, leaving behind a polluted sludge in the affected areas, as well as in other areas such as valleys, down-river flood plains, and river deltas. Threatening valuable agricultural lands and natural reserves. [6,9]

Many of the regions on Earth affected the most by these threats, are often lacking regulation and legislation to prevent and protect the hardship coming with it. Unfortunately, also in the more developed countries a lack of legislation can be found in topics regarding to water. Resulting in the irresponsible use of the still available water resources, as well as pollution of rivers, lakes, seas, and oceans, with a wide spectrum of unpunished abuse. [10,11]

The main global organization looking to discuss and implement regulation regarding global, regional, and local water management is the United Nations (UN). They recognized the access to water and sanitation to be a human right, using five definitions: *Sufficient, Safe, Acceptable, Physically accessible, and Affordable*. It

thereby aims to develop and implement several different sustainable technical methodologies and nature-based solutions for the management and protection of water sources, and the general validation of the value of water. [12–14]

Looking at a regional level, such as the European continent, the European Union (EU) aims to take and direct responsibilities regarding the management and protection of water sources and bodies. [15,16] The countries belonging to this union hosts around 450 million inhabitants and is one of the most densely populated and developed areas on Earth. The climate properties of this continent are diverse, ranging from a polar climate in the north, home to numerous petrochemical-, fishing, steel, and wood processing industries. The more moderate sea and continental climates in its center, home to some of the world's most industrialized areas for chemical production and the manufacturing of cars, machinery, and many other consumer products. As well as highly intensive agricultural activities, such as greenhouses and the dairy and meat industries. [17,18] The EU countries with a Mediterranean climate in the south, are keeping a high dependance on the agricultural industry to provide for the rest of the continent and beyond, on the fertile but semi-arid terrains, result in extremely high water pressures. [19,20] It is for these reasons that the EU in general, consumes one of the highest quantities of water per person in the world.

To ensure the supply of food and water within the EU, its central and local governments tend to enforce a variety of policies regarding water, such as the EU Council Directive 2000/60/EC of the European Parliament and of the Council. By the establishment of a framework for the Community action in the field of water policy, the Water Framework Directive, it makes it member states commit to the achievement of good qualitative and quantitative status of all of their water bodies. Moreover, and even more important, it declares that *water is not a commercial product like any other but, rather, a heritage which must be protected, defended and treated as such*. [21]

Also, the promotion and funding of research performed by the scientific community is part of this intent, looking e.g., at the Horizon 2020 and Horizon 2030 projects. The scientific community is entrusted to solve a part of the problems with water and environment related subjects, and more and more scientific focus is therefore directed to the production of food and the directly and indirectly related water topics. All to ensure a constant and reliable supply of good quality water now and for future generations, while promoting the synergy between the scientific community and industry at an international level, while keeping gender equality and an *open access* approach of results. [22,23]

The quality of water can be determined in many different ways, depending on the point in the water cycle. For example, at its primary source, being it a glacier, aquifer, river, lake or groundwater, the quality of water can be measured by the physicochemical parameters of the water. This is however as complex as the infinite

## I. Introduction

high number of water sources, and the exact point and time of the initial sample taken. The most reliable and utilized determination is a standardization of the water quality and the quantities of the compounds in it, based on its final application, such as drinking water and irrigation water. This standardization can be implemented as legislation at, for example, a national level, and be streamlined between nations that share the same river, lake or sea, throughout regional governments such as the EU. [24], potentially decreasing the chance of conflict between these countries and guaranteeing a more effective environmental policy. A quantification for the quality of water based on the physical characteristics can mainly be determined by the temperature, pH value, hardness, turbidity, total dissolved solids, and total suspended solids (TSS). The chemical characteristics are mainly determined by the chemical oxygen demand (COD), biological oxygen demand over five days (BOD<sub>5</sub>), total nitrogen (TN), nitrates, phosphorus, chloride, and sulfur, as well as the toxicity of the wastewater and pathogens present. [25]

As much as water is the first life necessity for humans and all other organisms on Earth, electricity, or energy in general, is the first life necessity for nowadays human society. Fossil fuels as a source for this energy is ever more accelerating the negative effects of its consumption on climate change, calling for a rapid change and implementation of sustainable energy sources. Most sustainable technologies, as well as some for the transport, heating, and other treatments of water, are based on the utilization of climate-depending sources, e.g., wind and tidal energy, biomass reactors and generators, and solar irradiation. As mentioned before, the climate within the EU and of course the rest of the world knows great variation. Therefore, the connection between water and energy demands its recognition. This can be found in the form of the 'Water-Energy Nexus'. [26,27]

Water, is used now for centuries in its gaseous phase to transfer thermal energy into mechanical and/or electrical energy in steam engines and turbines, plans for sustainable transport options aim to use hydrogen gas, produced from water from sustainable sources or as a rest of chemical processes, turned back into water after energy extraction in the fuel cell, and recently, the application of (sustainably produced) electricity for the treatment of polluted water. [28] Not only hydrogen, but also biogases such as methane can be utilized in this nexus, with potential (decentralized) applications at a local scale, or in otherwise desolated areas lacking the infrastructure. [29]

This all shows the great importance of the development, combination, and integration of novel and existing technologies, for the creation of sustainable circular economies. To increase the efficiency of water and energy use, in every process of modern society, in an intend to preserve and provide for human and organic life on Earth.

## 2.1. Wastewaters

### ***Urban wastewaters***

There are a variety of classes of wastewaters of which urban wastewater (UWW) is one. Coming from urban areas, they mainly come from direct domestic water use, rainwater and water runoffs, agricultural water-use and as a rest product, as well as from some small/simple industrial processes. As also described in the EU Council Directive for UWW, 91/271/EEC, differentiating domestic wastewaters as *wastewater from residential settlements and services which originates predominantly from the human metabolism and from household activities*. [30]

UWWs are treated in urban wastewater treatment plants (UWWTP). The different processes in the UWWTPs start with the mechanical separation of the big solids, ranging from sand, stones, wood, materials for cosmetic and hygienic use such as cleaning wipes, up to car tires, from the liquid bulk. Followed by the removal of fats and greases, and an aeration step as a preparation for biological treatments for the removal of different organic chemical compounds. If the then so-called secondary effluent still contains persistent pollutants, tertiary treatments, such as ozonation, UV irradiation and filtration over activated carbon and membranes, can be applied to further treat and purify the water, including disinfection for irrigation purposes. [31]

The size of UWWTPs and their specific treatment steps are determined by the size of the populations connected to them, the presence of hospitals, industrial areas, and agricultural zones. Apart from these dimensions, the UWWTP influent may thereby vary based on different seasonal and weather conditions, as rain may dilute the influent for short or temporal periods and tourism can significantly increase the population size for short periods, contributing to the level of organics present in the wastewater. In general, or based on the size of the UWWTP, analytics to monitor the different steps of the treatment process and the intermediate and final quality of the wastewater are performed on a weekly basis. The main indicators are the COD ranging between 250 and 1500 mg/L, BOD<sub>5</sub> ranging between 50 and 750 mg/L, TN ranging between 10 and 150 mg/L, ammonia ranging between 4 and 80 mg/L, phosphorous ranging between 0.5 and 25 mg/L, and finally, the TSS ranging between 100 and 750 mg/L, of which volatile solids ranging between 150 and 500 mg/L. [32–35]

The efforts in the EU to apply wastewater treatment before its discharge have significantly increased over the past decades. When looking at the most recent member states of the EU, mainly former Soviet countries in Eastern Europe and the Balkans, comparisons are made between 1990, just before the fall of the USSR, and 2014, when most of these countries joined the EU. [36]

Especially in the last years the EU made its final efforts by warning through infringements, and later fining the countries not complying to the implementation of more wastewater treatment for UWW. [37] However, the political means of sanctioning already economically vulnerable countries, such as Greece and different

## I. Introduction

other (South-)Eastern European countries, may not always be the solution. When also looking at geographical and other practical aspects, a more technical and decentralized approach should be taken in the construction of wastewater treatment infrastructure. Something opposite to the maintenance and improvement of highly developed inland areas regarding the UWW treatment infrastructure. [38]

### ***Industrial wastewaters***

Wastewaters coming from a variety of industries offer both great challenges and potential. It is in the same EU Council Directive, 91/271/EEC, the EU describes their definition for industrial wastewater: *any wastewater which is discharged from premises used for carrying on any trade or industry, other than domestic wastewater and run-off rainwater*. [30] Characterized by the significant volumes of process waters, often with high loads of COD, pigments, and/or pollutants ranging from slightly environmentally disturbing to extremely persistent and dangerous to all life on Earth. It is the chemical industry that is responsible for the highest production percentage of these pollutants, often not produced for itself, but for other industries. This is significantly extending its range of pollution, especially considering that efficient treatment methods are often failing, or are simply not applied. The further from the initial production process, the more often this is the case, as initial concentrations are ever further diluted. This failure on its turn, demands complicated clean-up operations after longer times, ranging from years to possibly centuries, when 'forgotten' polluted areas are then needed for the expansion of urban areas, or traces of pollutants are found back in drinking water. Oppositely to this problem, the immediate treatment of industrial wastewaters at their source offers great potential, by the recovery and elimination of chemicals from wastewater. [39,40]

### ***Agricultural and aquaculture industries***

One category of industrial wastewater comes from the agricultural industry, which ranges from everything between greenhouses and (urban) mushroom farms, to field crop and livestock meat and dairy farms. Their wastewaters are often characterized by the presence of high concentrations of ammonia and phosphates, a wide variety of pesticides, natural and artificial fertilizers, petrochemical products and a high (micro)biological load. [15,41] As much as these wastewaters can be a danger for the surrounding environment, they offer great opportunities for the application of technologies that enable the direct reuse of them. [42]

Aquaculture is the intensive breeding and growing of fish and other water animals and their wastewaters are often characterized by high COD values from feeding and excretion, contain high concentrations of medicine and pesticides, and when applied in open waters, are responsible for the excessive consumption of the naturally present smaller organisms, endangering the food supply of the naturally present sea life. The outbreak of diseases within this type of industry is despite their high (preventive) medicine use common, which brings more endangerment to the naturally present aqueous life, as well as species higher in the food chain. Recently, the introduction of

land-grown feed is also bringing disturbance in the biological balance of the areas in which aquaculture is practiced. Wastewater treatment in this industry is therefore of great importance to prevent these problems in the near and far future. [43,44]

### ***Chemical industry***

Wastewaters coming from the chemical industry are most often contaminated with high concentrations of contaminants. The chemicals are most often produced for other industries, thinking about softeners, fire retardants, and solvents for the polymer industry, heavy metals, anti-corrosion agents and high alkaline wastewaters for the metal industry, pigments and dyes for the textile and fiber industries, fertilizers, and pesticides for the agricultural industries, as well as the pharmaceutical and personal care industries. Their wastewaters are characterized by the presence of very artificial and persistent chemicals and their by-products and metabolites, moderate to extreme low and high pH values. [45–49]

### ***Food and beverage industry***

The agricultural product processing industry, thinking about the processing of sugarcane, potato and other root vegetables, the wine and beer producing industries, coffee, olive, and other vegetable oil industries, are all examples of food and beverage industries producing industrial wastewaters. Although the main priority is the processing of the actual agricultural product, the rest streams as also the wastewaters show great potential for the recovery of many valuable nutrients, which can be used for other products, or for example reused as fertilizer in the agricultural industry. Their wastewaters are mainly characterized by high COD (300-135,000 mg/L), high lipid and saline content and the presence of colorants and aromatic compounds. [50–54]

### ***Landfill leachates***

Basically, all the products mentioned in this chapter end up at the end of their lives in one of the following places, the atmosphere, or the landfill. Only a small percentage of all products produced in the world are being recycled or reused, all others are being dumped in landfills. The landfills are then becoming an infinite graveyard and mixing pot for all these products combined, creating gases leaking into the atmosphere, and after rains and floods from nearby surface waters, leachates. These leachates are a mix of highly complex and toxic chemical mixtures and heavy metals, almost always leaking into the soil without any regard or treatment. One of the most dangerous results is then not only the pollution of soil of the nearby area, but the transport by water sources to areas more distant to it. Their remediation is therefore a complicated and costly one. [55–57]

### ***Metal industry***

The metal industry starting with mining for its resources use and pollute huge amounts of water as well. Many environmental accidents and disasters occur during the mining,

## I. Introduction

quantities of alkaline, heavily polluted process waters leaking in to drinking water sources and rivers, killing all organisms and endangering water supplies. Process waters are mainly produced by the drilling, washing, sieving, and transporting of the raw products and ores. Thereby, especially so-called pit mines, destroy large parts of landscapes and so, natural habitats to flora and fauna, leaving deep empty spaces open to be filled with water, vulnerable to leaking into nearby water supplies. [58–60]

From an ethical point of view, many minorities lose their lands as well to governments and multinationals, by punishment of disownment, expulsion, or worse. [61,62]

The refinement process is furthermore energy extensive, using high quantities of water for e.g., cooling purposes, resulting in the leakage of the actual metals and the many by-products. This is not the last step for it to happen, as till the very last steps from the production of raw metal products, and the final product manufacturing and finishing, many pollutants end up as industrial wastewater by means of drilling oils, milling coolants, the painting and plating process, as well as the recycling of metals. [63–65]

### ***Textile industry***

Also the textile industry is an industry responsible for a high water pressure, the cotton production being one of the most water intensive agricultural processes, this continues with the dyeing and washing of fabrics, as well as the final product, clothes. [66] The industry is thereby highly susceptible to fashion, a definition that recently transformed to 'fast fashion' significantly shortening the lifetime of the products in this industry. Many of these clothing and textile products are exported to and ending up at economic weaker regions and countries without reaching their end of life state, or without even been used. Although efforts for the implementation of the circular economy principle are being made, many of these products finally end up in landfills, without proper processing. [67] Wastewaters from this industry are characterized by the presence of high pigment and chemical load, for e.g., bleaching and coloring, and it is estimated that the industry is good for 54% of the produced dye effluents in the World. Only 88% of this number is discharged in aquatic resources in an appropriate way. Further pollution from this industry can be found in the presence of fibers and microplastics coming from the laundry washing processes. [68–70]

### ***Paper and pulp industries***

Other water intensive industries are the paper and pulp industries. These industries consume huge amounts of water, starting already with their agricultural resources, the wood farming for the necessary pulp and fibers. Followed by the process waters, to produce the actual fibers and pulp from the bulk resources, necessary for the many applications, the many kinds of paper industrial wastewaters coming from these industries often contains a high variety of chemicals necessary for their process and finishing steps, think about lignin, resin, and tannin from wood extracts, but also dyes and heavy metals for coloring and printing. The industry is good for around 10% of produced dye effluents in the World. [68,71,72] A high microbial load is also a specific

problem due to the wet, warm, and nutrient-rich environments in the paper and pulp industries. [73]

### ***Pharmaceutical and personal care products industry***

Most wastewaters coming from the pharmaceutical industry contain large amounts of their production ingredients, as well as the actual drugs. Their discharge and presence in nature can result in a variety of problems such as bioaccumulation, birth and growth defects, and medicine resistance. [74]

The personal care products industry produces a great variety of contaminants in water, from sodium in detergents and shampoos, to microplastics and fibers, synthetic colorants, aromas and perfumes, polymers, wetting agents, synthetic and natural oils, and a wide variety of salts. Their consumption in the EU and is expected to grow annually with around 6% between 2020 and 2027. [75] It has thereby been registered that their use has significantly increased since the start of the Covid-19 pandemic. [76]

### ***Petrochemical and transport industries***

The production of petroleum products by 'onshore' and 'offshore' means, consumes high amounts of water as well. This mainly comes from the 'produced water' (PW), water that comes up from the reservoir or well, together with the oil and gas that are produced. The total volume of PW differs per case but can account for up to 10-20 times of the produced oil volume. Recently, it started to be common practice to reinject the PW back into the well, when possible. This, as a way to reuse it in the general oil and gas extraction operations. [77,78] Due to the constant threat of leakages from the oil, gas, and PW, which contain high concentrations of highly toxic and hazardous pollutants, that form significant danger to aquatic life, and the environment in general, the handling and discharge of PW created a public concern. Likewise for a relatively new process for the extraction of petrochemical products from soil, called 'fracking'. Over 1000 chemicals are currently being identified by the Environmental Protection Agency (EPA), with 27 chemicals being carcinogenic, or identified as hazardous pollutants impacting drinking water. Continuous efforts are made to fortify the regulations for the extensive treatments of these PWs, whose annual treatment and disposal costs for the industry reach now over 40 billion Euros. [79]

The main characteristics of these PWs are the presence of dissolved and dispersed oil compounds, dissolved formation of minerals, production chemicals, such as biocides, surfactants and corrosion inhibitors, production solids, such as formation solids, corrosion and scale products, bacteria, waxes and asphaltenes, as well as dissolved gases. [80,81]

Later, for the transport of oil and gas, and the transport of almost all other export products from all over the world, ships produce on their turn also polluted cooling water from the engine room, ballast waters when loading and unloading, as well as waters coming from the cargo holds. Ballast waters especially show biological danger



## I. Introduction

in this form of wastewater, as they can be discharged in different regions of the world. Other common practice is the dumping of all kinds of 'domestic' and 'industrial' waste from daily life and maintenance on ships during their long journeys in international waters, to prevent costs for the proper waste disposal when at the harbor. Fortunately, naval transport companies are more and more forced to treat their wastewaters before discharge, for which companies are developing ever more compact and efficient modular designs. [82–84]

These goods are then further transported inland by trucks, mainly powered by diesel oil, a transport mean relatively quick, as demanded more and more by shortening supply chains, but energy inefficient as compared by train or smaller ships. These trucks are thereby often leaking cooling liquids, oil, and grease along their way, produce dangerous exhaust fumes, and fine dust particles coming from their tires and other moving parts, polluting the air and water via clouds and rain. [85]

### ***Recycling industry***

At first instance, the recycling of rest materials, end-of-life products, and waste streams seems an environmentally friendly choice. However, many of these products, e.g., looking at metal and plastics recycling, are stored for longer time on plots of land till logistic and market prices are profitable for further processing. Furthermore, the recycling of paper waste is often paired with heavy metals and cancerogenic compounds from ink, whereas the stream for 'green' or biological waste, containing fruit, vegetable and garden material can contain plastics from tea bags and coffee pads, pesticides from e.g., banana and citrus peels, and non-recyclable plastic bags used for the initial collection in the kitchen container. [86]

Specifically, the recycling of post-consumer plastics waste knows great bias. Depending on the legislation of the countries in the EU, producers of consumer plastics are obliged to 'take back' their products post-consumer use. This already shows complication and confusion at the collection of the nowadays famous yellow bags and containers. Collectors are instructed to take-out and leave behind all other products other than packaging products, as well as different kinds of plastics and product morphologies. Latter contributing the most to the bias, the consumer is oftentimes not aware of the existence of different kind of plastics and polymers, their several additives and material properties, as well as the challenges that come with these differences during the recycle process and polymer recycle use. [87]

The separation and recycling processes for this post-consumer plastics are therefore extremely complicated processes, as conventional separation techniques are mainly based on optics and light diffraction, specific density, and morphology. The former conventional separation technique is especially hard to apply when the cultural and fashion tendencies direct to the preference of food consumption with black colored plastic disposables. During its separation processes, the products need washing, wetting, heating, and pH correction of process waters. All contributing to the necessity of water and its treatment, as well of the removal of the chemical products added during the treatment. Glues used for labelling on plastic bottles severely damages the

polymer chain cohesion in the recyclate, something which can be easily prevented by gluing on the label itself, label shrinking, or even better, the lack of labelling as such. [88]

Due to severe lack of legislation, thought of design, and civil knowledge and obedience in the packaging and recycling cycles, both polymeric and metallic material streams know a leaching similar to the ones at landfills when recycled or abandoned in nature, often not considered when being bought in stores, or even worse, promoted as 'greener', or 'good enough' than the use of virgin material, the choice for other (natural) materials, such as heavier glass, and the use of 'bio' plastics, something which only contributes to the incompatibility of the plastic recyclate pool, and its reuse. [89]

### 2.2. Modern concepts related with water and circular economy

One of the main solutions to lower the water stress, is to reuse the earlier mentioned wastewaters. Herefore it is necessary to (pre)treat the water for further use. One of the main reasons for this necessity is the presence of a variety of pollutions in the wastewaters. [90] These can be present at high concentrations, such as in industrial wastewaters, as also in very low concentration, such as domestic wastewaters, even after the conventional wastewater treatment methods. When so, a term used for these persistent contaminants is 'Contaminants of Emerging Concern' (CECs). [91] An advantage of this necessity for (pre)treatment is the possibility of the integration of an additional, or parallel, treatment step for the recovery of valuable nutrients from these wastewaters. [92,93] A challenge to this solution is the overall readiness of the existing UWWTPs to deliver waters conforming the developing regulations for the minimum quality requirements. [94,95]

#### ***Contaminants of Emerging Concern***

The term of CECs is given to unregulated microcontaminants (MCs) that are present in water in the range of ng/L to µg/L. Although still designated as 'emerging' their presence is known now for longer periods of time. They originate from the previously described UWWs, and their danger lies in acute and chronic toxicity, bioaccumulation, endocrine disruption and irreversible soil pollution and saturation. [96–98]

Although UWWs are being treated in UWWTPs, a high percentage of these MCs is still passing the conventional primary and secondary wastewater treatments methods, demanding the integration of more advanced tertiary treatments. Something that is not self-evident, as many of these methods are still in development, and their actual application stays behind. [99,100]

Also the lack of legislation for MC treatment is of great concern to many parties, though only one country till today, Switzerland, regulates that 80% of MCs present in urban wastewater treatment plant effluent are to be eliminated. [101] As for now, the most commonly practiced tertiary treatment methods for MCs in UWWTP effluents are ozonation, UV light irradiation, filtering over activated carbon, or a combination

## I. Introduction

thereof. Further promising treatment methods can be found in the application of 'Advanced Oxidation Processes' (AOPs). [102,103]

### ***Recovery of valuable nutrients***

Recently, interest in the recovery of valuable nutrients from wastewater streams surged. The term 'fertigation' (the combination of the words 'fertilization' and 'irrigation') emerged to describe irrigation water containing nitrogen compounds such as ammonium, as well as phosphorous compounds such as phosphates, different potassium, calcium, and magnesium compounds. Many of these valuable nutrients can be produced from urine rich wastewaters, but efficient systems and logistics for this production are still missing, or at best at very early state. [104,105] One of the main reasons to produce these nutrients by removing them from the wastewater streams is to decrease the production necessity from other artificial sources. These minerals are often only found in a few deposits around the world, bringing conflicts, unfair exploitation, and severe damage to natural habitats and the environment in general. [104] A part of these valuable resources can also be produced in a less centralized way, using chemical processes. However, these chemical processes for the production of the valuable nutrients consume huge amounts of energy, which significantly contribute to the emission of greenhouse gases, indirectly contributing to the aforementioned problems. Finding ways for the removal of valuable nutrients from wastewater streams, greatly improves the further decentralization of their production, and thereby prevents further problems in the natural surroundings when discharged. [7,106] A large variety of methods can be employed for the recovery of the valuable nutrients from UWW and waste streams coming from the UWW treatment processes, ranging from minerals to fatty acids, thinking about biological methods by employing microorganisms such as bacteria and algae, and physicochemical ways when employing treatments with membranes. [107–110] Although each of these methods have their advantages, they most certainly also bring their challenges.

## **2. Advanced oxidation processes**

### **2.1. Photooxidation processes**

Among the variety of AOPs there is the group of photooxidation processes with photocatalysis as the main mechanism. The photo-Fenton process is one of the main examples. In this photocatalytic process, the production of hydroxyl radicals ( $\cdot\text{OH}$ ) is based on a catalytic cycle of iron ( $\text{Fe}^{3+}$  and  $\text{Fe}^{2+}$ ). The iron complexes during the different stages of the catalytic cycle have the further advantage of being able to absorb light, something which further increases  $\cdot\text{OH}$  production. The  $\cdot\text{OH}$  production cycle is also promoted by hydrogen peroxide and irradiation by UV-vis light and needs only simple chemicals. To make this process renewable, solar radiation can be applied to power the solar photo-Fenton (SPF) process using different types of reactors such as compound parabolic reactors (CPC) or open raceway reactors. [111]

Despite its many advantages, there are also several risks that come with the operation of the photo-Fenton process. These risks can be observed in the handling, the transportation, and the storing of the different reagents, as well as the necessity for further processing of the produced polluted iron sludge. This form of secondary pollution can rapidly account for 35 – 50% of the total operational costs. Further challenges can also be found in the dosing of the reagent,  $\text{H}_2\text{O}_2$ , and the iron, as well as their exact application ratios. These ratios have to be determined empirically and differ to specific MCs, operational parameters, as also the properties of the to be treated matrices. Imbalance in these ratios can result in radical scavenging, recombination of  $\cdot\text{OH}$ , or other products of the catalytic cycle, and increased COD levels. [112]

Another important disadvantage is that the classical photo-Fenton process must be applied at pH 3, in order to prevent the iron from precipitating. There are several solutions to this problem, such as the application of iron oxides, iron immobilization on solid surfaces, iron chelation, or completely replacing the iron with other metal species. One specific solution to the problem of pH induced iron precipitation used in wastewater treatment is to apply iron complexing agents, to maintain the iron in solution at higher pHs. Examples of these iron complexing agents are citric acid, oxalic acid, and nitrilotriacetic acid (NTA). The use of these agents have the further advantage that they have a wider UV-vis wavelength range as compared to other  $\text{Fe}^{3+}$ -water complexes, something which promotes the reduction of ferric to ferrous ions, which results in higher regeneration of  $\cdot\text{OH}$ . The agents also promote the activation of  $\text{H}_2\text{O}_2$  and the generation of  $\cdot\text{OH}$ , while improving the dissolution of iron at circumneutral pH. [113,114]

Ethylenediamine tetra acetic acid (EDTA) is also such a complexing agent, and in the particular case for photo-Fenton in wastewater treatment, a commonly used one. A significant drawback for this chemical is that it is not biodegradable, and nowadays even classified as a persistent pollutant. [114,115]

Another well proven complexing agent of iron for photo-Fenton is Ethylenediamine-N, N'-disuccinic acid (EDDS), being effective at circumneutral pH, till even pH 9. It is thereby biodegradable and non-toxic, making it an environmentally friendly substance. Nowadays, it is even synthesized by biological methods, through fermentation and enzymatic synthesis. [116–118]

### 2.2. Electrochemical oxidation processes

A variety of electrochemical oxidation (EO) processes are applied in wastewater treatment, as they prove to be more efficient for the degradation of contaminants, produce less rest products, and consume less, as compared to chemical and other conventional treatment methods.

## I. Introduction

These methods can be applied solely or combined with the photooxidation processes. One of the most interesting characteristics of these processes is that it not only generates  $\cdot\text{OH}$ , but many different oxidizing species on the anode surface, such as  $\text{ClO}^-$  and  $\text{SO}_4^{\cdot-}$ , depending on the ionic composition and concentration of the matrix during the treatment. In certain cases, the electro cell contains a cathode, which surface produces  $\text{H}_2\text{O}_2$ , that when iron is added, further contributes to the Fenton process. The EO processes are, other than the photooxidation processes, thereby less sensitive to radical scavenging by e.g. bicarbonates. [119]

Different EO processes are anodic oxidation, electro-Fenton (EF), and when applied with photooxidation processes, such as with solar irradiation of the matrix, also solar assisted anodic oxidation (SAAO) and solar photo electro-Fenton (SPEF). Looking at its principles, EO processes show to be especially efficient when treating high saline effluents, as the high concentration of ions in the matrix facilitate an electron flow from the anode to the cathode as a result of the reduction of ohmic resistance, which lowers the required energy for the elimination of MCs. [120] The application of solar irradiation has proven to significantly lower the electrical consumption of beforementioned EO processes and reduces thereby less residual free available chlorine and chlorates, and by helping to remove otherwise persistent photoactive intermediates. [121]

### 2.2.1. The anodic oxidation process

Anodic oxidation (AO) is the application of EO processes using an anode. A current is applied, and an electron transfer occurs, resulting in the degradation of the contaminant in  $\text{CO}_2$  and  $\text{H}_2\text{O}$ . The electrodes anodic activity is depending on the overpotential for oxygen evolution. This is the case with e.g. Pt and boron doped diamond (BDD) electrodes. Recently, the application of BDD anodes showed to be specifically efficient for the application of EO, as  $\cdot\text{OH}$  production for the contaminant's oxidation can take place on its surface, at significantly higher current densities, at minimal oxygen evolution side reaction. There are two MC degradation mechanisms when using AO, direct oxidation, and indirect oxidation. [120,122]

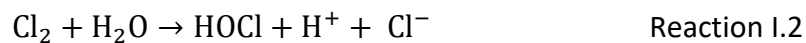
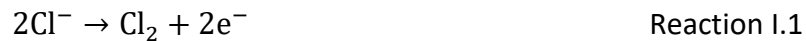
#### ***The direct oxidation process on the surface of the anode***

During EO the adsorption of MCs on the surface of the anode results in their degradation. This goes through an electron transfer from the molecule of the MCs to the anode, without need for an intermediate. The degradation efficiency is relatively low, as the total volume that is in direct contact with the anode surface, is only a fraction. Further limiting factors of this mechanism is related to the electrocatalytic activity of the anode, which is related to the applied electrical potential, which is most of the time also relatively low during the application of EO. [123]

***The indirect oxidation process through oxidants created at the anode surface***

Apart from the EO on the anode surface, there is the formation of oxidant species electrogenerated from precursor compounds. In this way, the degeneration of MCs does not occur directly on the surface, but in the matrix itself. The oxidant species have their origin in two sources, either through the  $\cdot\text{OH}$  cycle of the Fenton process, or through the formation of

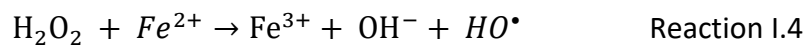
Chlorine, hypochlorous acid and hypochlorite, Reaction I.1 – I.3. [119]



Wherefor at alkaline pH, hypochlorite is the dominant specie, and at acidic pH hypochlorous acid is the dominant species. [124]

## 2.2.2. The electro-Fenton and (solar) photoelectro-Fenton processes

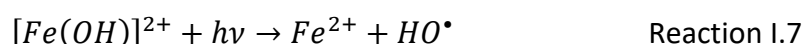
EF follows the same catalytic cycle as with the classic photo-Fenton process. Other than with the classical photo-Fenton process where the iron and  $\text{H}_2\text{O}_2$  reagents are consumed for the formation of  $\cdot\text{OH}$ , and so demanding a constant reagent dosage with a constant formation of  $\text{Fe}^{3+}$  sludge, both reagents can be (re)generated by electroreduction, Reaction I.4 and I.5. Making the classical photo-Fenton reaction unfavorable, as the  $\text{Fe}^{3+}$  sludge needs to be removed and treated after the application of the Fenton process, while its composition is thereby depending on the pH of the matrix. [125,126]



The EF process is ideal for highly saline matrices, which are greatly promoting the conductivity, and that may contain high concentrations of contaminants as well, as their specific EO necessities can be easily controlled by changing the applied current, or the applied potential. Making the overall system for EF easy to automate and monitor.

## I. Introduction

When the consumed iron in this process is regenerated by a UV irradiation source, such as a UV lamp or the Sun, it is called photoelectro-Fenton (PEF) and SPEF, respectively. A further advantage when a cathode is applied during these processes, is the production of  $H_2O_2$ , through the reduction of  $O_2$  gas. The (re)generation of these consumables save on process costs and it thereby avoids risks during transport, storage, and dosage. Reaction I.6 and I.7. [127]



The cathode material, just as the anode material, is an important parameter for the electro generation of  $H_2O_2$ . The commonly used electrode materials are based on carbon, and selected for their high conductivity, low costs, are stable and non-toxic. Furthermore, they demonstrate a high overpotential for  $H_2$  evolution at low catalytic activity for  $H_2O_2$ . Examples for these materials are poly tetra fluor ethylene (PTFE) and graphene. [128]

As can be seen in Reaction 2.6, to produce  $H_2O_2$ , it is important to have a high concentration of  $O_2$  present in the matrix. Therefore, an air chamber is commonly integrated in the EO cell, at the back of the cathode, for a forced  $O_2$  diffusion into the matrix. The name for this type of electrodes are so-called gas-diffusion electrodes (GDE). [129]

There are relatively few studies concerning the application of EF and SPEF on a pilot plant scale, while most of these studies focus on the material science of the electrodes, using only small electrode surfaces and batch volumes. It is therefore, that this work focusses on the treatment of different saline batch volumes of matrices containing MCs, after their preconcentration by nanofiltration (NF), with a parallel recovery of nutrients. This is followed by a comparison between the photo-Fenton processes, based on their relative ionic and bicarbonate content, process parameters, and consumable and energy consumption. [130,131]

### 3. Membranes for water treatment

In the field of water treatment technologies, membrane filtration offers one of the most economic- and energy efficient and promising applications. This is due to a wide variety of controllable physicochemical properties and process parameters, and therefore their wide technical and economic applicability.

### 2.1. Membrane separation

In membrane filtration the main separation mechanism is size exclusion, whereas the system parameters influencing this, and other separation mechanisms, are the system pressure, the trans membrane pressures (TMP), and the temperature. Therefore, being important parameters as well. Further functionality comes from physicochemical properties such as the Donnan-effect, solution-diffusion, as well as the molecular and surface charge, pore size and morphology, and pH. [132,133]

Membranes come in many forms and sizes, such as (spiral-wound or rolled) sheet membranes, single or multi-channel tubular membranes, plate-and-frame membranes, and hollow-fiber membranes. These different morphologies of membranes are commonly selected based on a modular designed system, placing them in series and/or parallel to save space. The specific membrane material built-up on its turn can be either symmetrical or anisotropic. Symmetrical membranes can be subdivided into isotropic microporous membranes, nonporous dense membranes, or electrically charged membranes. Anisotropic membranes can be divided in Loeb-Sourirajan anisotropic membranes, thin-film composite anisotropic membranes, and supported liquid membranes. The characterization and classification of membranes are mainly performed by determining the molecular weight cut-off (MWCO) and the bubble point porosimetry to determine pore size, morphology, and distribution. [133,134]

The separation processes for membranes driven by the difference in pressure in the liquid-liquid phase are mainly based on the type of compounds that are to be retained. The most common application range for membranes lies between 0.1 nm and 100  $\mu\text{m}$ . For this reason, a pretreatment of the following processes can significantly improve the total process costs. The cost price of these relatively simple but efficient water treatment processes is mainly calculated per unit of surface separation and volume, expressed as  $\text{m}^3 \text{m}^{-2} \text{h}^{-1}$ . The filtration process principles can be either dead-end, or the more common crossflow. With the former, the to be treated volume is forced against a membrane wall, forcing the permeate to flow until the rejected matter forms a cake and permeation is no longer possible. The process of this cake formation is called fouling, and once permeation is no longer possible, the cake needs to be removed before further operation is possible. [135]

### 2.2. Membrane systems

One of the oldest and most applied pressure driven filtration methods is microfiltration (MF). It has the largest pore size of the different membrane systems with a working range between 0.1 and 10  $\mu\text{m}$  and is good to retain bacteria, suspended solids, fine solids, and yeast cells, therefore reducing the COD and the total organic carbon (TOC). The membranes are relatively inexpensive and easy to apply, replace and maintain, and fouling can easily be reversed by back washing. MF membranes are produced from both polymeric, ceramic, and composite materials, whereas polymeric and ceramic MF membranes are generally used in UWW



## I. Introduction

treatment. As the main pore size of MF is larger than ultrafiltration (UF) and other membrane systems, the permeate flux is therefore also higher, and works with 0.2 - 5 bar at lower TMPs, though significantly reducing of fouling in the membrane systems having smaller pore sizes is obtained. [133,136,137]

UF is a membrane system with a working range of 0.01  $\mu\text{m}$  till 0.1  $\mu\text{m}$  in pore size and offers better selectivity than MF. Its TMP is operated between 1 – 10 bar, and depending on the pore size, these membranes are able to retain most bacteria and viruses, emulsions, suspended solids, colloids, natural organic matter (NOM), a selection of metal ions, and some of the larger MCs. UF finds its application mainly in the beverage processing, dairy, pharmaceutical industries, and is extensively used in the production of potable water and the treatment of UWW. [133,138,139]

From all classes of filtration based on pore size, NF is the most efficient for the treatment of potable water, as it retains almost everything up from pharmaceuticals, disinfection by-products, biological compounds such as sugars and polyphenols, inorganics, surfactants and solvents, dyes, up to a large variety of salts and the larger ions. Its working range is between 0.001  $\mu\text{m}$  and 0.010  $\mu\text{m}$ , at a TMP of 5 – 10 bar, and compared with reverse osmosis (RO) and forward osmosis (FO), has significantly lower operating and maintenance costs and is thereby less sensitive to fouling. [133,140,141]

Two of the most efficient water filtration processes regarding purity are the RO and FO membrane systems. Their working range starts already from 0.0001  $\mu\text{m}$ , with TMPs between 15 – 27 bar during brackish water desalination, and 50 – 80 bar during seawater desalination. These processes are able to retain minerals, salts, and metal ions. RO is the process of forcing liquid through a semipermeable membrane at very high pressures. FO is basically the same process, but this time directed towards the membrane as a dead end, producing clean water till severe fouling of the membrane prohibits the migration of the water molecules through the membrane. One of the problems of FO is the regeneration of the draw solution, which can be solved by combining it into a hybrid system with membrane distillation (MD). Other hybrid systems for treating the concentrates of RO and FO, and pretreatments with UF and NF, greatly enhance the process to circular economies and urban sustainability. [142–145]

Both osmosis filtration processes are extremely energy demanding as they work at very high pressures, and are thereby very sensitive to fouling, creating the necessity for already relatively clean influents or pretreatments. Apart from that, in the application of potable water production and irrigation activities, the addition of minerals after the treatment is necessary, as a lack of ions come along with a lack of taste and results in osmotic pressure on crops. In extreme cases, overconsumption of osmosis produced water without sufficient minerals can potentially drain these from the human body resulting in medical problems. [143,146,147]

MD is a membrane system that utilizes heat for vapor permeation through a hydrophobic membrane, which is based on the principle of the vapor pressure between its surfaces. MD uses a low pressure and has relatively low fouling rates when compared to the beforementioned high pressure membrane systems. Challenges to solve for this membrane system are mainly membrane wetting and fouling, both organic and inorganic. [148,149]

The hybridization of MD and the membrane bioreactor (MBR) makes it possible to deplete the concentrate of the anaerobic digester in order to produce a precipitation product, which can be utilized as a biofertilizer. Another product that can be produced in this way from UWW is struvite. [150]

### 2.3. Membrane materials

There are three main membrane materials used, polymeric, ceramic, and composite materials. Each having their outstanding advantages and disadvantages. [151]

**Polymeric membranes**, are characterized by their low costs and ease of application. The production of polymeric membranes can be performed by either stretching or as expanded film, melt extrusion, solution casting, phase precipitation, or also called phase inversion, template leaching, or sintering and annealing, in the case of isotropic membranes. Phase inversion is the most utilized method for the described membrane separation processes using polymeric membranes, especially considering anisotropic are the commonly used polymeric membranes. Anisotropic membranes are produced by means of template leaching or phase inversion by using different mechanisms controlling water and solvent concentrations, using cooling and heating for the precipitation mechanisms during the different production steps, as well as different chemical treatment steps. Further production methods are also dynamic formation, plasma polymerization, and selective reactive surface treatment. The anti-fouling treatments of polymeric membranes is mainly performed by backwashing and limited chemical treatment. Due to their low price, they are often simply replaced instead of applying extensive or frequent antifouling treatments. [152]

**Ceramic membranes**, are mainly used in the chemical industry, industrial wastewaters such as in the petrol, food, and metal industries. Although more expensive, ceramic membranes offer higher durability, have more temperature and pressure resistance, and have thereby also a wider pH application range. The production cost of these ceramic membranes is three to five times higher than polymeric membranes, as their production method consist out of multiple, energetically extensive steps. The different production methods consist out of the compounding of different ceramic materials, usually metal oxides, based on composition and size, most often with polymeric additives for binding and viscosity, to form a slip. This slip is than pressed, cast or extruded, and air dried to so called 'greens', before further thermal treatments are applied. These thermal treatments include pyrolysis of the greens and sintering of dip-coat layers. Other production methods also include anodic oxidation, chemical vapor deposition, hydrothermal treatment, and sol-gel synthesis. The fouling of ceramic

## I. Introduction

membranes can be reversed by backwashing, chemical treatment using strong acidic or basic chemicals, or by incineration of the fouling layer in an oven or furnace. The fouling of ceramic membranes can be reversed by backwashing, chemical treatment using strong acidic or basic chemicals, or by incineration of the fouling layer in an oven or furnace. [153,154]

The third membrane material is a combination of the former two, consisting out of two or more materials and layers, and are called **composite membranes**. The difference in material characteristics can provide a very specific solution to the treatment problem as related to the process parameters. An example of composite membranes can be a tubular ceramic membrane, or support, coated by so called dip-coating with a second ceramic membrane layer, that on its turn supports a polymeric membrane produced with the sol-gel method. Another example is the Layer-by-layer assembly of NF composite polymeric membranes. Backwashing and chemical treatments are mainly used for the removal of fouling in composite membranes. [155,156]

The use of engineered nanomaterials in UWW treatment is considered safe, as exposure to the human body is considered minimal. A vast growing number of research laboratories have analytical techniques available to quantify the presence of these nanomaterials in water and other systems. The different engineered nanomaterials of polymeric or ceramic origin greatly enhance the production possibilities of membranes in the nanofiltration range, when used solely or as composite. These nanomaterials possess thereby excellent (photo-)catalytic properties. [157]

### 2.4. Membrane fouling

The process of fouling of the membrane surface has many definitions. There are a wide variety of fouling mechanisms in membrane filtration processes that can be characterized by reversible and irreversible fouling, physical fouling in the form of a 'cake' formation consisting out of the retained particles and solids, chemical fouling by the deposition of salts, also called scaling, and other chemical compounds on the membrane surface from the matrix as function of time, supersaturation, or pH value. Another fouling mechanism is biological fouling, where bacteria form an extra-cellular polymeric substance (EPS) layer between themselves on the membrane surface, eventually blocking the pores of the membrane. [158,159]

There are two main processes for the anti-fouling treatment of membranes, backwashing, and chemical treatment. Backwashing is the process of reversing the flow direction of the permeate and concentrate through the membrane, to remove the build-up of particles and solids on the membrane surface. The small and highly polluted volume is then often disposed of, and the flow direction restored to continue the filtration process. The effectiveness of this anti-fouling treatment gets less

effective over time, as the irreversible fouling increases as well, which on its turn promotes the reversible fouling. The second process is a chemical anti-fouling treatment. During this treatment, the pH value is drastically changed to strongly acidic and basic. Commonly, first an acidic pH is applied on the membrane followed by neutralization. After this neutralization, a basic pH is applied, with another neutralization. The frequency of this cycle, as well as its sequence is highly dependent on the membrane's resistance to the extremes of this pH treatment. For polymeric membranes pH ranges lies between pH 3 – 10, with maximums of pH 2 – 11. Ceramic membranes have a wider pH range, often from pH 1- 14, due to their relatively inert nature, regarding this anti-fouling treatment. Once the chemical anti-fouling treatment also offers insufficient recovery of the flux, a third thermal treatment can be applied, before the necessity of replacing the membrane. This third option, only for ceramic and a selection of ceramic composite membranes, depending on their respective thermal expansion coefficient and degradation point, is incineration. Here the membranes are removed from the system and placed in an oven or furnace to burn away the fouling material on the membrane surface, as well as in the pores. [152,153,160]

Recently, the merging of a fourth type of anti-fouling treatment can be found in so called self-cleaning membrane surfaces. These membrane surfaces contain a thermo- or photocatalytic layer, creating radicals that prevent or reverse fouling to a certain extend. [161,162]

### 2.5. Prevention of fouling

Different fouling reversal mechanisms have to be applied during the membrane operation to guarantee the practical and economic viability of membranes. So-called 'back-wash' cycles are the main fouling reversal mechanism and is a process where the flow direction is reversed for a pre-determined period of time. Treatments using an acidic and/or basic medium for fouling prevention and reversal are often limited, as is foremost the case with polymeric membranes, which are known to be sensitive to extreme pH values by compromising their structural and chemical integrity. The application of this acid/base treatment is thereby only effective against reversible fouling, while membrane operation must be interrupted, and costs for the chemicals are to be considered. Ceramic membranes have the advantage that fouling can be reversed by the application of high temperature to incinerate the fouling layer. [158,163]

The emerging of novel fouling mechanisms can be found in systems utilizing super-hydrophilic and super-hydrophobic membrane surfaces, membrane pore design and development, as well as the pore morphology and density, sometimes even in the form of biomimicry and bioinspiration. [164–166]

An example of this are Janus membranes, after the two-faced Roman god, which are based on the application of subsequent membrane layers possessing opposite properties, such as hydrophilicity and hydrophobicity, chemical activity, pore size and/or structure, electrical and/or thermal conductivity, and wettability. Such

## I. Introduction

opposing properties offer a good preselection of compounds already on the membrane surface and thereby significantly increases the membrane separation efficiency. [167,168]

### 2.6. AOPs application as fouling prevention

Different AOPs can be utilized as a means to prevent fouling on membranes, and this combination of technologies can also be called Advanced Integrated Technology (AIT). Commonly used in wastewater treatment, ozonation can be applied both as pre- and post-treatment, and even in-situ. Hybrid systems using ozonation combined with polymeric membranes are not advised, as the majority of commercial polymeric membranes are degraded by the generated radicals. This is not a problem when combined with activated carbon or ceramic membranes and is therefore commonly used in UWW treatment. [169]

Photocatalytic membranes are a direct combination of AOP application with the membrane material, where membrane materials such as  $\text{TiO}_2$ ,  $\text{ZnO}$ , and  $\text{ZrO}_2$  on the membrane surface are producing radicals. As these materials are part of the membrane surface, and therefore immobilized photocatalytic material, they show to have a substantial lower number of active sites in comparison with suspended photocatalytic particles. Nonetheless, extended operation times are obtained when photocatalytic materials are applied in membranes to prevent fouling.  $\text{TiO}_2$  for example, is not only photocatalytic active, but it also possesses photo-induced super-hydrophilicity (PSH) under light irradiation. [170–172]

Other novel applications can be found in complex membrane systems that use photocatalytic membranes with aeration and oscillation. These systems are however still to be tested in real-life practical applications. [173]

## 4. Advanced integrated technologies and nutrient recovery in UWW treatment

Although many of the beforementioned technologies provide economically viable results and promising practical applications on their own, the combination of the different available technologies show even higher economic and practical efficiencies. Process efficiencies can be raised by applying different pretreatment methods, which include preconcentration of MCs while in parallel valuable nutrients are recovered in a direct way from the treated wastewater streams. [174] Great examples for this are the so-called membrane-based hybrid technologies, which utilize the combination of the different membrane systems with various AOPs as polishing treatments, along with nutrient recovery systems. [175,176]

A treatment train of different membrane systems to reach the full crystallization of brines, concentrates, such as reverse osmosis concentrates (ROC), industrial waters, and saline waters through the application of electrodialysis (ED), electrodialysis reversal (EDR), MD, membrane crystallization (MCR) are the base of the minimum-

liquid discharge (MLD) and zero-liquid discharge (ZLD) principles. The crystals coming from these processes can then be refined and processed into sustainable sourced nutrients, acids and bases, metals, minerals, and other salt compounds. These AITs are therefore greatly contributing to the circular economy and significantly reducing waste production. [177–179]

Different popular AITs combining membranes with in UWW treatment are for example the anaerobic membrane bioreactor (AnMBR), as well as the aerobic membrane bioreactor (aMBR), which are often combined. [180] The advantage of this system is that it produces biogases, such as CO, CO<sub>2</sub>, CH<sub>4</sub> and H<sub>2</sub>, which on its turn can be utilized for energy production, and so, not only removing nutrients from the UWWs, but can also lower its necessary energy consumption. Recently, significant interest into the P-to-X principle grew due to the current geo-political situation, for which this biogas is essential. [181–183]

Another microbiological AIT example is the application of algae, which include cyanobacteria, microalgae, and macroalgae, for the recovery of nutrients from wastewaters, and is called phycoremediation. [184] Algae contain a wide variety of biochemical compounds, such as enzymes, minerals, pigments, proteins

The process is characterized by the continuous feed of secondary UWW effluent into a high rate algal pond (HRAP), a raceway like reactor with a partition wall in the middle and a paddle wheel to create a current and turbulence to guarantee sufficient mixing of the algae. This is important in order to have repeated light irradiation, prevents sedimentation of the algae, the formation of algal/bacterial flocs, and nutrient diffusion. Parameters that are important in this system are the organic nutrient loading rate, the hydraulic retention time (HRT), flow rate, the pond depth, CO<sub>2</sub> supply, and pH value. Further importance should be given to the length to width ratio and optimized flow rate in order to prevent dead zones, as well dark zones next to the side- and partition walls. Once the HRT is obtained, the algae are harvested by concentrating the effluent stream through a DAF, and could be further concentrated by disc stack separator, or similar principles. The cultivated microalgae can later be processed from which biofuels, feeds, pigment, and biochar can be produced. [185]

The microalgae produced in the HRAP form a symbiosis with bacteria which produce CO<sub>2</sub> necessary for the growth of the microalgae that produce O<sub>2</sub>, necessary for the bacteria. Other symbioses are related to the reduction in NH<sub>4</sub><sup>+</sup>-N stress which promotes both microalgal lipid accumulation and growth, and the ability of bioflocculation by EPS production. These microalgal-bacterial symbiotic (MBS) systems can be divided in three categories based on the living state of the microalgae and bacteria: attached microalgal-bacterial (AMB), bioflocculated microalgal-bacterial (BMB) and free microalgal-bacterial (FMB) systems. Whereas the AMB system is preferred for UWW treatment. This technology can thereby be utilized after the AnMBR for even higher treatment and process efficiency. [50,186]

## I. Introduction

New developments can also be found in the previously mentioned HRAPs, this time not used for microalgae growth, but as a regular raceway pond reactor (RPR) for the tertiary treatment application of UWWTP effluents by SPF for disinfection and MC degradation. [187] The goal of the combination of these technologies is to improve the economic feasibility of the SPF AOP by decreasing the costs that the CPC reactors bring with it. Having thereby the advantage that the liquid depth can be changed during operation, as function of the natural solar irradiation and/or the turbidity, guaranteeing the availability of sufficient photons on the bottom of the pond. Something that cannot be done with the diameter of the CPC tubes. [188] The latest successful example of such AITs consisting out of the combined application of RPRs and AOPs can be found in a solar electrochemical raceway pond reactor (SEC-RPR), where an electrochemical filter press-cell is combined with an RPR, for the on-site electro generation of  $H_2O_2$ . Something that is advantage to transport and storage safety of latter, as well as the economic costs. The AIT shows the synergetic effects of the solar irradiation with the electro, improved dispersion of the on-site generated  $H_2O_2$  into the systems by combining them. [189] Challenges in RPR technologies lie in the necessary space, sensitivity of weather influences such as rain and evaporation, and the exposure of the matrix, which can contain harmful compounds, to the direct environment.

Further integrated technologies for the recovery of nutrients that use membrane separation processes are those that aim to produce fertilizers. [190]

One of the main sources for phosphorus can be found in urine, both from human and agricultural sources. Developing efficient systems in this promising technology can be an inexpensive and sustainable source. The actual recovery of this compound can be found through the way of struvite formation and harvesting. [191]

Despite the fact that the adaptation of AOPs and the number of AITs are growing, the real-life application of combined integrated technologies is lagging behind and is still considered to be a challenge, making the world miss out on their synergetic effects.

### **5. Future perspectives related to the main goal of this Ph.D.**

To obtain the goal of MC removal from UWWs by beforementioned technologies such as NF and its implementation into conventional UWW treatment systems, a contribution will have to be made by the mapping of the influence of several physicochemical properties of the selected MCs, such as the salinity of the matrix, the membrane surface and ionic composition. This, especially at pH values that are circumneutral, as this is the range of the majority of UWWs and with NF retentates at realistic concentration factors and MC concentrations. Different operational parameters within AOPs, such as SPF, will have to be compared in order to map the degradation mechanisms of the MCs, such as oxidation agent selectivity, as also the influence of different ratios and concentrations of the iron:EDDS complex.

The complex ionic compositions of UWWs are a great potential source for the recovery of valuable resources, and selective ion retention by NF, can therefore create MC free, ion enriched matrices for combined irrigation and fertilization, or fertigation. Thereby, to increase the applicability of SPF processes, combination with AOPs such as EO is relatively unknown and therefore to be researched. Due to the highly saline nature of NF concentrates, EO processes are good options for their treatment and have already shown great potential. However, relatively little is known about their individual efficiency differences on MC degradation when treating UWWs, or the effects when combined with SPF. An important parameter to the success of these combined AOPs into AITs, is their final toxicity. The toxicity determination of the treated matrices are key to their application of irrigation waters.

The development and application of low-cost, easy to apply, and self-cleaning membranes, such as ceramic UF membranes, can greatly contribute to (drinking)water safety and water security in areas with lower developed infrastructure for the treatment of UWW. The combination of AOPs combined with this novel type of membranes could strongly increase its synergetic effects, by prolonging operation times and anti-bacterial properties, while significantly lowering turbidity and bacterial load, all than not, prior to SPF treatment.



## I. Introduction

## Chapter II. Objectives and Experimental Plan

## II. Objectives and Experimental Plan

### 1. Objectives

This PhD thesis has the application of the combination of different Advanced Integrated Technologies (AITs), such as membranes, solar photooxidation and electrooxidation processes, to remove MCs from UWWs, as general objective. Prior to this removal, preconcentration of the components of a variety of water matrices by UF and NF was performed, partly with the parallel recovery of valuable nutrients from saline matrices for direct crop irrigation purposes. Furthermore, the development and assessment of novel photocatalytic self-cleaning membranes was also intended.

This general objective was subdivided in several proposed targets, that were developed in the scientific papers that compound this PhD thesis, for successful achievement:

**Target 1.** Determination of optimal operational parameters, concentration factors and retention mechanisms of MCs, for the preconcentration of saline waters by NF treatment, utilizing a pilot plant based on NF membranes. Followed by the assessment of oxidizing agents' effectiveness, iron concentration and EDDS complex ratios during solar photo-Fenton treatment of the different concentrate and permeate volumes, at different pHs.

**Target 2.** Recovery of valuable nutrients such as ammonium from saline waters during their preconcentration for the retention of MCs, with the aim to produce enriched crop irrigation waters for direct use. Followed by the application and assessment of different AOPs treatment methods for MC removal from the concentrate volumes, and a toxicity assessment of the permeate volumes.

**Target 3.** Development of novel self-cleaning photocatalytic membranes. The assessment of the fouling and self-cleaning capabilities by the registration of flux restoration during the filtration of real urban wastewaters, followed by membranes material evaluation, before and after solar irradiation. The quantification and effects of water turbidity reduction for the application of subsequent treatments were assessed. Quantification of the bacterial present in water retention by the newly developed photocatalytic membrane.

### 2. Experimental plan

The following tasks were assigned and completed based on the previously described target propositions, to guarantee their successful achievement.

#### **Task 1. MC retention determination by commercial polyamide NF membranes in a pilot plant, based on differences in operational parameters such as pressure, flow and physicochemical properties of MC and matrices for solar photo-Fenton tertiary treatment.**

##### 1.1. MC selection from lists of CECs and the development of a UPLC method

Representative MCs from different classes such as pharmaceuticals, technical chemicals, pesticides, and psycho-active drugs were chosen from lists of CECs coming from the EU and the AQUALity project consortium (H2020-MSCA-ITN-2017. European Innovative Training Network “Interdisciplinary cross-sectoral approach to effectively address the removal of contaminants of emerging concern from water”, Grant number 765860.), based on their persistence, danger to natural life, production and consumption quantities, and treatability by conventional wastewater treatment methods. A UPLC method was developed for the individual compound identification, guaranteeing their quantification till very low concentrations (5 µg/L) in complex saline composed matrices at a wide range of pH values.

##### 1.2. Mapping of the effects of the initial salinity concentration and the effects of ionic composition in demineralized and natural water on the operational parameters

Matrix preparation by using demineralized and natural water at different ratios, attaining an initial concentration of 3, 5 or 7 g/L of NaCl and 100 µg/L of each MC (caffeine (CAF), imidacloprid (IMI), thiacloprid (THI), carbamazepine (CAR) and diclofenac (DIC)), while operating the system at pressures of 5, 7 and 10 bars. Decision making based on the MC retention, flow, TMP and probability of real-life applications.

##### 1.3. Optimization of the solar photo-Fenton process parameters for the concentrate and permeate streams

After mapping and evaluating the effects of salinity and physicochemical properties of MCs towards retention of MCs in NF treatment, the different concentrate and permeate streams were treated by the solar photo-Fenton process on a lab scale. This, to determine the optimal process parameters for the specific salinity and ionic matrix composition, such as iron concentration at both pH 3 and circumneutral pH, as well as the influence of the iron:EDDS complex ratio at circumneutral pH. Furthermore, the sensitivity of the selected MCs towards different radical species, and the effects of radical scavengers were determined and evaluated, by comparing  $S_2O_8^{2-}$  and  $H_2O_2$  oxidizing agents. Once completed, the solar photo-Fenton process was then upscaled to the larger CPC reactors pilot plant and compared with the labs scale results.

## II. Objectives and Experimental Plan

### **Task 2. Recovery of valuable nutrients from saline water matrices and determination of different toxicity parameters of different enriched permeate volumes after ammonium recovery by the NF treatment of saline matrices.**

#### 2.1. Determination of the optimal parameters, such as pH, initial concentration, and salt concentration, for the recovery of ammonium from saline matrices by NF

Experiments were performed at pH 4, 7 and 9, with initial concentrations of  $\text{NH}_4^+$  of 250 and 500 mg/L in demineralized and natural water, utilizing the commercial polyamide membranes of the NF pilot plant at the PSA. Filtration experiments were performed till concentration factor (CF)= 2 and 4. A continuation was made with the addition of the previously selected MCs at a concentration of 100  $\mu\text{g/L}$  of each (CAF, IMI, THI, CAR and DIC), to determine the effects of the MCs on the  $\text{NH}_4^+$  permeation and vice versa. Next step was evaluation of the conductivity as a parameter of the permeation of  $\text{NH}_4^+$ , here an addition of 5 and 10 g/L NaCl was applied to obtain increased conductivity.

#### 2.2. Performance of phytotoxicity, acute and chronic toxicity tests

Phytotoxicity tests were performed by applying the enriched permeate streams to the seeds of three different plant species, *Sinapis alba*, *Sorghum saccharatum* and *Lepidium sativum*, following the instructions of the test kits. The rate of germination, sprouting and rooting provided a quantitative overview of toxicity for the specific plant species, of the specific permeate.

### **Task 3. Comparison of solar photo-Fenton treatment at lab and pilot plant scale of concentrate streams obtained after the application of NF treatment, at a low and a high concentration factor.**

The solar photo-Fenton process was applied on the different concentrate and permeate streams at a lab scale, applying the previously determined optimal process parameters for different saline matrices. A viability evaluation of the solar photo-Fenton process, mainly related to the stability of the iron:EDDS complex was necessary. Parallel to this, the effects of  $\text{NH}_4^+$  on radical formation, scavenging and stability was assessed by comparing  $\text{S}_2\text{O}_8^{2-}$  and  $\text{H}_2\text{O}_2$  as oxidizing agents. A scale up to pilot plant level was executed in a CPC reactor, using natural solar irradiation. Results between the lab and pilot plant scale were then evaluated.

### **Task 4. Assessment of the combined application of different electrooxidation and photooxidation treatments on highly saline NF concentrates after ammonium recovery.**

#### 4.1. Determination of efficacy of the individual EO processes using the iron:EDDS complex

A set of experiments was performed using a BDD anode, to perform AO and EF. Further observations of the synergy of combined EO and solar irradiation were performed. The effects of the different parameters were then evaluated and compared with solar photo-Fenton process.

### **Task 5. Comparison of self-cleaning capabilities of novel photo catalytic UF membrane.**

#### 5.1. Manufacturing of the novel self-cleaning photocatalytic TiO<sub>2</sub>-ZrO<sub>2</sub> UF membrane using a TiO<sub>2</sub> wash coat

The addition of a TiO<sub>2</sub> photocatalytic layer to a ZrO<sub>2</sub> membrane developed in previous work in collaboration with University of Turin, LiqTech Ceramics A/S and Aalborg University (partners of AQUAlity project) and not included in this thesis (Development of a photocatalytic zirconia-titania ultrafiltration membrane with anti-fouling and self-cleaning properties. *J. Environ. Chem. Eng.*, 9, 106671, 2021) was investigated. The application of the TiO<sub>2</sub> layer was performed by the use of so-called wash coats. These wash coats consisted out of TiO<sub>2</sub> nanoparticles in suspension in a chemical liquid mixture.

#### 5.2. Assessment of the self-cleaning capabilities of the UF membrane when using high volumes of UWW

The developed TiO<sub>2</sub>-ZrO<sub>2</sub> UF membrane was used to filter high volumes of UWWTP effluents from the EDAR 'El Bobar' in Almería, Spain, to induce severe fouling. A reversal of this fouling was then assessed by applying solar irradiation. Further determination of the optimal solar irradiation cleaning cycle was then investigated by irradiating the fouled membranes for different quantities of time, as function of the restored flux.

#### 5.3. SEM and EDX analysis of the membrane surface before and after severe fouling

To confirm the reversal of the fouling after solar irradiation, scanning electron microscopy (SEM) images were taken, along with Energy-dispersive X-ray spectroscopy (EDX) analyses, to confirm the removal of the fouling layer.

## II. Objectives and Experimental Plan

### 5.4. Assessment of solar photo-Fenton treatment at lab scale of the concentrate and permeate volumes

Produced concentrate and permeate volumes were treated with the solar photo-Fenton process, using the previously determined optimal parameters, in the solar simulator at lab scale.

### 5.5. Assessment of bacteria retention of the developed novel photocatalytic membrane

To determine the applicability of the UF membrane in disinfection, an assessment of the retention of the bacteria *P. Aeruginosa* was performed. The batch reactor set-up was prepared with natural water (Tabernas, Spain), and an initial concentration of  $1 \cdot 10^6$  CFU/ml of *P. Aeruginosa*.

## II. Objectives and Experimental Plan



## Chapter III. Materials and Methods



### III. Materials and Methods

#### 1. Chemicals

Throughout this work a selection of chemicals, reagents, and microorganisms have been used to conduct a wide variety of experiments. This selection on its turn was monitored by different advanced analysis methods mainly developed for water analysis of complex matrices, all taking place at the research facility of the 'Solar Treatment of Water' (Spanish language: TSA) unit of the Centro de Investigaciones Energéticas, Medioambientales y Tecnológicas – Plataforma Solar de Almería (CIEMAT - PSA; English language: Center for Energy-, Environmental-, and Technology Research - Solar Platform of Almería) located at Tabernas, Andalusia, Spain. The chemicals were delivered by Merck- Sigma Aldrich, Germany, unless otherwise designated.

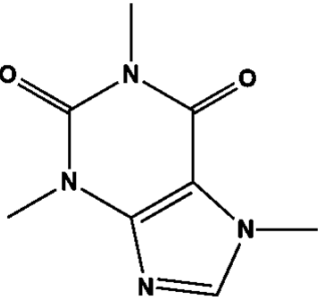
##### 2.1. Organic microcontaminants

In this study a selected variety of MCs were applied as target compounds based on their wide and global use, are characterized by poor biodegradability, and thereby possess a high biotoxicity. These target compounds, namely caffeine (CAF), Imidacloprid (IMI), Thiocloprid (THI), Carbamazepine (CAR), and Diclofenac (DIC), have been selected as a representative member of their chemical group. They thereby come from a list of preselected MCs selected by the AQUAlity project [192], which is based on a European database of CECs.

The selection of MCs chosen for this work is commonly found in UWWTP effluents in concentrations ranging from ng till  $\mu\text{g/L}$ , which make them particularly fit as target compounds.

In the used water matrixes for this work, different concentrations of these compounds have been spiked. An overview of some physicochemical parameters of these MCs can be found in Table III.1.

**Table III.1:** Characteristics of selected microcontaminants

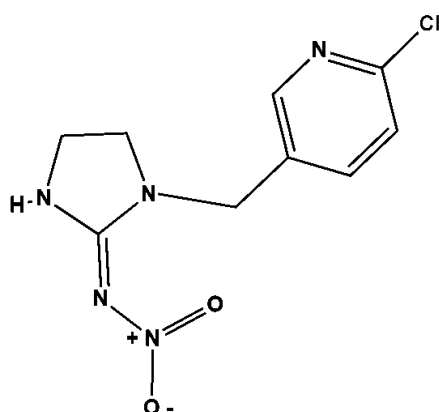
<b>Caffeine</b>	
	
<b>IUPAC ID</b>	1,3,7-Trimethylpurine-2,6-dione
<b>CAS number</b>	58-08-2
<b>Linear formula</b>	C <sub>8</sub> H <sub>10</sub> N <sub>4</sub> O <sub>2</sub>
<b>Molecular weight [g/mol]</b>	194.2
<b>Solubility in water [mg/L]</b>	21,700.0
<b>Class</b>	Psycho-active drug

### III. Materials and Methods

---

#### Imidacloprid

---



---

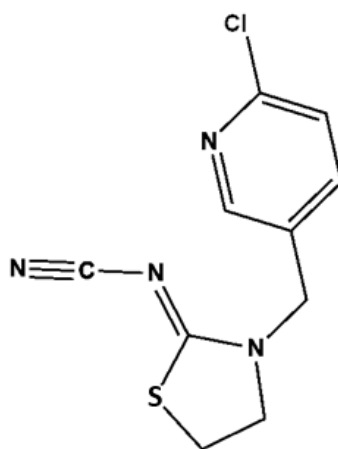
<b>IUPAC ID</b>	N-{1-[(6-Chloro-3-pyridyl)methyl]-4,5-dihydroimidazol-2-yl}nitramide
<b>CAS number</b>	138261-41-3
<b>Linear formula</b>	C <sub>9</sub> H <sub>10</sub> ClN <sub>5</sub> O <sub>2</sub>
<b>Molecular weight [g/mol]</b>	259.7
<b>Solubility in water [mg/L]</b>	610.0
<b>Class</b>	Insecticide

---

---

**Thiacloprid**

---



---

<b>UPAC ID</b>	[(2Z)-3-[(6-Chloropyridin-3-yl)methyl]-1,3-thiazolidin-2-ylidene]cyanamide
<b>CAS number</b>	111988-49-9
<b>Linear formula</b>	C <sub>10</sub> H <sub>9</sub> ClN <sub>4</sub> S
<b>Molecular weight [g/mol]</b>	252.7
<b>Solubility in water [mg/L]</b>	125.0
<b>Class</b>	Pesticide

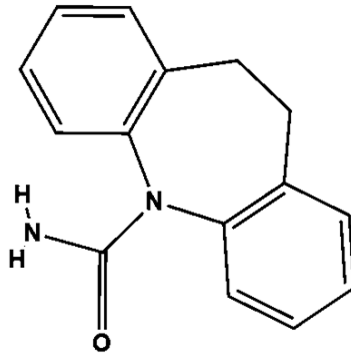
---

### III. Materials and Methods

---

#### Carbamazepine

---



---

<b>IUPAC ID</b>	5H-dibenzo[b,f]azepine-5-carboxamide
-----------------	--------------------------------------

---

<b>CAS number</b>	98-46-4
-------------------	---------

---

<b>Linear formula</b>	C <sub>15</sub> H <sub>12</sub> N <sub>2</sub> O
-----------------------	--

---

<b>Molecular weight [g/mol]</b>	236.27
---------------------------------	--------

---

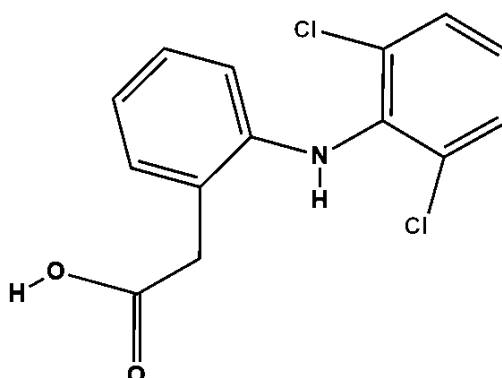
<b>Solubility in water [mg/L]</b>	17,7
-----------------------------------	------

---

<b>Class</b>	Anti-convulsant drug
--------------	----------------------

---

## Diclofenac



<b>IUPAC ID</b>	2-[2-(2,6-dichloroanilino)phenyl]acetic acid
<b>CAS number</b>	15307-86-5
<b>Linear formula</b>	C <sub>14</sub> H <sub>11</sub> Cl <sub>2</sub> NO <sub>2</sub>
<b>Molecular weight [g/mol]</b>	318.1
<b>Solubility in water [mg/L]</b>	2.4
<b>Class</b>	Non-steroidal anti-inflammatory drug

Prior to every series of experiments, a mixture of the previously mentioned MCs was prepared by predissolving them in the form of a so-called 'mother solution' (2.5 g/L each MC). This was performed by adding 250 mg of each MC into a 100 mL volumetric flask and filling it off with methanol. This method of predissolving the MCs in this specific type of solvent ensures a high solubility, while at the same time a low concentration of TOC is maintained. As it is otherwise impossible to dissolve MCs with low solubility efficiently and rapidly in water, through this method 100% dissolving is attained. Previous tests indicated also that it was not possible to dissolve several MCs in methanol at a concentration of >2.5 g/L of each MC. In any case, final TOC attained in treated water was always within the usual TOC found in UWWTP effluents.

## 2.2. Reagents

The main used reagents in this work were dissolvents and oxidizing agents. Acetonitrile was used as a solvent to dissolve the different organic microcontaminants, and in the case of the UPLC, acetonitrile was thereby also used as the mobile phase. The acetonitrile came from Sigma Aldrich, Germany, and was of analytical grade. Furthermore, ammonium sulfate was also used as a solvent, mainly for the UPLC as a mobile phase. The ammonium sulfate came from Sigma Aldrich, Germany and was also of analytical grade. The EDDS, the biodegradable complexing



### III. Materials and Methods

agent used in this work, was provided by Sigma Aldrich, Germany, and was used as provided. Another UPLC mobile phase, formic acid, was of analytical grade and provided by Sigma Aldrich, Germany. hydrogen peroxide (oxidizing agent), methanol (solvent). The alternative oxidizing agent used in this work, came as the precursor agent in the form of sodium persulfate, and was provided by Sigma Aldrich, Germany.

#### 2.3. Water matrices

A variety of water matrices has been used during the different experiments, ranging from ultrapure water, demineralized water, natural water and UWWTP effluents, depending on the specific experimental parameters and matrix properties.

#### Ultrapure water

The ultrapure water used in this work was produced by utilizing an ultrapure water system from Milli-Q (Merck Millipore), fed by demineralized water. The conductivity of this water was below 0.054  $\mu\text{S}/\text{cm}$  and a COD of <0.3 mg/L.

#### Demineralized water

At the PSA, an industrial plant (based on reverse osmosis and electro dialysis, in series) designated for the supply of demineralized water to the whole installation produces demineralized water with a conductivity <1  $\mu\text{S}/\text{cm}$ , a concentration of chlorides 0.7–0.8 mg/L, nitrates 0.5 mg/L and <0.5 mg/L of organic carbon. Conductivity was usually higher (<10  $\mu\text{S}/\text{cm}$ ), due to storage and transport before use in the experiments.

#### Natural water

On the terrain of the PSA, a well supplies natural water. The water characteristics show high hardness and ionic concentrations. An overview of the characteristics of this water is given in Table III.2.

**Table III.2:** Overview of the natural water characteristics at the PSA

Natural water (Tabernas, Spain)			
Cations	[mg/L]	Anions	[mg/L]
Ca <sup>2+</sup>	83.5	SO <sub>4</sub> <sup>2+</sup>	237.7
Mg <sup>2+</sup>	66.5	Cl <sup>-</sup>	376.7
K <sup>+</sup>	8.0	NO <sub>3</sub> <sup>-</sup>	20.7

<b>Na<sup>+</sup></b>	433.0
<b>Conductivity [mS/cm]</b>	2.7
<b>pH</b>	7.5
<b>TC [mg/L]</b>	3.8

### UWWTP effluent

The UWWTP effluent utilized in this work came from the EDAR 'El Bobar', Almería, Spain. This conventional medium sized UWWTP was designed to process UWW with a population equivalent (PE) of around 300.000 PE, while on average serving around 250.000 PE. The UWWTP effluent is built up by a pretreatment step, a primary-, and a secondary treatment step. The collected stream from this UWWTP came from the secondary bio-treatment step. An overview of representative characteristics are given in Table III.3.

**Table III.3:** Overview of the representative average secondary UWWTP effluent characteristics collected from the UWWTP EDAR 'El Bobar', Almería, Spain.

<b>UWWTP effluent (EDAR 'El Bobar' Almería, Spain)</b>			
<b>Cations</b>	[mg/L]	<b>Anions</b>	[mg/L]
<b>Ca<sup>2+</sup></b>	81	<b>SO<sub>4</sub><sup>2+</sup></b>	148
<b>Mg<sup>2+</sup></b>	48	<b>Cl<sup>-</sup></b>	489
<b>K<sup>+</sup></b>	30	<b>NO<sub>3</sub><sup>-</sup></b>	5
<b>Na<sup>+</sup></b>	314		
<b>Conductivity [mS/cm]</b>			2.7
<b>pH</b>			8.0
<b>TC [mg/L]</b>			30.0
<b>TSS [mg/L]</b>			60.0

### III. Materials and Methods

#### 2. Microorganisms

During this work a specific class of microorganisms has been used, naming the bacterium *Pseudomonas aeruginosa* (*P. aeruginosa*) for experiments related to bacteria elimination. This Gram-negative bacterium is characterized by its opportunistic behavior, as it is able to colonize a wide range of hosts due to its large genome, while it shows very high virulence and antibiotic resistance to commonly used antibiotics through its evolution in natural ecosystems. The bacterium is present in every healthcare location such as hospitals and clinics and is estimated to be present at any other sites where humans are or were present. These specifically include biocide polluted waters and sewage systems. Its survival strength and widespread presence is possible due to its clonal epidemic population structure. [193]

In order to utilize this bacterium for experimental work, 20 hours before the experiments an inoculum was prepared at a concentration of  $1 \cdot 10^6$  CFU/mL. For which the used materials to do so were Type CM0067 Nutrient Broth No. 2, supplied by OXCID LTD., England, and *P. Aeruginosa* supplied by the Spanish Culture Collection (CECT). This concentration is commonly used as a standard inoculum concentration for experiments that involve bacterial inactivation. [194,195]

For the quantifications of the *P. Aeruginosa*, sampling was performed by preparing a number of petri dishes containing Pseudomonas Chromogenic Agar bovine agar, supplied by Condalab, Spain, followed by the application of a 10-fold serial dilution at a sample size of 500  $\mu$ L when quantifying for the permeate volumes, and 50  $\mu$ L for the concentrate volumes. A swab was used for collecting samples from the membrane surfaces, every time prior to the experiments followed by sample collection after 90 minutes. The swabs were applied to the agar after sample collection for further cultivation. Samples taken from the experimental reactor, or concentrate volume, were taken at times 0, 30, 60, and 90 minutes. Samples taken from the permeate stream were taken at 30, 60, and 90 minutes. The filtration experiments were performed in double. The incubation of the *p. aeruginosa* in the Petri dishes took place by storing them in a Series BD type standard incubator at 36 °C for a time of 48 hours.

### 3. Analyses

#### 3.1 Physicochemical parameters

##### 3.1.1. Electrical conductivity and pH measurements

The electrical conductivity of the water matrices was measured using a CRISON GLP31 conductometer, Figure III.1.



**Figure III.1:** Conductivity meter used in the TSA lab of the PSA.

During the experiments, the pH values of the matrices were measured by using a portable pH meter of the type LAQUAact PH110, from HORIBA Advanced Techno Co., Ltd.



**Figure III.2:** The mobile pH meter used in the TSA lab at the PSA.

### III. Materials and Methods

#### 3.1.2. Turbidity measurement

The turbidity of the various matrices in this work was determined by utilizing a HACH 2100N Turbidimeter, as seen in Figure III.3. Samples with a turbidity between 0.1 and 4000 NTU could be measured, which was done by adding the samples to compatible glass vials, which were then cleaned, checked for cleanness, and then directly placed in the turbidimeter. Turbidity measurements consisted out of both forward- and scattered light detection, as well as transmitted light detection. The calibration was performed regularly using standards supplied by the manufacturer.



**Figure III.3:** Turbidity meter used in the TSA lab at the PSA, of the type HACH 2100N.

#### 3.1.3. UV-visible light spectrophotometry

For the determination of the concentration of a variety of chemical compounds present in the samples taken from the different water matrices and streams, a UV-visible light spectrophotometer was used, which was delivered by Thermo-Scientific, shown in Figure III.4.



**Figure III.4:** UV-vis set up used in the TSA lab at the PSA with on the right the UV-visible light spectrophotometer and on the right the computer connected to it with the compatible software.

#### 3.1.4. Chemical oxygen Demand determination

The chemical oxygen demand (COD) of samples taken during the experimental work performed in this thesis was determined by using special COD determination kits delivered by HACH, in the ranges of 0-150 and 150-1000 mg/L O<sub>2</sub>

An estimation of the COD present in the sample was made, and when applicable, further analysis was performed in a more specific range sample kit. Samples were taken and added to the testing vial at its indicated volume, shaken, and continued by a reaction time of two hours at a temperature of 148 °C. After this time, the vials were let to cool down to ambient temperature and analyzed at their specific wavelength as designated by the method.

#### 3.1.5. Free Available Chlorine measurement

During the experiments where EO was involved, the free available chlorine (FAC) was monitored by sampling the matrices and adding them to a vial containing N, N-diethyl-p-phenylenediamine (DPD) powder pillows provided by HACH. After the sample addition at given volumes based on the concentration and the given reaction time following the HACH DPD Method 10069, the samples were measured in the Evolution 220 UV-visible light Spectrophotometer of Thermo Scientific at a specific wavelength of 530 nm.

In Figure III.5, an example is given of a vial containing the buffer liquid that reacted with a sample coming from the EO pilot plant, with its characteristic faint pink color. A higher concentration of FAC resulted in a stronger color.

### III. Materials and Methods



**Figure III.5:** Vial with a sample containing free available chlorine as indicated by the faint pink color.

#### 3.1.6. Iron concentration determination

Determination of iron concentration during the different Fenton processes was performed following the ISO 6332 standard. The principle of the measurement comes from the complex formed between ferrous iron ( $\text{Fe}^{2+}$ ) and 1,10-phenantroline, taking place in an acetate/acetic acid buffer. The peak absorbance of this complex lies at 510 nm and is directly proportional to the ferrous iron concentration. The complex is characterized by a blue color, wherefore the intensity of the color increases proportional to the iron concentration, in visible light. Furthermore, when reducing the ferric iron ( $\text{Fe}^{3+}$ ) present in the sample by the addition of ascorbic acid, the total iron present in the sample can be measured. Meaning that the ferric iron concentration can be calculated by deducting the ferrous iron from the total iron.

A solution of 1,10-phenantroline was made at a concentration of 1 g/L, followed by a buffer solution containing 62.5 g of ammonium acetate and 175 mL acetic acid, which was then filled up to 250 mL.

Two series of samples were prepared, filtered and unfiltered, by adding 4 mL of sample into a testing tube, followed by adding 1 mL of the 1,10-phenantroline solution, 1 mL of the acetic acid/acetate buffer, and tip of a spatula of ascorbic acid.

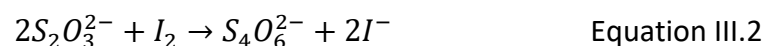
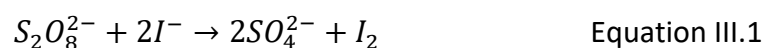
Prepared samples were then added to a quartz cuvette for the UV-visible spectrophotometer and measured in the spectrophotometer at a wavelength of 510 nm. The concentration of iron that could be measured with this method lies between 0.25 and 10 mg/L, with the possibility to dilute samples with demineralized water, as long as the sample size was kept at 4 mL. The reference sample was demineralized water.

## 3.1.7. Hydrogen peroxide measurement

Directly after sampling, H<sub>2</sub>O<sub>2</sub> was determined using titanium (IV) oxysulfate following DIN 38402H15. Herefore, 5 mL of sample was added to a volume of 0.5 mL of the titanium (IV) oxysulfate, mixed and then added to a quartz vial for the measurement in the UV-visible light spectrophotometer. The samples were yellow of color with an intensity depending on the height of the H<sub>2</sub>O<sub>2</sub> concentration and measured at a bandwidth of 410 nm, taking demineralized water as the reference sample.

## 3.1.8. Persulfate measurement

A spectrophotometric method was adapted from Liang et al [196], to determine the concentration of the persulfate present in the matrix, based on the oxidation of the iodide ion, which is characterized by a maximum absorption at 352 nm. The equations III.1 and III.2 show the chemical process that takes place:



The presence of NaHCO<sub>3</sub> prevents the premature oxidation of the iodide ion in the presence of oxygen. The time necessary for the spectrophotometric determination once the chemicals are combined lies around 15 minutes, so that even with a surplus of iodide complete oxidation is guaranteed.

In order to succeed with a complete and controlled oxidation two solutions were prepared, NaHCO<sub>3</sub> at a concentration of 50 g/L, and KI at a concentration of 71.4 g/L. The sample preparation took place by combining 1 mL of sample, with 0.5 mL of the NaHCO<sub>3</sub> solution, and 3.5 mL of the KI solution. This mixture was then stirred for 15 minutes to enable the oxidation reaction to take place, till a faint yellow color could be observed. The prepared sample was then measured in a compatible quartz cuvette in the UV-visible light spectrophotometer at a wavelength of 352 nm. The method was calibrated to be used for concentrations of S<sub>2</sub>O<sub>8</sub><sup>2-</sup> between 0.01-0.75 mM.



### III. Materials and Methods

#### 3.2 Dissolved organic carbon

A Shimadzu TOC-VCN analyzer was used to measure dissolved organic carbon (TOC), total carbon (TC), and inorganic carbon (IC). In order to measure the samples, compatible glass vials were filled with a sample volume of 25 mL and placed in the sample carousel.

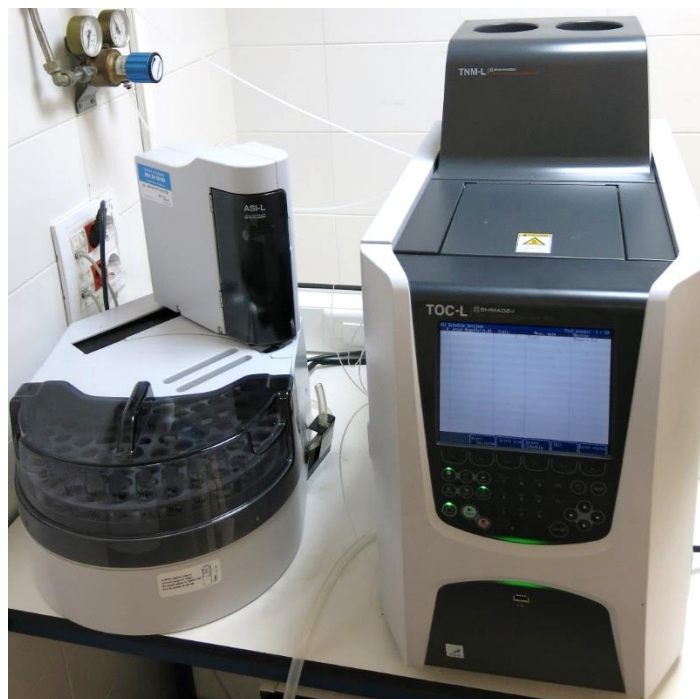


**Figure III.6:** Total Organic Carbon analyzer used at the TSA lab of the PSA, with on the right the analysis device and on the left the sample carousel and autosampler.

The TOC concentration of the wide variety of water samples containing high concentration of carbonate was determined by adding eight drops of pure  $\text{H}_2\text{SO}_4$  to samples with a volume of 25 mL, in order to lower the concentration of inorganic carbon to below 1 mg/L for a proper evaluation of TOC, as it is calculated from the difference between TC and IC. Once the pure acid was added, the samples were vigorously stirred to create a vortex on a magnetic stirrer plate, for at least four hours. Samples were filtered over an 0.45  $\mu\text{m}$  Nylon syringe filter to prevent any damage or clotting inside the catalytic reactor of the analyzer. Once the carbonates were removed and the sample volume was filtered, parafilm was used to cover the glass vials till further use and place them in the sample carousel. DOC named the content of TOC in filtered samples. The system determined IC by IR analyses of  $\text{CO}_2$  production after acidification of the sample and TC by  $\text{CO}_2$  production after combustion in a catalytic reactor at 680 °C.

### 3.3 Ionic chromatography

To determine the ionic composition of the matrices, samples were diluted with demineralized water at ratios of 1:20, 1:40, and 1:100, v/v; filtered over a 0.45  $\mu\text{m}$  Nylon filter in compatible glass vials of 15 mL, and analyzed by utilizing an ionic chromatograph from Metrohm, type 850 Professional. Dilution was necessary as the concentration of the main anions and cations was much higher than the quantification limit of the equipment. Dilution ratio was selected to quantify ions as close as possible to the center of the available calibration curves, which have a linear behavior ( $r^2 > 0.999$ ) between concentration and signal in the selected range (0,1 to 20 mg/L).

The used column for the determination of the anions was a Metrosep A Supp 7 150/40, which was thermoregulated at 45°C with 3.6 mM sodium carbonate as eluent, at a rate of 0.7 mL/min. The column for the determination of the cations was a Metrosep C6 150/4.0, with 1.7 mM dipicolinic acid at a rate of 1.2 mL/min. Figure III.7 shows a picture of the set-up.

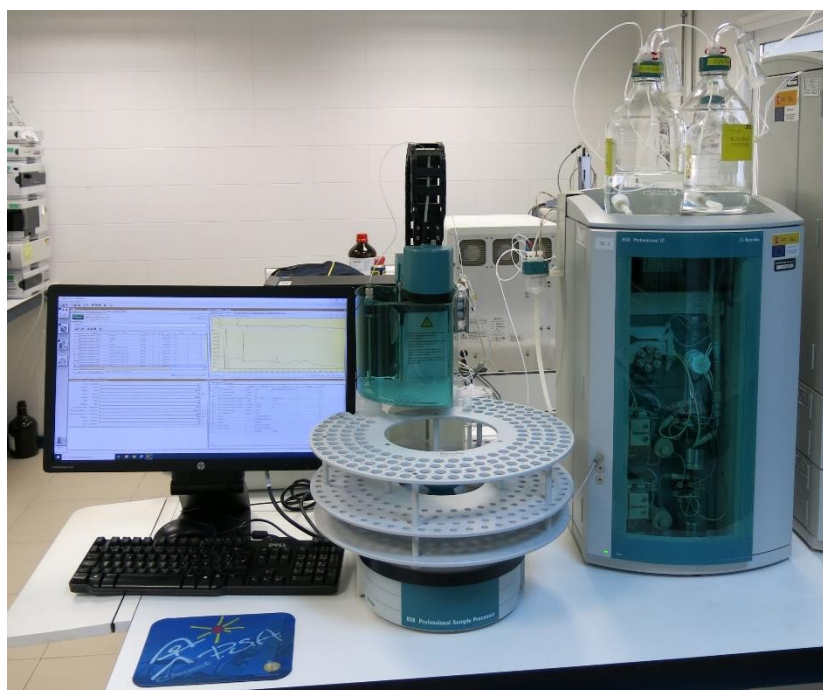


**Figure III.7:** The ionic chromatograph available at the PSA of the type Metrohm 850 Professional IC, with on the right the columns and the solvent tray, the autosampler in the middle, and the computer on the left.

### III. Materials and Methods

#### 3.4 Ultra-performance liquid chromatography

Ultra-performance liquid chromatography (UPLC) was used to determine the concentration of the selected MCs in the matrices. Figure III.8 shows the UPLC available at the PSA from Agilent Technologies, type 1200 series, which consisted of a UV-DAD detector and a Poroshell 120 EC-C18 column with a dimension of 3 x 50 mm. Initial eluent conditions were 95% water with 25 mM formic acid, designated as mobile phase A, and 5% acetonitrile (ACN), designated as mobile phase B, at a flow rate of 1 mL/min for 5 minutes. This was continued with a linear gradient for a time of ten minutes, till the ACN concentration was 68%, which was then maintained for two minutes. The injected sample volume was set at 100  $\mu$ L at a temperature of 30°C. Preparation of samples was performed by adding ACN to the samples at a ratio of 1:9, vigorously mixing and filtering over a hydrophobic PTFE 0.2 syringe filter from Millipore Millex-FG into 2 mL HPLC vials. The different specific parameters, the retention time  $t_R$ , the Limit of Quantification (LOQ), and the absorption  $\lambda$ , for this UPLC method are shown in Table III.4.



**Figure III.8:** UPLC used at the TSA lab of the PSA. With 1) Diode Array Detection (DAD), 2) column compartment with temperature control, 3) autosampler, 4) mobile phase pumps, 5) degasser, and 6) mobile phase tray.

**Table III.4:** Retention time, LOQ and maximum absorption of each contaminant.

Name	$t_R$ [min]	LOQ [ $\mu\text{g/L}$ ]	Absorption $\lambda$ [nm]
CAF	3.2	5	273
IMI	7.7	5	273
THI	9.4	5	213
CAR	10.7	5	267
DIC	13.8	5	285

### 3.5 Solar radiation measurement

Measurements of solar irradiation were performed by using a CUV 5 pyranometer by Kipp & Zonen, which registered the global UV radiation at an interval of 1 minute, in the wavelength range of <400 nm.

The UV radiation data was used to perform kinetic calculations for MC degradation and the formula used for these kinetic calculations is shown in Equation III.3, based on the work of Malato et al. [197]

$$Q_{UV,n} = Q_{UV,n-1} + (t_n - t_{n-1}) * \overline{UV}_{G,n} * A_i / V_t \quad \text{Equation III.3}$$

Equation III.3 describes the accumulated UV energy per unit of volume  $Q_{UV,n}$  [kJ/L], with the average solar ultraviolet radiation  $\overline{UV}_{G,n}$  [W/m<sup>2</sup>] in the range of <400 [nm] which is measured in a specific period of time, between  $t_n$  and  $t_{n-1}$ , where for  $n$  is the number of samples, the irradiated reactor surface  $A_i$  and the total treated volume  $V_t$ .

### 3.6 Phytotoxicity, acute- and chronic toxicity determination

Performed toxicity tests were performed by utilizing commercial kits supplied by MicroBioTests Inc., Belgium. The phytotoxicity determination was according to the ISO 18763 standard, using the PHYTOTOKIT for Liquid Samples. This kit assesses the direct effects of the chemicals on seed germination and early growth of plants.

### III. Materials and Methods

The tested permeate stream water samples were both kept at their natural pH of 9 and normalized prior to the phytotoxicity experiments by bringing them to a pH of 7 using a sulfuric acid solution. Three different test series were prepared, a control with demineralized water and two from the permeation streams produced at CF= 2 and CF= 4, for three different plant species, naming *Sinapis alba* (mustard), *Sorghum saccharatum* (sorgho), and *Lepidium sativum* (garden cress). These plant species are characterized by fast seed germination and root growth. A special black colored foam pad in a translucent cassette was soaked with the prepared volumes, after which the seeds were laid in a horizontal line and the cassettes closed. The cassettes were then placed in a special incubator to guarantee equal light and humidity conditions for three days. After this time, germination, shoot, and root length was determined, Figure III.9.



**Figure III.9:** The translucent plastic cassettes containing the black colored foam pad and the germinated seeds of the three plant species *Sorghum saccharatum* (left), *Sinapis alba* (middle), and *Lepidium sativum* (right).

The DAPHTOXKIT F was used to evaluate the acute and chronic toxicity of the permeate streams and was quantified by the number of immobilized individuals of the freshwater crustacean species *Daphnia magna*. The specific period of exposure time of 24 and 48 hours were used to determine the acute toxicity, and 72 hours of exposure time was used to determine the chronic toxicity.

Dormant eggs of the *Daphnia magna*, or *ephippia*, were hatched on a petri dish in a Standard Freshwater solution following ISO 6341, which were placed in an incubator at 20-22 °C for 72 hours, while continuously being irradiated by a lamp of 6000 lux.

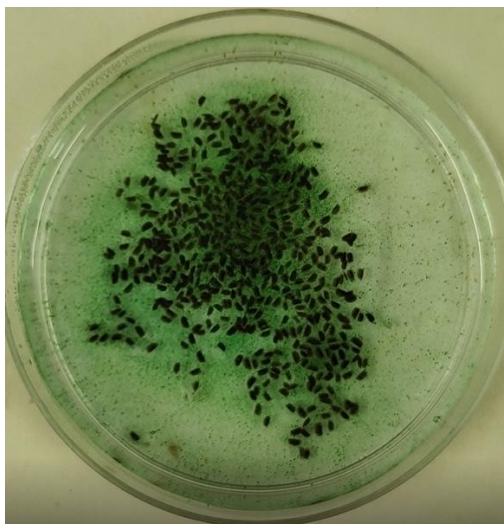


**Figure III.10:** *Ephippia* of *Daphnia magna* in the hatching process by placing them on a petri dish filled with Standard Freshwater solution, and algae to feed them.

Once the *Daphnia magna* hatched, they were transferred to a multiwell testing plate. First in a well for rinsing, followed by relocating them to four other wells, with five individuals per well. The well series contained a dilution row of 100, 50, 25, and 12.5% of the to be tested volume.

#### 4 Experimental set-ups and methodology

##### 4.2 Fe:EDDS complex preparation

In order to be able to apply the photo-Fenton process at circumneutral pH, and even up to a pH of almost 10, a complexing agent was used. The main used complexing agent to keep the Fe(III) in solution was the biodegradable EDDS.

The preparation of the Fe<sup>3+</sup>-EDDS complex was performed by taking (Fe<sub>2</sub>(SO<sub>4</sub>)<sub>3</sub> xH<sub>2</sub>O salt as a precursor agent. In order to prepare sufficient complex for 1 L of reactor volume, 26.3 mg of Fe(III) sulfate was dissolved in 40 mL water of MilliQ quality, and two drops of concentrated H<sub>2</sub>SO<sub>4</sub>, followed by stirring for at least 30 minutes. Once the salt was fully dissolved, aluminum foil was wrapped around the beaker glass to ensure no light was able to enter, which could later degrade the complex. An EDDS volume of 201.6 μL was added to the wrapped beaker glass and left to homogenize for at least 15 minutes, until a faint yellow color could be observed. It is of the utmost importance that the complex was kept in the dark till further.

### III. Materials and Methods

#### 4.3 Sand filtration system

UWWTP effluents was pretreated for further experimental work in this PhD thesis by the filtration system shown in Figure III.11.



**Figure III.11:** UWWTP effluent pretreatment filtration system available at the PSA. Consisting out of a feed tank for UWWTP effluent, a sand filter (75  $\mu\text{m}$ ) and two cartridge filters (25  $\mu\text{m}$  and 5  $\mu\text{m}$ ) in series, and a storage tank (1  $\text{m}^3$ ) for the filtered UWWTP effluent. The systems flow is powered by two centrifugal pumps.

The system was operated by filling the 1  $\text{m}^3$  black polypropylene feed tank with fresh UWWTP effluent collected from the EDAR, water is then pumped at a flow rate of 1  $\text{m}^3/\text{h}$  by two ESPA Techno 15 5 M centrifugal pumps to the sand filter containing 75  $\mu\text{m}$  SETA 16x44 (PEVASA) material. Further filtration is performed by pumping the UWWTP effluent through the 25  $\mu\text{m}$  and then the 5  $\mu\text{m}$  AMETEK string wound filter cartridges. Finally, the fully filtered UWWTP effluent is then stored in the second 1  $\text{m}^3$  black polypropylene storage tank.

The system is equipped with an automated operation and washing system of the sand filter, which is furthermore equipped with a flow meter and two WIKA 232.50 manometers at the inlet and outlet, ranging from 0 to 6 bars for fitness monitoring. The fitness of both cartridge filters is monitored by two WIKA 232.50 manometers at their relative outlets. A pressure difference between both filters higher than 0.7 bars indicates the necessity of filter replacement.

#### 4.4 Nanofiltration pilot plant

The utilized NF pilot plant, Figure III.12, for this work available at the PSA consisted of a 500 L batch tank in which the desired matrix was prepared. The batch tank had its own recirculation pump and a lid to prevent evaporation. From the batch tank, the matrix was led through a tube to a multistage pump which fed the NF rolled sheet membranes. The pilot plant had three different membrane slots available, which gave the possibility to operate different membranes at the same time, or easily change between different membranes based on type, age, or preference.



**Figure III.12:** The pilot plant for NF available at the PSA

The working pressure of the system was measured by pressure meters after the pump, as well as before and after the membrane to monitor the trans membrane pressure (TMP) and was controlled by the speed of the pump. Three flowmeters, after the pump, and one for each the concentrate and the permeate stream, enabled to monitor the flow throughout the system. A bypass was built around the pump to be able to control the system flow, an important parameter as it determines the crossflow velocity of the membrane. Furthermore, three conductivity meters placed after the previously mentioned flowmeters enabled to monitor the conductivity of the different stream in the pilot plant.

The NF pilot plant was digitally controlled by a computer with compatible software in the form of a SCADA interface, which also digitally monitored the flow and conductivity, while providing to save this data. Figure III.13.



### III. Materials and Methods

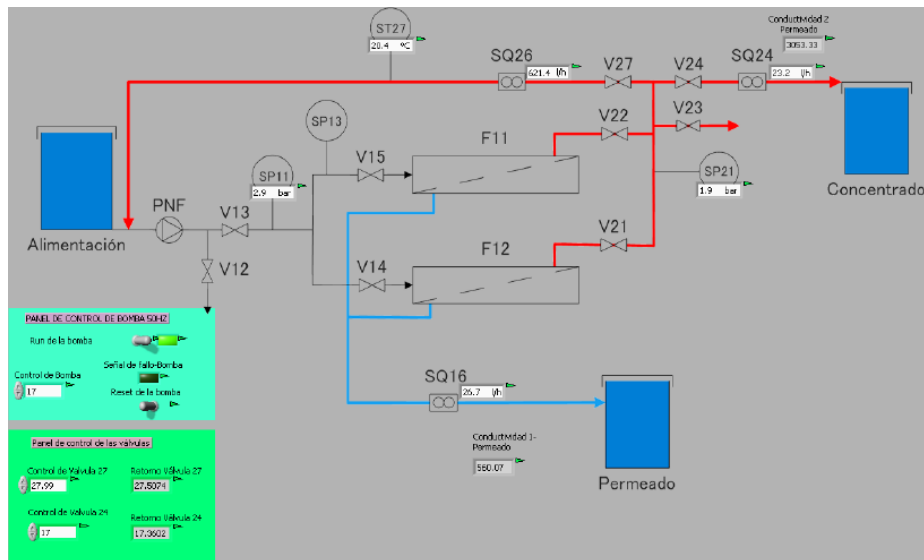


**Figure III.13:** Screenshot of the SCADA control software of the pilot plant.

The permeate stream coming from the membrane was collected through a tube placed in an external container, whereas the concentrate stream was led back into the feed tank when operating in batch mode. The maximum operating pressure of the system was 10 bars. The used NF membranes for this work were commercial grade polyamide thin-film composite membranes of the type NF90-2540 FILMTEC™ Membranes delivered by DOW, characterized by an active area of 2.6 m<sup>2</sup>, a maximum operating temperature of 45°C, a maximum operating pressure of 41 bars, within a pH range during continuous operation between pH 2-11.

The membranes were chemically cleaned in order to reverse fouling by preparing an acidic solution in the feed tank of demineralized water and HCl at pH 1.7. After operating this solution for one hour, leading both the concentrate and permeate streams back into the feed tank, the acidic solution was discharged, and the system was rinsed three times with demineralized water. This was also performed with a basic solution by dissolving NaOH in demineralized water till a pH was reached of pH 11.

In the case the pilot plant was not used for long times, a biocide was used to prevent an outbreak of microbiological growth, as the pilot plant system, and especially the NF membranes needs to be wet at all times.

**Table III.5:** Predetermined concentrations of biocide needed for set periods of time.

<b>Period</b>	<b>Concentration of the Biocide</b>
<b>&lt; 2 days</b>	180 mg/L
<b>1 – 7 days</b>	360 mg/L
<b>1 – 4 weeks</b>	540 mg/L
<b>1 – 6 months</b>	900 mg/L

Irreversible fouling, and the degree thereof, was monitored by preparing a standard NaCl solution in the feed tank, and operating the system at a relatively low pressure, while both the concentrate stream and the permeate stream was led back to the feed tank. The system pressure was then gradually increased, while the TMP increase and the permeate flow decrease was monitored. The difference between the produced curves for a new membrane, and a membrane used for a certain amount of time, gave a quantitative insight of the degree of irreversible fouling.

#### 4.5 Solar photoelectro-Fenton pilot plant

The EO pilot plant available at the PSA for SPEF experiments was build up from four commercial Electro MP-Cell plate-and-frame cells, which was delivered by ElectroCell A/S, Denmark, Figure III.14. The anode of every cell was a BDD thin film which was deposited on a Nb mesh and the cathode was a carbon-polytetrafluorethylen GDE, characterized by an effective area of 100 cm<sup>2</sup> for both the anode and the cathode, which was connected to a feed tank containing an experimental volume of 100 L. The feed tank was connected to a 2 m<sup>2</sup> CPC photoreactor having a total irradiated volume of 23 L, Figure III.15. The cell was set to maintain a constant current density ( $j$ ) of 74 mA/cm<sup>2</sup>. A constant flow of air was led into the cell at a pressure of 0.7 bar and a flow rate of 10 L/min, something fundamental for the prevention of water flowing into the air circuit, as the treated water was led to the cell at a pressure of 0.5 bar and a flow rate of 4 L/min, Figure III.16. The electrochemical system had an experimental volume of 30 L, with a total volume of 75 L when combined with the CPC photoreactor. A schematic overview of the set-up is shown in Figure III.17. An automated cooling system set at 25-30 °C was used for cooling the pilot plant set-up when needed.

### III. Materials and Methods



**Figure III.14**Error! No bookmark name given.: Photo of the system wall containing four cells for EO treatment of water.



**Figure III.15:** Photo of the CPC reactor connected to the EO cell system as part of the EO pilot plant.



**Figure III.16:** The EO cell set-up, with 1) the air-inlet and pressure meter, 2) the EO cell, 3) the water-inlet and pressure meter.

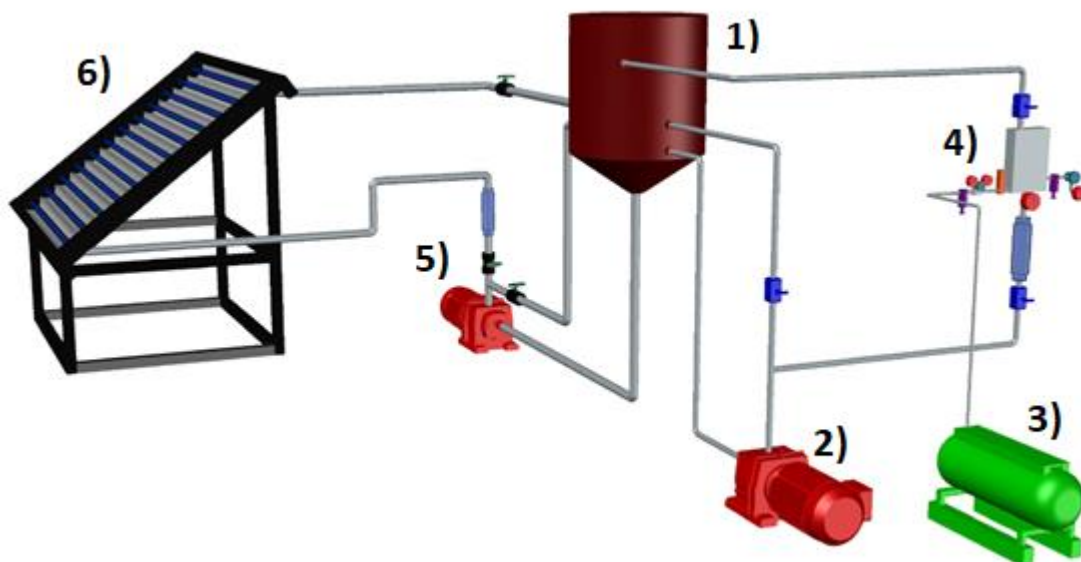


**Figure III.17:** Schematic overview of the SPEF pilot plant available at the PSA, consisting out of 1) the feed tank, 2) the feed tank pump, 3) the compressor, 4) the EO cell set-up, 5) CPC-feed tank circulation pump, and 6) the CPC reactor.

### III. Materials and Methods

The experimental procedure was:

- Filling of the 30 L feed tank with the experimental batch volume. When connected to the CPC, the total system volume is 75 L. The batch volume was homogenized for a duration of 30 minutes by continuous pumping.
- Temperature control by an external heat exchange system to keep the temperature of the batch volume at a temperature of 25 °C.
- The pH value was measured and corrected when needed, using H<sub>2</sub>SO<sub>4</sub> for acidification and NaOH for alkalization.
- Addition of the Fe: EDDS complex, followed by homogenization for 30 minutes, with a covered CPC reactor.
- Adjustment of the operational parameters, such as the batch volume flow, air flow, and pre-setting the current at the PSU.
- Taking the initial sample, followed by switching on the PSU, along with the immediate uncovering of the CPC reactor when SAAO and SPEF experiments are performed.
- Sampling at short intervals in the first 30 minutes, then extended to an interval of 30 and 60 minutes.

At the end of the experiments the system was emptied and cleaned with demineralized water, sequentially with an acidic solution of pH 3, by adding HCl to the demineralized water, for a total amount of three times.

#### 4.6 Solar simulator

Performed experiments in this work included ones solely, or prior to further experiments in pilot plants, small scale batches in a solar simulator, Figure III.18. The solar simulator available at the PSA is the Atlas-SunTest XLS+, which has a daylight filter and a xenon lamp placed on the ceiling of the irradiation chamber ceiling. The solar simulator was programmed to produce a total irradiation potential of  $365 \text{ W/m}^2$  in the wavelength range of 300-800 nm, along with temperature control venting system set at  $25 \text{ }^\circ\text{C}$ . UV irradiation was  $30 \text{ W/m}^2$  in the range of 300-400 nm.



**Figure III.18:** The Atlas-SunTest XLS+ available at the PSA, equipped with a xenon lamp and a daylight filter.

### III. Materials and Methods

A 1 L cylindrical container was placed in the middle of the solar simulator platform and was magnetically stirred, which had a diameter of 18.5 cm and a depth of 4.0 cm, as shown in Figure III.19.

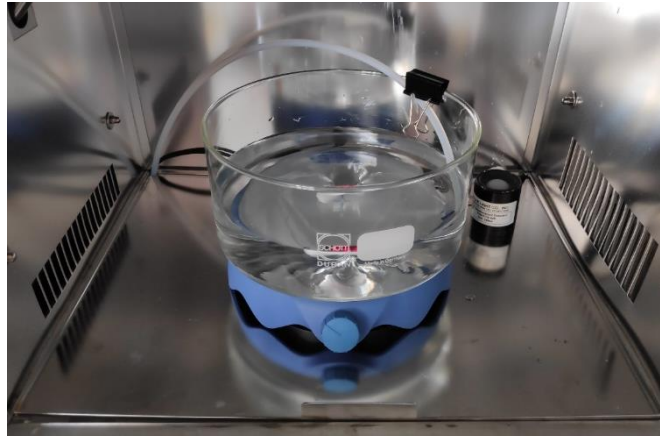


**Figure III.19:** The 1 L cylindrical glass container placed in the solar simulator on a magnetic stirrer plate, a tube for sampling, and on the side a solar irradiation meter. The perpendicular holes on both sides belong to the venting system that control the air temperature.





## Chapter IV. Results and Discussion



**Target 1. Determination of optimal operational parameters, concentration factors and retention mechanisms of MCs, for the preconcentration of saline waters by NF treatment, utilizing a pilot plant containing NF membranes. Followed by the assessment of oxidizing agents' effectiveness, iron concentration and EDDS complex ratios during solar photo-Fenton treatment of the different concentrate and permeate volumes, at different pHs.**

### 1. The Effects of salinity on NF membranes

The influence of the water matrices, salinity, and system pressure on the performance of the NF pilot plant was investigated. Two water matrices were chosen, demineralized water and natural water from Tabernas, Spain. The different system pressures were set at 5, 7, and 10 bars, at salinity levels of 3, 5, and 7 g/L of NaCl. The NF experiments started by spiking the prepared water matrices with the previously chosen target MCs from the stock solution prepared as described in Chapter III – 2.3, till a tank concentration of 100 µg/L of each MC.

For the experiments using the demineralized water, the total experimental time was set at 360 minutes to reach a maximum CF of CF= 4. The permeability of the three MCs, THI, CAF, and CAR, was detected after 180 minutes of operation of the NF pilot plant, something indicating the membrane surface saturation point time. The permeability order of the MCs was THI, CAF, and CAR, while only very low concentrations of DIC were detected.

In all experiments, the MC permeability order was the following: THI, CAF, and CAR, sometimes with very low concentrations of DIC. This permeation order can be attributed to the specific molecular morphology, flexibility, and weight (252.7, 194.2, and 236.3 g/mol, respectively) of the first three MCs, as compared to DIC (318.1 g/mol), and the MWCO of the NF membrane, which lies around 250 g/mol. Furthermore, positively charged molecules also enhance the MC membrane permeability, as the membrane surface is negatively charged.

The MC concentration increase over time in the concentrate stream showed to be inversely related to the CF. Meaning that operating at higher system pressures, the NF pilot plant obtained higher CFs, as was expected.

During experiments where 3 g/L of NaCl was added to the matrix, the same conditions were observed regarding the pressure as compared to the previous experiments. The MC permeability order stayed the same as without the addition of NaCl, with THI, CAF, and CAR as the most permeable MCs. Not in any case was DIC observed in the permeate stream.

The total time required to reach a concentration of 10 µg/L per MC in the permeate stream is shown in Table IV.1. CFs of 2, 3, and 4 were obtained at 120, 180, and 300 minutes, respectively, at a system pressure of 10 bars. Operating at lower system pressures resulted in longer times to reach the desired CF. Over time, the salinity increased with a factor 2 in the feed tank at 180, 150, and 90 minutes for 5, 7, and 10 bars, respectively.

#### IV. Results and Discussion

**Table IV.1:** Overview of the times necessary to reach a concentration of 10 µg/L of each MC in the permeate stream, while operating with demineralized water as the matrix and an addition of 3 g/L NaCl.

<b>Pressure, bars</b>	<b>5</b>	<b>7</b>	<b>10</b>	
<b>THI</b>	180	150	120	min.
<b>CAF</b>	420	300	210	min.
<b>CAR</b>	-	-	300	min.
<b>DIC</b>	-	-	-	min.

The maximum applied system pressure was set at 10 bars, which is the maximum system pressure of the NF pilot plant. However, for further commercial applications higher operation pressures are expected to be utilized, especially for water matrices possessing higher saline conditions than with the addition of 5, 7, and 10 g/L of NaCl to the water matrix. Unfortunately, this lower pressure prohibited obtaining the desired CF= 4 within the previously determined experimental time of 360 minutes, for which the data is not shown. As an example, when 5 g/L of NaCl was added to demineralized water, and the NF pilot plant was operated at 10 bars, the CF only reached CF= 2 and CF= 3 at 210 and 360 minutes, respectively.

In order to further investigate the effect of salinity on the NF membrane, the complexity of the water matrix was increased by using natural water from Tabernas, Spain. The composition of this matrix can be found in Table III.2.

Additionally, IMI, a neonicotinoid pesticide comparable to THI, was added as selected MC with the other MCs in order to extend the variability of the NF permeability and retention, as also enriching the results. Just as THI, IMI is well known for its persistence in the environment and its potential negative effects on bees worldwide. [198,199]

The use of natural water as the matrix increased the salinity as compared to the demineralized water due to the presence of NaCl and other salts, while no differentiation in MC membrane permeability order was observed after the addition of 3, 5, or 7 g/L NaCl. The total matrix salinity after the addition of NaCl was 8,200, 11,100, and 14,500 µS/cm, respectively.

In Figure IV.1 the changes in the total MC concentration in both the permeate and concentrate (inset) streams are shown throughout the 360 minutes of experiment time. The final MC concentration increment over time in the permeate stream was 25.7, 3.2, and 3.8 times higher as compared to the experiments with demineralized water, and in the concentrate stream 2.3, 1.7, and 1.4 times higher with the addition of 3, 5, and 7 g/L of NaCl, respectively.

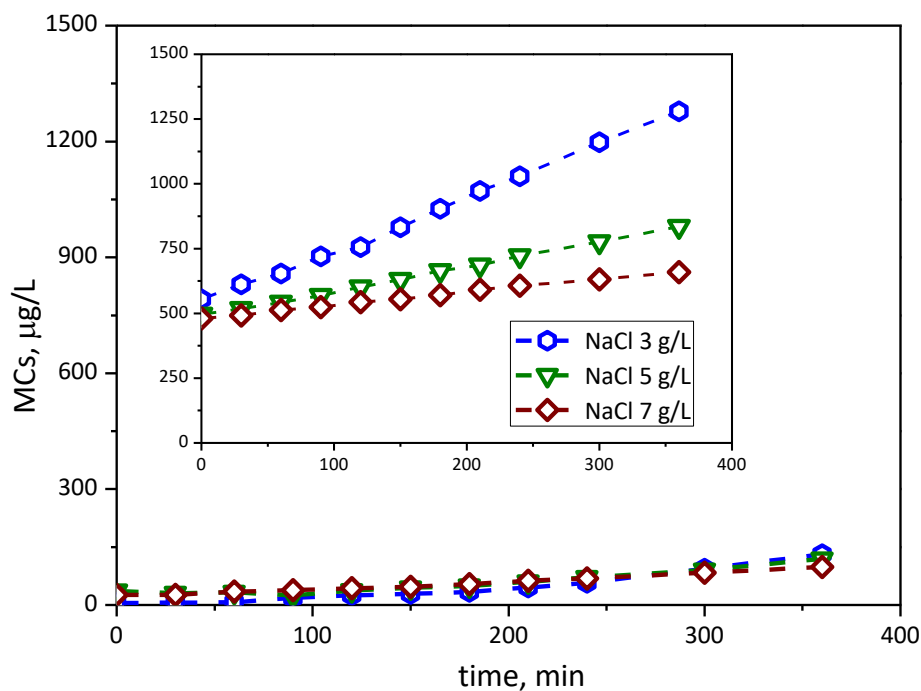


**Figure IV.1:** The concentration of the sum of MCs, and the evolution thereof, in the permeate stream and the concentrate stream (inset). The natural water matrix had 3, 5, and 7 g/L NaCl added to it.

After the addition of 3 g/L of NaCl, the initial conductivities of the permeate and the concentrate streams at  $t=0$  minutes were 430 and 10500  $\mu\text{S}/\text{cm}$ , respectively, which then increased to 2400 and 20200  $\mu\text{S}/\text{cm}$  after the total experiment time of  $t=360$  minutes. Thus, the increment in salinity in the permeate stream was a factor of 5.7, while in the tank and concentrate stream, it had an increment factor of 2.3 and 1.9, respectively. The CF obtained after this time was  $\text{CF}=3.3$ .

Secondly, after the addition of 5 g/L of NaCl, the initial conductivities of the permeate and the concentrate streams at  $t=0$  minutes were 650 and 13700  $\mu\text{S}/\text{cm}$ , respectively. At the end of the total experiment time,  $t=360$  minutes, the conductivities were 4300 and 21400  $\mu\text{S}/\text{cm}$ . The salinity in the permeate stream had increased by a factor of 6.5, while in the tank and the concentrate stream, the increment factors were 1.8 and 1.6, respectively. The CF obtained after this time was  $\text{CF}=2.4$ .

As last, after the addition of 7 g/L of NaCl, the permeate and concentrate stream had initial conductivities of 1400 and 17900  $\mu\text{S}/\text{cm}$ , respectively. At a total experiment time of  $t=360$  minutes, their relative conductivities increased to 4600 and 22700  $\mu\text{S}/\text{cm}$ . The salinity in the permeate stream increased with a factor of 3.2, whereas in the tank and concentrate stream, the increment factors were 1.5 and 1.3 respectively. The obtained CF after 360 minutes of experiment time was  $\text{CF}=1.6$ , indicating that a significant decrease in the concentration capacity of the NF system utilized in this

#### IV. Results and Discussion

work. An CF of CF= 4 was only obtained with the addition of 3 g/L NaCl to the natural water, which had already an initial conductivity of 2300  $\mu\text{S}/\text{cm}$ .

During all experiments, the MC membrane permeability order was IMI, THI, CAF, and CAR. DIC was not detected in the permeate stream, which could be assigned to its molecular weight and charge, as mentioned before. An increasing CF and salinity were observed with increasing MC permeation, in particular with the increased permeation of THI and IMI, which showed a disproportionate increase in the permeate stream. This is suggesting that a higher salinity leads to reduced membrane efficiency and MC retention.

The most unfavorable operating conditions for the NF pilot plant were determined and simulated based on this conclusion, resulting in performing the following experiments with an addition of 7 g/L of NaCl at a system pressure of 10 bars. Under these conditions, at an experiment time of  $t= 360$  minutes, the total MC concentration in both the permeate and the concentrate streams were 104  $\mu\text{g}/\text{L}$  (IMI: 30  $\mu\text{g}/\text{L}$ , THI: 39  $\mu\text{g}/\text{L}$ , CAF: 19  $\mu\text{g}/\text{L}$ , CAR: 11  $\mu\text{g}/\text{L}$ , and DIC: 5  $\mu\text{g}/\text{L}$ ) and 659  $\mu\text{g}/\text{L}$  (IMI: 130  $\mu\text{g}/\text{L}$ , THI: 129  $\mu\text{g}/\text{L}$ , CAF: 156  $\mu\text{g}/\text{L}$ , CAR: 162  $\mu\text{g}/\text{L}$ , and DIC: 82  $\mu\text{g}/\text{L}$ ), respectively. The final MC concentration in the feed tank was 659  $\mu\text{g}/\text{L}$ .

Based on these results, multiple batches were produced at an isobaric pressure of 10 bars in order to generate sufficient concentrate and permeate volume to perform further tertiary treatment using the solar photo-Fenton process. As the matrix, the natural water from Tabernas, Spain was chosen and 7 g/L of NaCl was added, as it resulted in the highest salinity and ionic variation coming closest to highly saline effluents coming from UWW, which is the main objective of this work. While additionally, the NF pilot plant was operated at more challenging conditions in order to obtain more conservative results rather than optimistic ones.

Starting with batch P1 with a volume of  $v_0= 400$  L and operating for 180 minutes, as the permeability of the four MCs, IMI, THI, CAF, and CAR, was detected within this timeframe. After 180 minutes, a total volume of  $v_{P1}= 100$  L was produced. The NF pilot plant was still being operated with the residual 300 L for an addition of 660 minutes, which resulted in batches P2 and C1, having an equal volume of  $v_{P2} = v_{C1} = 150$  L. The operation time of 660 minutes for these batches was chosen to obtain a final batch volume ratio close to 4.

The produced batches P1 and P2, each with different MC concentrations, low and high, and batch C1 with very high MC concentrations, were prepared for subsequent treatment by the solar photo-Fenton process under a variety of operating conditions. The main objective of all the different treatments applied to both permeate streams and the concentrate stream was to achieve a total degradation of 90% of the sum of the MCs. An ambitious objective and something which comes only close to the

regulation in Switzerland, where current requirements dictate 80% of CECs are to be removed from raw wastewater in UWWTP effluents. [101]

## 2 Solar photo-Fenton as tertiary treatment

### 2.2 Treatment with the conventional solar photo-Fenton process at a pH of 3

In order to minimize the economic and environmental impacts of the treatment with the solar photo-Fenton process, a set of initial conditions were chosen to still obtain a high efficiency in the removal of a wide range of MCs, based on previous findings. [200,201]

In Figure IV.2, the results of the treatment by solar photo-Fenton at a pH of 3 are shown, using mild experimental parameters (0.10 Fe(II) and 1.50 mM H<sub>2</sub>O<sub>2</sub>). These results demonstrate that in volume C1, the MCs CAF, CAR, and DIC were eliminated till under the LOQ in less than five minutes. IMI and THI showed more persistence, for which only 70% elimination was obtained after 30 minutes of treatment time. The H<sub>2</sub>O<sub>2</sub> consumption at the end of the experiment was determined at 0.70 mM, which is around half of the initial amount. Derived from these results the first-order kinetic constants ( $r = kC$ ) were calculated, being 0.770 min<sup>-1</sup>, 0.042 min<sup>-1</sup>, 0.041 min<sup>-1</sup>, 0.793 min<sup>-1</sup>, 0.737 min<sup>-1</sup> for the selected MCs CAF, IMI, THI, CAR, and DIC, respectively.

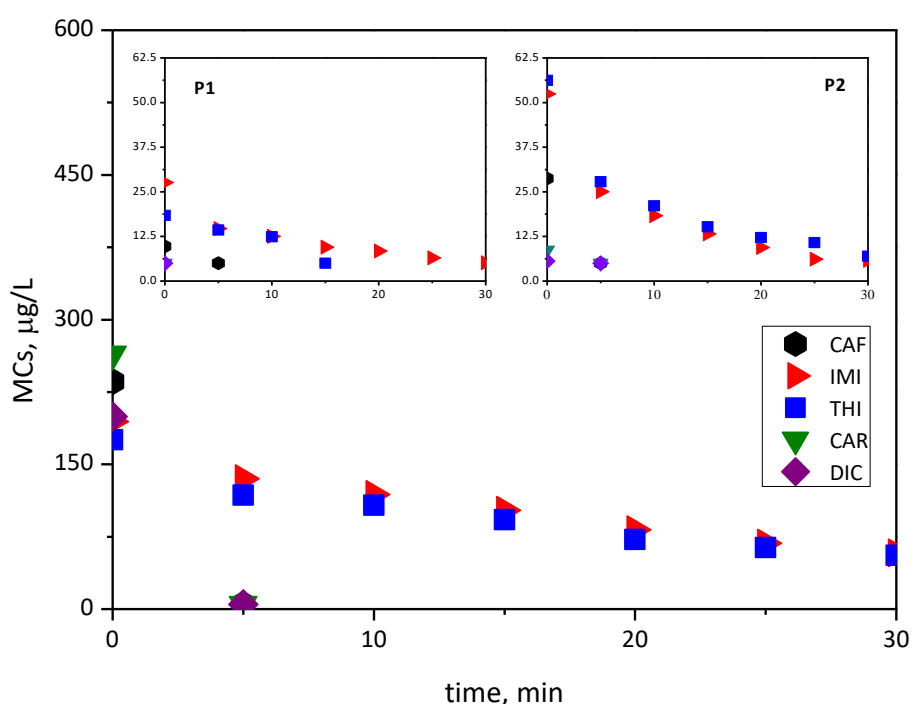


**Figure IV.2:** Solar photo-Fenton treatment applied on concentrate volume C1, at a pH of 3. The treatment applied on permeate streams P1 and P2 are shown in the insets.



#### IV. Results and Discussion

Also in volumes P1 and P2, CAF, CAR, and DIC were rapidly eliminated to the LOQ within the first five minutes of treatment. Remarkably, DIC was already eliminated by the Fenton process even before illumination ( $t < 0$ ), in the dark. The more persistent IMI and THI showed to be harder to eliminate as compared to the other MCs, as only 90% elimination was obtained in volumes P1 and P2 after 25 and 30 minutes of treatment, respectively. The first-order kinetic constants for volume P1 were  $0.133 \text{ min}^{-1}$ ,  $0.060 \text{ min}^{-1}$ , and  $0.071 \text{ min}^{-1}$  for CAF, IMI, and THI, respectively. For volume P2, the values of the first-order kinetic constants were  $0.350 \text{ min}^{-1}$ ,  $0.083 \text{ min}^{-1}$ , and  $0.074 \text{ min}^{-1}$  for CAF, IMI, and THI, respectively.

The  $\text{H}_2\text{O}_2$  consumption after 30 minutes of treatment time was 0.50 mM and 0.80 mM for volumes P1 and P2, respectively. Therefore,  $\text{H}_2\text{O}_2$  consumption was not mainly determined by MC concentration, which was comparable in volumes P1, P2, and C1. Although the treatment of the volumes was slower, they were still successful, reaching a MC elimination of over 90% of the total MCs after 20 minutes of treatment and kept consistently above 70% for individual MCs after 30 minutes of treatment time with the solar photo-Fenton process as tertiary treatment.

##### 2.3 The application of EDDS for the solar photo-Fenton process at natural pH

The results of the treatment of the volumes P1, P2, and C1, with the solar photo-Fenton process under mild conditions at a natural pH (0.10 mM Fe(III):EDDS; [1:2] and 1.50 mM  $\text{H}_2\text{O}_2$ ) are shown in Figure IV.3. These initial operational parameters for the solar photo-Fenton process were chosen based on previous work also applying low initial concentrations of Fe(II) and  $\text{H}_2\text{O}_2$ . [202]

For volume C1, an elimination of CAF, CAR, and DIC to the LOQ was reached in less than five minutes. An elimination of 90% was obtained for the more persistent IMI and THI in a treatment time less than 15 minutes. The degradation of the Fe(III):EDDS complex paralleled to the evolution of the dissolved Fe, which is consistent with the finding from other studies that extensively evaluated the complex. [203,204] The iron precipitation, an indicator for the degradation of the Fe(III):EDDS complex, was first observed at just under 20 minutes, which resulted in a total loss of 0.03 mm of dissolved iron after 30 minutes. The  $\text{H}_2\text{O}_2$  consumption was approximately 1.20 mM after 30 minutes reaching a MC degradation of 90%, while only 0.80 mM was consumed after fifteen minutes of treatment. The calculated first-order kinetics were  $0.768 \text{ min}^{-1}$ ,  $0.150 \text{ min}^{-1}$ ,  $0.126 \text{ min}^{-1}$ ,  $0.792 \text{ min}^{-1}$ , and  $0.732 \text{ min}^{-1}$  for CAF, IMI, THI, CAR, and DIC, respectively.

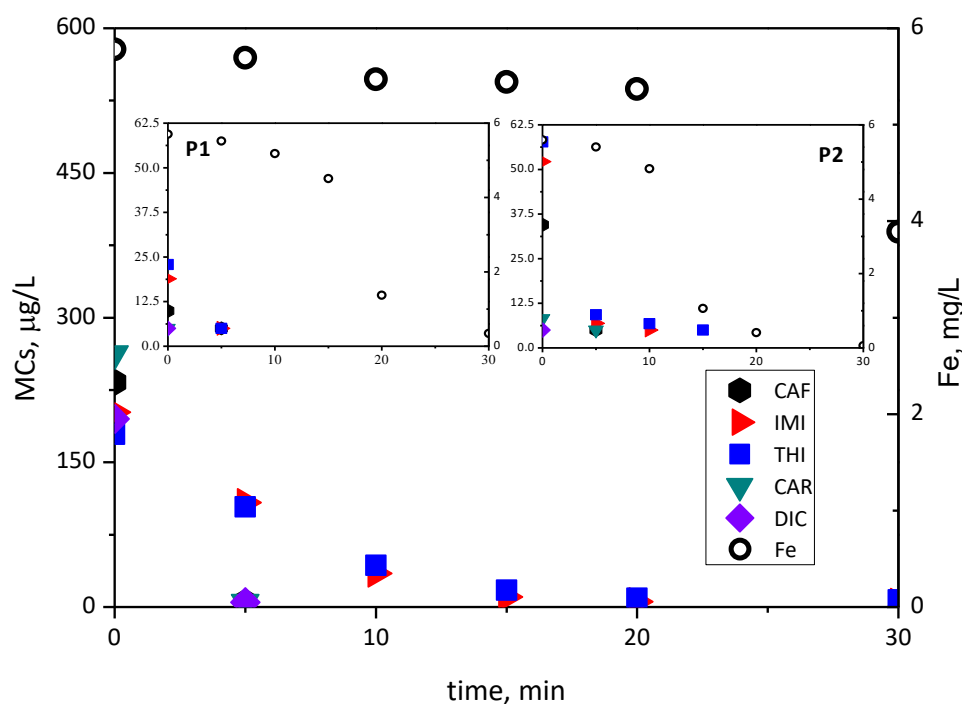


**Figure IV.3:** Evolution of dissolved iron and MC concentration decline by solar photo-Fenton treatment of concentrate volume C1, applied at a natural pH of 7, using Fe(III):EDDS at a ratio of [1:2], with the insets showing the results of the treatment applied to permeate volumes P1 and P2.

In Figure IV.3, the rapid elimination till the LOQ of all MCs in volumes P1 and P2 is shown. Within the first five minutes of treatment time, 90% of all MCs was obtained. Iron precipitation due to EDDS degradation started after ten minutes and was completed after 30 minutes of treatment. The  $\text{H}_2\text{O}_2$  consumption was not affected by the MC concentration but decomposed naturally over the treatment time. The calculated first-order kinetic constants for volume P1 were  $0.137 \text{ min}^{-1}$ ,  $0.266 \text{ min}^{-1}$ , and  $0.304 \text{ min}^{-1}$  for CAF, IMI, and THI, respectively. For volume P2, the corresponding values were  $0.386 \text{ min}^{-1}$ ,  $0.269 \text{ min}^{-1}$ , and  $0.192 \text{ min}^{-1}$  for CAF, IMI, and THI, respectively. The Fe(III):EDDS complex at circumneutral pH demonstrated the ability to rapidly eliminate the selected MCs in the volumes treated by NF, or at least being as effective as compared to the classic photo-Fenton process at acidic pH, or potentially even more so, looking at the first-order kinetic constants of the different MCs. IMI and THI were the most persistent MCs in both treatments.

The solar photo-Fenton experiments were applied to waters containing high chloride concentrations, without any significant adverse effects regarding the photo degradation of the selected MCs. The effects of different AOPs due to the main compounds present in wastewater, including the previously mentioned chloride ions, were reviewed by Lado Ribeiro et al. (2019). [205] Furthermore, it was reported that the high chloride concentrations had no effect of a slight improvement in the reaction rate due to the involvement of chloride radicals in MC degradation. [206]

## IV. Results and Discussion

### 2.4 The NF operating parameter effect on the solar photo-Fenton process as tertiary treatment at a pH of 3

Previous studies indicate that sulfate can reduce the efficiency of treatment by the photo-Fenton process by scavenging hydroxyl and other radicals. [207–209] The experiments in this work, where the pH was lowered to a pH of 3 by the addition of sulfuric acid, the sulfate concentration was nearly four times higher as compared to a pH of 7. The higher reaction rates observed by utilizing Fe(III):EDDS at a natural pH, as compared to the photo-Fenton process at a pH of 3, could therefore be assigned to the scavenging of hydroxyl radicals by sulfate.

In order to counter the negative effects of the scavenging sulfate, an additional 0.60 mM of H<sub>2</sub>O<sub>2</sub> was added to the reactor after 15 minutes at pH 3. As the MCs CAF, CAR, and DIC reached the LOQ in less than five minutes, the more recalcitrant IMI and THI had not yet reached 90% of elimination after 30 minutes. However, the second H<sub>2</sub>O<sub>2</sub> addition did not show to have a positive effect on the MC elimination, especially considering an equal amount (0.70 mM) of H<sub>2</sub>O<sub>2</sub> was consumed as compared to the experimental results shown in Figure IV.2.

Similar to this, further experimental work to enhance the solar photo-Fenton at a pH of 3, the iron concentration was doubled to a concentration of 0.2 mM. Figure IV.4, illustrates the elimination of the MCs CAF, CAR, and DIC to the LOQ within the first five minutes.

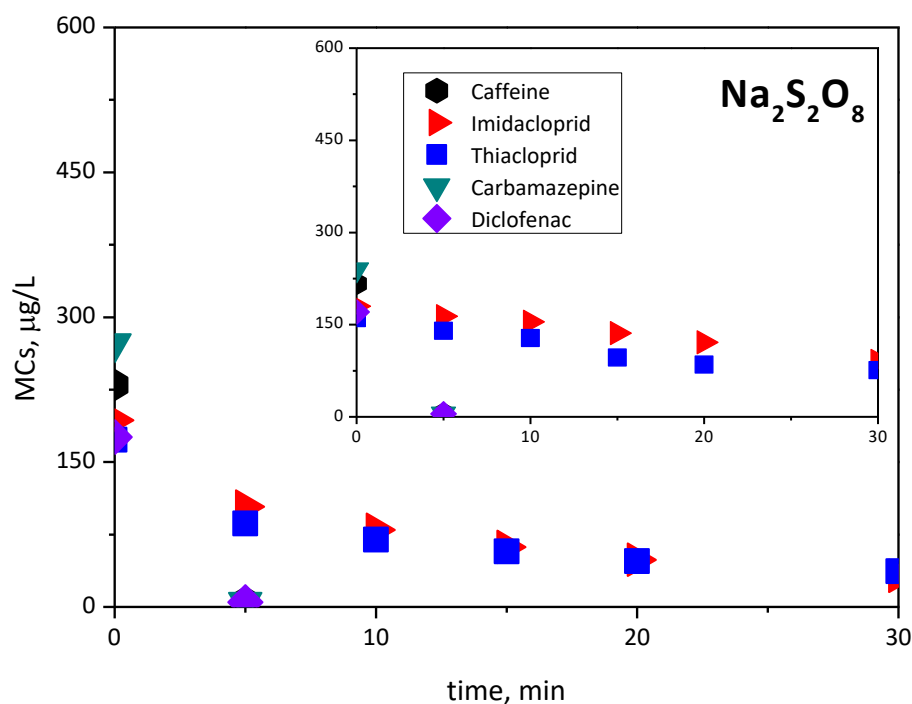


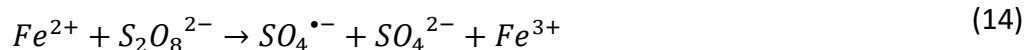
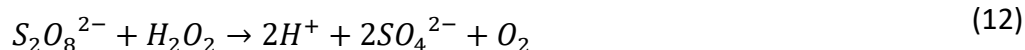
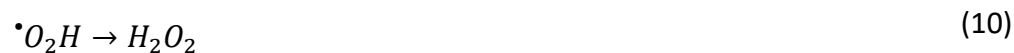
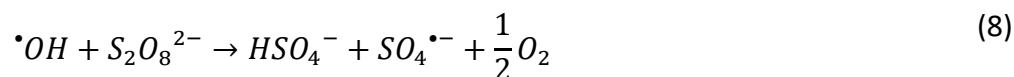
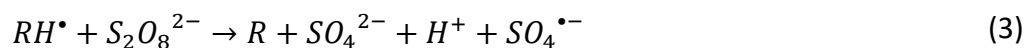
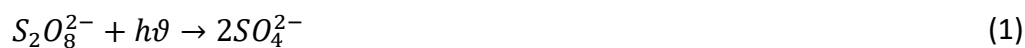
**Figure IV.4:** The solar photo-Fenton treatment applied at a pH of 3, with 0.20 mM of Fe(II) and 1.50 mM of H<sub>2</sub>O<sub>2</sub> on concentrate volume C1, showing the degrading concentrations of the MCs. When persulfate is used as an alternative oxidizing agent, the MC concentration decline is shown in the inset.

After 30 minutes of treatment, an IMI and THI elimination of 85 and 80%, respectively, was obtained. However, the increased iron concentration showed to have a minimal positive effect when comparing the first-order kinetic constants as calculated from the results in Figure IV.3. The H<sub>2</sub>O<sub>2</sub> consumption of 0.95 mM after 30 minutes was 20% higher than the basic experimental parameters (Fe 0.10 mM and 1.50 mM H<sub>2</sub>O<sub>2</sub>). Additionally to this, after a treatment time of five minutes, the H<sub>2</sub>O<sub>2</sub> consumption was 0.36 mM, which is over two times that of 0.1 mM of Fe(II). It is therefore, that the observed higher reaction rate with Fe(III):EDDS at natural pH at a pH of 3 cannot be assigned to the lack of oxidizing radicals caused by a low iron concentration. Instead, the high reaction rate could be assigned to the high sulfate concentration in volume C1, which scavenged hydroxyl and other radicals, or could be related to the different photoreactivity of the formed iron species formed with Fe(III):EDDS at a natural pH or a pH of 3.

Finally, persulfate was utilized as an alternative to H<sub>2</sub>O<sub>2</sub> as an oxidizing agent in order to find out if any improvement can be obtained when utilizing the traditional solar photo-Fenton process for the elimination of the selected MCs present in volume C1 at a pH of 3. Using persulfate as an oxidizing agent in the photo-Fenton process was previously described. [210,211]

#### IV. Results and Discussion

The mechanism behind the persulfate lies in its activation by a combination of factors such as an increase in temperature, radiation by UV-light, or through transition metals such as Fe(II) and Fe(III):EDDS (reactions (13-14); Figure IV.4 and Figure IV.5), which can all lead to the generation of highly oxidizing sulfate radicals ( $SO_4^{\bullet-}$ ), as is shown following reactions (1-12). [209]



These radicals possess a high redox potential, which is similar to the redox potential of  $\bullet\text{OH}$ , and rather than a direct reaction, react with the MCs through an electron transfer. This preference for an electron transfer provides a synergistic effect for the elimination of the MCs and thereby strengthens the Fenton process by reducing the pH of the water through the generation of sulfuric acid, as shown in Reaction (12). [212,213] Consequently, this approach delivers a promising alternative to the treatment with the conventional photo-Fenton process at a pH of 3, as it combines the presence of both  $\bullet\text{OH}$  and sulfate radicals, potentially with higher reaction rates as a result. However, in this work no clear improvement in the elimination of the selected MCs was observed when using persulfate as an oxidizing agent at a pH of 3, as shown in Figure IV.4.

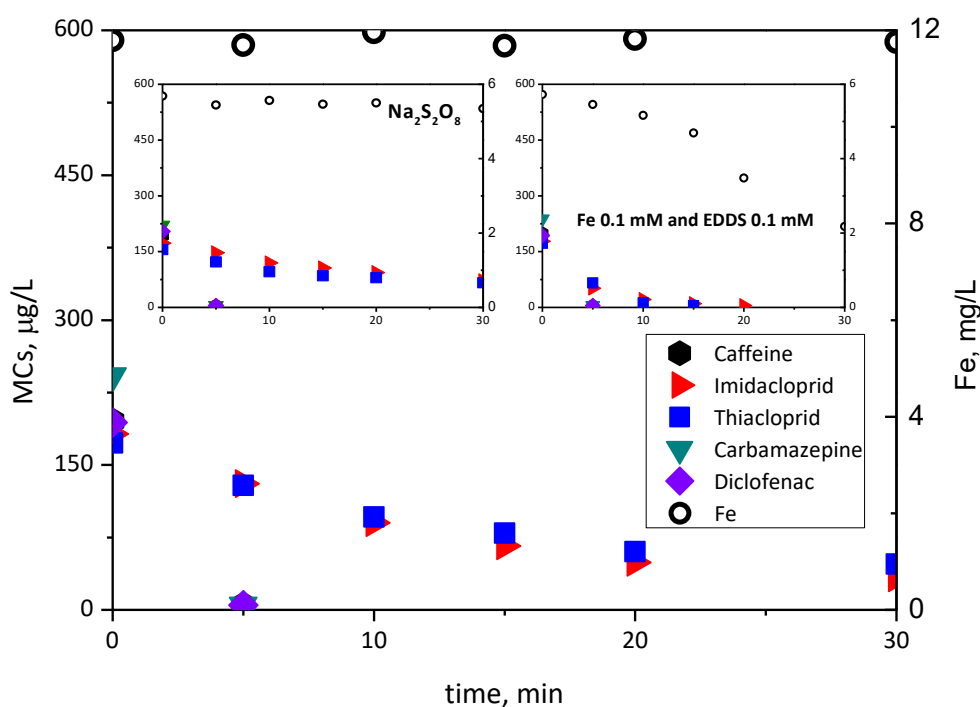


**Figure IV.5:** Dissolved iron evolution and MC concentration decline when applying the solar photo-Fenton treatment at a natural pH on concentrate volume C1, utilizing 0.20 mM of Fe(III): EDSS [1:1], and 1.50 mM of  $\text{H}_2\text{O}_2$ . The results when 0.10 mM of Fe(III):EDSS and the same ratio with persulfate (1.50 mM) as an alternative oxidizing agent are shown in the insets.

The MCs CAF, CAR, and DIC were eliminated to the LOQ of  $5 \mu\text{g/L}$  in less than five minutes. Generally, the first-order kinetic constants were lower when using persulfate as compared to the treatment with the classic photo-Fenton process using  $\text{H}_2\text{O}_2$  at a pH of 3. The values for CAF, IMI, THI, CAR, and DIC were  $0.753 \text{ min}^{-1}$ ,  $0.021 \text{ min}^{-1}$ ,  $0.028 \text{ min}^{-1}$ ,  $0.774 \text{ min}^{-1}$ ,  $0.706 \text{ min}^{-1}$ , respectively. The total persulfate consumption accounted for only 10% of the initial amount. Whereby, after 30 minutes of treatment, only 90% of IMI and THI were eliminated, at similar elimination rates as when using

## IV. Results and Discussion

H<sub>2</sub>O<sub>2</sub>. However, IMI exhibited greater persistence when persulfate was used as the oxidizing agent.

### 2.5 The Solar photo-Fenton process as tertiary treatment

Different operating parameters and their effects on the solar photo-Fenton method as a tertiary treatment at natural pH were investigated. Different factors, such as the concentration and ratio of Fe(III):EDDS (0.20 mM iron or half EDDS, 0.10 mM) and the use of an alternative oxidizing agent, persulfate instead of H<sub>2</sub>O<sub>2</sub>, was examined.

Starting with the first variety of the different operating parameters, Figure IV.5, where the concentration of the iron was doubled (0.20 mM, Fe:EDDS [1:1]), the MCs CAF, CAR, and DIC reached the LOQ by UPLC determination of 5 µg/L in less than five minutes. After 30 minutes, approximately 80% of IMI and 70% of THI was eliminated. The first-order kinetic constants were determined for all of the MCs, CAF, IMI, THI, CAR, and DIC, being 0.732 min<sup>-1</sup>, 0.061 min<sup>-1</sup>, 0.048 min<sup>-1</sup>, 0.776 min<sup>-1</sup>, and 0.732 min<sup>-1</sup>, respectively. During this time no iron precipitation was observed, while H<sub>2</sub>O<sub>2</sub> consumption was determined to be 1.35 mM. However, the increased iron concentration of 0.20 mM showed to result in negative effects regarding the elimination of IMI and THI at natural pH, which could be assigned to an excess of •OH, leading to its recombination into H<sub>2</sub>O<sub>2</sub>. A competition between EDDS and the MCs for the •OH seemed unlikely, as no iron precipitation was observed, which indicated stability of the Fe(III):EDDS complex during the experiment time.

In the case only half of the base concentration of EDDS was utilized (0.10mM), the MCs CAF, CAR, and DIC were eliminated to a concentration under the LOQ in less than five minutes. In total, over 90% of the total concentration of MCs were already eliminated after 15 minutes, having consumed 0.70 mM of H<sub>2</sub>O<sub>2</sub>, which totaled to 1.00 mM after 30 minutes of experiment time. The first-order kinetic constants for CAF, IMI, THI, CAR and DIC were calculated to be 0.737 min<sup>-1</sup>, 0.189 min<sup>-1</sup>, 0.241 min<sup>-1</sup>, 0.772 min<sup>-1</sup>, and 0.731 min<sup>-1</sup>, respectively. In comparison with the basic experimental parameters, slightly better MC elimination rates were obtained at lower H<sub>2</sub>O<sub>2</sub> consumption. Iron precipitation was however observed at an earlier time, resulting in a loss of iron during the solar photo-Fenton process. By reducing the DOC and minimizing the competition for the oxidants with the selected MCs, the lower EDDS concentration had a positive effect on the MC elimination at a natural pH.

When persulfate was used as an oxidizing agent at natural pH, the MCs CAF, CAR, and DIC were eliminated till under the LOQ in less than five minutes. A maximum elimination of 60% of the more recalcitrant IMI and THI was obtained after 30 minutes. The elimination rates were similar to those observed when using H<sub>2</sub>O<sub>2</sub> at neutral pH. Although, the persulfate consumption was significantly higher as compared to the experiment performed at a pH of 3. Overall, a substantial improvement in MC

degradation was not observed as compared to H<sub>2</sub>O<sub>2</sub> as an oxidizing agent at a neutral pH.

The reduction of toxicity of the treated water and effluents containing the selected MCs through treatment with the solar photo-Fenton process was extensively studied in recent research. [188,214,215] Given the existing abundance of information regarding the evolution of toxicity during the treatment with the solar photo-Fenton process, this aspect was chosen to be outside of the scope of Target 1. However, the toxicity reduction was confirmed by various bioanalytical tools, as is more extensively described in Target 2.

This Chapter IV – Target 1 corresponds to article:

Dennis Deemter, Isabel Oller, Ana M. Amat, Sixto Malato, **Effect of salinity on preconcentration of contaminants of emerging concern by nanofiltration: Application of solar photo-Fenton as a tertiary treatment**, *Science of The Total Environment*, **Volume 756**, 2021, 143593, ISSN 0048-9697, Available at: <https://doi.org/10.1016/j.scitotenv.2020.143593>. It is included as part of Annex B.



**Target 2. Recovery of valuable nutrients such as ammonium from saline waters during their preconcentration for the retention of MCs, with the aim to produce enriched crop irrigation waters for direct use. Followed by the application and assessment of different AOPs treatment methods for MC removal from the concentrate volumes, and a toxicity assessment of the permeate volumes.**

### 3 Applying Nanofiltration for ammonium recovery

The  $\text{NH}_4^+$  permeation through commercial NF membranes was investigated by utilizing demineralized water. In Figure IV.6 can be seen that the  $\text{NH}_4^+$  permeation was minimal at a pH of 4 and 7. At a pH of 9 however, there was a notable increase in permeation, especially when the feed tank had an initial concentration of 250 mg/L and 500 mg/L  $\text{NH}_4^+$ .

The permeation rate further increased as the CF reached CF= 4. This behavior can be assigned to the speciation of ammonia at different pH levels, while as the ammonia molecules dominate at a high pH value, the ammonium ions prevail at an acidic to neutral pH value. In effect, the non-charged ammonia species was rejected to a greater extent at a lower pH value as compared to the charged ammonium ions. The increment of the permeation volume over time, and so the CF, was influenced by the concentration polarization, which is the phenomenon where the concentration gradient across the membrane surface is affected by the transport of solutes.

The necessary  $\text{NH}_4^+$  concentration in the permeate stream, which can be used as a water for irrigation, could be decided based on various factors such as the crop type, the soil pH value, the soil composition, and the availability and preference for other nitrogen sources such as  $\text{NO}_3^-$ . Considering the specific requirements and characteristics of the crops being grown is therefore important.

#### IV. Results and Discussion

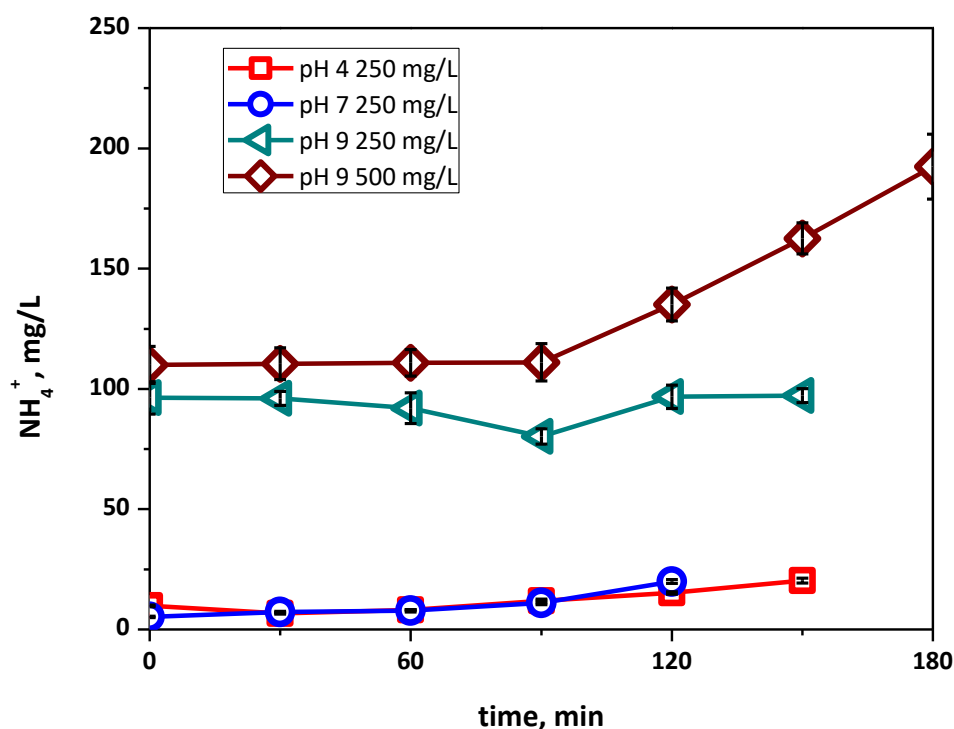


**Figure IV.6:** The concentration of  $\text{NH}_4^+$  in mg/L present in the permeate stream at different pH values and feed tank concentrations. The different experiments were performed till  $\text{CF} = 4$  was reached.

One of the potential drawbacks of  $\text{NH}_4^+$  is that when the plant absorbs it, the  $\text{H}^+$  ions are released, which leads to soil acidification. In certain cases, the  $\text{NH}_4^+$  fertilization can even be associated with toxicity, making its application somewhat contradictory. Nonetheless, it is essential to evaluate the potential negative effects of the soil acidification and toxicity against the provided benefits of this renewable and sustainable source of nitrogen in irrigation water, particularly in regions that are (semi-)arid where NF permeates have often a high pH value and the soil types been typically alkaline. The overall impact of  $\text{NH}_4^+$  rich irrigation water on the pH of the soil and the plant health must be carefully considered, while considering factors such as the nutrient availability, the necessity of the crop, and sustainability of the agricultural practices. [216–218]

Experiments were performed to investigate if the presence of the selected MCs at an initial concentration of  $100 \mu\text{g/L}$  each has an influence on the permeation of the  $\text{NH}_4^+$ . The experiments were performed at a pH of 9 with a concentration of  $500 \text{ mg/L}$   $\text{NH}_4^+$ . The results showed that the permeation of  $\text{NH}_4^+$  was similar to that shown in Figure IV.6, which indicates that the presence of the MCs in the wastewater did not significantly influence the  $\text{NH}_4^+$  permeation. In addition to this, when the experiments were repeated with an increased water conductivity, obtained by adding  $5 \text{ g/L}$  NaCl, the permeation volume of the  $\text{NH}_4^+$  stood the same.

Furthermore, the  $\text{NH}_4^+$  recovery was found to be highest at a  $\text{CF}=4$ , despite the higher MC permeation seen at this  $\text{CF}$ . This suggests that if the permeate is supposed to be utilized directly as a revalorized irrigation water, a  $\text{CF}=2$  is preferred. This, while at this  $\text{CF}$  the concentration of the recovered  $\text{NH}_4^+$  is high, while the MC permeation is relatively low, suggesting better suitability for irrigation purposes.

#### **4 Treatment of the Nanofiltration concentrate stream by the solar photo-Fenton process at lab and pilot scale**

Chosen experimental parameters for the treatment of the NF concentrate, in order to eliminate the present MCs, were based on previous results achieved with similar saline NF concentrates. [219] The goal was to minimize the concentration of consumables, such as the  $\text{Fe(III):EDDS}$  complex and the  $\text{H}_2\text{O}_2$  oxidizing agent, to keep the environmental and economic impacts low, while maintaining a high elimination efficiency.

The concentrate streams were created by operating the NF plant till 150 L of permeate, designated P1. After this, the NF was further operated till a permeate volume of 50 L was obtained and was designated as P2. The final result, a concentrate volume of around 200 L ( $\text{CF}=2$ ), was labelled C1. Another batch was created by directly permeating the starting volume of 400 L, till 100 L of concentrate was left. This concentrate was then designated as C2 ( $\text{CF}=4$ ).

For the treatment of sample C2, which had a  $\text{CF}=4$ , on a lab scale level in a solar simulator with solar photo-Fenton, a concentration of 0.10 mM  $\text{Fe(III):EDDS}$  [1:1] and 1.50 mM  $\text{H}_2\text{O}_2$  at pH 9 were used.

As high concentrations of bicarbonates can be found in natural water at a pH of 9 (450 mg/L), the reaction rates for the solar photo-Fenton were very slow. Also when utilizing persulfate as an oxidizing agent at a concentration of 1.50 mM did not yield satisfactory results. The reason for this is that bicarbonates are known scavengers of  $\bullet\text{OH}$  and other radicals and can lower the performance of the solar photo-Fenton process, as was also reported in previous studies. [205] In order to address this issue, further experiments were performed at a circumneutral pH (between pH 6.5 and 7.9) by adding  $\text{H}_2\text{SO}_4$  and air stripping to lower the bicarbonate concentration to under 75 mg/L.

In Figure IV.7 the elimination of CAR and DIC to the Limit of Quantification (LOQ) (5  $\mu\text{g/L}$ ) in respectively 15 and 10 minutes can be seen. CAF, IMI, and THI had lower elimination rates, with only 82, 54 and 55% of degradation in the first 15 minutes, and a bare minimum of degradation between 15 and 30 minutes. The reason for this was the low concentration of iron in solution available as the  $\text{Fe(III):EDDS}$  complex decomposed. [203,214] As the iron precipitated directly, a strong decline was observed foremost between 5 and 10 minutes while completely precipitated at 20 minutes. After 30 minutes the  $\text{H}_2\text{O}_2$  consumption was 0.95 mM with the highest consumption during the first 5 minutes.

#### IV. Results and Discussion

In order to determine the degradation by photolysis, blank experiments were performed where CAF, IMI, THI, CAR and DIC did not show significant degradation after illumination by simulated sunlight for 30 minutes.

When using persulfate as the oxidizing agent at circumneutral pH, lower elimination rates for the MCs were observed. The LOQ was reached for both CAR and DIC, which were both degraded in under 5 minutes, while CAF was degraded in 15 minutes. Nonetheless, IMI and THI showed more persistence, with only 24 and 20% of degradation, respectively. The iron concentration declined gradually from the start of the treatment, with only 10% remaining after 30 minutes. The persulfate consumption during the first 5 minutes of the treatment was 0.87 mM. Normally, sulfate radicals show slower reaction rates than  $\bullet\text{OH}$ , while strongly depending on the target MCs, the initial iron concentration, and the EDDS concentration, as was also reported in previous studies. [220,221]

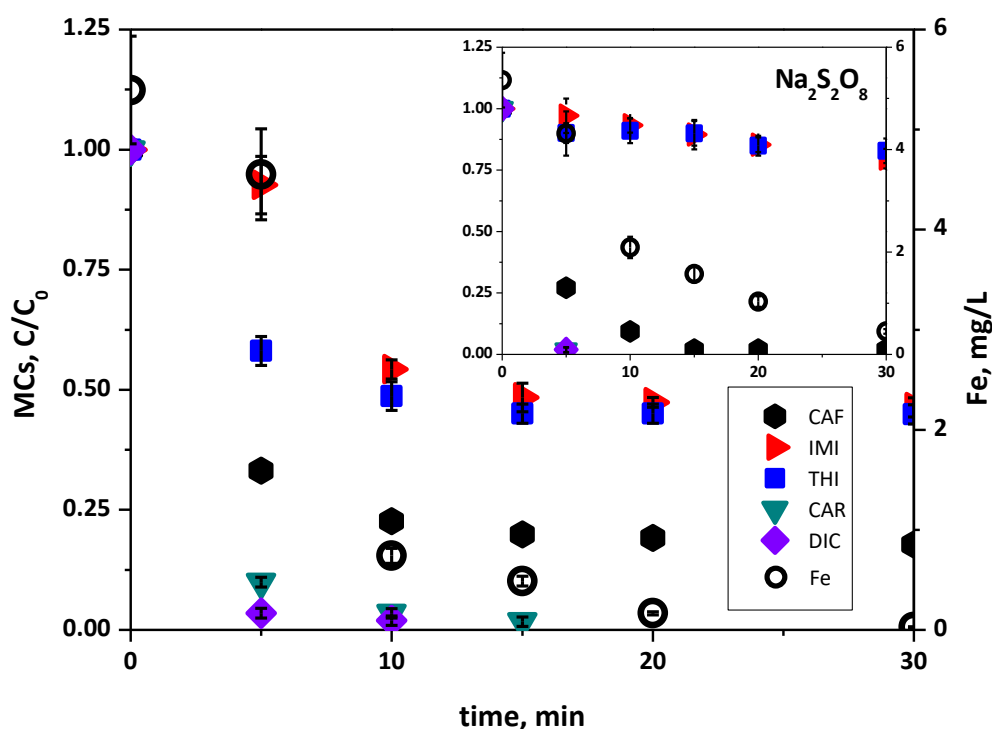


**Figure IV.7:** The evolution of the dissolved iron and MC concentration during the treatment of concentrate volume C2 with photo-Fenton, with an initial concentration of Fe(III):EDDS of 0.10 mM [1:1], applying H<sub>2</sub>O<sub>2</sub> and persulfate at a concentration of 1.50 mM in the solar simulator at a circumneutral pH.

Figure IV.8 shows the solar photo-Fenton treatment applied on concentrate volume C2 at pilot scale in an 80 L CPC photoreactor, with solar accumulated UV energy (Equation III.3) measured in the photoreactor after 30 minutes. As only DIC was degraded to the LOQ after 30 minutes, and 93% degradation of CAR. CAF, IMI, and THI, showed once again similar results as in the solar simulator with only 70, 49 and 39% of degradation, respectively, at 30 minutes. The total MC degradation reached

76% with only 1.6 kJ/L of accumulated UV energy. During the 30 minutes over 90% of the Fe(III):EDDS complex was degraded, which confirms the inefficiency of the MC elimination at circumneutral pH after the degradation of the complex. At the end of the experiment, H<sub>2</sub>O<sub>2</sub> consumption accounted for a total of 0.83 mM.

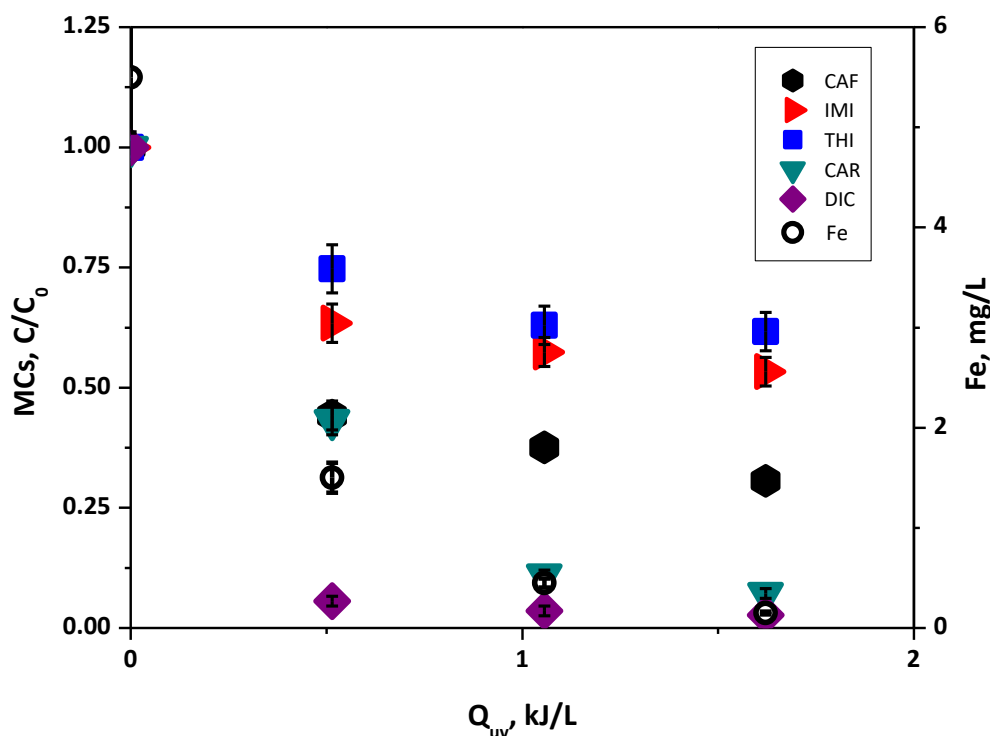


**Figure IV.8:** The evolution of the dissolved iron and MC concentration during the treatment of concentrate volume C2 with solar photo-Fenton at a circumneutral pH, performed in the pilot plant.

## 5 Treatment of the concentrate stream volumes by electrooxidation

In a solar photoelectron-Fenton (SPEF) pilot plant electrooxidation (EO) experiments were conducted using the experimental parameters previously given in Chapter III – 4.5. First, the EO experiments were applied on concentrate volume C2 (CF=4), as it is the most concentrated stream. This will make it a viable comparison with following EO treatments. It is noteworthy that however, that higher concentrations of ions, carbonates, and MCs could result in increased radical scavenging effects, which was also mentioned before.

In Figure IV.9 the results can be seen when treating concentrate volume C1, containing its natural concentration of carbonates and pH, with AO, SAAO, EF, and SPEF oxidation treatment methods. In the case AO was applied, the degradation of MCs till the LOQ was achieved at different times for the different compounds. CAF, THI, CAR, and DIC, were degraded in less than 150, 180, 45, and 150 minutes, respectively. IMI showed to be more persistent reaching only 67% of degradation, still leading to a total MC

#### IV. Results and Discussion

degradation of 88%. When applying solar assisted anodic oxidation (SAAO), CAR and DIC were the only two MCs that were degraded to the LOQ, at 180 and 45 minutes respectively, while CAF showed degradation to 84%. Once again IMI, and this time also THI, showed themselves to be more persistent with 44 and 57%, respectively, resulting in a total MC degradation of 78%. Lastly, when applying SPEF, CAR and DIC were degraded to the LOQ, in less than 180 and 45 minutes, respectively. The MCs CAF, IMI, THI were once again more persistent, showing only 82, 44, and 78%, respectively, with a total MC degradation of 80%.

Looking at the results of the treatment of concentrate volume C1, the target of a degradation of 80% was not reached by EF, not even after a treatment time of 240 minutes. In addition to this, more consumables, such as the complexing agent EDDS were consumed, which in its turn significantly increases the DOC in the matrix, making it compete with the MCs for the radicals. Also, EF consumed over 50% more electric energy than AO, while producing more free available chlorine. Noting that its chlorate production was 15% lower. For these reasons, EF was considered unsuitable for the treatment of this type of water, which was also reported in previous work. [222]

When applying the AO treatment the target of 80% MC degradation was obtained after a treatment time of 120 minutes. The electric energy consumption for the treatment of 30 L was 6.1 kWh/m<sup>3</sup>. The final concentration of produced free available chlorine (FAC) was 3.4 mg/L, while the chlorate production was registered after 10 minutes of treatment time from 20.4 mg/L progressing linearly to 70.0 mg/L after 240 minutes of treatment time.

The beforementioned compounds FAC and chlorate are by products of the EO process. The formation of these compounds proceed from the high concentrations of free dissolved ions, in particular chloride ions, present in the water matrix. Active chlorine, a compound generated from free dissolved chloride ions, is commonly used in wastewater treatment. Active chlorine species (ACS) are created by the adsorption of free dissolved ions from the water matrix on the surface of the anode, which leads to the formation of radical or other oxidizing species related to the specific ions. The formation of indirect ACSs are taking place when these oxidizing species, which were generated previously, act as intermediates in the degradation reactions of the MCs in the bulk of the treated water matrices, furthest from the anode. [223] The ACSs which usually play a crucial role in the MC degradation is also known as electrochlorination, which offers certain advantages over the conventional water treatment methods that involve only chlorine. These include improved performance and the absence of dangerous chlorine transport and storage. [224,225] In the case a BDD anode is used for the treatment of wastewater, chlorates are formed through the reaction of an ACS with an  $\bullet\text{OH}$ . [226]

When applying the SAAO treatment on concentrate volume C1, the MC degradation target of 80% was just not reached with a total degradation of 78% after 240 minutes. The electric energy consumption was in total 3.8 kWh/m<sup>3</sup>, which is 62% as compared to AO. The required UV energy consumption ( $Q_{UV}$ ) was 13.3 kJ for a total volume of 75 L. The final FAC concentration was 4.2 g/L, while the chlorate concentration was 33.3 mg/L, good for an increase of 23% in FAC and 52% in chlorate, as compared to AO.

SPEF treatment was able to obtain an 80% degradation of MCs in less than 240 minutes of treatment time. To reach this, 4.2 kWh/m<sup>3</sup> of electric energy was consumed and 14.2 kJ/L for a total volume of 75 L, being 11 and 7 % higher, respectively, when comparing to SAAO. The enhancement of the process by Fe:EDDS showed no significant improvement on the degradation of the MCs, as also the DOC is increased by this addition. The concentration of FAC at the end of the experiment was in total 2.1 mg/L, while chlorate was only 16.4 mg/L, 50% lower than with the SAAO treatment. This can be assigned to the reaction between H<sub>2</sub>O<sub>2</sub> and ACS.

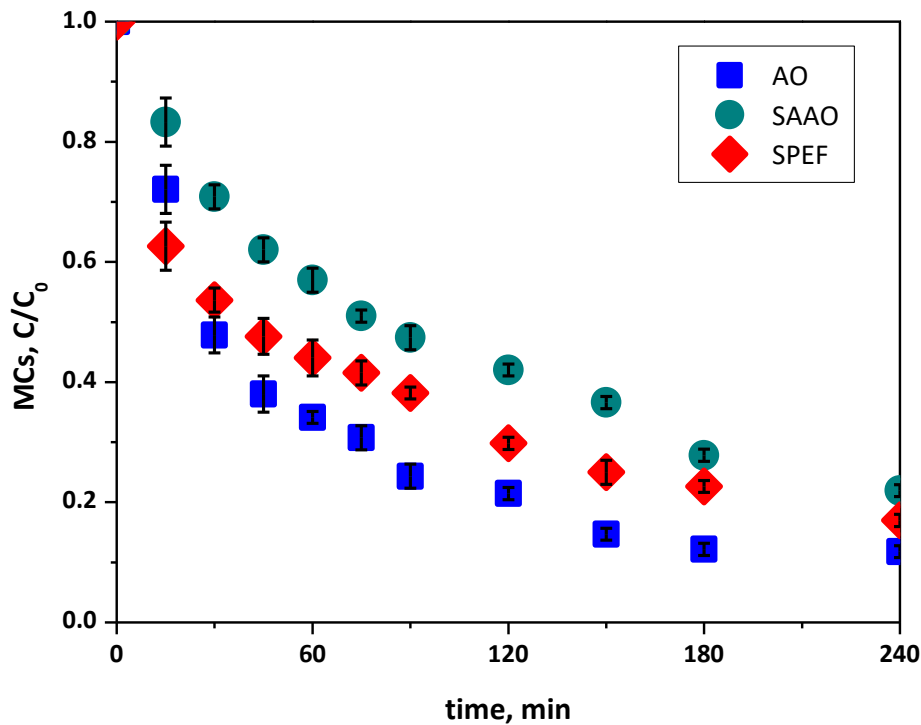


**Figure IV.9:** The evolution of the MC concentration in concentrate volume C1 (CF= 2) during the treatment with AO, SAAO, and SPEF, at its natural pH.

The initial reaction rate ( $r_0$ ) was calculated in order to make a comparison between the different EO treatment methods by utilizing the MC mass instead of the MC concentration as a function of the experimental volume, as described in Equation IV.1.

$$r_0 = \frac{(m_{n+1} - m_n)}{(t_{n+1} - t_n)} \quad \text{Equation IV.1}$$



#### IV. Results and Discussion

For which  $m_n$  is the cumulative mass of MCs at a designated time in mg, as calculated for the concentration of MCs and the water volume that is treated, which were 30 L for AO and 75 L for both SAAO and SPEF, and  $t_n$  the time interval in minutes for yielding  $r_0$  in mg/min. For the treatment methods AO, SAAO and SPEF  $r_0 = -0.337$  mg/min;  $-0.0696$  mg/min; and  $-1.305$  mg/min, respectively.

Figure IV.10 shows the results of the treatment of concentrate volume C1 with SPEF, this time with lower concentrations of bicarbonates (76.3 g/L). The goal of this experiment was to discover if high concentrations of carbonates are as disadvantageous as during treatment with the photo-Fenton process. [219] Only CAR and DIC were degraded to the LOQ in 150 and 60 minutes, respectively, whereas CAF and THI were both degraded with 82%, while IMI persisted with only 49% of degradation. The total MC degradation was just over the target of 80% with 82%. This demonstrates that the influence of carbonates on the SPEF treatment is negligible, and that the oxidation of MCs mainly occurred through oxidants other than  $\bullet\text{OH}$ . Therefore, the analysis of the chlorinated byproducts would be crucial for a comprehensive assessment of the system and for the design of the most applicable treatment.

Performed at low concentrations of carbonates, the SPEF treatment obtained the target degradation of 80% in less than 220 minutes, while consuming 4.3 kWh/m<sup>3</sup> and a  $Q_{UV}$  of 11.6 kJ/L. The FAC production was the highest of all treatment methods with a final concentration of 5.7 mg/L, whereas the final chlorate concentration was 18.2 mg/L, which is similar to the treatment with a high carbonate concentration. In addition to this, the SPEF treatment at low carbonate concentrations had a reaction rate of -1.155 mg/min, which was 11% lower than that observed at high carbonate concentrations.

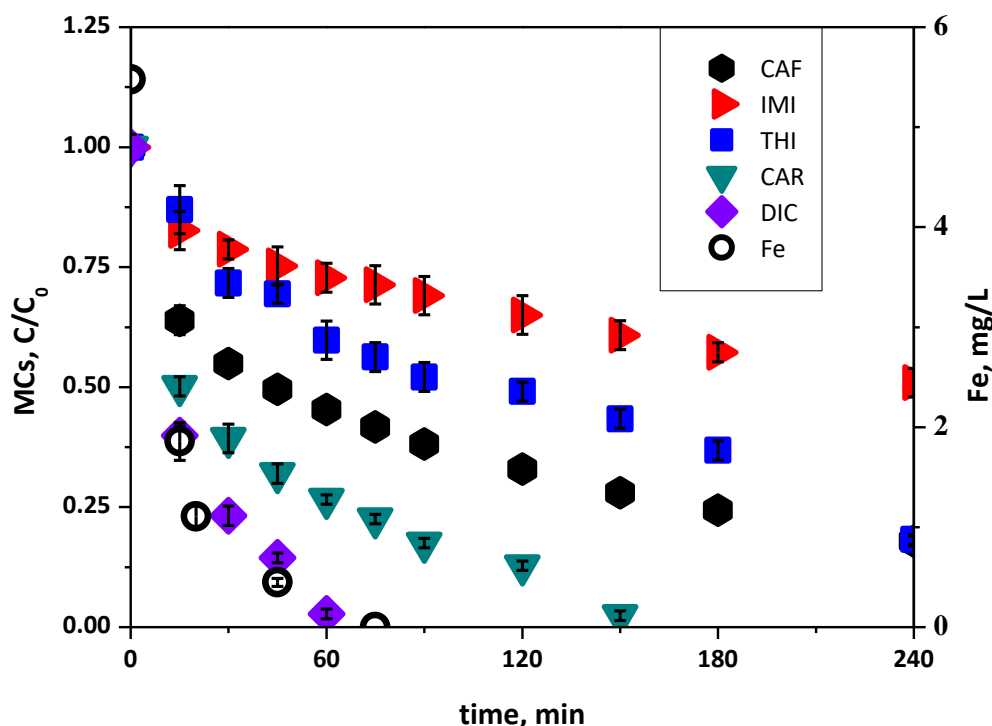


**Figure IV.10:** The evolution of the MC concentrations in concentrate volume C1 (CF= 2) at its natural pH during the treatment with SPEF at pilot scale, performed at low concentrations of carbonate.

## 6 Determination of acute and chronic toxicity of the Nanofiltration streams

One of the principal objectives of this work was to recover and reuse the  $\text{NH}_4^+$  present in the NF permeate stream obtained from the preconcentration of the UWWTP effluent for crop irrigation. In order to assess the impact of the produced permeate volumes on the seed germination, root and shoot growth, phytotoxicity tests were performed on the permeate volumes at a concentration of CF= 2 and CF= 4. The toxicity of the permeate volumes were tested at pH 7. Both the permeates of CF= 2 and CF= 4 showed a minor impact on the germination of *Sorghum saccharatum*, by causing a reduction of 10%. In addition to this, the permeate volume with CF= 2 also caused a reduction of 10% in germination of *Sinapis alba*.

The root development of *Sorghum saccharatum* was positively affected by the permeate volume at CF= 2, which increased it by 45% as compared to the reference sample for which demineralized water was used. A similar case was observed for *Sinapis alba* which showed a 17% increase in root development with the same CF= 2. For *Lepidium sativum*, a significant decrease was observed in its root development, showing a decrease of 27% and 46% for CF= 2 and CF= 4, respectively.

#### IV. Results and Discussion

When observing the shoot length, permeate volume CF= 4 caused a 40% reduction in *Sorghum saccharatum*, while permeate volume CF= 2 led to a 13% increase. *Sinapis alba* showed a 9% reduction in its shoot growth when applying CF= 2 and even a 39% reduction with permeate volume CF= 4. Also this time *Lepidium sativum* showed different results, whereas its shoot growth was positively affected by permeate volume CF= 2, increasing it by 11%, and for permeate volume CF= 4 an increase of 17% was observed.

Evaluating these results, it can be concluded that in the case of direct use of the permeate stream for crop irrigation of CF= 2 is suitable, looking at the root and shoot growth. However, the application of the permeate volume with CF= 4 cannot be advised due to its relatively high MC concentration and salt content.

Further testing was performed by using the DAPHTOXKIT F in order to determine the acute toxicity at 24 and 48 hours and its chronic toxicity at 72 hours, by observing the immobilization of *Daphnia magna* in the permeate volumes and comparing them to standard freshwater samples. The results of these tests can be seen in Figure IV.11. After 24 hours, no immobilization of the *Daphnia magna* was observed at dilutions of 12.5%, 25%, and 50% of permeate volume CF= 2. In the case of a concentration of pure (100 %) CF= 2, only one organism showed movement. Similar results were observed for permeate volume CF= 4, excluding the 100% sample, where immobilization of all *Daphnia magna* was observed. After a time of 48 hours, the dilutions of 12.5%, 25%, and 50% of permeate volume CF= 2 showed 0, 2, and 3 out of 5 immobilized organisms, respectively. Once again with the 100% sample, all *Daphnia magna* were immobilized, showing similar results for the permeate volume with CF= 4. After 72 hours, immobilization was observed for 3 out of 5 *Daphnia magna* in the control sample. In the case of the permeate volume with CF= 2, looking at the dilutions with a concentration of 12.5%, 25%, and 50%, 2, 3, and 4 organisms were immobilized, which was comparable with the permeate sample with CF= 4. It was therefore concluded that both permeate volumes should be diluted with at least 50% in order to prevent osmotic stress and acute toxicity. Thereby, it was notable that at a 25% dilution, only the permeate volume of CF= 2 showed chronic toxicity results similar to the standard freshwater conditions.

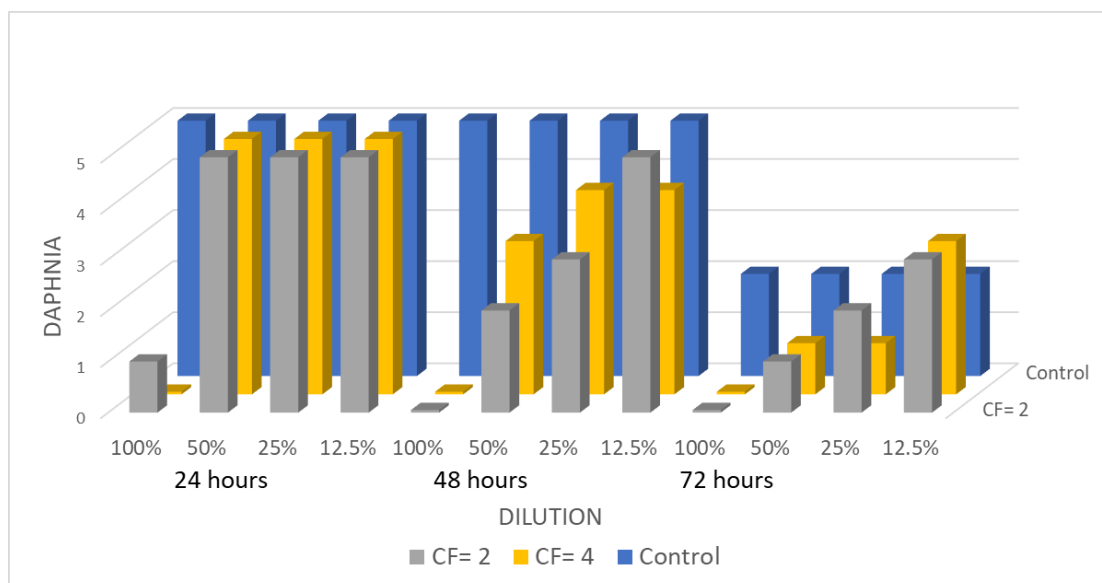


**Figure IV.11:** Performed toxicity tests, acute toxicity measured at 24 and 48 hours, and chronic toxicity measured at 72 hours, applying *Daphnia magna* organisms at different dilutions in freshwater. In the front permeate volume CF= 2 is shown, followed by permeate volume CF= 4 in the middle and the freshwater control in the back.

**This Chapter IV – Target 2 corresponds to article:**

Dennis Deemter, Irene Salmerón, Isabel Oller, Ana M. Amat, Sixto Malato, **Valorization of UWWTP effluents for ammonium recovery and MC elimination by advanced AOPs**, *Science of The Total Environment*, **Volume 823**, 2022, 153693, ISSN 0048-9697, Available at: <https://doi.org/10.1016/j.scitotenv.2022.153693>. It is included as part of Annex B.

**Target 3. Development of a novel self-cleaning photocatalytic membrane. The assessment of the fouling and self-cleaning capabilities by the registration of flux restoration during the filtration of real urban wastewaters, followed by material evaluation, before and after solar irradiation. The quantification and effects of water turbidity reduction for the application of subsequent treatments. Quantification of the bacterial present in water retention by the newly developed photocatalytic membrane.**

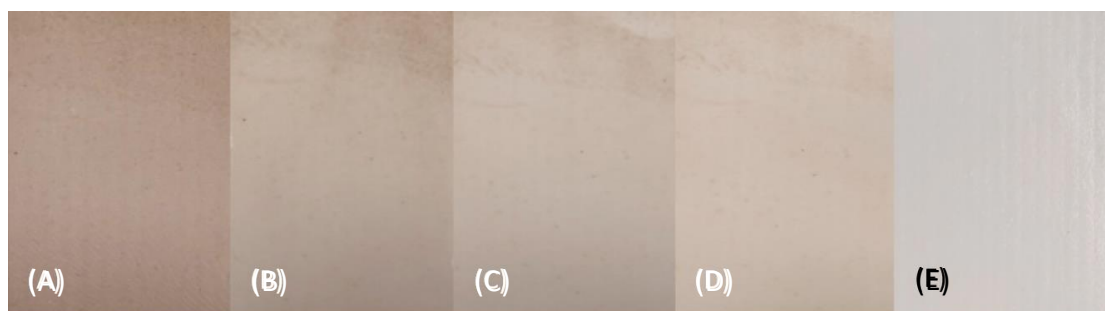
## 7 The fouling and self-cleaning properties of the photocatalytic membrane

A ceramic UF membrane, which was developed in previous work and is made from  $\text{TiO}_2\text{-ZrO}_2$ , was assessed for its self-cleaning properties, and fouling reversing capabilities. [227] The ceramic UF membrane can be used to filter UWWTP effluents, as a pretreatment to further water treatment such as with AOPs, by significantly lowering the turbidity of these matrices, which enhances the efficacy of the applied AOP treatments. The photocatalytic capabilities are potentially able to prolong the operation times of the membrane before it is too severely fouled to operate. Furthermore, the irradiation of the ceramic UF membranes surface by sunlight could be able to reverse the fouling of the membrane when filtering UWWTP effluents, and prevent the formation of a biofilm, which is also known as biofouling. Finally, the ability of the ceramic UF membrane to retain bacteria such as *E. Coli* and *P. Aeruginosa* is of great use when the UWWTP effluents are to be used for direct crop irrigation or simply discharged into nature, under conditions where multidrug resistance can be developed.

The  $\text{TiO}_2\text{-ZrO}_2$  self-cleaning UF membrane was used to filter multiple batches of UWWTP effluent. The turbidity of these batches ranged between 8.7 and 21.3 NTU. The filtration was performed till a concentration factor of  $\text{CF} = 2$  was achieved, showing a slight increase in the pH value for the concentrate volume. The turbidity of the resulting permeate volume, measured at regular intervals, increased from 0.4 to 0.6 NTU. The TSS concentration in the different produced permeate volumes ranged from 0.6 to 1.3 mg/L.

In order to evaluate the self-cleaning capabilities of the UF membrane, a continuous filtration of UWWTP effluent was performed for six hours to foul the UF membrane, Figure IV.12-A. After this period of time, the fouled UF membrane was irradiated by simulated sunlight in a beaker glass filled with demineralized water, while gently stirred. The beaker was placed in the middle of the solar simulator while being irradiated for one hour following the settings as described in Chapter III – 4.6 to reverse the fouling, Figure IV.12-B. This was followed by another hour (Figure IV.12-C), and again for another hour (Figure IV.12-D), having irradiated the UF membrane for a total of three hours. Figure IV.12 shows a consistent gradual cleaning of the membrane surface, although a full reversal of the fouling to its initial state, Figure IV.12-E, was not achieved.

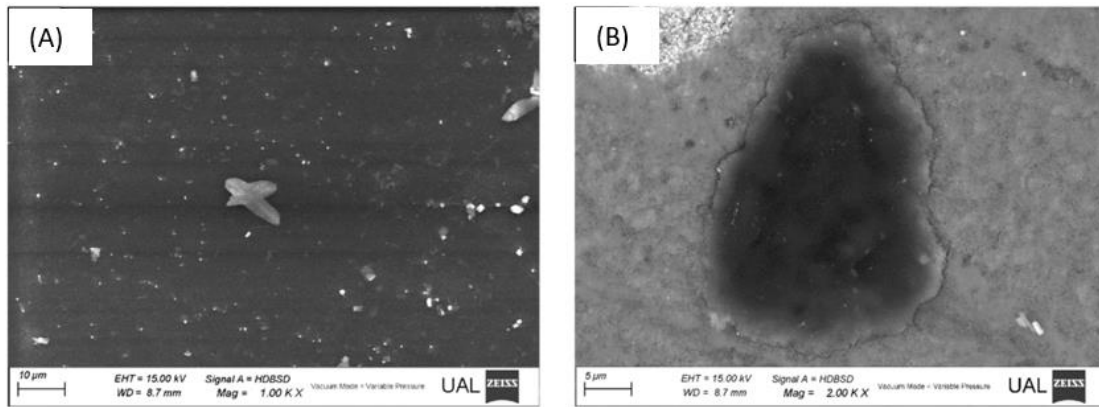
#### IV. Results and Discussion



**Figure IV.12:** The cleaning evolution of the membrane surface in demineralized water in the solar simulator. The pictures were taken by conventional photography of the surface, after operating for 6 hours during the filtration of UWWTP effluent (A), and after irradiation with simulated sunlight for 1 hour (B), 2 hours (C) and 3 hours (D), as compared to a fresh membrane surface (E).

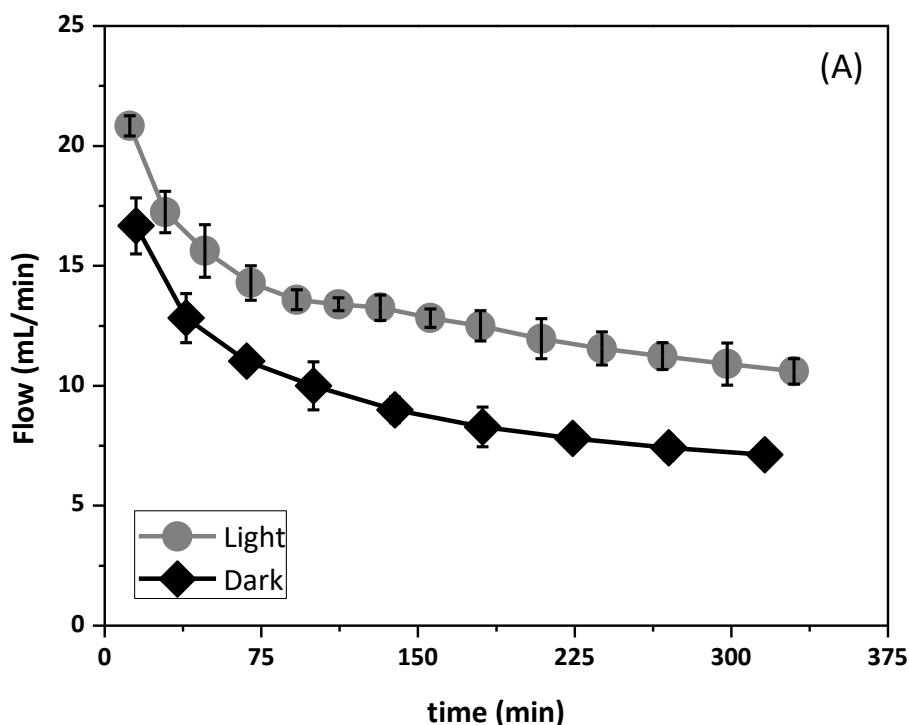
After irradiating the severely fouled membrane for three one-hour periods, an improvement in condition could clearly be observed. Therefore, another fouled membrane sample was rinsed and placed in a beaker glass with demineralized water under gentle stirring for three hours without irradiation, in order to validate the self-cleaning effect. Not even after manual cleaning of the UF membrane the fouling was reversed to the degree as was observed before with irradiation, showing the efficacy of the photocatalytic membrane surface when irradiated.

Both the initial state of the fouled UF membrane (Figure IV.13-A) and after three hours of self-cleaning under simulated solar irradiation (Figure IV.13-B) were examined by SEM. The surface of the UF membrane appears dark grey due to the presence of organic material and fouling, which was confirmed by EDX, having a carbon atomic percentage of over 90%. The dark spot that can be observed in Figure IV.13-B can be identified as residual fouling surrounded by the  $\text{TiO}_2$  photocatalytic layer. The light-white area in the upper left corner can be identified as a minor defect in the  $\text{TiO}_2$  layer resulting from the previously mentioned manual cleaning.



**Figure IV.13:** Images made by SEM after 6 hours of filtrations (A), and after cleaning by irradiation with simulated sunlight (B).

In order to validate the recovery of the membrane's physical properties, that is the porosity and not simply the visual properties of the membrane, further filtration experiments were conducted, to specifically measure the time required to obtain 250 mL of permeate volumes. This was performed to assess if the cleaning process could affect the filtration time and restore the UF membrane's initial filtration capability, Figure IV.14. The normalized flow rate, as seen in Figure IV.14-B, shows the change in flow rate relative to the initial flow and how it decreases due to the reasons stated below. Remarkably, a clear difference can be observed between the UF membrane kept in the dark and the UF membrane that was irradiated with simulated sunlight during filtration. This further demonstrates the self-cleaning properties of the TiO<sub>2</sub> photocatalytic UF-membrane when applied for the filtration of UWWTP effluent under solar irradiation.





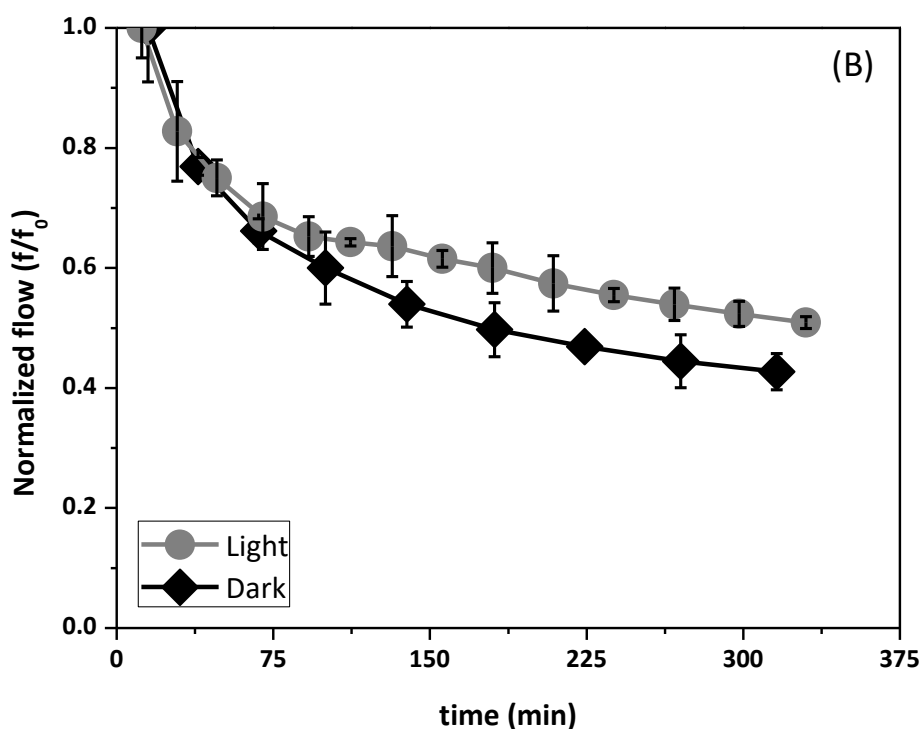


**Figure IV.14:** The measured flow during filtration experiments of UWWTP effluent, with flow rates in mL/min in the dark and in the light (A), and normalized flow rates ( $f/f_0$ ) in the dark and under irradiation by simulated sunlight.

The comparison between flow rates reveals that the original flow rate of 21 mL/min observed when irradiating is higher than the 17 mL/min rate when kept in the dark. This difference can be assigned to the inhibitory effect of the membrane's photocatalytic surface on the attachment of the suspended matter present in the UWWTP effluent. Furthermore, the phenomenon of photo-induced superhydrophilicity (PSH) caused by the  $\text{TiO}_2$  contributes to even higher flow rates and reduced fouling, as was also previously observed, and reported in other studies. [227–229]

A substantial decrease in flow rate can be observed within the first 60 minutes of the experiment, both when kept in the dark and when irradiated by simulated sunlight. This can be assigned to the accumulation of fouling within the membrane pores that are shielded from the irradiated light. Between 60 and 120 minutes, a clear distinction can be made between the curves of the normalized flow rate under irradiation with simulated sunlight (Figure IV.14-B), indicating that there is no photodegradation of fouling on the outer membrane surface when the UF membrane is kept in the dark. After 120 minutes, the curve of when the UF membrane is irradiated follows a similar trend as compared to the curve when the UF membrane is kept in the dark, which suggests that both membranes experience comparable trends of internal fouling, while the outer surface of the irradiated membrane remains clean.

During the experiment in the dark, a total of 1 L of permeate was produced when operating for 120 minutes.

The following experiment was the examination of the impact of the self-cleaning on the fouled membrane after 60 minutes of irradiation by simulated sunlight on the membrane surface, which corresponds to the required filtration duration, as derived from the deviation in the curve of normalized flow between the experiments when the UF membrane was kept in the dark and when irradiated. In addition, the UWWTP effluent was spiked with 100 µg/L of each of the target MCs, CAF, IMI, THI, CAR, and DIC.

In Figure IV.15, the flow rate is shown during the initial filtration of 1 L of UWWTP effluent while the UF membrane was kept in the dark. Then, the UF membrane was irradiated for 60 minutes without filtration. Followed by a second cycle where 2 L of UWWTP effluent was filtered in the dark, and cleaning once again for 60 minutes equally to the first time. Finally, a third (final) filtration of UWWTP effluent was performed. The results show that filtration of a certain volume of UWWTP effluent in the dark is only possible till a certain level of fouling. However, the initial conditions can be restored after irradiation if the fouling degree was not too severe.

This shows the essence of defining and optimize the operating variables when utilizing the photocatalytic UF membranes to preserve their self-cleaning capabilities. Due to the high porosity of the membrane no retention of the target MCs was observed, nor any difference in the operation of the membranes with UWWTP effluent, with or without MCs, as the self-cleaning properties eliminated most of the fouling.

#### IV. Results and Discussion

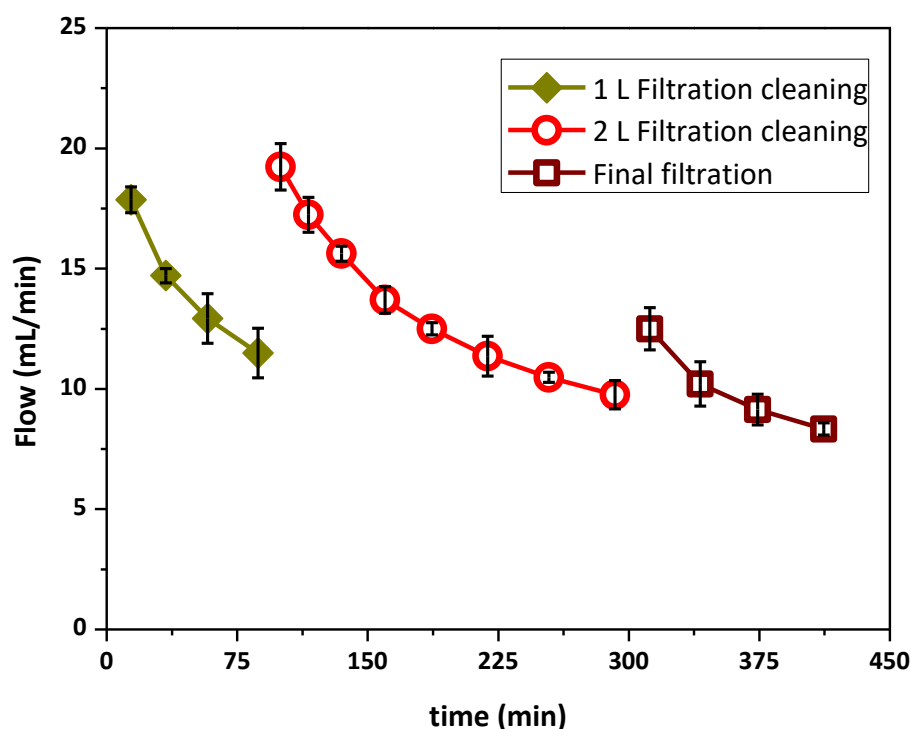


**Figure IV.15:** The measured flow and its recovery during filtration of UWWTP effluent spiked with 100  $\mu\text{g/L}$  of each MC, in the dark and the recovery due to the self-cleaning properties under irradiation with simulated sunlight. Filtering first 1 L of UWWTP effluent, followed by 60 minutes of irradiation; the filtration of 2 L of UWWTP effluent, followed by 60 minutes of cleaning; and consecutively another filtration of 1 L of UWWTP effluent.

Not only the previously mentioned super-hydrophilicity mechanisms of the  $\text{TiO}_2\text{-ZrO}_2$  UF membrane contribute to the self-cleaning capabilities. Another mechanism that prevents the fouling by various compounds on the membrane surface is the formation of radical species, such as  $\cdot\text{OH}$  and others, when the membrane surface is irradiated by a photon energy equal or greater than the semiconductor band gap energy. These radical species are able to degrade organic material and to eliminate biofouling. [230] The specific band gaps of the UF membrane are 2.5 and 3.1 eV, as a result of the  $\text{TiO}_2\text{-ZrO}_2$  mixture, as described in previous work. [227]

### 8 Treatment of the membrane streams by solar photo-Fenton

The photocatalytic UF membrane's impact on the filtration of UWWTP effluent was assessed during further treatment of the produced concentrate and permeate volumes by solar photo-Fenton treatment. Whereas both volumes still contained the initial concentrations of the target MCs as they were not retained by the UF membrane. The photocatalytic UF membrane offers the advantage of pretreating the UWWTP effluents, and so, reducing their turbidity and particle concentration, enhancing the photon availability for the solar photo-Fenton process. Experiments were performed using 0.1 mM  $\text{Fe(III):EDDS}$  [1:1] and 1.50 mM  $\text{H}_2\text{O}_2$  as the oxidizing

agent for solar photo-Fenton treatment, as was found to be the optimum in Chapter IV – Target 1.

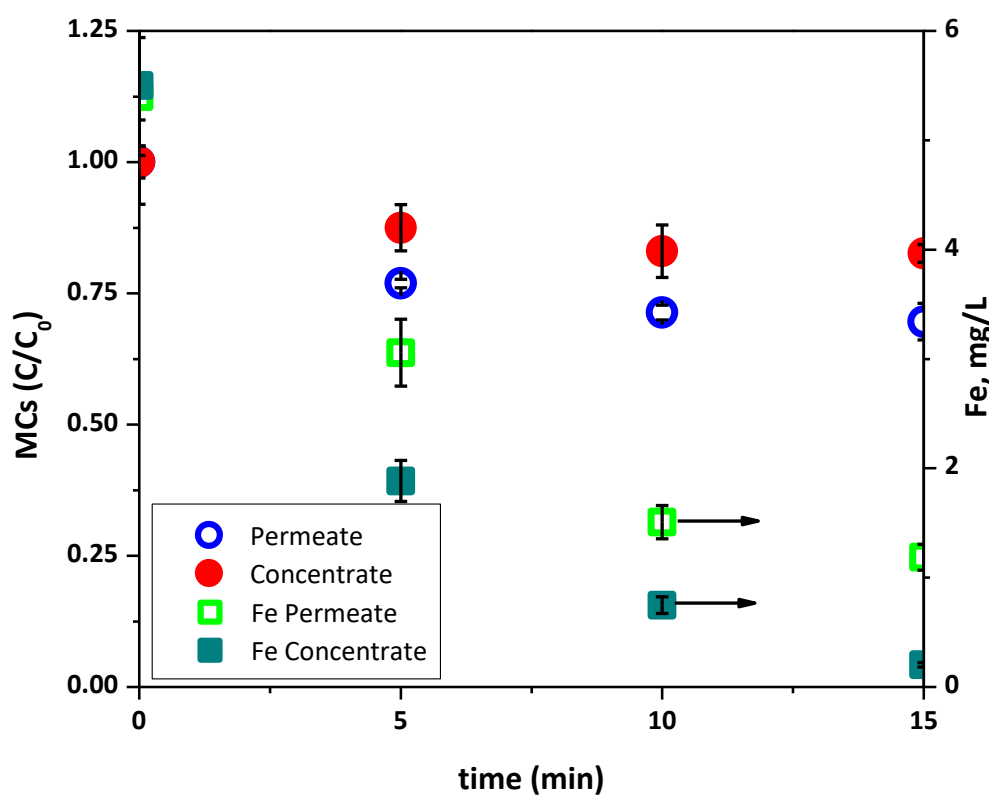


**Figure IV.16:** The evolution of the MC concentration of the permeate stream and the concentrate stream in the UWWTP effluent during solar photo-Fenton treatment and the evolution of the dissolved iron in the solar simulator, using 0.10 mM of Fe(III):EDDS and 1.50 mM of H<sub>2</sub>O<sub>2</sub>.

Applying solar photo-Fenton treatment on the concentrate volume, containing its natural bicarbonate concentration of 720 mg/L, a slight degradation of MCs was achieved. A degradation of 16, 12, 9 and 27% of CAF, IMI, THI, and CAR was achieved, respectively, whereas DIC was either degraded during the filtration step by photolysis, or below the LOD. The overall MC degradation rate was 17%, along with a H<sub>2</sub>O<sub>2</sub> consumption of 12.5 mg/L. Within 15 minutes, all dissolved iron had precipitated, as the Fe(III):EDDS complex degrades faster in the presence of particulate organic matter.

A similar solar photo-Fenton treatment was applied to the permeate volume, resulting in higher MC degradation rates. A degradation of 32, 22, 19, 42 and 81% of CAF, IMI, THI, CAR, and DIC was achieved, respectively, totaling a 32% MC degradation rate. The consumption of H<sub>2</sub>O<sub>2</sub> at the end of the experiment was 18 mg/L, while the dissolved iron concentration remained at 15 minutes at 22% higher than the treatment of the concentrate volume. This can be attributed to the slower degradation of the Fe(III):EDDS complex due to the lower concentration of particulate organic matter,

#### IV. Results and Discussion

which was effectively removed from the matrix by the self-cleaning UF membrane. These findings indicate that lowering the turbidity and particle concentrations by the UF membrane positively impacts the applicability of the solar photo-Fenton treatment. However, the overall MC degradation rates were relatively low in both cases.

It is thereby known that the presence of high concentrations of bicarbonates in the concentrate and the permeate volumes act as radical scavengers, obstructing the full potential of the solar photo-Fenton process, which results in the observed low MC degradation rates. This phenomenon has also been documented in other studies. [231,232] In order to address this issue, additional experiments were performed on the same concentrate and permeate volumes, which is shown in Figure IV.17, this time with the bicarbonates removed. Air-stripping using  $H_2SO_4$  was applied to lower the initial bicarbonate concentration of 720 mg/L to 75 mg/L, which resulted in a pH decrease from pH 8 to circumneutral pH.

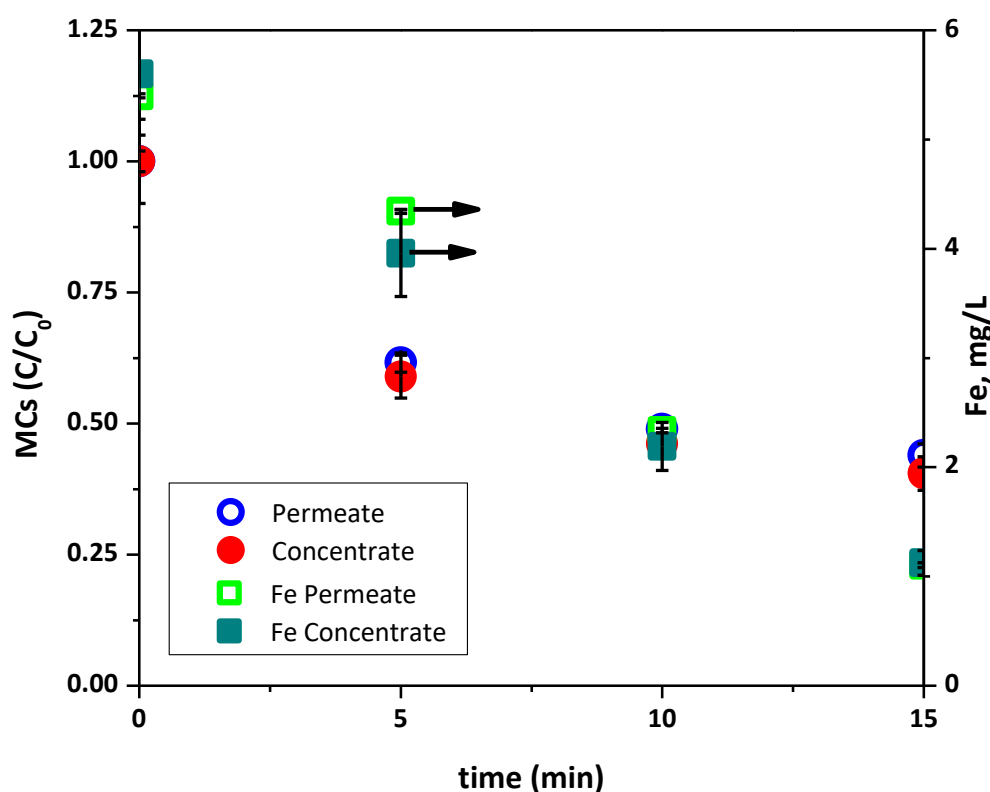
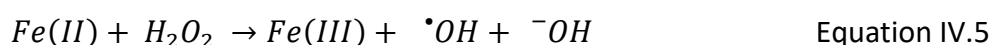


**Figure IV.17:** The evolution of the MC concentration of the permeate and the concentrate stream, and the dissolved iron concentration during treatment with solar photo-Fenton in the solar simulator, with UWWTP effluents containing a low concentration (75 mg/L) of bicarbonates, using 0.10 mM of Fe(III):EDDS and 1.50 mM of  $H_2O_2$ .

When removing the bicarbonates, the MC degradation efficiency of the concentrate showed significant improvement. A MC degradation of 66, 52, 45 and 83% for CAF, IMI, THI, and CAR, respectively, was obtained. Similar to the previous experiment, DIC

was degraded through photolysis during the filtration step. The overall MC degradation rate reached a total of 64%, more than three times higher as compared to the treatment with natural bicarbonate concentration. The H<sub>2</sub>O<sub>2</sub> consumption also increased to 30 mg/L, indicating a slower decrease in dissolved iron concentration and better stability of the Fe(III):EDDS complex. Around 80% of the iron was consumed after 15 minutes, which was consistent with the treatment of the permeate volume containing its natural bicarbonate concentration. A lower bicarbonate concentration resulted in reduced scavenging effects on the •OH radicals during the solar photo-Fenton at circumneutral pH (Equations IV.2-4)). [233] The regeneration of the Fe(III):EDDS complex occurred from the Fe(II):EDDS complex when reacting with H<sub>2</sub>O<sub>2</sub>, formed after the rapid degradation of the Fe(III):EDDS complex in the initial minutes of the experiment, along with the reaction of Fe(II) with H<sub>2</sub>O<sub>2</sub> to form Fe(III) and •OH (Equation IV.5)) It explains the higher H<sub>2</sub>O<sub>2</sub> consumption rates.



In the permeate volume, the degradation efficiency was also higher, with 60, 46, 39, and 78% of CAF, IMI, THI, CAR, and DIC, respectively within 15 minutes. The total MC degradation rate was 59%, which is double the degradation rate of the permeate volume with the natural bicarbonate concentration. However, the H<sub>2</sub>O<sub>2</sub> consumption was almost three times lower at 12.7 mg/L, while reaching a similar iron concentration as the concentrate volume with 20% remaining. The lower H<sub>2</sub>O<sub>2</sub> consumption can be attributed to the lower turbidity and the MC concentrations. Despite having similar total MC concentrations of 450 mg/L total, the relative MC concentrations in the concentrate and permeate volumes were significantly different. The lack of the bicarbonates and so the absence of radical scavenging in the solar photo-Fenton cycle, resulted in significant more production of •OH. The resulting significantly lower H<sub>2</sub>O<sub>2</sub> consumption at similar MC degradation rates highlights the economic advantages of the pretreatment with the photocatalytic UF membrane. In addition, an attempt to use persulfate as an oxidizing agent instead of H<sub>2</sub>O<sub>2</sub> resulted in ineffective degradation of the selected MCs in the UWWTP effluent, as only a degradation of 19.6% was achieved, as compared to 64% with the conventional solar photo-Fenton treatment.

### 9 The membrane retention of the *Pseudomonas Aeruginosa* bacterial species

The retention of the *P. Aeruginosa* bacterial species by the photocatalytic TiO<sub>2</sub>-ZrO<sub>2</sub> UF membrane was also tested. Figure IV.18 shows the results of filtering natural water from Tabernas, Spain, which had an initial concentration of  $1 \cdot 10^6$  CFU/mL. The membrane demonstrated to have a stable flow rate of 31 mL/min through its effective surface of 150 cm<sup>2</sup>. The samples were collected and processed as described in Chapter III – 2, where *P. Aeruginosa* CFU counting, and calculation took place after 48 hours cultivation at 36 °C. the permeate volume samples at t= 0 minutes showed no presence of *P. Aeruginosa*, or it was below the LOD. The experiment include two replicates, designated as Repetition 1 and Repetition 2.

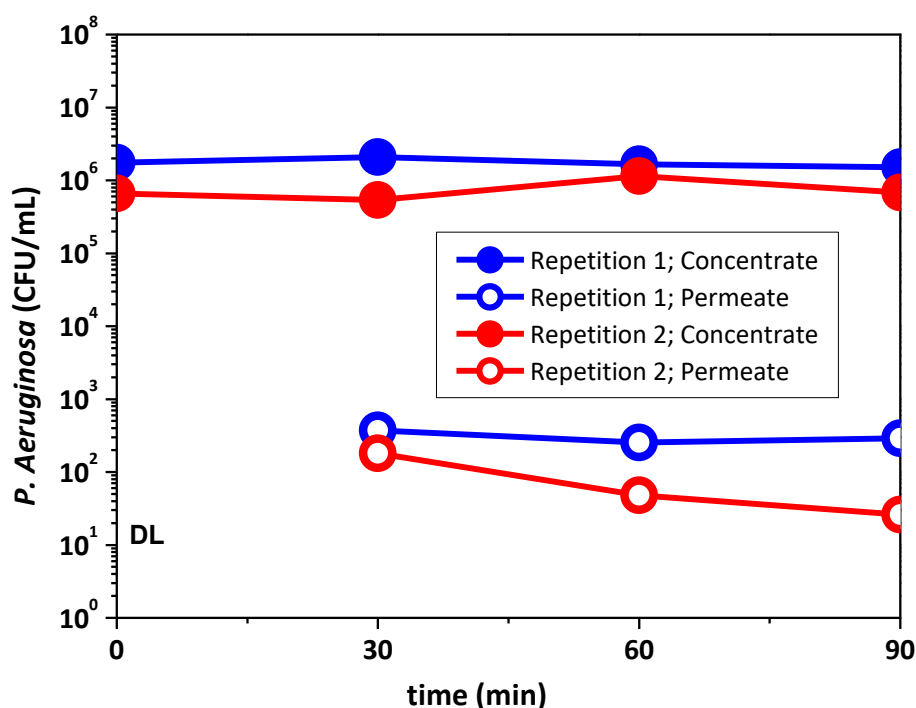


**Figure IV.18:** The retention by the self-cleaning membrane of *P. Aeruginosa* at an initial concentration of  $1 \cdot 10^6$  CFU/mL in natural water (Tabernas, Spain). The detection limit (DL) of for the *P. Aeruginosa* was  $1 \cdot 10^6$  CFU/mL.

The results shown in Figure IV.18 demonstrate that the photocatalytic UF membrane is able to consistently retain the *P. Aeruginosa* at levels ranging from  $1 \cdot 10^3$  to  $1 \cdot 10^4$  CFU/mL within 90 minutes of filtration in Repetition 1, when looking at the permeate. While the concentration of the *P. Aeruginosa* in the permeate volume decreased significantly as compared to the concentrate, it was expected when looking at the pore size of the photocatalytic UF membrane, the thickness of the zirconia intermediate layer of 60 nm, and the size of the rod-like *P. Aeruginosa*, ranging between 500-800 nm by 1500-3000 nm. [234–236] The retention rate of the *P. Aeruginosa* was lower than expected and it may be attributed to minor damages in the surface of the photocatalytic UF membrane caused by manual cleaning, as was observed in Figure IV.13-B, and minor defects in the intermediate zirconia layer, allowing some *P. Aeruginosa* to permeate through. On the other hand, the decreasing trend observed in Repetition 2 of the permeate, indicates the irreversible effects of fouling at these

sites with minor damages. The continuous fouling mechanisms, as observed in Figure IV.15, result in satisfactory concentrations of *P. Aeruginosa* in the permeate volume when the photocatalytic UF membrane was operated for more than 180 minutes. Controlled fouling mechanisms are commonly employed in ceramic membrane production and various industries as a treatment strategy for similar reasons.

Irradiating the photocatalytic membrane surface results in increased hydrophilic properties, which helps to prevent bacterial adhesion. Furthermore, irradiation can prevent and degrade the formation of EPS, which bacteria produce to bind themselves to surfaces and protect them from unfavorable conditions. This results that the membrane is less likely to foul and can be operated for longer periods without significant decline in performance. The EPS can be observed to a typical slimy biofilm layer. [237]

This Chapter IV – Target 3 corresponds to article:

Dennis Deemter, Fabricio Eduardo Bortot Coelho, Isabel Oller, Sixto Malato, Ana M. Amat, **Assessment of a Novel Photocatalytic TiO<sub>2</sub>-Zirconia Ultrafiltration Membrane and Combination with Solar Photo-Fenton Tertiary Treatment of Urban Wastewater**, *Catalysts* 12, no. 5: 552, 2022. Available at: <https://doi.org/10.3390/catal12050552>. It is included as part of Annex B.



## IV. Results and Discussion

## Chapter V. Conclusions

## V. Conclusions

**Target 1.** *Determination of optimal operational parameters, concentration factors and retention mechanisms of MCs, for the preconcentration of saline waters by NF treatment, utilizing a pilot plant containing NF membranes. Followed by the assessment of oxidizing agents' effectiveness, iron concentration and EDDS complex ratios during solar photo-Fenton treatment of the different concentrate and permeate volumes, at different pHs.*

- Microcontaminant retention experiments were successfully conducted for the preconcentration of saline matrices.
- Operational parameters such as the increase of the working pressure, as also increasing the salinity of the utilized matrices did not show to have any effects on the permeation order of selected contaminants.
- Selected contaminants had a membrane permeability order of imidacloprid, thiacloprid, caffeine, and carbamazepine. Not in any case was diclofenac detected in any of the produced permeate streams. Permeation order was assigned to both molecular weight and molecular charge, whereas diclofenac is the largest of the selected microcontaminants.
- Concentration factor (CF) showed to be the controlling factor of the microcontaminant and ionic permeation.
- The classic (solar) photo-Fenton process has to be applied at low pH 3 in order to prevent the precipitation of iron, which significantly decreases the economic viability of the solar photo-Fenton process as a tertiary treatment method for urban wastewater treatment plant effluents. Chelating agents, such as Ethylenediamine-N, N'-disuccinic acid (EDDS), were found to be a viable option to be able to apply the solar photo-Fenton process at circumneutral pH.
- The most effective concentration and ratio was then to be 0.10 mM at a ratio of [1:2] Fe(III):EDDS.
- The two tested oxidizing agents, H<sub>2</sub>O<sub>2</sub> and persulfate, showed significantly different selectivity for the selected microcontaminants. Persulphate was less effective.
- It was found that solar photo-Fenton can also be applied as a tertiary treatment polishing step when treating the permeate streams by rapidly degrading all the present microcontaminants.

**Target 2.** *Recovery of valuable nutrients such as ammonium from saline waters during their preconcentration for the retention of MCs, with the aim to produce enriched crop irrigation waters for direct use. Followed by the application and assessment of different AOPs treatment methods for MC removal from the concentrate volumes, and a toxicity assessment of the permeate volumes.*

- The recovery of  $\text{NH}_4^+$  from saline wastewater matrices was effectively obtained when utilizing Nanofiltration at pH 9.
- Treatment of wastewaters with NF does produce permeate streams basically free from bacteria but could still contain antibiotic resistant genes and antibiotic resistant bacteria. Something which has to be further researched before applying the produced streams for direct crop irrigation.

The target compounds, caffeine, imidacloprid, thiacloprid, carbamazepine and diclofenac showed faster degradation by utilizing  $\text{H}_2\text{O}_2$  instead of persulfate.

- Electrooxidation proved to be an effective treatment method of nanofiltration produced concentrate streams, due to their high conductive potential.
- Solar-assisted treatment significantly reduced the electricity consumption, at lower produced concentrations of free available chlorine and chlorate as compared to sole application of anodic oxidation. It was found that the permeate streams are suitable for crop irrigation as long as  $\text{CF} = 2$  is not exceeded.
- Specific  $\text{NH}_4^+$  enriched permeate streams are to be used to irrigate specific crops only, thereby also looking at soil composition.
- Acute and chronic toxicity tests also showed that the concentration factor should not exceed  $\text{CF} = 2$ .
- Permeate streams are only to be used for direct crop irrigation and fertigation when  $\text{CF} = 2$  is not exceeded and a diluted is made first at a ratio of two, or more.

## V. Conclusions

**Target 3.** *Development of a novel self-cleaning photocatalytic membranes. The assessment of the fouling and self-cleaning capabilities by the registration of flux restoration during the filtration of real urban wastewaters, followed by material evaluation, before and after solar irradiation. The quantification and effects of water turbidity reduction for the application of subsequent treatments. Quantification of the bacterial present in water retention by the newly developed photocatalytic membrane.*

- Self-cleaning photocatalytic TiO<sub>2</sub>-ZrO<sub>2</sub> ceramic ultrafiltration membrane was successfully used for the (pre) treatment of urban wastewater treatment plant effluents.
- Obtaining longer operational times was possible when the membrane surface was irradiated with light that reached the semiconductor's band gap energy.
- After a period of irradiation, a cleaner membrane surface was observed, as also a significant restoration of the membrane flux.
- Fouling prevention and flux increasing mechanism was found by photo-induced super-hydrophilicity.
- *Pseudomonas aeruginosa* showed to be retained by membrane with an order of magnitude of  $1 \times 10^3 - 1 \times 10^4$  CFU/mL. Fouling positively contributed by closing larger pores and minor defects in the membrane. Fouling was reversible when the surface was irradiated.



## References

- [1] P. Westerhoff, P.J. Alvarez, J. Kim, Q. Li, A. Alabastri, N.J. Halas, D. Villagran, J. Zimmerman, M.S. Wong, Utilizing the broad electromagnetic spectrum and unique nanoscale properties for chemical-free water treatment, *Curr. Opin. Chem. Eng.* 33 (2021) 100709. <https://doi.org/10.1016/j.coche.2021.100709>.
- [2] D. Yang, Y. Yang, J. Xia, Hydrological cycle and water resources in a changing world: A review, *Geogr. Sustain.* 2 (2021) 115–122. <https://doi.org/10.1016/j.geosus.2021.05.003>.
- [3] S. Uhlenbrook, W. Yu, P. Schmitter, D.M. Smith, Optimising the water we eat — rethinking policy to enhance productive and sustainable use of water in agri-food systems across scales, *Lancet Planet. Heal.* 6 (2022) e59–e65. [https://doi.org/10.1016/S2542-5196\(21\)00264-3](https://doi.org/10.1016/S2542-5196(21)00264-3).
- [4] G. Konapala, A. Mishra, Dynamics of virtual water networks: Role of national socio-economic indicators across the world, *J. Hydrol.* 589 (2020) 125171. <https://doi.org/10.1016/j.jhydrol.2020.125171>.
- [5] D. Zetland, The role of prices in managing water scarcity, *Water Secur.* 12 (2021) 100081. <https://doi.org/10.1016/j.wasec.2020.100081>.
- [6] N.N. Kourgialas, A critical review of water resources in Greece: The key role of agricultural adaptation to climate-water effects, *Sci. Total Environ.* 775 (2021) 145857. <https://doi.org/10.1016/j.scitotenv.2021.145857>.
- [7] A. Altieri, *Dead zones: Low oxygen in coastal waters*, Elsevier Ltd., 2018. <https://doi.org/10.1016/B978-0-12-409548-9.10616-5>.
- [8] C. Ramis, A. Amengual, *Climate change effects on European heat waves and human health*, Elsevier Inc., 2017. <https://doi.org/10.1016/B978-0-12-809665-9.09798-6>.
- [9] C. Wasko, A. Sharma, A. Pui, Linking temperature to catastrophe damages from hydrologic and meteorological extremes, *J. Hydrol.* 602 (2021) 126731. <https://doi.org/10.1016/j.jhydrol.2021.126731>.
- [10] J. Hipólito, J. Coutinho, T. Mahlmann, T.B.R. Santana, W.E. Magnusson, Legislation and pollination: Recommendations for policymakers and scientists, *Perspect. Ecol. Conserv.* 19 (2021) 1–9. <https://doi.org/10.1016/j.pecon.2021.01.003>.
- [11] K. Oelkers, Is the objective of the Water Framework Directive to deal with pollutant emissions at source coherently implemented by the EU's substance-specific legal acts? A comparison of the environmental risk control of pharmaceutical legislation with the REACH-, *Bi, Sustain. Chem. Pharm.* 20 (2021) 100386. <https://doi.org/10.1016/j.scp.2021.100386>.
- [12] Z.A. Smith, K.L. Ross, Human Rights to Water, *Handb. Glob. Environ.* (2018) 115–133. <https://doi.org/10.4324/9781315093253-7>.
- [13] S.F.O.R. Water, World Water Assessment Programme (Nations Unies), The United Nations World Water Development Report 2018 (United Nations Educational, Scientific and Cultural Organization, New York, United States) [www.unwater.org/publications/world-water-development-repor](http://www.unwater.org/publications/world-water-development-repor), 2018.
- [14] UN Water, *Compendium of Water Quality Regulatory Frameworks: Which Water for Which Use?*, Report: (2015) 69. [www.iwa-network.org/which-water-for-which-use](http://www.iwa-network.org/which-water-for-which-use).
- [15] C. Campanale, C. Massarelli, D. Losacco, D. Bisaccia, M. Triozzi, V.F. Uricchio, The monitoring of Pesticides in water matrices and the analytical criticalities: a



## References

- review, *TrAC Trends Anal. Chem.* 144 (2021) 116423. <https://doi.org/10.1016/j.trac.2021.116423>.
- [16] A.B. Ndah, C.L. Meunier, I. V. Kirstein, J. Göbel, L. Rönn, M. Boersma, A systematic study of zooplankton-based indices of marine ecological change and water quality: Application to the European marine strategy framework Directive (MSFD), *Ecol. Indic.* 135 (2022) 0–3. <https://doi.org/10.1016/j.ecolind.2022.108587>.
- [17] A.S. Stasinakis, P. Charalambous, I. Vyrides, Dairy wastewater management in EU: Produced amounts, existing legislation, applied treatment processes and future challenges, *J. Environ. Manage.* 303 (2022) 114152. <https://doi.org/10.1016/j.jenvman.2021.114152>.
- [18] H. Guyomard, Z. Bouamra-mechemache, V. Chatellier, L. Delaby, C. Détang-dessendre, Review: Why and how to regulate animal production and consumption : The case of the European Union, *Animal.* 15 (2021) 100283. <https://doi.org/10.1016/j.animal.2021.100283>.
- [19] R. Duarte, V. Pinilla, A. Serrano, The globalization of Mediterranean agriculture: A long-term view of the impact on water consumption, *Ecol. Econ.* 183 (2021) 106964. <https://doi.org/10.1016/j.ecolecon.2021.106964>.
- [20] C.S.S. Ferreira, S. Seifollahi-Aghmiuni, G. Destouni, N. Ghajarnia, Z. Kalantari, Soil degradation in the European Mediterranean region: Processes, status and consequences, *Sci. Total Environ.* 805 (2022) 150106. <https://doi.org/10.1016/j.scitotenv.2021.150106>.
- [21] E.P. and of the Council, Directive 2000/60/EC, 2000.
- [22] European Commission, HORIZON 2020, 2014. <https://doi.org/10.2777/3719>.
- [23] European Commission, HORIZON 2030, 2019. <https://doi.org/10.1017/9781108339216.019>.
- [24] B.C. Gordalla, Standardized Methods for Water-Quality Assessment, *Treatise Water Sci.* 3 (2011) 263–302. <https://doi.org/10.1016/B978-0-444-53199-5.00060-9>.
- [25] Y. Jia, F. Zheng, H.R. Maier, A. Ostfeld, E. Creaco, D. Savic, J. Langeveld, Z. Kapelan, Water quality modeling in sewer networks: Review and future research directions, *Water Res.* 202 (2021) 117419. <https://doi.org/10.1016/j.watres.2021.117419>.
- [26] E.J. Okampo, N. Nwulu, Optimisation of renewable energy powered reverse osmosis desalination systems: A state-of-the-art review, *Renew. Sustain. Energy Rev.* 140 (2021) 110712. <https://doi.org/10.1016/j.rser.2021.110712>.
- [27] T. Ding, L. Liang, K. Zhou, M. Yang, Y. Wei, Water-energy nexus: The origin, development and prospect, *Ecol. Modell.* 419 (2020) 108943. <https://doi.org/10.1016/j.ecolmodel.2020.108943>.
- [28] L. Cheng, Energy prediction for community water supply: An integrative application of scaling analysis and life cycle assessment, *Water-Energy Nexus.* 4 (2021) 1–9. <https://doi.org/10.1016/j.wen.2020.12.003>.
- [29] G.N. Ijoma, A. Mutungwazi, T. Mannie, W. Nurmahomed, T.S. Matambo, D. Hildebrandt, Addressing the water-energy nexus : A focus on the barriers and potentials of harnessing wastewater treatment processes for biogas production in Sub Saharan Africa, *Heliyon.* 8 (2022) e09385. <https://doi.org/10.1016/j.heliyon.2022.e09385>.

- [30] European Union Council Directive, The urban waste water treatment directive, 1991.
- [31] L. Rizzo, W. Gernjak, P. Krzeminski, S. Malato, C.S. McArdell, J.A.S. Perez, H. Schaar, D. Fatta-Kassinos, Best available technologies and treatment trains to address current challenges in urban wastewater reuse for irrigation of crops in EU countries, *Sci. Total Environ.* 710 (2020) 136312. <https://doi.org/10.1016/j.scitotenv.2019.136312>.
- [32] C. Martin, P.A. Vanrolleghem, Environmental Modelling & Software Analysing, completing, and generating influent data for WWTP modelling: A critical review, *Environ. Model. Softw.* 60 (2014) 188–201. <https://doi.org/10.1016/j.envsoft.2014.05.008>.
- [33] S. Jafarinejad, A framework for the design of the future energy-efficient , cost-effective, reliable, resilient, and sustainable full-scale wastewater treatment plants, *Curr. Opin. Environ. Sci. Heal.* 13 (2020) 91–100. <https://doi.org/10.1016/j.coesh.2020.01.001>.
- [34] K.Y. Fung, C. Wibowo, Design of industrial wastewater treatment plants : a multi-faceted problem, *Curr. Opin. Chem. Eng.* 2 (2013) 455–460. <https://doi.org/10.1016/j.coche.2013.09.003>.
- [35] Frank R. Spellman, Handbook of Water and Wastewater Treatment Plant Operations, 4th Editio, CRC Press, 2020. <https://doi.org/https://doi.org/10.1201/9781003038351>.
- [36] EAA, Urban waste water treatment in Europe — European Environment Agency, (2021). <https://www.eea.europa.eu/data-and-maps/indicators/urban-waste-water-treatment/urban-waste-water-treatment-assessment-5>.
- [37] EC, MEMO/19/1472, 2019.
- [38] European Commission, Urban Waste Water: Commission decides to refer SPAIN to the Court of Justice of the European Union over its failure to comply with the Urban Waste Water Directive, 06.04.2022. (2022). [https://ec.europa.eu/commission/presscorner/detail/en/IP\\_22\\_1923](https://ec.europa.eu/commission/presscorner/detail/en/IP_22_1923).
- [39] B. Narayan, R. Kumar, Current technologies and future perspectives for the treatment of complex petroleum refinery wastewater : A review, *Bioresour. Technol.* 355 (2022) 127263. <https://doi.org/10.1016/j.biortech.2022.127263>.
- [40] R. Sirohi, J. Joun, J.Y. Lee, B.S. Yu, S.J. Sim, Waste mitigation and resource recovery from food industry wastewater employing microalgae-bacterial consortium, *Bioresour. Technol.* 352 (2022) 127129. <https://doi.org/10.1016/j.biortech.2022.127129>.
- [41] R. Paarlberg, The trans-Atlantic conflict over “green” farming, *Food Policy.* 108 (2022) 102229. <https://doi.org/10.1016/j.foodpol.2022.102229>.
- [42] M. Reda, W. Zam, M. El, State of knowledge on chemical, biological and nutritional properties of olive mill wastewater, *Food Chem.* 381 (2022) 132238. <https://doi.org/10.1016/j.foodchem.2022.132238>.
- [43] A.M. Gorito, A.R. Lado Ribeiro, M.F.R. Pereira, C.M.R. Almeida, A.M.T. Silva, Advanced oxidation technologies and constructed wetlands in aquaculture farms: What do we know so far about micropollutant removal?, *Environ. Res.* 204 (2022). <https://doi.org/10.1016/j.envres.2021.111955>.
- [44] A. Ahmad, S. Budi, S. Rozaimah, S. Abdullah, A. Razi, H. Abu, Contaminants of emerging concern (CECs) in aquaculture effluent: Insight into breeding and

## References

- rearing activities, alarming impacts, regulations, performance of wastewater treatment unit and future approaches, *Chemosphere*. 290 (2022) 133319. <https://doi.org/10.1016/j.chemosphere.2021.133319>.
- [45] S. Bapu, Y. Jawaharlal, N. Lakshaman, Industrial wastewater treatment using oxidative integrated approach, *South African J. Chem. Eng.* 40 (2022) 100–106. <https://doi.org/10.1016/j.sajce.2022.02.004>.
- [46] S. Nair, B. Manu, A. Azhoni, Sustainable treatment of paint industry wastewater: Current techniques and challenges, *J. Environ. Manage.* 296 (2021) 113105. <https://doi.org/10.1016/j.jenvman.2021.113105>.
- [47] P. Bhanot, S.M. Celin, T.R. Sreekrishnan, A. Kalsi, S.K. Sahai, Application of integrated treatment strategies for explosive industry wastewater — A critical review, *J. Water Process Eng.* 35 (2020) 101232. <https://doi.org/10.1016/j.jwpe.2020.101232>.
- [48] L. Mishra, K.K. Paul, S. Jena, Coke wastewater treatment methods: Mini review, *J. Indian Chem. Soc.* 98 (2021) 100133. <https://doi.org/10.1016/j.jics.2021.100133>.
- [49] W. Dou, X. Peng, L. Kong, X. Hu, A review on the removal of Cl<sup>-</sup> with high concentration from industrial wastewater: Approaches and mechanisms, *Sci. Total Environ.* 824 (2022) 153909. <https://doi.org/10.1016/j.scitotenv.2022.153909>.
- [50] H. Wang, L. Deng, Z. Qi, W. Wang, Constructed microalgal-bacterial symbiotic (MBS) system: Classification, performance, partnerships and perspectives, *Sci. Total Environ.* 803 (2021) 150082. <https://doi.org/10.1016/j.scitotenv.2021.150082>.
- [51] V. Shrivastava, I. Ali, M. Maskawat, E.R. Rene, Wastewater in the food industry: Treatment technologies and reuse potential, *Chemosphere*. 293 (2022). <https://doi.org/10.1016/j.chemosphere.2022.133553>.
- [52] T. Ahmad, T. Belwal, L. Li, S. Ramola, R. Muhammad, Y. Xu, L. Zisheng, Utilization of wastewater from edible oil industry, turning waste into valuable products: A review, *Trends Food Sci. Technol.* 99 (2020) 21–33. <https://doi.org/10.1016/j.tifs.2020.02.017>.
- [53] S. Ying, D.C. Stuckey, Separation and biosynthesis of value-added compounds from food-processing wastewater: Towards sustainable wastewater resource recovery, *J. Clean. Prod.* 357 (2022) 131975. <https://doi.org/10.1016/j.jclepro.2022.131975>.
- [54] R. Cássia, V. Rodrigues, A. Pinto, L. Fernandes, S. José, S. Soares, J. Sélia, New sustainable perspectives for “Coffee Wastewater” and other by-products: A critical review, *Futur. Foods.* 4 (2021). <https://doi.org/10.1016/j.fufo.2021.100058>.
- [55] A. Hussain, F. Rehman, H. Rafeeq, M. Waqas, A. Asghar, N. Afsheen, A. Rahdar, M. Bilal, H.M.N. Iqbal, In-situ, Ex-situ, and nano-remediation strategies to treat polluted soil, water, and air – A review, *Chemosphere*. 289 (2022) 133252. <https://doi.org/10.1016/j.chemosphere.2021.133252>.
- [56] S. Li, Y. Yang, H. Zheng, Y. Zheng, T. Jing, J. Ma, J. Nan, Advanced oxidation process based on hydroxyl and sulfate radicals to degrade refractory organic pollutants in landfill leachate, *Chemosphere*. 297 (2022) 134214. <https://doi.org/10.1016/j.chemosphere.2022.134214>.

- [57] Z. Guo, Y. Zhang, H. Jia, J. Guo, X. Meng, J. Wang, Electrochemical methods for land fill leachate treatment: A review on electrocoagulation and electrooxidation, *Sci. Total Environ.* 806 (2022) 150529. <https://doi.org/10.1016/j.scitotenv.2021.150529>.
- [58] L. Chen, M. Zhou, J. Wang, Z. Zhang, C. Duan, X. Wang, S. Zhao, A global meta-analysis of heavy metal (loid) s pollution in soils near copper mines: Evaluation of pollution level and probabilistic health risks, *Sci. Total Environ.* 835 (2022) 155441. <https://doi.org/10.1016/j.scitotenv.2022.155441>.
- [59] G. Chen, Y. Ye, N. Yao, N. Hu, J. Zhang, Y. Huang, A critical review of prevention, treatment, reuse, and resource recovery from acid mine drainage, *J. Clean. Prod.* 329 (2021) 129666. <https://doi.org/10.1016/j.jclepro.2021.129666>.
- [60] S. Tomiyama, T. Igarashi, The potential threat of mine drainage to groundwater resources, *Curr. Opin. Environ. Sci. Heal.* 27 (n.d.) 100347. <https://doi.org/10.1016/j.coesh.2022.100347>.
- [61] A.B. Adam, J.R. Owen, D. Kemp, The Extractive Industries and Society Households, livelihoods and mining-induced displacement and resettlement, *Biochem. Pharmacol.* 2 (2015) 581–589. <https://doi.org/10.1016/j.exis.2015.05.002>.
- [62] J.R. Owen, D. Kemp, Mining-induced displacement and resettlement: a critical appraisal, *J. Clean. Prod.* 87 (2015) 478–488. <https://doi.org/10.1016/j.jclepro.2014.09.087>.
- [63] A.M. Elgarahy, K.Z. Elwakeel, S.H. Mohammad, G.A. Elshoubaky, A critical review of biosorption of dyes, heavy metals and metalloids from wastewater as an efficient and green process, *Clean. Eng. Technol.* 4 (2021) 100209. <https://doi.org/10.1016/j.clet.2021.100209>.
- [64] F. Arshad, M. Selvaraj, F. Banat, M. Abu, Removal of metal ions and organics from real refinery wastewater using double- functionalized graphene oxide in alginate beads, *J. Water Process Eng.* 38 (2020) 101635. <https://doi.org/10.1016/j.jwpe.2020.101635>.
- [65] J.M. Costa, J. Grisente, Techniques of nickel (II) removal from electroplating industry wastewater: Overview and trends, *J. Water Process Eng.* 46 (2022). <https://doi.org/https://doi.org/10.1016/j.jwpe.2022.102593>.
- [66] R. Abduraupov, G. Akhmadjanova, A. Ibragimov, B.K. Bala, S.F. Sidique, M. Makhmudov, K. Angelina, Modeling of water management for cotton production in Uzbekistan, *Agric. Water Manag.* 265 (2022) 107535. <https://doi.org/10.1016/j.agwat.2022.107535>.
- [67] A. Abdelmeguid, M. Afy-shararah, K. Salonitis, Investigating the challenges of applying the principles of the circular economy in the fashion industry : A systematic review, *Sustain. Prod. Consum.* 32 (2022) 505–518. <https://doi.org/10.1016/j.spc.2022.05.009>.
- [68] S. Samsami, M. Mohamadizani, M. Sarrafzadeh, E.R. Rene, M. Firoozbahr, Recent advances in the treatment of dye-containing wastewater from textile industries : Overview and perspectives, 143 (2020) 138–163. <https://doi.org/10.1016/j.psep.2020.05.034>.
- [69] A. Ulson, W. Artifon, K. Cesca, C. Jos, Dyestuffs from textile industry wastewaters : Trends and gaps in the use of bioflocclants, 111 (2021) 181–190. <https://doi.org/10.1016/j.procbio.2021.10.030>.

## References

- [70] J. Li, M. Dagneu, M.B. Ray, Effect of coagulation on microfibers in laundry wastewater, *Environ. Res.* (2022) 113401. <https://doi.org/10.1016/j.envres.2022.113401>.
- [71] I. Haq, P. Mazumder, A.S. Kalamdhad, Recent advances in removal of lignin from paper industry wastewater and its industrial applications – A review, *Bioresour. Technol.* 312 (2020) 123636. <https://doi.org/10.1016/j.biortech.2020.123636>.
- [72] A. Kumar, N.K. Srivastava, P. Gera, Removal of color from pulp and paper mill wastewater- methods and techniques- A review, *J. Environ. Manage.* 298 (2021) 113527. <https://doi.org/10.1016/j.jenvman.2021.113527>.
- [73] G.K. Gupta, H. Liu, P. Shukla, Pulp and paper industry – based pollutants , their health hazards and environmental risks, *Curr. Opin. Environ. Sci. Heal.* 12 (2019) 48–56. <https://doi.org/10.1016/j.coesh.2019.09.010>.
- [74] A. Sousa, H. Sousa, L. Santos, M. Sim, F. Vale, Parabens as emerging contaminants : Environmental persistence , current practices and treatment processes, 347 (2022). <https://doi.org/10.1016/j.jclepro.2022.131244>.
- [75] GrandViewResearch, Personal Care Contract Manufacturing Market Size, Share & Trends Analysis Report By Service (Manufacturing, Packaging), By Region (APAC, North America, Europe, RoW), And Segment Forecasts, 2020 - 2027, 2019. <https://www.grandviewresearch.com/industry-analysis/personal-care-product-contract-manufacturing-market>.
- [76] X. Chen, L. Lei, S. Liu, J. Han, R. Li, J. Men, L. Li, L. Wei, Y. Sheng, L. Yang, B. Zhou, L. Zhu, Occurrence and risk assessment of pharmaceuticals and personal care products (PPCPs) against COVID-19 in lakes and WWTP-river-estuary system in Wuhan, China, *Sci. Total Environ.* 792 (2021) 148352. <https://doi.org/10.1016/j.scitotenv.2021.148352>.
- [77] I. Azizov, M. Dudek, G. Øye, Emulsions in porous media from the perspective of produced water re-injection – A review, *J. Pet. Sci. Eng.* 206 (2021). <https://doi.org/10.1016/j.petrol.2021.109057>.
- [78] A.A. Olajire, Recent advances on the treatment technology of oil and gas produced water for sustainable energy industry-mechanistic aspects and process chemistry perspectives, *Chem. Eng. J. Adv.* 4 (2020) 100049. <https://doi.org/10.1016/j.cej.2020.100049>.
- [79] U.S.E. Agency, Hydraulic Fracturing for Oil and Gas: Impacts from the Hydraulic Fracturing, EPA’s Study Hydraul. Fract. Its Potential Impact Drink. Water Resour. (2016).
- [80] J. Njuguna, S. Siddique, L. Bakah Kwroffie, S. Piromrat, K. Addae-Afoakwa, U. Ekeh-Adegbotolu, G. Oluyemi, K. Yates, A. Kumar Mishra, L. Moller, The fate of waste drilling fluids from oil & gas industry activities in the exploration and production operations, *Waste Manag.* 139 (2022) 362–380. <https://doi.org/10.1016/j.wasman.2021.12.025>.
- [81] Y. Liu, H. Lu, Y. Li, H. Xu, Z. Pan, P. Dai, H. Wang, Q. Yang, A review of treatment technologies for produced water in offshore oil and gas fields, *Sci. Total Environ.* 775 (2021) 145485. <https://doi.org/10.1016/j.scitotenv.2021.145485>.
- [82] K. Andersson, F. Baldi, S. Brynolf, J.F. Lindgren, L. Granhag, E. Svensson, Shipping and the environment, *Shipp. Environ. Improv. Environ. Perform. Mar. Transp.* (2016) 3–27. [https://doi.org/10.1007/978-3-662-49045-7\\_1](https://doi.org/10.1007/978-3-662-49045-7_1).
- [83] M. Pe, M. Brailo, New role of hydrocyclone in ballast water treatment, 188

- (2018) 339–346. <https://doi.org/10.1016/j.jclepro.2018.03.299>.
- [84] H. Kim, S. Lee, B. Son, J. Jeon, D. Kim, Biocidal effect of thymol and carvacrol on aquatic organisms : Possible application in ballast water management systems, *Mar. Pollut. Bull.* 133 (2018) 734–740. <https://doi.org/10.1016/j.marpolbul.2018.06.025>.
- [85] L. Sun, T. Zhang, S. Liu, K. Wang, T. Rogers, L. Yao, Reducing energy consumption and pollution in the urban transportation sector : A review of policies and regulations in Beijing, *J. Clean. Prod.* 285 (2021) 125339. <https://doi.org/10.1016/j.jclepro.2020.125339>.
- [86] N. Han, J. Zhang, M. Hoang, S. Gray, Z. Xie, A review of process and wastewater reuse in the recycled paper industry, *Environ. Technol. Innov.* 24 (2021) 101860. <https://doi.org/10.1016/j.eti.2021.101860>.
- [87] G. Cabrera-papamija, F. Machuca-martínez, R.A. Mu, L.A. Rodríguez, J.E. Diosa, E. Mosquera-vargas, Plastic recycling and their use as raw material for the synthesis of carbonaceous materials, 8 (2022). <https://doi.org/10.1016/j.heliyon.2022.e09028>.
- [88] K. Hu, Y. Yang, J. Zuo, W. Tian, Y. Wang, X. Duan, S. Wang, Emerging microplastics in the environment : Properties, distributions, and impacts, *Chemosphere.* 297 (2022) 134118. <https://doi.org/10.1016/j.chemosphere.2022.134118>.
- [89] M. Sajjad, Q. Huang, S. Khan, Microplastics in the soil environment: A critical review, *Environ. Technol. Innov.* 27 (2022) 102408. <https://doi.org/10.1016/j.eti.2022.102408>.
- [90] P. Jeffrey, Z. Yang, S.J. Judd, The status of potable water reuse implementation, *Water Res.* 214 (2022) 118198. <https://doi.org/10.1016/j.watres.2022.118198>.
- [91] D. Palma, C. Richard, M. Minella, State of the art and perspectives about non-thermal plasma applications for the removal of PFAS in water, *Chem. Eng. J. Adv.* 10 (2022) 100253. <https://doi.org/10.1016/j.cej.2022.100253>.
- [92] H. Wu, Nutrient recovery from wastewater : A review on the integrated Physicochemical technologies of ammonia stripping , adsorption and struvite precipitation, 433 (2022). <https://doi.org/10.1016/j.cej.2021.133664>.
- [93] L. Rizzo, W. Gernjak, P. Krzeminski, S. Malato, C.S. Mcardell, J. Antonio, S. Perez, H. Schaar, D. Fatta-kassinou, Best available technologies and treatment trains to address current challenges in urban wastewater reuse for irrigation of crops in EU countries, *Sci. Total Environ.* 710 (2020) 136312. <https://doi.org/10.1016/j.scitotenv.2019.136312>.
- [94] P. Sauri, David, Rodríguez-Villanueva, Wastewater Treatment Plants in Mediterranean Spain: An Exploration of Relations between Water Treatments, Water Reuse, and Governance, *Water.* 13 (2021) 1710. <https://doi.org/https://doi.org/10.3390/w13121710>.
- [95] A. Garre, F. L. P. Truchado, M.I. Gil, L. Cecilia, New standards at European Union level on water reuse for agricultural irrigation: Are the Spanish wastewater treatment plants ready to produce and distribute reclaimed water within the minimum quality requirements ? *Water Reuse System - 1, Int. J. Food Microbiol.* 356 (2022). <https://doi.org/10.1016/j.ijfoodmicro.2021.109352>.
- [96] S. de Boer, J. González-Rodríguez, J.J. Conde, M.T. Moreira, Benchmarking tertiary water treatments for the removal of micropollutants and pathogens

## References

- based on operational and sustainability criteria, *J. Water Process Eng.* 46 (2022). <https://doi.org/10.1016/j.jwpe.2022.102587>.
- [97] X. Tong, S. Mohapatra, J. Zhang, N. Han, L. You, Source, fate, transport and modelling of selected emerging contaminants in the aquatic environment : Current status and future perspectives, *Water Res.* 217 (2022) 118418. <https://doi.org/10.1016/j.watres.2022.118418>.
- [98] M. Antoniadou, P.P. Falara, V. Likodimos, Photocatalytic degradation of pharmaceuticals and organic contaminants of emerging concern using nanotubular structures, *Curr. Opin. Green Sustain. Chem.* 29 (2021) 100470. <https://doi.org/10.1016/j.cogsc.2021.100470>.
- [99] A. Sousa, L.C. Sim, M. Sim, Microalgal-based removal of contaminants of emerging concern, 423 (2022) 0–2. <https://doi.org/10.1016/j.jhazmat.2021.127153>.
- [100] E.O. Marson, C.E.S. Paniagua, O. Gomes, B.R. Gonçalves, V.M. Silva, I.A. Ricardo, M. Clara, V.M. Starling, C.C. Amorim, A.G. Trovó, A review toward contaminants of emerging concern in Brazil: Occurrence, impact and their degradation by advanced oxidation process in aquatic matrices, *Sci. Total Environ.* 836 (2022) 155605. <https://doi.org/10.1016/j.scitotenv.2022.155605>.
- [101] Federal Office for the Environment FOEN Water Division, Reporting for Switzerland under the Protocol on Water and Health, 2019.
- [102] M. Pei, B. Zhang, Y. He, J. Su, K. Gin, O. Lev, G. Shen, S. Hu, State of the art of tertiary treatment technologies for controlling antibiotic resistance in wastewater treatment plants, *Environ. Int.* 131 (2019) 105026. <https://doi.org/10.1016/j.envint.2019.105026>.
- [103] L. Rizzo, S. Malato, D. Antakyali, V.G. Beretsou, M.B. Đolić, W. Gernjak, E. Heath, I. Ivancev-Tumbas, P. Karaolia, A.R. Lado Ribeiro, G. Mascolo, C.S. McArdell, H. Schaar, A.M.T. Silva, D. Fatta-Kassinos, Consolidated vs new advanced treatment methods for the removal of contaminants of emerging concern from urban wastewater, *Sci. Total Environ.* 655 (2019) 986–1008. <https://doi.org/10.1016/J.SCITOTENV.2018.11.265>.
- [104] A. Kunhikrishnan, A. Rahman, D. Lamb, N.S. Bolan, Rare earth elements (REE) for the removal and recovery of phosphorus : A review, *Chemosphere.* 286 (2022) 131661. <https://doi.org/10.1016/j.chemosphere.2021.131661>.
- [105] A. Finzi, V. Guido, E. Riva, O. Ferrari, D. Quilez, E. Herrero, G. Provolo, Performance and sizing of filtration equipment to replace mineral fertilizer with digestate in drip and sprinkler fertigation, *J. Clean. Prod.* 317 (2021) 128431. <https://doi.org/10.1016/j.jclepro.2021.128431>.
- [106] S. Kundu, B.K. Pramanik, P. Halder, S. Patel, M. Ramezani, M.A. Khairul, M.H. Marzbali, J. Paz-Ferreiro, S. Crosher, G. Short, A. Surapaneni, D. Bergmann, K. Shah, Source and central level recovery of nutrients from urine and wastewater: A state-of-art on nutrients mapping and potential technological solutions, *J. Environ. Chem. Eng.* 10 (2022) 107146. <https://doi.org/10.1016/j.jece.2022.107146>.
- [107] C. Magoni, S. Bertacchi, C.M. Giustra, L. Guzzetti, R. Cozza, M. Ferrari, A. Torelli, M. Marieschi, D. Porro, P. Branduardi, M. Labra, Could microalgae be a strategic choice for responding to the demand for omega-3 fatty acids? A European perspective, *Trends Food Sci. Technol.* 121 (2022) 142–155.

- <https://doi.org/10.1016/j.tifs.2022.01.030>.
- [108] E. Kendir, M. Hartl, J. Kisser, Z. Cetecioglu, Phosphorus mining from eutrophic marine environment towards a blue economy: The role of bio-based applications, *Water Res.* 219 (2022) 118505. <https://doi.org/10.1016/j.watres.2022.118505>.
- [109] P.S. Goh, K.C. Wong, A.F. Ismail, Membrane technology: A versatile tool for saline wastewater treatment and resource recovery, *Desalination.* 521 (2022) 115377. <https://doi.org/10.1016/j.desal.2021.115377>.
- [110] M. Sobhi, J. Guo, M.S. Gaballah, B. Li, J. Zheng, X. Cui, H. Sun, R. Dong, Selecting the optimal nutrients recovery application for a biogas slurry based on its characteristics and the local environmental conditions: A critical review, *Sci. Total Environ.* 814 (2022) 152700. <https://doi.org/10.1016/j.scitotenv.2021.152700>.
- [111] S. Malato, P. Fernández-Ibáñez, M.I. Maldonado, J. Blanco, W. Gernjak, Decontamination and disinfection of water by solar photocatalysis: Recent overview and trends, *Catal. Today.* 147 (2009) 1–59. <https://doi.org/10.1016/j.cattod.2009.06.018>.
- [112] S. Ziembowicz, M. Kida, Limitations and future directions of application of the Fenton-like process in micropollutants degradation in water and wastewater treatment: A critical review, *Chemosphere.* 296 (2022). <https://doi.org/10.1016/j.chemosphere.2022.134041>.
- [113] U.J. Ahile, R.A. Wuana, A.U. Itodo, R. Sha’Ato, R.F. Dantas, A review on the use of chelating agents as an alternative to promote photo-Fenton at neutral pH: Current trends, knowledge gap and future studies, *Sci. Total Environ.* 710 (2020) 134872. <https://doi.org/10.1016/j.scitotenv.2019.134872>.
- [114] M.E.T. Sillanpää, T.A. Kurniawan, W. hung Lo, Degradation of chelating agents in aqueous solution using advanced oxidation process (AOP), *Chemosphere.* 83 (2011) 1443–1460. <https://doi.org/10.1016/j.chemosphere.2011.01.007>.
- [115] C. Oviedo, J. Rodríguez, EDTA: The chelating agent under environmental scrutiny, *Quim. Nova.* 26 (2003) 901–905. <https://doi.org/10.1590/S0100-40422003000600020>.
- [116] Y. Wang, Y. Lu, J. Lu, Z. Yang, Z. Yang, Research progress on the biosynthesis and bioproduction of the biodegradable chelating agent ( S , S ) -EDDS, *Process Biochem.* 116 (2022) 38–48. <https://doi.org/10.1016/j.procbio.2022.02.025>.
- [117] S. Tandy, A. Ammann, R. Schulin, B. Nowack, Biodegradation and speciation of residual SS-ethylenediaminedisuccinic acid (EDDS) in soil solution left after soil washing, *Environ. Pollut.* 142 (2006) 191–199. <https://doi.org/10.1016/j.envpol.2005.10.013>.
- [118] L. Clarizia, D. Russo, I. Di Somma, R. Marotta, R. Andreatti, Environmental Homogeneous photo-Fenton processes at near neutral pH: A review, *Applied Catal. B, Environ.* 209 (2017) 358–371. <https://doi.org/10.1016/j.apcatb.2017.03.011>.
- [119] C.A. Martínez-huitle, M.A. Rodrigo, *Electrochemical Water and Wastewater Treatment*, First Edit, Elsevier Inc., 2018.
- [120] S. Garcia-Segura, E.B. Cavalcanti, E. Brillas, Mineralization of the antibiotic chloramphenicol by solar photoelectro-Fenton. From stirred tank reactor to solar pre-pilot plant., *Appl. Catal. B Environ.* 144 (2014) 588–598.



## References

- <https://doi.org/10.1016/j.apcatb.2013.07.071>.
- [121] M.C. Santos, V.S. Antonin, F.M. Souza, L.R. Aveiro, P.C. Moura, C.R. Silva, V.S. Pinheiro, T.C. Gentil, T.S. Lima, L.E.B. Lucchetti, L. Codognoto, I. Robles, M.R. V Lanza, Decontamination of wastewater containing contaminants of emerging concern by electrooxidation and Fenton-based processes – A review on the relevance of materials and methods, *Chemosphere*. 307 (2022). <https://doi.org/10.1016/j.chemosphere.2022.135763>.
- [122] J.C. Murillo-Sierra, E. Ruiz-Ruiz, L. Hinojosa-Reyes, J.L. Guzmán-Mar, F. Machuca-Martínez, A. Hernández-Ramírez, Sulfamethoxazole mineralization by solar photo electro-Fenton process in a pilot plant, *Catal. Today*. 313 (2018) 175–181. <https://doi.org/10.1016/j.cattod.2017.11.003>.
- [123] A. Li, J. Weng, X. Yan, H. Li, H. Shi, X. Wu, Electrochemical oxidation of acid orange 74 using Ru, IrO<sub>2</sub>, PbO<sub>2</sub>, and boron doped diamond anodes: Direct and indirect oxidation, *J. Electroanal. Chem.* 898 (2021) 115622. <https://doi.org/10.1016/j.jelechem.2021.115622>.
- [124] C. LeFrou, P. Fabry, J.-C. Poignet, *Electrochemistry - The Basics, With Examples*, Springer Berlin Heidelberg, 2009.
- [125] P. V. Nidheesh, A. Adeyemi, N.G. Yasri, A.R. Laiju, V.R.S. Cheela, A. Thiam, Y.G. Asfaha, S. Kanmani, E. Ted, P.L. Roberts, Emerging applications, reactor design and recent advances of electrocoagulation process, *Process Saf. Environ. Prot.* 166 (2022) 600–616. <https://doi.org/10.1016/j.psep.2022.08.051>.
- [126] Z. Hu, J. Cai, G. Song, Y. Tian, Electrochemistry Anodic oxidation of organic pollutants: Anode fabrication, process hybrid and environmental applications, *Curr. Opin. Electrochem.* 26 (2021) 100659. <https://doi.org/10.1016/j.coelec.2020.100659>.
- [127] E. Brillas, Fenton, photo-Fenton, electro-Fenton, and their combined treatments for the removal of insecticides from waters and soils. A review, *Sep. Purif. Technol.* 284 (2022) 120290. <https://doi.org/10.1016/j.seppur.2021.120290>.
- [128] J. Casado, Towards industrial implementation of Electro-Fenton and derived technologies for wastewater treatment: A review, *J. Environ. Chem. Eng.* 7 (2019) 102823. <https://doi.org/10.1016/j.jece.2018.102823>.
- [129] D. Li, T. Zheng, Y. Liu, D. Hou, K.K. Yao, W. Zhang, H. Song, H. He, W. Shi, L. Wang, J. Ma, A novel Electro-Fenton process characterized by aeration from inside a graphite felt electrode with enhanced electrogeneration of H<sub>2</sub>O<sub>2</sub> and cycle of Fe<sup>3+</sup>/Fe<sup>2+</sup>, *J. Hazard. Mater.* 396 (2020) 122591. <https://doi.org/10.1016/j.jhazmat.2020.122591>.
- [130] K. V. Plakas, S.D. Sklari, D.A. Yiankakis, G. Th. V.T. Zaspalis, A.J. Karabelas, Removal of organic micropollutants from drinking water by a novel electro-Fenton filter: Pilot-scale studies, *Water Res.* 91 (2016) 183–194. <https://doi.org/10.1016/j.watres.2016.01.013>.
- [131] I. Salmerón, I. Oller, S. Malato, Solar photo-assisted electrochemical processes applied to actual industrial and urban wastewaters: A practical approach based on recent literature, *Chemosphere*. 279 (2021). <https://doi.org/10.1016/j.chemosphere.2021.130560>.
- [132] D. Lu, Z. Yao, L. Jiao, M. Waheed, Z. Sun, L. Zhang, Separation mechanism, selectivity enhancement strategies and advanced materials for mono-

- /multivalent ion-selective nanofiltration membrane, *Adv. Membr.* 2 (2022) 100032. <https://doi.org/10.1016/j.advmem.2022.100032>.
- [133] E.M. V Hoek, M.M. Pendergast, V. V Tarabara, *Encyclopedia of Membrane Science and Technology*, John Wiley & Sons, Inc., 2013. <https://doi.org/9781118522318>.
- [134] R.B. Merlet, M.A. Pizzoccaro-Zilamy, A. Nijmeijer, L. Winnubst, Hybrid ceramic membranes for organic solvent nanofiltration: State-of-the-art and challenges, *J. Memb. Sci.* 599 (2020) 117839. <https://doi.org/10.1016/j.memsci.2020.117839>.
- [135] A.F. Ismail, T. Matsuura, *Membrane Technology for Water and Wastewater Treatment*, Energy and Environment, 2016. <https://doi.org/10.1201/b19702>.
- [136] J. Wei, J. Kilduff, G. Belfort, The behavior of suspensions and macromolecular solutions in crossflow microfiltration: An update, *J. Memb. Sci.* 601 (2020) 117865. <https://doi.org/10.1016/j.memsci.2020.117865>.
- [137] S. Fatima, R. Hashaikeh, N. Hilal, Microfiltration membrane processes: A review of research trends over the past decade, *J. Water Process Eng.* 32 (2019). <https://doi.org/10.1016/j.jwpe.2019.100941>.
- [138] C.D. Peters, T. Rantissi, V. Gitis, N.P. Hankins, Retention of natural organic matter by ultrafiltration and the mitigation of membrane fouling through pre-treatment, membrane enhancement, and cleaning - A review, *J. Water Process Eng.* 44 (2021) 102374. <https://doi.org/10.1016/j.jwpe.2021.102374>.
- [139] R.K. Manoharan, F. Ishaque, Y.H. Ahn, Fate of antibiotic resistant genes in wastewater environments and treatment strategies - A review, *Chemosphere.* 298 (2022) 134671. <https://doi.org/10.1016/j.chemosphere.2022.134671>.
- [140] D. Yadav, S. Karki, P.G. Ingole, Current advances and opportunities in the development of nanofiltration (NF) membranes in the area of wastewater treatment, water desalination, biotechnological and pharmaceutical applications, *J. Environ. Chem. Eng.* 10 (2022) 108109. <https://doi.org/10.1016/j.jece.2022.108109>.
- [141] G.M. Shi, Y. Feng, B. Li, H.M. Tham, J.Y. Lai, T.S. Chung, Recent progress of organic solvent nanofiltration membranes, *Prog. Polym. Sci.* 123 (2021) 101470. <https://doi.org/10.1016/j.progpolymsci.2021.101470>.
- [142] I. Ibrar, S. Yadav, O. Najj, A.A. Alanezi, N. Ghaffour, S. Déon, S. Subbiah, A. Altaee, Development in forward Osmosis-Membrane distillation hybrid system for wastewater treatment, *Sep. Purif. Technol.* 286 (2022). <https://doi.org/10.1016/j.seppur.2022.120498>.
- [143] American Water Works Association, *Reverse Osmosis and Nanofiltration Manual of Water Supply Practices*, 2nd Ed., 2007.
- [144] X. Zhang, Y. Liu, Reverse osmosis concentrate: An essential link for closing loop of municipal wastewater reclamation towards urban sustainability, *Chem. Eng. J.* 421 (2021) 127773. <https://doi.org/10.1016/j.cej.2020.127773>.
- [145] Q.V. Ly, Y. Hu, J. Li, J. Cho, J. Hur, Characteristics and influencing factors of organic fouling in forward osmosis operation for wastewater applications: A comprehensive review, *Environ. Int.* 129 (2019) 164–184. <https://doi.org/10.1016/j.envint.2019.05.033>.
- [146] A. Lesimple, F.E. Ahmed, N. Hilal, Remineralization of desalinated water: Methods and environmental impact, *Desalination.* 496 (2020) 114692.

## References

- <https://doi.org/10.1016/j.desal.2020.114692>.
- [147] M. Philibert, A. Filingeri, C. Natalello, N. Moe, E. Filloux, A. Cipollina, Surface water RO permeate remineralization through minerals recovery from brines, *Desalination*. 531 (2022) 115725. <https://doi.org/10.1016/j.desal.2022.115725>.
- [148] H. Julian, N. Nurgirisia, G. Qiu, Y.P. Ting, I.G. Wenten, Membrane distillation for wastewater treatment: Current trends, challenges and prospects of dense membrane distillation, *J. Water Process Eng.* 46 (2022) 102615. <https://doi.org/10.1016/j.jwpe.2022.102615>.
- [149] T. Khayet, Mohamed; Matsuura, *Membrane Distillation Principles and Applications*, 2011. <https://doi.org/10.1016/b978-0-444-53126-1.10017-x>.
- [150] J.A. Kharraz, N.K. Khanzada, M.U. Farid, J. Kim, S. Jeong, A.K. An, Membrane distillation bioreactor (MDBR) for wastewater treatment, water reuse, and resource recovery: A review, *J. Water Process Eng.* 47 (2022) 102687. <https://doi.org/10.1016/j.jwpe.2022.102687>.
- [151] D. da Silva Biron, V. dos Santos, M. Zeni, *Ceramic Membranes Applied in Separation Processes*, 2017. <https://doi.org/10.1007/978-3-319-58604-5>.
- [152] N.Y. Ahmad Fauzi Ismail Ph.D, Wan Norharyati Wan Salleh, *Synthetic Polymeric Membranes for Advanced Water Treatment, Gas Separation, and Energy Sustainability (Ahmad Fauzi Ismail Ph.D (editor) etc.) (z-lib.org).pdf*, 2020. <https://doi.org/https://doi.org/10.1016/C2018-0-04133-X>.
- [153] C. Das, S. Bose, *Advanced Ceramic Membranes and Applications*, 2017. <https://doi.org/https://doi.org/10.1201/9781315165530>.
- [154] E. Eray, V.M. Candelario, V. Boffa, H. Safafar, D.N. Østedgaard-Munck, N. Zahrtmann, H. Kadrispahic, M.K. Jørgensen, A roadmap for the development and applications of silicon carbide membranes for liquid filtration: Recent advancements, challenges, and perspectives, *Chem. Eng. J.* 414 (2021). <https://doi.org/10.1016/j.cej.2021.128826>.
- [155] C. Wang, M. Jun, H. Yu, H. Matsuyama, E. Drioli, H. Kyong, Recent advances of nanocomposite membranes using layer-by-layer assembly, *J. Memb. Sci.* 661 (2022) 120926. <https://doi.org/10.1016/j.memsci.2022.120926>.
- [156] X. Jin, C. Wu, L. Fu, X. Tian, P. Wang, Y. Zhou, J. Zuo, Development, dilemma and potential strategies for the application of nanocatalysts in wastewater catalytic ozonation: A review, *J. Environ. Sci.* 124 (2023) 330–349. <https://doi.org/10.1016/j.jes.2021.09.041>.
- [157] H.R. Tschiche, F.S. Bierkandt, O. Creutzenberg, V. Fessard, R. Franz, B. Giese, R. Greiner, K. Haas, A. Haase, A. Hartwig, K. Hund-rinke, P. Iden, C. Kromer, D. Mutz, A. Rakow, K. Rasmussen, H. Richter, J. Schoon, O. Schmid, C. Som, G.E.M. Tovar, P. Westerhoff, W. Wohlleben, A. Luch, P. Laux, Environmental considerations and current status of grouping and regulation of engineered nanomaterials, *Environ. Nanotechnology, Monit. Manag.* (2022) 100707. <https://doi.org/10.1016/j.enmm.2022.100707>.
- [158] V. Gitis, *Ceramic Membranes*, 2016. <https://doi.org/10.2138/rmg.2014.78.16>.
- [159] A. Kim, J. Hak Kim, R. Patel, Modification strategies of membranes with enhanced Anti-biofouling properties for wastewater Treatment: A review, *Bioresour. Technol.* 345 (2022) 126501. <https://doi.org/10.1016/j.biortech.2021.126501>.

- [160] G. Bargeman, Recent developments in the preparation of improved nanofiltration membranes for extreme pH conditions, *Sep. Purif. Technol.* 279 (2021) 119725. <https://doi.org/10.1016/j.seppur.2021.119725>.
- [161] F.E. Bortot Coelho, F. Nurisso, V. Boffa, X. Ma, F.A.O. Rasse-Suriani, P. Roslev, G. Magnacca, V. Candelario, F. Deganello, V. La Parola, A thermocatalytic perovskite-graphene oxide nanofiltration membrane for water depollution, *J. Water Process Eng.* 49 (2022) 102941. <https://doi.org/10.1016/j.jwpe.2022.102941>.
- [162] O. Samuel, M.H.D. Othman, R. Kamaludin, T.A. Kurniawan, T. Li, H. Dzinun, A. Imtiaz, Treatment of oily wastewater using photocatalytic membrane reactors: A critical review, *J. Environ. Chem. Eng.* 10 (2022) 108539. <https://doi.org/10.1016/j.jece.2022.108539>.
- [163] M. Bilal, Z. Zhang, Ceramic membrane technology for water and wastewater treatment: A critical review of performance, full-scale applications, membrane fouling and prospects, *Chem. Eng. J.* 418 (2021) 129481. <https://doi.org/10.1016/j.cej.2021.129481>.
- [164] Y. Tu, L. Samineni, T. Ren, A.B. Schantz, W. Song, S. Sharma, M. Kumar, Prospective applications of nanometer-scale pore size biomimetic and bioinspired membranes, *J. Memb. Sci.* 620 (2021) 118968. <https://doi.org/10.1016/j.memsci.2020.118968>.
- [165] Y. Wang, Y. Liu, Z. Chen, Y. Liu, J. Guo, W. Zhang, Recent progress in the pore size control of silicon carbide ceramic membranes, *Ceram. Int.* 48 (2022) 8960–8971. <https://doi.org/10.1016/j.ceramint.2022.01.092>.
- [166] J. Usman, M. Hafiz, D. Othman, A. Fauzi, M.A. Rahman, J. Jaafar, Y. Olabode, A.O. Gbadamosi, T. Hassan, E. Badawy, An overview of superhydrophobic ceramic membrane surface modification for oil-water separation, *J. Mater. Res. Technol.* 12 (2021) 643–667. <https://doi.org/10.1016/j.jmrt.2021.02.068>.
- [167] L. Yan, X. Yang, Y. Zhang, Y. Wu, Z. Cheng, S.B. Darling, L. Shao, Porous Janus materials with unique asymmetries and functionality, *Mater. Today.* 51 (2021) 626–647. <https://doi.org/10.1016/j.mattod.2021.07.001>.
- [168] M. Afsari, H.K. Shon, L.D. Tijng, Janus membranes for membrane distillation : Recent advances and challenges, *Adv. Colloid Interface Sci.* 289 (2021) 102362. <https://doi.org/10.1016/j.cis.2021.102362>.
- [169] S.N. Malik, P.C. Ghosh, A.N. Vaidya, S.N. Mudliar, Hybrid ozonation process for industrial wastewater treatment: Principles and applications: A review, *J. Water Process Eng.* 35 (2020). <https://doi.org/10.1016/j.jwpe.2020.101193>.
- [170] Y. Ren, Y. Ma, G. Min, W. Zhang, L. Lv, W. Zhang, A mini review of multifunctional ultrafiltration membranes for wastewater decontamination: Additional functions of adsorption and catalytic oxidation, *Sci. Total Environ.* 762 (2021). <https://doi.org/10.1016/j.scitotenv.2020.143083>.
- [171] S. Mathew, G. George, M.S. Sajna, V.P. Prakashan, T. Anna, P. Vasudevan, A.C. Saritha, P.R. Biju, C. Joseph, N. V Unnikrishnan, Recent advancements in multifunctional applications of sol-gel derived polymer incorporated TiO<sub>2</sub>-ZrO<sub>2</sub> composite coatings : A comprehensive review, *Appl. Surf. Sci. Adv.* 6 (2021) 100173. <https://doi.org/10.1016/j.apsadv.2021.100173>.
- [172] S. Banerjee, D.D. Dionysiou, S.C. Pillai, Self-cleaning applications of TiO<sub>2</sub> by photo-induced hydrophilicity and photocatalysis, "Applied Catal. B, Environ.

## References

- 176–177 (2015) 396–428. <https://doi.org/10.1016/j.apcatb.2015.03.058>.
- [173] S. Gupta, H. Gomaa, M.B. Ray, A novel submerged photocatalytic oscillatory membrane reactor for water polishing, *J. Environ. Chem. Eng.* 9 (2021) 105562. <https://doi.org/10.1016/j.jece.2021.105562>.
- [174] V.R. Moreira, Y. Abner, R. Lebron, M. Cristina, S. Amaral, Enhancing industries exploitation : Integrated and hybrid membrane separation processes applied to industrial effluents beyond the treatment for disposal, *Chem. Eng. J.* 430 (2022) 133006. <https://doi.org/10.1016/j.cej.2021.133006>.
- [175] P. Luis, Chapter 8 - Hybrid processes based on membrane technology, Elsevier Inc., 2018. <https://doi.org/10.1016/B978-0-12-813483-2.00008-3>.
- [176] Z. Adlan, M. Hir, A. Halim, Hybrid polymer-based photocatalytic materials for the removal of selected endocrine disrupting chemicals ( EDCs ) from aqueous media : A review, *J. Mol. Liq.* 361 (2022) 119632. <https://doi.org/10.1016/j.molliq.2022.119632>.
- [177] R. Mohammadi, W. Tang, M. Sillanpää, A systematic review and statistical analysis of nutrient recovery from municipal wastewater by electro dialysis, *Desalination.* 498 (2021) 114626. <https://doi.org/10.1016/j.desal.2020.114626>.
- [178] A.L. Eusebi, F. Fatone, G. Cipolletta, N. Lancioni, Brine treatment technologies towards minimum / zero liquid discharge and resource recovery : State of the art and techno-economic assessment, 300 (2021). <https://doi.org/10.1016/j.jenvman.2021.113681>.
- [179] A. Panagopoulos, Process Intensification Brine management ( saline water & wastewater effluents ): Sustainable utilization and resource recovery strategy through Minimal and Zero Liquid Discharge ( MLD & ZLD ) desalination systems, *Chem. Eng. Process. - Process Intensif.* 176 (2022) 108944. <https://doi.org/10.1016/j.cep.2022.108944>.
- [180] T.N. Cao, X. Bui, L. Le, B. Dang, An overview of deploying membrane bioreactors in saline wastewater treatment from perspectives of microbial and treatment performance, *Bioresour. Technol.* 363 (2022) 127831. <https://doi.org/10.1016/j.biortech.2022.127831>.
- [181] A. Singh, K.C. Surendra, D. Wu, H. Lu, J.W.C. Wong, S. Kumar, Anaerobic membrane bioreactors for pharmaceutical-laden wastewater treatment : A critical review, 361 (2022). <https://doi.org/10.1016/j.biortech.2022.127667>.
- [182] J. Matinmikko, S. Kinnunen, T. Sinkkonen, K. Timo, Towards sustainable feasibility studies for P2X investments, 365 (2022). <https://doi.org/10.1016/j.jclepro.2022.132641>.
- [183] B. Akkoyunlu, S. Daly, E. Casey, Membrane bioreactors for the production of value-added products : Recent developments , challenges and perspectives, *Bioresour. Technol.* 341 (2021) 125793. <https://doi.org/10.1016/j.biortech.2021.125793>.
- [184] S. Dayana, P. Suresh, S. Manikandan, R. Subbaiya, M. Govarthan, N. Karmegam, Phycoremediation of wastewater for pollutant removal : A green approach to environmental protection and long-term remediation, *Environ. Pollut.* 290 (2021) 117989. <https://doi.org/10.1016/j.envpol.2021.117989>.
- [185] P. Verma, Phycology-Based Approaches for Wastewater Treatment and Resource Recovery, 1st Editio, M.P. Shah, Ed., 2021.

- <https://doi.org/https://doi.org/10.1201/9781003155713>.
- [186] L. Jiang, Y. Liu, F. Guo, Z. Zhou, J. Jiang, Z. You, Q. Wang, Z. Wang, Z. Wu, Evaluation of nutrient removal performance and resource recovery potential of anaerobic/anoxic/aerobic membrane bioreactor with limited aeration, *Bioresour. Technol.* 340 (2021) 125728. <https://doi.org/10.1016/j.biortech.2021.125728>.
- [187] P. Soriano-Molina, P. Plaza-Bolaños, A. Lorenzo, A. Agüera, J.L. García Sánchez, S. Malato, J.A. Sánchez Pérez, Assessment of solar raceway pond reactors for removal of contaminants of emerging concern by photo-Fenton at circumneutral pH from very different municipal wastewater effluents, *Chem. Eng. J.* 366 (2019) 141–149. <https://doi.org/10.1016/j.cej.2019.02.074>.
- [188] A. Cabrera-Reina, S. Miralles-Cuevas, J.A. Sánchez Pérez, R. Salazar, Application of solar photo-Fenton in raceway pond reactors: A review, *Sci. Total Environ.* 800 (2021) 149653. <https://doi.org/10.1016/j.scitotenv.2021.149653>.
- [189] R. Salazar, S. Campos, J. Martínez, F. Luna, A. Thiam, M. Aranda, W. Calzadilla, S. Miralles-Cuevas, A. Cabrera-Reina, New development of a solar electrochemical raceway pond reactor for industrial wastewater treatment, *Environ. Res.* 212 (2022). <https://doi.org/10.1016/j.envres.2022.113553>.
- [190] S. Jafarinejad, Forward osmosis membrane technology for nutrient removal/recovery from wastewater: Recent advances, proposed designs, and future directions, *Chemosphere.* 263 (2021) 128116. <https://doi.org/10.1016/j.chemosphere.2020.128116>.
- [191] N. Krishnamoorthy, T. Arunachalam, B. Paramasivan, A comparative study of phosphorus recovery as struvite from cow and human urine, *Mater. Today Proc.* (2021) 7–11. <https://doi.org/10.1016/j.matpr.2021.04.587>.
- [192] AQUAlity - European Union's Horizon 2020 research and innovation programme under the Marie Skłodowska-Curie grant agreement N. 765860, (n.d.). <https://www.aquality-etn.eu/the-project/>.
- [193] P. Laborda, F. Sanz-García, S. Hernando-Amado, J.L. Martínez, *Pseudomonas aeruginosa*: an antibiotic resilient pathogen with environmental origin, *Curr. Opin. Microbiol.* 64 (2021) 125–132. <https://doi.org/10.1016/j.mib.2021.09.010>.
- [194] C. Lozano, M. López, B. Rojo-Bezares, Y. Sáenz, Antimicrobial susceptibility testing in *pseudomonas aeruginosa* biofilms: One step closer to a standardized method, *Antibiotics.* 9 (2020) 1–11. <https://doi.org/10.3390/antibiotics9120880>.
- [195] S. Mizunaga, T. Kamiyama, Y. Fukuda, M. Takahata, J. Mitsuyama, Influence of inoculum size of *Staphylococcus aureus* and *Pseudomonas aeruginosa* on in vitro activities and in vivo efficacy of fluoroquinolones and carbapenems, *J. Antimicrob. Chemother.* 56 (2005) 91–96. <https://doi.org/10.1093/jac/dki163>.
- [196] C. Liang, C.F. Huang, N. Mohanty, R.M. Kurakalva, A rapid spectrophotometric determination of persulfate anion in ISCO, *Chemosphere.* 73 (2008) 1540–1543. <https://doi.org/10.1016/j.chemosphere.2008.08.043>.
- [197] S. Malato, J. Blanco, A. Campos, J. Cáceres, C. Guillard, J.M. Herrmann, A.R. Fernández-Alba, Effect of operating parameters on the testing of new industrial titania catalysts at solar pilot plant scale, *Appl. Catal. B Environ.* 42 (2003) 349–357. [https://doi.org/10.1016/S0926-3373\(02\)00270-9](https://doi.org/10.1016/S0926-3373(02)00270-9).

## References

- [198] J.P. Van der Sluijs, N. Simon-Delso, D. Goulson, L. Maxim, J.M. Bonmatin, L.P. Belzunces, Neonicotinoids, bee disorders and the sustainability of pollinator services, *Curr. Opin. Environ. Sustain.* 5 (2013) 293–305. <https://doi.org/10.1016/j.cosust.2013.05.007>.
- [199] D. Klingelhöfer, M. Braun, D. Brüggmann, D.A. Groneberg, Neonicotinoids: A critical assessment of the global research landscape of the most extensively used insecticide, *Environ. Res.* 213 (2022). <https://doi.org/10.1016/j.envres.2022.113727>.
- [200] N. Klammerth, S. Malato, M. Maldonado, A. Agüery, A. Fernandez-Alba, Application of Photo-Fenton as a Tertiary Treatment of Emerging Contaminants in Municipal, *CEUR Workshop Proc.* 44 (2010) 1792–1798.
- [201] S. Miralles-Cuevas, A. Arqués, M.I. Maldonado, J.A. Sánchez-Pérez, S. Malato Rodríguez, Combined nanofiltration and photo-Fenton treatment of water containing micropollutants, *Chem. Eng. J.* (2013). <https://doi.org/10.1016/j.cej.2012.09.068>.
- [202] S. Miralles-Cuevas, I. Oller, J.A.S. Pérez, S. Malato, Application of solar photo-Fenton at circumneutral pH to nanofiltration concentrates for removal of pharmaceuticals in MWTP effluents, *Environ. Sci. Pollut. Res.* (2014). <https://doi.org/10.1007/s11356-014-2871-2>.
- [203] P. Soriano-Molina, J.L. García Sánchez, S. Malato, L.A. Pérez-Estrada, J.A. Sánchez Pérez, Effect of volumetric rate of photon absorption on the kinetics of micropollutant removal by solar photo-Fenton with Fe<sup>3+</sup>-EDDS at neutral pH, *Chem. Eng. J.* 331 (2018). <https://doi.org/10.1016/j.cej.2017.08.096>.
- [204] E.P. Costa, M. Roccamante, C.C. Amorim, I. Oller, J.A. Sánchez Pérez, S. Malato, New trend on open solar photoreactors to treat micropollutants by photo-Fenton at circumneutral pH: Increasing optical pathway, *Chem. Eng. J.* 385 (2020) 123982. <https://doi.org/10.1016/j.cej.2019.123982>.
- [205] A.R. Lado Ribeiro, N.F.F. Moreira, G. Li Puma, A.M.T. Silva, Impact of water matrix on the removal of micropollutants by advanced oxidation technologies, *Chem. Eng. J.* 363 (2019) 155–173. <https://doi.org/10.1016/j.cej.2019.01.080>.
- [206] P. Soriano-molina, P. Plaza-bolaños, A. Lorenzo, A. Agüera, J.L.G. Sánchez, Assessment of solar raceway pond reactors for removal of contaminants of emerging concern by photo-Fenton at circumneutral pH from very different municipal wastewater effluents, *Chem. Eng. J.* 366 (2019) 141–149. <https://doi.org/10.1016/j.cej.2019.02.074>.
- [207] J. De Laat, G. Truong Le, B. Legube, A comparative study of the effects of chloride, sulfate and nitrate ions on the rates of decomposition of H<sub>2</sub>O<sub>2</sub> and organic compounds by Fe(II)/H<sub>2</sub>O<sub>2</sub> and Fe(III)/H<sub>2</sub>O<sub>2</sub>, *Chemosphere.* 55 (2004) 715–723. <https://doi.org/10.1016/j.chemosphere.2003.11.021>.
- [208] A. Zapata, I. Oller, E. Bizani, J.A. Sánchez-Pérez, M.I. Maldonado, S. Malato, Evaluation of operational parameters involved in solar photo-Fenton degradation of a commercial pesticide mixture, *Catal. Today.* 144 (2009) 94–99. <https://doi.org/10.1016/j.cattod.2008.12.030>.
- [209] M. Sánchez-Polo, M.M. Abdel daiem, R. Ocampo-Pérez, J. Rivera-Utrilla, A.J. Mota, Comparative study of the photodegradation of bisphenol A by HO<sup>•</sup>, SO<sub>4</sub><sup>•-</sup> and CO<sub>3</sub><sup>•-</sup>/HCO<sub>3</sub><sup>•-</sup> radicals in aqueous phase, *Sci. Total Environ.* 463–464 (2013) 423–431. <https://doi.org/10.1016/j.scitotenv.2013.06.012>.

- [210] S. Wang, J. Wang, Trimethoprim degradation by Fenton and Fe(II)-activated persulfate processes, *Chemosphere*. 191 (2018) 97–105. <https://doi.org/10.1016/j.chemosphere.2017.10.040>.
- [211] X. Wang, W. Dong, M. Brigante, G. Mailhot, Hydroxyl and sulfate radicals activated by Fe(III)-EDDS/UV: Comparison of their degradation efficiencies and influence of critical parameters, *Appl. Catal. B Environ.* 245 (2019) 271–278. <https://doi.org/10.1016/j.apcatb.2018.12.052>.
- [212] Y. Wu, A. Bianco, M. Brigante, W. Dong, P. De Sainte-Claire, K. Hanna, G. Mailhot, Sulfate Radical Photogeneration Using Fe-EDDS: Influence of Critical Parameters and Naturally Occurring Scavengers, *Environ. Sci. Technol.* 49 (2015) 14343–14349. <https://doi.org/10.1021/acs.est.5b03316>.
- [213] L. Lian, B. Yao, S. Hou, J. Fang, S. Yan, W. Song, Kinetic Study of Hydroxyl and Sulfate Radical-Mediated Oxidation of Pharmaceuticals in Wastewater Effluents, *Environ. Sci. Technol.* 51 (2017) 2954–2962. <https://doi.org/10.1021/acs.est.6b05536>.
- [214] B.R. Gonçalves, R.O. Guimarães, L.L. Batista, C. Ueira-Vieira, M.C.V.M. Starling, A.G. Trovó, Reducing toxicity and antimicrobial activity of a pesticide mixture via photo-Fenton in different aqueous matrices using iron complexes, *Sci. Total Environ.* 740 (2020) 140152. <https://doi.org/10.1016/j.scitotenv.2020.140152>.
- [215] F. Rodrigues-Silva, M.C. Maria, C.C. Amorim, Challenges on solar oxidation as post-treatment of municipal wastewater from UASB systems: Treatment efficiency, disinfection and toxicity, *Sci. Total Environ.* 850 (2022) 157940. <https://doi.org/10.1016/j.scitotenv.2022.157940>.
- [216] D.T. Britto, H.J. Kronzucker, NH<sub>4</sub><sup>+</sup> toxicity in higher plants: A critical review, *J. Plant Physiol.* 159 (2002) 567–584. <https://doi.org/10.1078/0176-1617-0774>.
- [217] A.R. Conklin, *Introduction to Soil Chemistry: Analysis and Instrumentation*, 2005. <https://doi.org/10.1002/0471728225>.
- [218] S. Hülsmann, *Managing Water, Soil and Waste Resources to Achieve Sustainable Development Goals*, 2018. <https://doi.org/10.1007/978-3-319-75163-4>.
- [219] D. Deemter, I. Oller, A.M. Amat, S. Malato, Effect of salinity on preconcentration of contaminants of emerging concern by nanofiltration: Application of solar photo-Fenton as a tertiary treatment, *Sci. Total Environ.* (2020) 143593. <https://doi.org/https://doi.org/10.1016/j.scitotenv.2020.143593>.
- [220] A. Cabrera-Reina, S. Miralles-Cuevas, I. Oller, J.A. Sánchez-Pérez, S. Malato, Modeling persulfate activation by iron and heat for the removal of contaminants of emerging concern using carbamazepine as model pollutant, *Chem. Eng. J.* 389 (2020) 124445. <https://doi.org/10.1016/j.cej.2020.124445>.
- [221] R.R. Solís, F.J. Rivas, A.M. Chávez, D.D. Dionysiou, Peroxymonosulfate/solar radiation process for the removal of aqueous microcontaminants. Kinetic modeling, influence of variables and matrix constituents, *J. Hazard. Mater.* 400 (2020). <https://doi.org/10.1016/j.jhazmat.2020.123118>.
- [222] I. Salmerón, G. Rivas, I. Oller, A. Martínez-Piernas, A. Agüera, S. Malato, Nanofiltration retentate treatment from urban wastewater secondary effluent by solar electrochemical oxidation processes, *Sep. Purif. Technol.* 254 (2021) 117614. <https://doi.org/10.1016/j.seppur.2020.117614>.
- [223] M. Panizza, G. Cerisola, Direct and mediated anodic oxidation of organic



## References

- pollutants, *Chem. Rev.* 109 (2009) 6541–6569. <https://doi.org/10.1021/cr9001319>.
- [224] C.A. Martínez-Huitle, E. Brillas, Decontamination of wastewaters containing synthetic organic dyes by electrochemical methods: A general review, *Appl. Catal. B Environ.* 87 (2009) 105–145. <https://doi.org/10.1016/j.apcatb.2008.09.017>.
- [225] E. Mostafa, P. Reinsberg, S. Garcia-Segura, H. Baltruschat, Chlorine species evolution during electrochlorination on boron-doped diamond anodes: In-situ electrogeneration of Cl<sub>2</sub>, Cl<sub>2</sub>O and ClO<sub>2</sub>, *Electrochim. Acta.* 281 (2018) 831–840. <https://doi.org/10.1016/j.electacta.2018.05.099>.
- [226] A. Sánchez-Carretero, C. Sáez, P. Cañizares, M.A. Rodrigo, Electrochemical production of perchlorates using conductive diamond electrolyses, *Chem. Eng. J.* 166 (2011) 710–714. <https://doi.org/10.1016/j.cej.2010.11.037>.
- [227] F.E.B. Coelho, D. Deemter, V.M. Candelario, V. Boffa, S. Malato, G. Magnacca, Development of a Photocatalytic Zirconia-Titania Ultrafiltration Membrane with Anti-fouling and Self-cleaning Properties, *J. Environ. Chem. Eng.* 9 (2021) 106671. <https://doi.org/10.1016/j.jece.2021.106671>.
- [228] S.M. Kim, I. In, S.Y. Park, Study of photo-induced hydrophilicity and self-cleaning property of glass surfaces immobilized with TiO<sub>2</sub> nanoparticles using catechol chemistry, *Surf. Coatings Technol.* 294 (2016) 75–82. <https://doi.org/10.1016/j.surfcoat.2016.03.080>.
- [229] A. Saini, I. Arora, J.K. Ratan, Photo-induced hydrophilicity of micro-sized-TiO<sub>2</sub> based self-cleaning cement, *Mater. Lett.* 260 (2020) 126888. <https://doi.org/10.1016/j.matlet.2019.126888>.
- [230] C.N. Rani, S. Karthikeyan, S. Prince Arockia Doss, Photocatalytic ultrafiltration membrane reactors in water and wastewater treatment - A review, *Chem. Eng. Process. - Process Intensif.* 165 (2021) 108445. <https://doi.org/10.1016/j.cep.2021.108445>.
- [231] E. Rommozzi, S. Giannakis, R. Giovannetti, D. Vione, C. Pulgarin, Detrimental vs. beneficial influence of ions during solar (SODIS) and photo-Fenton disinfection of *E. coli* in water: (Bi)carbonate, chloride, nitrate and nitrite effects, *Appl. Catal. B Environ.* 270 (2020). <https://doi.org/10.1016/j.apcatb.2020.118877>.
- [232] B.R. Gonçalves, R.O. Guimarães, L.L. Batista, C. Ueira-Vieira, M.C.V.M. Starling, A.G. Trovó, Reducing toxicity and antimicrobial activity of a pesticide mixture via photo-Fenton in different aqueous matrices using iron complexes, *Sci. Total Environ.* 740 (2020) 140152. <https://doi.org/10.1016/j.scitotenv.2020.140152>.
- [233] P. Soriano-molina, J.L.G. Sánchez, S. Malato, L.A. Pérez-estrada, Effect of volumetric rate of photon absorption on the kinetics of micropollutant removal by solar photo-Fenton with Fe<sup>3+</sup> -EDDS at neutral pH, *Chem. Eng. J.* 331 (2018) 84–92. <https://doi.org/10.1016/j.cej.2017.08.096>.
- [234] B. Iglewski, *Pseudomonas*, in: Baron S. (Ed.), *Med. Microbiol.* 4th Ed., University, Galveston (TX), 1996. <https://www.ncbi.nlm.nih.gov/books/NBK8326/%0A>.
- [235] C. Formosa, M. Grare, R.E. Duval, E. Dague, Nanoscale effects of antibiotics on *P. aeruginosa*, *Nanomedicine Nanotechnology, Biol. Med.* 8 (2012) 12–16. <https://doi.org/10.1016/j.nano.2011.09.009>.
- [236] M. del M. Cendra, E. Torrents, *Pseudomonas aeruginosa* biofilms and their partners in crime, *Biotechnol. Adv.* 49 (2021) 107734.

- <https://doi.org/10.1016/j.biotechadv.2021.107734>.
- [237] A. Harimawan, Y. Ting, Colloids and Surfaces B : Biointerfaces Investigation of extracellular polymeric substances ( EPS ) properties of P . aeruginosa and B . subtilis and their role in bacterial adhesion, Colloids Surfaces B Biointerfaces. 146 (2016) 459–467. <https://doi.org/10.1016/j.colsurfb.2016.06.039>.

## References

## List of abbreviations

## Abbreviations

ACN - Acetonitrile

ACS – Active chlorine species

AMB – Attached microalgal-bacterial

aMBR – Aerobic membrane bioreactor

AMR – Antimicrobial resistance

AnMBR – Anaerobic membrane bioreactor

AIT – Advanced Integrated Technology

AO – Anodic oxidation

AOP – Advanced Oxidation Process

BMB – Biofloculated microalgal-bacterial

BDD – Boron doped diamond

CFU – Colony forming unit

CAF – Caffeine

CAR – Carbamazepine

CBA – Cost benefit analysis

CF – Concentration factor

COD – Chemical Oxygen Demand

CPC – Compound Parabolic Collector

DAD – Diode Array Detector

DC – Direct Current

DIC – Diclofenac

DOC – Dissolved Organic Carbon

DPD – N, N-diethyl-p-phenylenediamine

ED – Electrodialysis

EDR – Electrodialysis reversal

EDDS – Ethylenediamine-N, N'-disuccinic acid

EDTA – Ethylenediamine tetra-acetic acid

EDX – Energy-dispersive X-ray spectroscopy

EF – Electro-Fenton

EO – Electrooxidation  
EPA – Environmental Protection Agency  
EPS – Extra-cellular polymeric substances  
EU – European Union  
FAC – Free Available Chlorine  
FMB – Free microalgal-bacterial  
FO – Forward Osmosis  
GDE – Gas diffusion electrodes  
HPLC – High Performance Liquid Chromatography  
HRAP – High-rate algal pond  
HRT – Hydraulic retention time  
IC – Ionic chromatograph  
IMI – Imidacloprid  
LCA – Life cycle analysis  
LOQ – Limit of quantification  
MBR – Membrane bioreactor  
MC – Micro contaminant  
MCr – Membrane crystallization  
MD – Membrane distillation  
MF – Microfiltration  
MLD – Minimum-liquid discharge – MLD  
MWCO – Molecular weight cut-off  
NF – Nanofiltration  
NTA – Nitrilotriacetic acid  
NOM – Natural organic matter  
PE – Population equivalent  
PEF – Photoelectro-Fenton  
PPCP – Pharmaceutical and personal care products  
PSA – Plataforma Solar de Almería

## Abbreviations

PSH – Photo-induced super-hydrophilicity

PSU – Power supply unit

PTFE - Polytetrafluoroethylene

PW – Produced water

RO – Reverse osmosis

ROC – Reverse osmosis concentrate

RPR – Raceway pond reactor

SAAO – Solar assisted anodic oxidation

SEC-RPR – Solar electrochemical raceway pond reactor

SEM – Scanning electron microscopy

SPEF – Solar photoelectro-Fenton

SPF – Solar photo-Fenton

THI – Thiacloprid

TMP – Trans membrane pressure

TOC – Total organic carbon

TSS – Total suspended solids

UF – Ultrafiltration

UPLC – Ultra-Performance Liquid Chromatography

UWW – Urban wastewater

UWWTP – Urban wastewater treatment plant

WHO – World Health Organization

ZLD – Zero-liquid discharge





## Annex A



## Advances in membrane separation of urban wastewater effluents for (pre) concentration of microcontaminants and nutrient recovery: A mini review

Dennis Deemter<sup>a</sup>, Isabel Oller<sup>a</sup>, Ana M. Amat<sup>b</sup>, Sixto Malato<sup>a,\*</sup>

<sup>a</sup> Plataforma Solar de Almería-CIEMAT, Carretera de Senés Km 4, Tabernas, Almería, Spain

<sup>b</sup> Grupo Procesos de Oxidación Avanzada, Universitat Politècnica de València, Campus de Alcoy, Spain

### ARTICLE INFO

#### Keywords:

Integrated technologies  
Advanced oxidation processes  
Wastewater reclamation  
Urban wastewater  
Zero-liquid discharge

### ABSTRACT

This revision work focuses on the recent advances in the separation of microcontaminants from urban wastewaters, using ultrafiltration and Nanofiltration membranes. Conventional systems show advantages such as low pressure and fouling, competitive energetic- and maintenance costs compared to reverse osmosis, and higher rejection rates of organic microcontaminants compared to membrane distillation. However, these rejection rates strongly depend on temperature, flow, and pressure, as well as surface charge and concentration, challenging the adequate treatment of more complex matrices. Recent advances in material science strongly improved the implementation possibilities of different membrane types. In conventional industrial processes and especially in wastewater treatment, offering not only cost reducing solutions for urban wastewaters, but also more efficiency for the remediation of a high variety of industrial wastewaters. Moreover, membrane separation systems show great potential and applicability for added value substance recovery from wastewaters for the agricultural, chemical and consumer industry, for more sustainable natural resources use. Finally, perspectives on promising technologies for the implementation and combination of different membrane separation methods in treatment trains, such as advanced oxidation processes, are given, also aiming for zero-liquid discharge, to prevent microcontaminants and valuable resources from passing through conventional methods and focusing on closing the water cycle.

### Abbreviations

AnMBR	anaerobic membrane bioreactor
ACS	activated chlorine species
AO	anodic oxidation
AOPs	advanced oxidation processes
BBM	biomimetic and bioinspired membrane
BDD	boron doped diamond
CEC	contaminants of emerging concern
CNT	carbon Nanotubes
COD	chemical oxygen demand
CPC	compound parabolic collector
CVD	chemical vapor deposition
EAOP	electrochemical advanced oxidation process
EC	electro coagulation
EDDS	ethylenediamine-N, N'-disuccinic acid
EF	electro-Fenton
EO	electrooxidation

EPS	extracellular polymeric substances
FO	forward osmosis
GAC	granulated activated carbon
IC	inorganic carbon
MABR	membrane aerated biofilm reactor
MBBR	moving bed bioreactor
MBMBR	moving bed Membrane bioreactor
MBR	membrane bioreactor
MCS	micro contaminants
MD	membrane distillation
MF	microfiltration
MFC	microbial fuel cell
MLD	minimum-liquid discharge
MNB	micro nano-bubble
MWCO	molecular weight cut-off
NF	nanofiltration
PA	polyamide
PAC	powdered activated carbon

\* Corresponding author.

E-mail address: [sixto.malato@psa.es](mailto:sixto.malato@psa.es) (S. Malato).

<https://doi.org/10.1016/j.cej.2022.100298>

Available online 31 March 2022

2666-8211/© 2022 The Author(s). Published by Elsevier B.V. This is an open access article under the CC BY-NC-ND license (<http://creativecommons.org/licenses/by-nc-nd/4.0/>).

PhF	Photo-Fenton
RO	reverse osmosis
ROC	reverse osmosis concentrate
SAAO	solar assisted anodic oxidation
SGM	sol-gel method
SMBR	submerged membrane bioreactor
TMP	trans-membrane pressure
TOC	total organic carbon
UF	ultrafiltration
UWW	urban wastewater
UWWTP	urban wastewater treatment plant
ZLD	zero-liquid discharge

## Introduction

Water can be considered as a commodity nowadays as it is the most important requisite to organic life on Earth. The decrease in water availability provoked by the Climate Change, specifically sweet water, jointly with the significant increase in water consumption and the pollution of available sources due to the increasing world population and wealth, require a continuous development of water technologies [1, 2].

These water technologies are not only necessary for the treatment of used water, but even more for the creation of alternative water sources, such as desalination systems. One of the main usages of such reclaimed water would be irrigation in agriculture, which accounts for around 70% of the global water consumption, as well as for human consumption and energy production [3].

One of the most efficient ways to meet these challenges is the direct reuse of treated (waste)water to close the water cycle guaranteeing, at the same time, a full control of the quality of the water in every step of the cycle. The practice of water reuse is not new, as it is known to be applied in irrigation as early as the Bronze Age (3200 – 1100 BC), by ancient civilizations such as the Cretans, the Egyptians, and the Mesopotamians. Greek and Roman civilizations (1000 BC – 330 AD) are known to have applied wastewater for both irrigation and fertilization around their major cities. This dangerous unplanned use of raw wastewater is something that is still nowadays being done at small scale in arid regions, for example in Algeria, Morocco and Egypt [4,5]. Urban wastewater (UWW) consists out of effluents coming from domestic, industrial, and agricultural areas. Their composition may vary as well as the concentrations of the present ions, pollutants, and physicochemical parameters, [6] having substantial influence on soil composition, including its fauna and flora, such as earthworms [4].

In order to be able to safely reuse the wastewaters coming from agricultural and industrial activities, as well as UWW treatment plant (UWWTP) effluents, they need to be treated to prevent elevated concentrations of organic compounds, salts, and microbiological matter. Especially in UWWTP effluents, a cocktail of different organic compounds at low concentrations can be found which are identified as 'Contaminants of Emerging Concern' (CEC) [7,8]. These microcontaminants (MCs) coming from the use of pharmaceuticals, pesticides, cosmetics, and other organic compounds show concentrations ranging from  $\mu\text{g/L}$  till  $\text{ng/L}$ . [9] As conventional UWWTPs are not efficient enough for their removal, they often end up in the environment after discharge, resulting in bioaccumulation, chronic toxicity, endocrine disruption and irreversible soil pollution, calling for the rapid application and integration of novel treatment technologies [10,11].

Many different UWW treatment methods and processes are available, although the actual implementation of these applications is staying behind, mainly for economic reasons due to the extra-cost of the treatment itself [12–15]. Another highly important reason is the lack of legislation to regulate the safe reuse of these effluents containing CECs. In Europe, only Switzerland has specific legislation about this matter, which enforces, since 2016, the removal of 80% of MCs in UWWTPs. This is mainly performed by applying ozonation combined with

adsorption techniques with powdered activated carbon (PAC) and granular activated carbon (GAC), additionally to the traditional biological and physical UWW treatment systems. Furthermore, the footprint of both activated carbon forms is intended to be reduced by producing biochar regionally from wood, biogenic waste and sewage sludge [16,17].

At the European level, the recently published EU Regulation 2020/741 regarding the minimum requirements for the reuse of water (EC Water Reuse, 2020), establishes provisions on comprehensive water management in order to guarantee the safe use of reclaimed water, promoting the circular economy and supporting adaptation to climate change [18].

Therefore, combination and integration of different novel and already available technologies is considered a challenge to tackle, not only to raise the economic efficiency, but also the practical one. This can be found in different pretreatment methods to raise process efficiencies, such as the pre-concentration of microcontaminants at the same time valuable nutrients are directly recovered in treated streams [19]. A clear example can be found in the combination of different membrane systems with different Advanced Oxidation Processes (AOPs) as polishing treatments, as well as nutrient recovery systems, or also called membrane-based hybrid technologies [20,21].

In this sense, the principles of minimum-liquid discharge (MLD) and zero-liquid discharge (ZLD) show increased research interest for the full crystallization of, for example, reverse osmosis concentrates (ROC), saline wastewaters, and industrial wastewaters by applying electrodialysis (ED), electrodialysis reversal (EDR) and membrane distillation (MD) [22–25]. The crystals on their turn, can be refined and further processed into sustainable acids and bases, metals, minerals, nutrients, and salt compounds as a recovery mechanism of added value substances from wastewater [23,26].

This revision work describes the main technologies applied in UWW treatment, based on membranes, AOPs and the recovery of valuable nutrients from wastewater. Starting with the advances made in the development of different membrane materials, as also the improvement of their working principle and selectivity, including the prevention of fouling mechanisms to improve their operation time by surface functionalization. Following with the implementation of different AOPs in the treatment processes using membranes and novel methods for valuable nutrients recovery, at the different stages of the treatment.

## Membrane separation

The principle of membrane separation is based on the different physicochemical parameters. Further mechanisms are the Donnan effect, molecular charge, surface charge, the trans-membrane pressure (TMP), and the crossflow velocity. Combination of membrane separation with pretreatments such as acidification, coagulation, flotation, and physical adsorption are very common, as they greatly extend membrane operation and lifetime.

The subject of specific rejection of compounds by membranes is important, as it is depending on several physico-chemical parameters. The importance of mapping and reporting the efficiency of different membranes and membrane systems is very high. It makes possible to effectively combine two or more different membrane types or systems, which would solely be inefficient for the treatment of UWW, greatly increasing their synergy. It would also make possible to develop custom-fit systems to treat wastewaters directly on-site, thinking about several industrial and agricultural areas, or for example effluents coming from hospitals. Both on a large or small scale, preventing the relatively concentrated wastewater streams to dilute with other wastewaters on its way to the UWWTP must be considered an important issue [27]. In Table 1 an overview of main membrane types, their materials, and drawbacks described in this work can be found.

**Table 1**  
Overview of main membrane types, their materials, and their drawbacks.

Membrane type	Membrane material	Drawback
Size exclusion	Polymeric Ceramic	Chemical sensitivity Expensive
Membrane distillation	Polymeric/ceramic	High energy consumption
Membrane bioreactor	Polymeric/ceramic	Fouling High energy consumption Microbiological stability

### Membrane systems

Microfiltration (MF) is one of the oldest pressure-driven membrane applications and has the largest pore size of membrane separation technologies, ranging from 10 – 0.1  $\mu\text{m}$ , with TMP between 0.2 and 5 bar. These inexpensive membranes are commonly used to filter out large particles, to reduce the total organic carbon (TOC) and the chemical oxygen demand (COD). Both ceramic and polymeric MF membranes are commonly used for wastewater filtration, and significantly decrease fouling in the following smaller pore size membranes [28,29].

Ultrafiltration (UF) has better selectivity than MF, but lower selectivity compared to NF membranes, as their pore size range between 0.1 – 0.01  $\mu\text{m}$ , with a TMP between 1 and 10 bar. They operate commonly in the dairy, beverage processing and pharmaceutical industry, as well as in UWW treatment. It is able to retain suspended solids, colloids, emulsions, bacteria, and viruses [30].

Nanofiltration (NF) is a relatively simple and inexpensive technology that operates under lower pressures compared to RO, showing still excellent retention capacity towards MCs and a selection of ions. The pore size lies between 0.010 and 0.001  $\mu\text{m}$ , with a TMP 5 – 10 bar. Commercially, polymeric polyamide (PA) NF membranes are mainly used as they offer excellent results regarding the retention till particles as small as monovalent ions [29].

In Reverse osmosis (RO) everything is retained except water molecules. The TMP when operating RO is between 15 and 27 bar for brackish water, and 50–80 bar for seawater desalination, with a pore size of 0.001–0.0001  $\mu\text{m}$ . Although RO obtains excellent results, and is therefore the most used process in desalination, it operates at very high pressures which come along with high energy consumption. In addition, when considered as alternative water source for irrigation activities, remineralization of the obtained distilled water (or mix with freshwater) is required beforehand. Another downfall is the fact that RO membranes are highly susceptible to fouling, such as scaling, which makes pre-filtration of the matrix highly necessary [31,32].

Forward osmosis (FO) is a process where the osmotic pressure difference is used to draw water to the feed solution through a selectively or semi-permeable membrane, and so, rejecting molecules and ions. FO offers in this way lower and reversible fouling, with lower operation and equipment costs, as well as higher water recovery rates as compared to before mentioned pressure driven categories [33].

In membrane distillation (MD), heat is used to let vapor permeate through a hydrophobic membrane based on the vapor pressure difference between its surfaces. The process is performed at low pressures and has low fouling rates compared to high pressure membrane processes, such as the previously described RO. The main challenges to overcome in this type of membrane separation system are the membrane wetting and membrane fouling, latter being both organic and inorganic [34,35]. A new development is the hybridization of MD with the membrane bioreactor (MBR), into a system where the dewatered concentrate coming from the anaerobic digester is depleted of water, resulting in a precipitation product that can be applied as a liquid biofertilizer, of which also struvite can be recovered [34].

### Membrane bioreactor systems

The membrane bioreactor (MBR) is a hybrid system that exist out of a membrane unit for physical filtration, as well as a bioreactor for biodegradation which can be used as treatment of wastewaters. MBRs have a small ecological footprint, high effluent quality, and less sludge production than conventional biotreatment. There are two general types of MBRs, the aerobic and the anaerobic MBR, though in both the high consumption of energy is considered an important drawback. New advances in this membrane-based technology show that they can be combined with microbial fuel cells (MFC), to efficiently treat wastewater, while also recover energy [36,37]. A variety on the MBR, where the biomass is suspended in the matrix, is the moving bed bioreactor (MBBR), where the biomass is grown as a biofilm on carriers made out of plastic, spongelike, or other materials. Lately, there is increased interest in combining conventional MBRs with MBBR into hybrid systems, also called moving bed membrane bioreactor (MBMBR), which further extends the advantages of high specific biomass, higher efficiency in nutrient removal, and flexible operation [38,39].

Aerobic MBR systems utilize the metabolism of microbes to breakdown matter in UWW treatment, mainly existing out of C, N, P, and S, while using oxygen. The efficiency is strongly depending on the bioactivity and the biodiversity of the microorganisms, and physicochemical factors such as temperature and salinity [40].

Opposite to this, the anaerobic MBR (AnMBR) operates without oxygen, produces like aerobic MBR high quality permeate, but due to the anaerobic environment, it produces less sludge and is also able to produce methane gas, which can be used as a combustible for the production of energy, in order to balance the energy consumption of the overall process, like with an MFC [36,41].

Submerged MBR (SMBR) are also highly employed and available at commercial level. The SMBR offers one of the most efficient solutions to limit fouling in MBRs. This is performed by enhancing the mass transfer by applying a gas/liquid two-phase flow. The permeate stream is taken from the matrix by vacuum while air washing is applied to prevent cake layer formation, whereas fouling is reversed by sequenced aeration and filtration-relaxation, backwashing [42].

Other novel variations within the MBR principles include the membrane-aerated biofilm reactor (MABR). In this type of MBR, gaseous electron acceptor, such as  $\text{O}_2$ , or electron donors, such as  $\text{H}_2$  and  $\text{CH}_4$ , are fed inside of a usually hydrophobic membrane on which a biofilm grows, significantly reducing the necessary aeration, as the gas is directly delivered to the organism, instead of dispersed into the aqueous medium. The feeding of the gas can be either dead-end or flow-through, and in the case of  $\text{CH}_4$  could be delivered from a coupled AnMBR [43]. Ren et al. recently developed an electrochemical MABR for the removal of antibiotics. The system enhanced the degradation of both sulfamethoxazole and trimethoprim, as also enriched the genus of *Xanthobacter*, which is able to degrade intermediate degradation products of the two compounds [44].

One of the drawbacks of MBRs is their low ability to reduce or eliminate unwanted microorganisms within its microbiological community, as compared to conventional biological treatment. This thereby reduces the ability of the system to biodegrade highly persistent MCs and the reduction of COD. A solution to this problem is the addition of Nano- $\text{Fe}_3\text{O}_4$  particles, resulting in decreased membrane fouling, lowering the *Bacteroidetes* and increasing the *Proteobacteria* growth in the microbial community, which results in a decrease of COD in the effluent [45]. Another solution to this problem can be found in the addition of PAC to the MBR. Asif et al. found that the PAC addition promotes the growth of 24 out of 31 genera of bacteria for a more diverse microbial community, especially for denitrifying bacteria, as well as for nitrifying and denitrifying functional genes, and MC biodegrading bacteria and genes. High concentrations of PAC in the MBR did not compromise the MC removal, nor the microbial community evolution [46].

Further challenges in the application of MBR techniques lie in the treatment of high saline wastewaters (10–100 g/L), as well as in concentration shocks, sudden changes in compound concentration such as antibiotics. These extreme conditions for bacteria, sudden or constant, cause them to increase their defense mechanism in the form of extracellular polymeric substances (EPS) production, one of the main fouling mechanisms in MBR systems and membrane systems in general. Therefore, specific microbial communities have to be found, formed, and conditioned for the treatment of such wastewaters, as well as studying of the effects of these conditions on the microorganisms. Halophilic microorganisms are such microbes that can successfully be applied till salinities of 150 g/L in wastewater treatment by MBR system [40].

### Membrane materials

One of the main classes of membranes applied in wastewater treatment are ceramic membranes. Relatively expensive, ceramic membranes offer excellent properties regarding pH and temperature operation range, and mechanical strength. Ceramic membranes can be produced from many different materials, but mainly oxides of aluminum, titanium, silicon and zirconium [47].

Ceramic membrane supports are generally produced by the compounding of different ceramic oxide materials, (polymeric) binders, and stabilizers. Mixtures of these materials are then pre-formed by extrusion or slip casting in the desired forms and air dried into so-called 'greens' before further thermal treatment. The different thermal treatments, e.g., sintering, determine the integral strength of the membranes, the pore size, pore morphology and distribution, and layer thicknesses. Mainly based on the different times and temperatures maintained. The main build-up of ceramic membranes consists out of the support material, (multiple) intermediate layers, and the final membrane layer [48].

The different pore sizes and pore morphologies of ceramic membranes are mainly based on their prime material, which is most often particles. There are numerous limitations to produce smaller ceramic particles, that, on their turn, behave differently in the production process as smaller they get, based on the volume to surface ratio. Therefore, another approach to produce membranes in the Nano range is the application of the sol-gel method (SGM). This method uses different precursor compounds to produce a gel-like substance, which is then applied on the support and sintered. Something performed by Qin et al. who prepared yttria-stabilized ZrO<sub>2</sub> NF membranes from size-controlled spherical ZrO<sub>2</sub> Nanoparticles produced by a reversed micelles-mediated SGM, for the treatment of wastewaters containing pesticides. The successfully prepared NF membranes with a MWCO of  $800 \pm 50$  Da were able to obtain a carbofuran removal of over 80% and fouled membranes were easily cleaned by an alkali washing treatment and low-temperature calcination [49,50]. Another commonly used method for the production of ceramic membranes is the chemical vapor deposition (CVD). Here a precursor vapor material is applied on the support to obtain small particles that are then sintered, obtaining small pore sizes. Pore sizes and morphologies are on their turn also strongly dependent on sintering times, temperatures, and atmosphere [51,52]. The geometries of the different ceramic membranes are mainly the disk, flat-sheet, and the tubular and hollow fiber membranes, latter being able to have multiple channels. The produced ceramic membranes are most often combined in modular set-ups and applications can often be found in industrial wastewaters for their stability, which is necessary due to the often-harsh conditions that come in these industries, such as extreme pH values, high temperatures, and abrasive chemicals [48].

Efforts to lower the price of ceramic membranes are found in methods to lower the sintering-energy consumption, as it is good for 60% of the membrane price, where material cost and fabrication procedure are good for another 20% each. To obtain this, research is mainly performed to decrease the sintering temperature by applying materials with low melting point such as kaolin and fly ash, to accelerate the

sintering speed by applying spark plasma sintering or microwave heating and decreasing the sintering time by applying co-sintering or membrane structure optimization. Another recent development is the development of no-sintering processes such as with geopolymer and Portland cement-based membranes for industrial applications [53,54]. Enhanced fabrication procedures for the production of ceramic membranes for wastewater treatment and desalination in the future is mainly expected to be found in 3D printing as a decline in costs of 50–75% is expected in the next decade. 3D printing significantly increases customization, low-cost to prototype and test designs, has sustainability benefits, and reduces production time. However, its current difficulties are the lack of resolution, appropriate materials and build volume scale [55,56].

New developments in the production of ceramic membranes can be found in the application of materials coming from other industries such as solid municipal waste treatment, or the cement and concrete industry. Materials recovered from different waste streams within these industries are used following the principle of Circular Economy and with the aim to produce significantly cheaper ceramic membranes. Examples of the use of these materials can be found in the work of Mouratib et al. who developed low-cost ceramic MF membranes made from alumina- and silica-rich water treatment sludge, to filter wastewater [57]. Khadijah et al., developed low cost, green silica based ceramic hollow fiber membranes from waste rice husk for water filtration [58]. Lorente-Ayza et al. compared the extrusion and the pressing method for the successful production of low-cost ceramic support material for MF membranes. They used as raw material chamotte coming from the Spanish tile industry, a local Spanish clay mixture, and low-cost potato starch as an organic pore former. It was found that extruded material resulted in less porous material and smaller pore sizes, than material formed by dry pressing. Their work will be utilized in the near future to produce multilayer ceramic membranes for UF and NF as well. Planning to do so, by developing thinner and selective layers [59].

Waste materials are not only used to produce the ceramics, but recycling wastes from the food, agricultural and industry are also used as pore-forming agents to produce porous ceramics [60].

Another main class of membranes in water treatment are polymeric membranes. Although significantly cheaper than ceramic membranes, polymeric membranes are more sensitive to chemicals, and are more prone to fouling. They can be categorized in two process classes, non-pressure driven, such as pervaporation, dialysis, and membrane distillation, and pressure driven such as MF, UF, NF, RO, and FO [61,62].

All of these processes are widely applied in successful technologies ranging from the removal of natural organics, microbes, MCs, and heavy metals from UWWs, dyes and oily substances from industrial wastewaters, biomedical applications such as kidney dialysis, due to their low energy use and simplicity as compared to thermal separation processes. Their many forms come as hollow fiber membranes, (rolled) flat sheet membranes, tubular, and electro-spun nanofiber. All coming with their unique material properties and pore design, based on their polymerization method [63].

In order to make these commonly used polymeric membranes more sustainable, new ways are investigated to produce them from biodegradable polymers instead of oil based polymers. Main examples regarding biodegradable polymeric membranes in wastewater treatment are the application of cellulose acetate, chitosan, and chitin membranes. Disadvantages, however, are their oftentimes even more limited pH range, particle affinity, and the biodegradation, and so, selectivity rate, environmental pollution by its non-biodegradable counterpart in the case of blends and composites, and inferior mechanical properties in comparison to conventional materials [64,65].

There are different movements in the development of composite membranes, such as with the combination of polymers, or the application of e.g., a polymer layer on ceramics. The most common type of polymeric composite membranes are thin film composite (TFC) membranes, existing out of three layers, a woven or non-woven fabric, to

support the intermediate layer with micro sized pores, and finally the PA selective layer. The pore size of each layer is around 60–80  $\mu\text{m}$ , 50–100  $\mu\text{m}$ , and 100–200 nm, respectively [66]. Saini et al. writes about the tremendous potential of new polymer membrane technologies that make use of polymer nanocomposite membranes for applications as small as of synthetically produced hydrogen gas, filtering out  $\text{CO}_2$ ,  $\text{N}_2$ , and  $\text{CH}_4$ . Something that can be useful when applying novel EO reactors, that produces this gas [67]. Another example of highly advanced membranes are the biomimetic and bioinspired membranes (BBM). These BBMs consist of membranes with integrated biological functional molecules or bioinspired functional elements that are able to separate compounds in the sub-Nanometer scale. Examples for these molecules are artificial water channels, membrane protein channels, and carbon Nanotubes (CNT). Their application can currently be found in water purification, but finds significant potential in the specific separation of antibiotics, homogeneous catalyst retention, organic acid and gas separation as well [68].

Another way to effectively apply membrane separation is to pre-concentrate water contaminated streams for a subsequent AOP application to rejection streams, mainly for lowering the volume to be treated and to reduce the consumption of reagents as the concentration of contaminants would be higher than in the raw wastewater. This is a key topic for the elimination of MCs [69].

Oftentimes, permeate volumes still contain very low concentrations of (certain) MCs, as the membrane selectivity is determined by factors such as system parameters, physicochemical properties, and concentration factor. The permeate volumes can then be polished by different selected AOPs that are to be matched with the MCs that are insufficiently retained by the different membrane types and systems, in order to obtain significantly higher removal of MC [70].

#### Membrane fouling

Fouling is the process in which a variety of undesired organic and inorganic matter is deposited onto the membrane, eventually leading to the blockade of the membrane pores, after increasingly reducing the flux and the selectivity of the membrane. Organic membrane fouling is induced by the collection of organic material on the membrane surface, as well as in the pores, by proteins, humic acids, polymers, and polysaccharides. Inorganic fouling is the crystallization and precipitation of salts in the matrix on the membrane surface, mainly due to supersaturation. In the case of metallic deposition it is called scaling. Common salts in wastewater are carbonates, phosphates, sulfates, and sodium chloride [71].

The term biofouling is used for the formation of biological material, such as algae, bacteria, fungi, and plankton on the membrane surface. Bacterial EPS can be formed helping bacteria to resist flow and turbulence from the surrounding matrix. In MD for example, the thermal stress can elevate the formation of EPS. Over time, the biofouling is initiated by the formation of the conditioning film through scaling and organic fouling, followed by their reversible attachment by the formation of the protobiofilm. The bacteria in this protobiofilm then form the EPS, due to which an irreversible attachment of the biofilm on the membrane surface starts, maturing over time. Once matured, parts of the biofilm start to detach itself into the matrix, contributing to the protobiofilm formation [71]. The communication by the bacteria to produce EPS under stress conditions, is done via quorum sensing, performed by the secretion and detection of diffusible molecules named autoinducer, or signal molecules. A relatively new solution to this problem can be found in the deployment of functional bacteria, fungi, or enzymes to suppress this communication, what is called quorum quenching [45,72,73].

#### Fouling prevention

In order to guarantee the viability of membranes, the prevention and reversal of fouling is of the utmost importance. The main fouling

reversal mechanism is the application of ‘back-wash’ cycles, whereby the flow direction is reversed for a certain period of time. Other treatments can be found in chemical cleaning, which involves the use of an acidic and/or basic medium, often limited, especially in the case of polymeric membranes as extreme pH values are detrimental to their structural and chemical integrity [74,75]. Acid-base treatment is thereby also a temporary solution to remove reversible fouling layers. However, operation must be put on-hold and the chemicals bring extra cost with them. In the case of ceramic membranes, fouling can also be reversed by the incineration of the fouling layer. An effective solution, but replacement of the membranes or a full stop of the system during the incineration treatment is necessary [76].

Other antifouling mechanisms are also emerging. This can be found in the form of super-hydrophilic or super-hydrophobic membrane surfaces, the development and design of the pores, the pore-density, and morphology within these materials. The Janus membrane, named after the two-faced Roman god Janus, is based on the principle of applying different membrane layers on each other, with opposite properties, such as hydrophilic and hydrophobic, wettability, pore size or structure, thermal/electrical conductivity, and chemical activity. It offers a good option towards the preselection of compounds directly on the membrane surface and can prevent fouling to a great extent [77].

MBR system aeration, which is essential to keep the desired dissolved oxygen concentration for the biomass metabolism, can be used as anti-fouling mechanism. However, the agitation that aeration creates towards the bacteria can also increase the formation of EPS and foam. As different aeration patterns are continuously being researched for the different MBR principles, as a way to decrease energy costs as well, it was found that coarser bubbles are preferred over finer bubbles, as they remove more cake on the membrane [39,78,79].

#### The application of AOPs against fouling

To prevent fouling of membranes, different AOPs can be utilized. Ozonation, commonly used in UWW treatment, can be deployed as pre- or post-treatment, as well as *in-situ* cases. Special care should be taken when considering ozonation in hybrid systems using polymeric membranes, as only few commercial polymer membranes do not degrade by the generated radicals [80].

Photocatalytic membranes directly combine the application of AOPs with the membrane material, by producing them from photoactive materials such as  $\text{TiO}_2$  and  $\text{ZrO}_2$ . The efficiency of these novel membranes is lower for the degradation of MCs, as the immobilized photocatalytic material has significantly less active site as compared to suspended photocatalytic particles. However, the application of photocatalytic materials in membranes resulted to require extended operation times by other means of fouling prevention, such as with photocatalytic  $\text{TiO}_2$ . This material possesses the property of photo-induced super-hydrophilicity (PSH) when irradiated by light [81].

Brillas et al. observed that current research regarding these materials do not consider the light transport as fundamental aspect of light-matter interaction. They suggest applying biomimicry from phototroph organisms to improve the quantum yield of such surfaces by taking nature as an alternative guide in the development of novel materials. They identified micro- and nanostructures present in nature to prepare new bio-inspired photocatalytic and photo electrocatalytic material and reactor design, rather than focusing on the development of the composition of the semiconductor photo(electro)catalyst [82].

Gupta et al. reported a complex membrane system that exists out of the combination of many anti-fouling and membrane-based-AOP technologies. They developed a submerged photocatalytic oscillatory membrane reactor, with membrane aeration, for the removal of MCs from UWW as a tertiary treatment. The reactor uses suspended nano-sized  $\text{TiO}_2$ , which is irradiated with UV light to produce hydroxyl radicals for the removal of MCs, while the aeration and oscillation is utilized to prevent the  $\text{TiO}_2$  from fouling the membrane. They reached 90% MC removal of diclofenac, sulfamethoxazole, and hydrochlorothiazide, in

Milli-Q water. Practical applications of this kind of membrane systems must be tested in actual wastewater treatment integration systems [83].

### Combination of membranes and AOPs

Advanced oxidation processes are characterized by the production of hydroxyl radicals that can degrade MCs in UWWTP effluents. AOPs are an important solution for a sustainable tertiary treatment of UWWTP effluents, as only simple chemicals are necessary, and the irradiation can be provided in a renewable form, with solar radiation, using reactors such as the compound parabolic collectors (CPC) [84]. An example of these AOPs, which uses the Sun and CPC reactors, is solar photo-Fenton and is based on catalytic iron cycles, using  $\text{H}_2\text{O}_2$  as an oxidant, and UV-vis light from the Sun to produce the hydroxyl radicals [85].

Although UV-C on its own is not an AOP [86], its application is essential to many AOPs. UV-C is UV light applied in the range of 254 nm and its source varies from the Sun, as also different kinds of lamps. UV radiation is commonly applied with oxidants such as  $\text{H}_2\text{O}_2$ ,  $\text{O}_3$ , and  $\text{Cl}_2$ , catalyzing them or the production of related radical species. The application of UV lamps is still very expensive and uses electricity that is often not generated from sustainable sources. Great advantage of UV lamps, however, is the fact that they can be applied throughout the day and any day of the year, by disregarding the weather conditions. New types of lamps, such as UV-C LEDs and the lamp design rapidly raises the effectiveness of this promising technology. An example of this is the development of UV-C LED and light fabric combinations [87].

#### Photo-Fenton

Photo-Fenton (PhF) is based on the catalytic cycle of Fe species ( $\text{Fe}^{2+}/\text{Fe}^{3+}$ ) and is promoted by the presence of  $\text{H}_2\text{O}_2$  and UV-vis light for the production of hydroxyl radicals. Hydroxyl radicals are a highly reactive and non-selective radical species which can be generated by different processes. These fast reaction rates are ideal in effluents coming from membrane-based treatments such as UF and NF, which, in the case of the permeate volume contains minimal amounts natural organic matter (NOM) and other radical scavenging compounds, competing with the MCs for the generated radicals. The same goes for concentrate volumes containing high concentrations of MCs. Significantly, increasing the change for the hydroxyl radicals to encounter MCs for degradation [88]. One of the main disadvantages of classic PhF is that has to be applied at pH 3 to prevent the Fe to precipitate, making it necessary to acidify the UWW with costly chemicals, that come with danger during transport and storage. A solution to this problem is the application of Fe complexing agents, such as Ethylenediamine-N, N'-disuccinic acid (EDDS), which is an environmentally friendly solution as it is nontoxic and biodegradable [89,90]. When utilizing EDDS to keep the Fe in solution, the PhF process can be applied up to pH 9 [91].

Another oxidant that can be used in this AOP is persulfate. Reaction rates of persulfate radicals are generally slower and more selective as compared to hydroxyl radicals. Nevertheless, high efficiencies of MC removal in UWWs can still be obtained with this oxidant during (solar) PhF, being, in many cases, even a better choice, depending on the consistency of the matrix [92].

In areas with less sun hours and intensity, other AOPs are preferred. Electrooxidation (EO) is one of them, an AOP needing electricity instead of sunlight which can be generated by renewable energy, such as wind energy and modern biomass energy technologies. A further advantage of this technology is that it can also be deployed when there is very-low till no sun irradiation, such as during cloudy weather and at night [93]; or for wastewater treatment applications at a small scale in remote areas where no energy grid is available [94].

Another non-selective, relatively expensive, but highly effective AOP is ozonation. It can thereby not only be used as a MC degradation treatment, but also in different ways as a pretreatment of UWWTP effluents. Ozone is able to break down organic macromolecules, such as

microbial cell walls, into shorter chain intermediate products, making it possible to enter other cells for biodegradation. This process generates the highly reactive hydroxyl radicals on the way. Thereby, ozonation can be applied at room temperature and ambient pressure and does not produce sludge, while residual ozone decomposes in water and oxygen [95].

#### Electrooxidation

EO and electrochemical AOPs (EAOP) have drawn a lot of attention lately, as they offer a high efficiency, cost effectiveness and environmental compatibility [96]. EO creates the possibility to directly electrooxidize absorbed MCs on the electrode surface, as well as the significantly larger production of different radicals into the matrix for MC degradation, such as  $\cdot\text{OH}$ ,  $\text{ClO}^-$  and  $\text{SO}_4^{\cdot-}$ . As the system needs wastewaters with high conductivity, and therefore high ionic loads, to easier generate an electron flow, EO is especially eligible for the treatment of concentrate volumes coming from membrane treated wastewaters. The higher the conductivity is, the lower the ohmic resistance, and so the required energy consumption. The production of the different radical species on the anode surface is directly related to the presence and concentration of the different ions. A common ion specie in wastewater is  $\text{Cl}^-$ , from which active chlorine can be generated, by the adsorption of free dissolved ions on the anode surface in the form of direct active chlorine species (ACS) formation. Indirect ACS formation takes place in the matrix, where the resulting compounds degrade the MCs. The higher the current density is, the higher the production of ACS [97].

One of the challenges within EO is the stability of the electrodes. It is therefore one of the most important subjects, and studies are mainly focused on the further development and application of the widely implemented boron doped diamond (BDD) electrodes. BDD's success is mainly due to its large potential window (2.4 – 2.6 V against a standard hydrogen electrode (SHE)), allowing high oxygen evolution over-voltage, and so permitting the oxidation of water into physisorbed hydroxyl radicals [94,98]. When a cathode is applied it is even possible to produce onsite  $\text{H}_2\text{O}_2$ , which contributes to the PhF process in the presence of Fe through the reduction of produced  $\text{O}_2$  gas [93].

There are several processes through which EO can be applied. Anodic oxidation (AO) is the technique of direct oxidation of MCs on the anode surface by electron transfer, or by the oxidation of hydroxyl radicals,  $\text{H}_2\text{O}_2$ ,  $\text{O}_3$ , ACS, and peroxyxynitrate produced on the anode surface [99].

Electro-Fenton (EF) is also an EO process, here chemicals such as Fe and  $\text{H}_2\text{O}_2$  are used to produce hydroxyl radicals, by  $\text{H}_2\text{O}_2$  through the Fenton process. In this case,  $\text{H}_2\text{O}_2$  consumption as a consumable to be added, can be reduced by applying a cathode as mentioned before [100]. Variations on this AOP can be found by the combination of before mentioned EO processes with sunlight, known as solar assisted AO and (solar) photoelectro-Fenton. These combined processes have the advantage of the degradation by the sun light, or photolysis, as well as the activation of the oxidants and generation of the radical species by UVC. Thereby, the self-quenching effect of the free radicals is restrained, increasing the number of radicals, and so, the system oxidation capacity [101].

#### Ozonation

Ozonation is an efficient technology for the treatment of UWWTP effluents, where ozone is directly oxidizing the MCs in UWW, or indirectly through other processes by means of hydroxyl radicals. Ozone has a relatively slow dissolution rate and rapid decomposition in the aqueous phase. A solution to this problem can be found by producing ozone micro- and Nano-bubbles (MNB), significantly increasing the lifespan as they have higher mass transfer efficiency, less rising velocity, higher persistence time and bursting energy, and so, the reactivity in the aqueous phase. Another advantage is the much higher volume to surface

ratio at nano scale, making the production of hydroxyl radicals more likely and easier [102]. Ozonation is often combined with other reagents such as  $H_2O_2$  and UV irradiation, to obtain synergetic performances and catalytic effects towards the production of hydroxyl radicals. However, the  $H_2O_2/O_3$  ratio and the pH should be carefully monitored, to avoid the over-production of hydroxyl radicals, inducing scavenging and their recombination. Furthermore, ozonation can also be combined with electro coagulation (EC) where the metal ions catalyze the ozone production to produce more hydroxyl radicals [70,95]. Switzerland, the first country in the world to enforce legislation related the treatment of UWW to a minimum of 80% MC removal, is widely applying ozonation, with or without GAC filters, proving the effectiveness of this technology [16].

A recent advance with this process in combination with membrane separation in a hybrid system is presented by Khalifa et al., where ozonation is used as an EC enhancer, facilitating the size-exclusion of the emerged SiC ceramic flat sheet microfiltration membrane for the treatment of oily wastewaters [47].

### Nutrient recovery

Treated UWWs are characterized by containing a wide variety of different ions and other compounds. These ions and compounds can be recovered, which significantly contribute to the self-proficiency and environmental gains that could be obtained. Furthermore, other than with desalinated waters from RO, they can be utilized directly for crop irrigation, where even positive effects have been reported thanks to the consequent reduction on fertilizer use. It significantly reduces the needed quantities, and so, the crop production price. Water reuse for irrigation of crops by nutrient rich wastewaters is also called 'fertigation', and its application aims to significantly lower or even eliminate the use of mineral fertilizers [6,103,104]. The practice of fertigation has beneficial effects on the growth of crops and is expected to be increasing, as 35% of rainfed and 60% of irrigated crops is located within a 20 km proximity of a UWWTP, its practical implementation is thereby relatively accessible as well [105,106].

An example of this nutrient recovery is the recovery of ammonia from wastewaters. Nitrogen, along with phosphor and potassium, is one of the major components in fertilizers, as its availability as a macro-nutrient is essential to crop growth and development [107]. Ammonia can be recovered from UWWs by applying membrane-based systems such as NF to concentrate such wastewaters, and so creating ammonia enriched permeate streams [108,109].

### Phosphate recovery from UWW

Phosphates account for another major part of used artificial fertilizers and can be recovered from UWW, such as from the dairy industry, winery and olive mill wastewater, and domestic and livestock wastewaters [110,111]. The recovery of phosphates from UWW decreases the risk of environmental disruption after their discharge, something which can result in the eutrophication of different surface waters [112]. The availability of mineral phosphates in the world is relatively low and rapidly decreasing, and so, contributes to geopolitical tensions, while its refinery process is an energy intensive one, strongly contributing to greenhouse gas emissions [113]. Phosphate species in UWW can be organic and inorganic and can be found in both solid and dissolved phase. Its removal can be performed through biological, chemical, and physical processes. Phosphate solids or particles in UWW can be removed by different clarification steps. One of the main technologies for the removal of dissolved phosphate in UWW is through the formation of struvite. The struvite is produced by the precipitation of dissolved phosphoric compounds coming from the before mentioned industries and urine present in UWW. Membrane technologies can offer different solutions to the production of struvite: Firstly, from the separation of urine from any possible unwanted solids coming from concentrated

sources, such as urinary and mobile toilets, and collection basins used in intensive animal husbandry, as well as the separation of phosphate compounds coming from industrial sources; Secondly, in the pre-concentration of more diluted sources such as UWW or contaminated surface waters. A positive side effect is the prevention of undesired struvite formation on surfaces in the equipment and treatment processes of UWWTPs [114,115]. Recently, an advance in the recovery of phosphate has been found in the application of rare earth elements (REE) for its adsorption [116].

Both FO and MD can be applied to extract water from dewatered sludge centrate coming from anaerobic digesters used to digest sludge coming from the primary settler in UWWTPs or rest products coming from algae production from UWWTPs. The extracted water can directly be used for the irrigation of crops, whereas the retentate can be used as a liquid biofertilizer, from which struvite and nitrogen fertilizers can be produced by precipitation [117,118]. Simoni et al. compared two forms of MD, vacuum MD, and direct contact MD, for the application of simultaneous recovery of phosphorous and ammonia from UWW. Finding that vacuum MD showed better results at low pH values, and direct contact MD at high pH values [119]. Further novel applications of MD can be found in membrane crystallization through MD. Where traditionally MD is used to concentrate water and crystallization is performed by utilizing crystallizers and evaporators. Membrane crystallization through MD utilizes a membrane contactor, making it possible to use residual heat at temperatures as low as room temperature. This significantly reduces the energy consumption and thereby offers well-controlled nucleation and growth kinetics, fast crystallization rates, the promotion of heterogeneous nucleation or good control of the supersaturation by the membrane surface [120]. MD-crystallization already showed that it can be economically profitable, although is strongly depending on market value of the crystallized salts. Other factors contributing to the viability of this system is the membrane price, the overall mass transfer coefficient, and the membrane area, which depends strongly on the concentration of the osmotic agent [121].

Another recent advance in the production of struvite from UWW is the biomineralization by microorganisms to produce biological struvite. This principle could potentially be integrated in existing UWWTPs, by using one of the previously described MBR systems [122–124].

### Toxicity of resources used for fertigation

One of the main concerns of the application of these water and nutrient sources is their toxicity induced by residual MCs and their degradation products, which could obstruct or prohibit the germination of seeds, as well as the root and shoot development [104,105]. Other concerns are changes in the soil microbiome and the accumulation of salts and heavy metals [125,126]. Therefore, multiple authors performed different toxicity tests to map the acute and chronic toxicities of created waters for crop irrigation, as well as the potential applicability based on soil and crop types [127–130].

When looking at the presence of MCs in precipitation products such as struvite, it has been found that MCs do not sorb themselves on the surface of these precipitation products. However, MCs can be included when struvite nucleates on colloidal particles containing them. MC presence has only been registered in significant lower concentrations as compared to land applied biosolids [131].

### Lipid extraction from UWW

Another application of nutrient recovery can be found in the extraction of lipids from UWWs. Where, otherwise, these lipids are produced from different crops and livestock sources, even more increasing the pressure on available agricultural lands, water, and food products. Therefore, instead of producing them from raw food resources, these lipids can be recovered from UWWs as large amounts of them are originating from domestic use. Estimations of the total amount of lipids



available in European UWWs depend on the specific treatment step and their yield but could be good for up to 24% of the EU diesel demand. Significantly contributing to the creation and closing its circular economy [132].

### Main remarks and future outlook

Membrane separation has already shown its potential and wide array of applications for water and wastewater restoration, including combination with biotreatment for UWW effluents remediation or direct UWWTP effluent polishing. However, further treatment of rejection streams containing different contaminants at higher concentration than in the initial source is needed. The combination of different classes of membranes within an UWWTP, as well as the combination with AOPs and other wastewater treatment methods into hybrid systems is essential to obtain their maximum efficiency and synergy.

Another essential topic is fouling of all membrane materials. The solution to prevent and control fouling can be found in the hybridization of materials and composite membranes, with the use of stronger (but more expensive) ceramic membranes also being a choice. Ceramic membranes are better adapted to be combined with AOPs, including being part of the AOP treatment through the use of photocatalytic membranes. Otherwise, the efficiency of these novel membranes should be enhanced before being a consistent alternative.

Hydroxyl radicals generated by AOPs produce fast degradation reaction rates favored by higher concentration of contaminants. Therefore, they are ideal to be applied to effluents coming from rejection streams of membrane-based UWWTP effluent treatments, such as UF and NF.

More research focused on the economic viability of membranes in UWW treatment is desired, especially on large scale applications already installed in running UWWTPs. This will help to convince the short-term, as well as the long-term advantages of the already existing technologies, freeing subsidies and helping in the further development of membrane systems used for UWW treatment.

Membrane technologies must be considered as part of the UWW reclamation strategy, even more when recovery of nutrients and added value substances are to be tackled. Membranes significantly increase process efficiency, by offering economically and sustainable competing alternatives to the use of artificial fertilizers coming from energy extensive production in the case of nitrogen and phosphorus compounds.

### Declaration of Competing Interest

The authors declare that they have no known competing financial interest or personal relationship that could have appeared to influence the work reported in this paper.

### Acknowledgement

This paper is part of a project that has received funding from the European Union's Horizon 2020 research and innovation program under the Marie Skłodowska-Curie grant agreement No 765860. The authors wish to thank the Spanish Ministry of Science, Innovation and Universities (MCIU), AEI and FEDER for funding under the CalypSol Project (Reference: RTI2018-097997-B-C32 and RTI2018-097997-B-C31). Furthermore, Dennis Deemter would like to give his thanks to the personnel at the Plataforma Solar de Almería.

### References

- [1] B. Maryam, H. Büyükgüngör, Wastewater reclamation and reuse trends in Turkey: opportunities and challenges, *J. Water Process Eng.* 30 (2019), 100501, <https://doi.org/10.1016/j.jwpe.2017.10.001>.
- [2] A. Ishaq, M.U. Din, R. Ahmad, J.P. Singh, K. Singh, S. Ahmad, Prospectives and challenges of wastewater treatment technologies to combat contaminants of emerging concerns, *Ecol. Eng.* 152 (2020), 105882, <https://doi.org/10.1016/j.ecoleng.2020.105882>.
- [3] A. Guadie, A. Yesigat, S. Gatew, A. Worku, W. Liu, M. Minale, A. Wang, Effluent quality and reuse potential of urban wastewater treated with aerobic-anoxic system: a practical illustration for environmental contamination and human health risk assessment, *J. Water Process Eng.* 40 (2021), 101891, <https://doi.org/10.1016/j.jwpe.2020.101891>.
- [4] N. Ababsa, M. Kribaa, L. Tamrabet, D. Addad, V. Hallaire, A. Ouldjaoui, Long-term effects of wastewater reuse on hydro physicals characteristics of grassland grown soil in semi-arid Algeria, *J. King Saud Univ. Sci.* 32 (2020) 1004–1013, <https://doi.org/10.1016/j.jksus.2019.09.007>.
- [5] N. Ait-Mouheeb, P.-L. Mayaux, J. Mateo-Sagasta, T. Hartani, B. Molle, Water reuse: A resource For Mediterranean Agriculture, Elsevier Inc., 2020, <https://doi.org/10.1016/b978-0-12-818086-0.00005-4>.
- [6] L.P. Leonel, A.L. Tonetti, Wastewater reuse for crop irrigation: crop yield, soil and human health implications based on giardiasis epidemiology, *Sci. Total Environ.* 775 (2021), 145833, <https://doi.org/10.1016/j.scitotenv.2021.145833>.
- [7] H. Sousa, C.A. Sousa, L.C. Simões, M. Simões, Microalgal-based removal of contaminants of emerging concern 423 (2022), 127153, <https://doi.org/10.1016/j.jhazmat.2021.127153>.
- [8] W. Mccance, O.A.H. Jones, M. Edwards, A. Surapaneni, S. Chadalavada, Contaminants of emerging concern as novel groundwater tracers for delineating wastewater impacts in urban and peri-urban areas, *Water Res.* 146 (2018) 118–133, <https://doi.org/10.1016/j.watres.2018.09.013>.
- [9] M. Antonio, R. Cardenas, I. Ali, F.Y. Lai, L. Dawes, R. Thier, J. Rajapakse, Removal of micropollutants through a biological wastewater treatment plant in a subtropical climate, Queensland-Australia, *J. Environ. Health Sci. Eng.* (2016) 1–10, <https://doi.org/10.1186/s40201-016-0257-8>.
- [10] J.F.J.R. Pesqueira, M.F.R. Pereira, A.M.T. Silva, Environmental impact assessment of advanced urban wastewater treatment technologies for the removal of priority substances and contaminants of emerging concern, *A review* 261 (2020), 121078, <https://doi.org/10.1016/j.jclepro.2020.121078>.
- [11] T. Kabeya, M.A.A. Coetzee, I. Kamika, V.M. Ngole-jeme, M. Ndombo, B. Momba, Endocrine-disruptive chemicals as contaminants of emerging concern in wastewater and surface water : a review, *J. Environ. Manag.* 277 (2021), 111485, <https://doi.org/10.1016/j.jenvman.2020.111485>.
- [12] J.A. Sánchez Pérez, S. Arzate, P. Soriano-Molina, J.L. García Sánchez, J.L. Casas López, P. Plaza-Bolaños, Neutral or acidic pH for the removal of contaminants of emerging concern in wastewater by solar photo-Fenton? A techno-economic assessment of continuous raceway pond reactors, *Sci. Total Environ.* 736 (2020), 139681, <https://doi.org/10.1016/j.scitotenv.2020.139681>.
- [13] J. Mendret, A. Azais, T. Favier, S. Brosillon, Urban wastewater reuse using a coupling between nanofiltration and ozonation: techno-economic assessment, *Chem. Eng. Res. Des.* 145 (2019) 19–28, <https://doi.org/10.1016/j.cherd.2019.02.034>.
- [14] M. Capocelli, M. Prisciandaro, V. Piemonte, D. Barba, A technical-economical approach to promote the water treatment & reuse processes, *J. Clean. Prod.* 207 (2019) 85–96, <https://doi.org/10.1016/j.jclepro.2018.09.135>.
- [15] L. García, J.C. Leyva-díaz, E. Díaz, S. Ordóñez, A review of the adsorption-biological hybrid processes for the abatement of emerging pollutants : removal of fi ciencias, physicochemical analysis, and economic evaluation, *Sci. Total Environ.* 780 (2021), <https://doi.org/10.1016/j.scitotenv.2021.146554>.
- [16] Federal Office for the Environment FOEN Water Division, Reporting for Switzerland under the Protocol on Water and Health, Federal Office for the Environment FOEN Water Division, 2019.
- [17] N. Hagemann, K. Spokas, H.P. Schmidt, R. Kägi, M. Boehler, T. Bucheli, Activated carbon, biochar and charcoal: linkages and synergies across pyrogenic carbon's ABCs, *Water* 10 (2018) 182, <https://doi.org/10.3390/w10020182>.
- [18] The European parliament and the council, regulation (EU) 2020/741, minimum requirements for water reuse, *Off. J. Eur. Union* 177 (33) (2020) 32–55.
- [19] Y.G. Asfaha, A. Kebede, F. Zewge, Hybrid process of electrocoagulation and electrooxidation system for wastewater treatment : a review, *Clean. Eng. Technol.* 4 (2021), 100261, <https://doi.org/10.1016/j.clet.2021.100261>.
- [20] V.R. Moreira, Y. Abner, R. Lebron, M. Cristina, S. Amaral, Enhancing industries exploitation : integrated and hybrid membrane separation processes applied to industrial effluents beyond the treatment for disposal, *Chem. Eng. J.* 430 (2022), 133006, <https://doi.org/10.1016/j.cej.2021.133006>.
- [21] P. Luis, Chapter 8 - Hybrid processes Based On Membrane Technology, Elsevier Inc., 2018, <https://doi.org/10.1016/B978-0-12-813483-2.00008-3>.
- [22] X. Zhang, Y. Liu, Reverse osmosis concentrate: an essential link for closing loop of municipal wastewater reclamation towards urban sustainability, *Chem. Eng. J.* 421 (2021), 127773, <https://doi.org/10.1016/j.cej.2020.127773>.
- [23] M.O. Mavukkandy, C.M. Chabib, I. Mustafa, A. Al, Brine management in desalination industry : from waste to resources generation, *Desalination* 472 (2019), 114187, <https://doi.org/10.1016/j.desal.2019.114187>.
- [24] N. Naimah, R. Ahmad, W. Lun, C. Peng, A. Wahab, N. Hilal, Current advances in membrane technologies for saline wastewater treatment : a comprehensive review, *Desalination* 517 (2021), 115170, <https://doi.org/10.1016/j.desal.2021.115170>.
- [25] M. Yaqub, W. Lee, Zero-liquid discharge (ZLD) technology for resource recovery from wastewater : a review, *Sci. Total Environ.* 681 (2019) 551–563, <https://doi.org/10.1016/j.scitotenv.2019.05.062>.
- [26] A.S. Bello, N. Zouari, D.A. Da, J.N. Hahladakis, M.A. Al-ghouthi, An overview of brine management : emerging desalination technologies, life cycle assessment, and metal recovery methodologies, *J. Environ. Manag.* 288 (2021), 112358, <https://doi.org/10.1016/j.jenvman.2021.112358>.

- [27] J. U.J. Y. Gonz, Improved integrated dynamic model for the simulation of submerged membrane bioreactors for urban and hospital wastewater treatment, *J. Membr. Sci.* 624 (2021), <https://doi.org/10.1016/j.memsci.2021.119053>.
- [28] A.H. Behroozi, M.R. Ataabadi, Improvement in microfiltration process of oily wastewater : a comprehensive review over two decades, *J. Environ. Chem. Eng.* 9 (2021), 104981, <https://doi.org/10.1016/j.jece.2020.104981>.
- [29] S. Fatima, R. Hashaikheh, N. Hilal, Microfiltration membrane processes : a review of research trends over the past decade, *J. Water Process Eng.* 32 (2019), <https://doi.org/10.1016/j.jwpe.2019.100941>.
- [30] C.N. Rani, S. Karthikeyan, S.P. Arockia, Photocatalytic ultrafiltration membrane reactors in water and wastewater treatment-a review, *Chem. Eng. Process. Process Intensif* 165 (2021), 108445, <https://doi.org/10.1016/j.ccep.2021.108445>.
- [31] W. Yu, D. Song, W. Chen, H. Yang, Antiscalants in RO membrane scaling control, *Water Res.* 183 (2020), 115985, <https://doi.org/10.1016/j.watres.2020.115985>.
- [32] H. Rabiee, K.R. Khalilpour, J.M. Betts, Energy-Water Nexus : Renewable-Integrated Hybridized Desalination Systems, Elsevier Inc, 2019, <https://doi.org/10.1016/B978-0-12-813306-4.00013-6>.
- [33] S. Jafarnejad, Forward osmosis membrane technology for nutrient removal/recovery from wastewater: recent advances, proposed designs, and future directions, *Chemosphere* 263 (2021), 128116, <https://doi.org/10.1016/j.chemosphere.2020.128116>.
- [34] F. Tibi, A. Charfi, J. Cho, J. Kim, Fabrication of polymeric membranes for membrane distillation process and application for wastewater treatment : critical review, *Process Saf. Environ. Prot.* 141 (2020) 190–201, <https://doi.org/10.1016/j.psep.2020.05.026>.
- [35] A. Alkhatib, M.A. Ayari, A.H. Hawari, Fouling mitigation strategies for different foulants in membrane distillation, *Chem. Eng. Process. Process Intensif.* 167 (2021), 108517, <https://doi.org/10.1016/j.ccep.2021.108517>.
- [36] M.N. Ardakani, G.B. Gholikandi, Biomass and Bioenergy Microbial fuel cells (MFCs) in integration with anaerobic treatment processes (AnTPs) and membrane bioreactors (MBRs) for simultaneous efficient wastewater/sludge treatment and energy recovery-a state-of-the-art review, *Biomass Bioenergy* 141 (2020), 105726, <https://doi.org/10.1016/j.biombioe.2020.105726>.
- [37] Y. Wang, H. Jia, J. Wang, B. Cheng, G. Yang, F. Gao, Impacts of energy distribution and electric field on membrane fouling control in microbial fuel cell-membrane bioreactor (MFC-MBR) coupling system, *Bioresour. Technol.* 269 (2018) 339–345, <https://doi.org/10.1016/j.biortech.2018.08.122>.
- [38] D. Saidulu, A. Majumder, A. Kumar, A systematic review of moving bed biofilm reactor, membrane bioreactor, and moving bed membrane bioreactor for wastewater treatment : comparison of research trends, removal mechanisms, and performance, *J. Environ. Chem. Eng.* 9 (2021), 106112, <https://doi.org/10.1016/j.jece.2021.106112>.
- [39] D. Zhao, C. Fu, X. Bi, H. Yong, X. Shi, Effects of coarse and fine bubble aeration on performances of membrane filtration and denitrification in moving bed membrane bioreactors, *Sci. Total Environ.* 772 (2021), <https://doi.org/10.1016/j.scitotenv.2021.145513>.
- [40] X. Tan, I. Acquah, H. Liu, W. Li, S. Tan, A critical review on saline wastewater treatment by membrane bioreactor (MBR) from a microbial perspective, *Chemosphere* 220 (2019) 1150–1162, <https://doi.org/10.1016/j.chemosphere.2019.01.027>.
- [41] A. Aslam, S.J. Khan, A. Shahzad, Anaerobic membrane bioreactors (AnMBRs) for municipal wastewater treatment- potential benefits, constraints, and future perspectives : an updated review, *Sci. Total Environ.* 802 (2022), <https://doi.org/10.1016/j.scitotenv.2021.149612>.
- [42] K. Nadeem, M. Alliet, Q. Plana, J. Bernier, S. Azimi, V. Rocher, C. Albasi, Modeling, simulation and control of biological and chemical P-removal processes for membrane bioreactors (MBRs) from lab to full-scale applications: state of the art, *Sci. Total Environ.* (2021), 151109, <https://doi.org/10.1016/j.scitotenv.2021.151109>.
- [43] Z. Li, L. Ren, Y. Qiao, X. Li, J. Zheng, J. Ma, Z. Wang, Recent advances in membrane biofilm reactor for micropollutants removal : fundamentals, performance and microbial communities, *Bioresour. Technol.* 343 (2022), 126139, <https://doi.org/10.1016/j.biortech.2021.126139>.
- [44] L. Ren, M. Chen, J. Zheng, Z. Li, C. Tian, Q. Wang, Z. Wang, Efficacy of a novel electro-chemical membrane-aerated biofilm reactor for removal of antibiotics from micro-polluted surface water and suppression of antibiotic resistance genes, *Bioresour. Technol.* 338 (2021), 125527, <https://doi.org/10.1016/j.biortech.2021.125527>.
- [45] H. He, X. Xin, W. Qiu, D. Li, Z. Liu, J. Ma, Role of nano-Fe<sub>3</sub>O<sub>4</sub> particle on improving membrane bioreactor (MBR) performance: alleviating membrane fouling and microbial mechanism, *Water Res.* 209 (2022), 117897, <https://doi.org/10.1016/j.watres.2021.117897>.
- [46] M.B. Asif, B. Ren, C. Li, T. Maqbool, X. Zhang, Z. Zhang, Powdered activated carbon-membrane bioreactor (PAC-MBR): impacts of high PAC concentration on micropollutant removal and microbial communities, *Sci. Total Environ.* 745 (2020), 141090, <https://doi.org/10.1016/j.scitotenv.2020.141090>.
- [47] O. Khalifa, F. Banat, C. Srinivasakannan, F. Almarzooqi, S.W. Hasan, Ozonation-assisted electro-membrane hybrid reactor for oily wastewater treatment : a methodological approach and synergy effects, *J. Clean. Prod.* 289 (2021), 125764, <https://doi.org/10.1016/j.jclepro.2020.125764>.
- [48] V. Gitis, Vitaly Gitis and Gadi Rothenberg Ceramic Membranes, 2016. 10.2138/rmg.2014.78.16.
- [49] N. Duan, X. Zhang, C. Lu, Y. Zhang, C. Li, J. Xiong, Effect of rheological properties of AlOOH sol on the preparation of Al<sub>2</sub>O<sub>3</sub> nanofiltration membrane by sol-gel method, *Ceram. Int.* (2021), <https://doi.org/10.1016/j.ceramint.2021.11.200>.
- [50] H. Qin, W. Guo, X. Huang, P. Gao, H. Xiao, Preparation of yttria-stabilized ZrO<sub>2</sub> nanofiltration membrane by reverse micelles-mediated sol-gel process and its application in pesticide wastewater treatment, *J. Eur. Ceram. Soc.* 40 (2020) 145–154, <https://doi.org/10.1016/j.jeurceramsoc.2019.09.023>.
- [51] E. Eray, V.M. Candelario, V. Boffa, H. Safaar, D.N. Østedgaard-Munck, N. Zahrtmann, H. Kadrispahic, M.K. Jørgensen, A roadmap for the development and applications of silicon carbide membranes for liquid filtration : Recent advancements, challenges , and perspectives 414 (2021) 128826, <https://doi.org/10.1016/j.cej.2021.128826>.
- [52] M. Chen, R. Shang, P.M. Sberna, M.W.J. Luiten-olieman, L.C. Rietveld, S.G. J. Heijman, Highly permeable silicon carbide-alumina ultra filtration membranes for oil-in-water filtration produced with low-pressure chemical vapor deposition, *Sep. Purif. Technol.* 253 (2020), 117496, <https://doi.org/10.1016/j.seppur.2020.117496>.
- [53] D. Zou, Y. Fan, State-of-the-art developments in fabricating ceramic membranes with low energy consumption, *Ceram. Int.* 47 (2021) 14966–14987, <https://doi.org/10.1016/j.ceramint.2021.02.195>.
- [54] K.P. Goswami, K. Pakshirajan, G. Pugazhenthii, Process intensification through waste fly ash conversion and application as ceramic membranes: a review, *Sci. Total Environ.* 808 (2022), 151968, <https://doi.org/10.1016/j.scitotenv.2021.151968>.
- [55] A. Soo, S.M. Ali, H.K. Shon, 3D printing for membrane desalination: challenges and future prospects, *Desalination* 520 (2021), 115366, <https://doi.org/10.1016/j.desal.2021.115366>.
- [56] H.A. Balogun, R. Sulaiman, S.S. Marzouk, A. Giwa, S.W. Hasan, 3D printing and surface imprinting technologies for water treatment : a review, *J. Water Process Eng.* 31 (2019), 100786, <https://doi.org/10.1016/j.jwpe.2019.100786>.
- [57] R. Mouratib, B. Achiou, M. El. S. Alami, Low-cost ceramic membrane made from alumina- and silica-rich water treatment sludge and its application to wastewater filtration, *J. Eur. Ceram. Soc.* 40 (2020) 5942–5950, <https://doi.org/10.1016/j.jeurceramsoc.2020.07.050>.
- [58] S. Khadjah, M.H.D. Othman, A.F. Ismail, M.A. Rahman, J. Jaafar, Y. Iwamoto, S. Honda, M.I.H.M. Dzhahir, M.Z.M. Yusop, Fabrication of low cost, green silica based ceramic hollow fibre membrane prepared from waste rice husk for water filtration application 44 (2018) 10498–10509, <https://doi.org/10.1016/j.ceramint.2018.03.067>.
- [59] M. Lorente-ayza, S. Mestre, M. Menéndez, E. Sánchez, Comparison of extruded and pressed low cost ceramic supports for microfiltration membranes, *J. Eur. Ceram. Soc.* 35 (2015) 3681–3691, <https://doi.org/10.1016/j.jeurceramsoc.2015.06.010>.
- [60] S.Z. Zalleh, A.A. Kechik, A.H. Yusoff, M.A.A. Taib, M.M. Nor, M. Mohamad, P. G. Tan, A. Ali, M.N. Masri, J.J. Mohamed, S.K. Zakaria, J.G. Boon, F. Budiman, T. Teo, Recycling food, agricultural, and industrial wastes as pore-forming agents for sustainable porous ceramic production, *A review* 306 (2021) 127264, <https://doi.org/10.1016/j.jclepro.2021.127264>.
- [61] A. Nasir, F. Masood, T. Yasin, A. Hameed, Progress in polymeric nanocomposite membranes for wastewater treatment: preparation, properties and applications, *J. Ind. Eng. Chem.* 79 (2019) 29–40, <https://doi.org/10.1016/j.jiec.2019.06.052>.
- [62] M. Khodakarami, M. Bagheri, Recent advances in synthesis and application of polymer nanocomposites for water and wastewater treatment, *J. Clean. Prod.* 296 (2021), 126404, <https://doi.org/10.1016/j.jclepro.2021.126404>.
- [63] M. Radjabian, V. Abetz, Advanced porous polymer membranes from self-assembling block copolymers, *Prog. Polym. Sci.* 102 (2020), 101219, <https://doi.org/10.1016/j.progpolymsci.2020.101219>.
- [64] S. Bandeali, H. Sanaeepur, A. Ebadi, S. Shirazian, Biodegradable polymers for membrane separation, *Sep. Purif. Technol.* 269 (2021), 118731, <https://doi.org/10.1016/j.seppur.2021.118731>.
- [65] S. Sarode, P. Upadhyay, M.A. Khosa, T. Mak, A. Shakir, S. Song, A. Ullah, Overview of wastewater treatment methods with special focus on biopolymer chitin-chitosan, *Int. J. Biol. Macromol.* 121 (2019) 1086–1100, <https://doi.org/10.1016/j.ijbiomac.2018.10.089>.
- [66] J. Farahbakhsh, V. Vatanpour, M. Khoshnam, M. Zargar, Recent advancements in the application of new monomers and membrane modification techniques for the fabrication of thin film composite membranes : a review, *React. Funct. Polym.* 166 (2021), 105015, <https://doi.org/10.1016/j.reactfunctpolym.2021.105015>.
- [67] A. Saini, I. Arora, J.K. Ratan, Photo-induced hydrophilicity of micro-sized-TiO<sub>2</sub> based self-cleaning cement, *Mater. Lett.* 260 (2020), 126888, <https://doi.org/10.1016/j.matlet.2019.126888>.
- [68] Y. Tu, L. Samineni, T. Ren, A.B. Schantz, W. Song, S. Sharma, M. Kumar, Prospective applications of nanometer-scale pore size biomimetic and bioinspired membranes, *J. Membr. Sci.* 620 (2021), 118968, <https://doi.org/10.1016/j.memsci.2020.118968>.
- [69] Y.L. Brasil, V.R. Moreira, Y.A.R. Lebron, W.G. Moravia, C. Míriam, S. Amaral, Combining yeast MBR, Fenton and nanofiltration for landfill leachate reclamation, *Waste Manag.* 132 (2021) 105–114, <https://doi.org/10.1016/j.wasman.2021.07.027>.
- [70] D. Deemter, I. Oller, A.M. Amat, S. Malato, Effect of salinity on precontamination of contaminants of emerging concern by nanofiltration: application of solar photo-Fenton as a tertiary treatment, *Sci. Total Environ.* (2020), 143593, <https://doi.org/10.1016/j.scitotenv.2020.143593>.
- [71] F.C.R. Costa, B.C. Ricci, B. Teodoro, K. Koch, J.E. Drewes, M.C.S. Amaral, Biofouling in membrane distillation applications - a review 516 (2021), 115241, <https://doi.org/10.1016/j.desal.2021.115241>.
- [72] Q. Liu, J. Ren, Y. Lu, X. Zhang, F.A. Roddick, L. Fan, Y. Wang, H. Yu, P. Yao, A review of the current *in-situ* fouling control strategies in MBR : biological versus

- physicochemical, *J. Ind. Eng. Chem.* 98 (2021) 42–59, <https://doi.org/10.1016/j.jiec.2021.03.042>.
- [73] H. Oh, C. Lee, Origin and evolution of quorum quenching technology for biofouling control in MBRs for wastewater treatment, *J. Membr. Sci.* 554 (2018) 331–345, <https://doi.org/10.1016/j.memsci.2018.03.019>.
- [74] A.I. Schäfer, A.G. Fane, *Nanofiltration. Principles. Applications and New Materials*, Wiley-VCH, 2021.
- [75] S.M. Mohan, S. Nagalakshmi, A review on aerobic self-forming dynamic membrane bioreactor: formation, performance, fouling and cleaning, *J. Water Process Eng.* 37 (2020), 101541, <https://doi.org/10.1016/j.jwpe.2020.101541>.
- [76] Y.J. Shih, R.R.M. Abarca, M.D.G. de Luna, Y.H. Huang, M.C. Lu, Recovery of phosphorus from synthetic wastewaters by struvite crystallization in a fluidized-bed reactor: effects of pH, phosphate concentration and coexisting ions, *Chemosphere* 173 (2017) 466–473, <https://doi.org/10.1016/j.chemosphere.2017.01.088>.
- [77] L. Yan, X. Yang, Y. Zhang, Y. Wu, Z. Cheng, S.B. Darling, L. Shao, Porous Janus materials with unique asymmetries and functionality, *Mater. Today* (2021) 1–22, <https://doi.org/10.1016/j.mattod.2021.07.001>, xxx.
- [78] O. Díaz, E. González, L. Vera, J.J. Macías-hernández, J. Rodríguez-sevilla, Fouling analysis and mitigation in a tertiary MBR operated under restricted aeration, *J. Membr. Sci.* 525 (2017) 368–377, <https://doi.org/10.1016/j.memsci.2016.12.014>.
- [79] R. Campo, M. Capodici, G. Di, M. Torregrossa, The role of EPS in the foaming and fouling for a MBR operated in intermittent aeration conditions, *Biochem. Eng. J.* 118 (2017) 41–52, <https://doi.org/10.1016/j.bej.2016.11.012>.
- [80] S. Ouali, P. Loulergue, P. Biard, N. Nasrallah, A. Szymczyk, Ozone compatibility with polymer nanofiltration membranes, *J. Membr. Sci.* 618 (2021), 118656, <https://doi.org/10.1016/j.memsci.2020.118656>.
- [81] F.E.B. Coelho, D. Deemter, V.M. Candelario, V. Boffa, S. Malato, G. Magnacca, Development of a photocatalytic Zirconia-Titania ultrafiltration membrane with anti-fouling and self-cleaning properties, *J. Environ. Chem. Eng.* 9 (2021), 106671, <https://doi.org/10.1016/j.jece.2021.106671>.
- [82] E. Brillas, A. Serrà, S. Garcia-segura, Biomimicry designs for photoelectrochemical systems: strategies to improve light delivery efficiency, *Curr. Opin. Electrochem.* 26 (2021), 100660, <https://doi.org/10.1016/j.coelec.2020.100660>.
- [83] S. Gupta, H. Goma, M.B. Ray, A novel submerged photocatalytic oscillatory membrane reactor for water polishing, *J. Environ. Chem. Eng.* 9 (2021), 105562, <https://doi.org/10.1016/j.jece.2021.105562>.
- [84] S. Malato Rodriguez, J. Blanco Galvez, M.I. Maldonado Rubio, P. Fernandez Ibañez, D. Alarcon Padilla, M. Collares Pereira, J. Farinha Mendes, J. Correia de Oliveira, Engineering of solar photocatalytic collectors, *Solar Energy* 77 (2004) 513–524, <https://doi.org/10.1016/j.solener.2004.03.020>.
- [85] A. Della-flora, M.L. Wilde, D. Lima, E.C. Lima, C. Sirtori, Combination of tertiary solar photo-Fenton and adsorption processes in the treatment of hospital wastewater : the removal of pharmaceuticals and their transformation products, *J. Environ. Chem. Eng.* 9 (2021), 105666, <https://doi.org/10.1016/j.jece.2021.105666>.
- [86] L. Fan, J. Wang, Y. Huang, L. Su, C. Li, Y. Hui, C.J. Martyniuk, Comparative analysis on the photolysis kinetics of four neonicotinoid pesticides and their photo-induced toxicity to *Vibrio Fischeri* : pathway and toxic mechanism, *Chemosphere* 287 (2022), 132303, <https://doi.org/10.1016/j.chemosphere.2021.132303>.
- [87] Towards an innovative wastewater treatment by UV-C LED technology combined with light-conducting fabrics. <https://apriasytems.es/uv-cleaning/> (accessed November 28, 2021).
- [88] T. Hwang, S. Nam, J. Lee, J. Koo, E. Kim, Hydroxyl radical scavenging factor measurement using a fluorescence excitation-emission matrix and parallel factor analysis in ultraviolet advanced oxidation processes, *Chemosphere* 259 (2020), 127396, <https://doi.org/10.1016/j.chemosphere.2020.127396>.
- [89] I. Oller, S. Malato, Photo-Fenton applied to the removal of pharmaceutical and other pollutants of emerging concern, *Curr. Opin. Green Sustain. Chem.* 29 (2021), 100458, <https://doi.org/10.1016/j.cogsc.2021.100458>.
- [90] S. Tandy, A. Ammann, R. Schulin, B. Nowack, Biodegradation and speciation of residual SS-ethylenediaminedisuccinic acid (EDDS) in soil solution left after soil washing, *Environ. Pollut.* 142 (2006) 191–199, <https://doi.org/10.1016/j.envpol.2005.10.013>.
- [91] X. Wang, W. Dong, M. Brigante, G. Mailhot, Hydroxyl and sulfate radicals activated by Fe(III)-EDDS/UV: comparison of their degradation efficiencies and influence of critical parameters, *Appl. Catal. B Environ.* 245 (2019) 271–278, <https://doi.org/10.1016/j.apcatb.2018.12.052>.
- [92] G. Chen, Y. Yu, L. Liang, X. Duan, R. Li, X. Lu, B. Yan, N. Li, S. Wang, Remediation of antibiotic wastewater by coupled photocatalytic and persulfate oxidation system : a critical review, *J. Hazard. Mater.* 408 (2021), 124461, <https://doi.org/10.1016/j.jhazmat.2020.124461>.
- [93] S.O. Ganiyu, C.A. Martínez-Huitle, M.A. Rodrigo, Renewable energies driven electrochemical wastewater/soil decontamination technologies: a critical review of fundamental concepts and applications, *Appl. Catal. B Environ.* 270 (2020), 118857, <https://doi.org/10.1016/j.apcatb.2020.118857>.
- [94] F.L. Souza, M.R.V. Lanza, J. Llanos, C. Sáez, M.A. Rodrigo, P. Cañizares, A wind-powered BDD electrochemical oxidation process for the removal of herbicides, *J. Environ. Manag.* 158 (2015) 36–39, <https://doi.org/10.1016/j.jenvman.2015.04.040>.
- [95] S.N. Malik, P.C. Ghosh, A.N. Vaidya, S.N. Mudliar, Hybrid ozonation process for industrial wastewater treatment : principles and applications : a review, *J. Water Process Eng.* 35 (2020), <https://doi.org/10.1016/j.jwpe.2020.101193>.
- [96] Z. Hu, J. Cai, G. Song, Y. Tian, Anodic oxidation of organic pollutants : anode fabrication, process hybrid and environmental applications, *Curr. Opin. Electrochem.* 26 (2021), 100659, <https://doi.org/10.1016/j.coelec.2020.100659>.
- [97] Z. Guo, Y. Zhang, H. Jia, J. Guo, X. Meng, J. Wang, Electrochemical methods for landfill leachate treatment: a review on electrocoagulation and electrooxidation, *Sci. Total Environ.* 806 (2022), 150529, <https://doi.org/10.1016/j.scitotenv.2021.150529>.
- [98] E. Mousset, Interest of micro-reactors for the implementation of advanced electrocatalytic oxidation with boron-doped diamond anode for wastewater treatment, *Curr. Opin. Electrochem.* (2021), <https://doi.org/10.1016/j.coelec.2021.100897>.
- [99] K. Liu, Y. Yi, N. Zhang, Anodic oxidation produces active chlorine to treat oilfield wastewater and prepare ferrate (VI), *J. Water Process Eng.* 41 (2021), 101998, <https://doi.org/10.1016/j.jwpe.2021.101998>.
- [100] I. Salmerón, G. Rivas, I. Oller, A. Martínez-Piernas, A. Agüera, S. Malato, Nanofiltration retentate treatment from urban wastewater secondary effluent by solar electrochemical oxidation processes, *Sep. Purif. Technol.* 254 (2021), 117614, <https://doi.org/10.1016/j.seppur.2020.117614>.
- [101] J. Ding, Q. Gao, B. Cui, Q. Zhao, G. Zhao, S. Qiu, L. Bu, S. Zhou, Solar-assisted electrooxidation process for enhanced degradation of bisphenol A: performance and mechanism, *Sep. Purif. Technol.* 277 (2021), 119467, <https://doi.org/10.1016/j.seppur.2021.119467>.
- [102] T. Temesgen, T. Thuy, M. Han, T. Kim, H. Park, Micro and nanobubble technologies as a new horizon for water-treatment techniques: a review, *Adv. Colloid Interface Sci* 246 (2017) 40–51, <https://doi.org/10.1016/j.cis.2017.06.011>.
- [103] A. Finzi, V. Guido, E. Riva, O. Ferrari, D. Quilez, E. Herrero, G. Provolo, Performance and sizing of filtration equipment to replace mineral fertilizer with digestate in drip and sprinkler fertigation, *J. Clean. Prod.* 317 (2021), 128431, <https://doi.org/10.1016/j.jclepro.2021.128431>.
- [104] A. Singh, Resources, Conservation & Recycling A review of wastewater irrigation : environmental implications, *Resour. Conserv. Recycl.* 168 (2021), 105454, <https://doi.org/10.1016/j.resconrec.2021.105454>.
- [105] A. Poustie, Y. Yang, P. Verburg, K. Pagilla, D. Hanigan, Science of the Total Environment Reclaimed wastewater as a viable water source for agricultural irrigation : a review of food crop growth inhibition and promotion in the context of environmental change, *Sci. Total Environ.* 739 (2020), 139756, <https://doi.org/10.1016/j.scitotenv.2020.139756>.
- [106] S. Elfanssi, N. Ouazzani, L. Mandi, Soil properties and agro-physiological responses of alfalfa (*Medicago sativa* L.) irrigated by treated domestic wastewater, *Agric. Water Manag.* 202 (2018) 231–240, <https://doi.org/10.1016/j.agwat.2018.02.003>.
- [107] N. Soobhany, Insight into the recovery of nutrients from organic solid waste through biochemical conversion processes for fertilizer production : a review, *J. Clean. Prod.* 241 (2019), 118413, <https://doi.org/10.1016/j.jclepro.2019.118413>.
- [108] M.L. Gerardo, N.H.M. Aljohani, D.L. Oatley-Radcliffe, R.W. Lovitt, Moving towards sustainable resources: recovery and fractionation of nutrients from dairy manure digestate using membranes, *Water Res.* 80 (2015) 80–89, <https://doi.org/10.1016/j.watres.2015.05.016>.
- [109] A. Patel, A.A. Mungray, A.K. Mungray, Technologies for the recovery of nutrients, water and energy from human urine: a review, *Chemosphere* 259 (2020), 127372, <https://doi.org/10.1016/j.chemosphere.2020.127372>.
- [110] C. Numviyimana, J. Warchoń, G. Izydorczyk, S. Baśladyńska, K. Chojnacka, Struvite production from dairy processing wastewater: optimizing reaction conditions and effects of foreign ions through multi-response experimental models, *J. Taiwan Inst. Chem. Eng.* 117 (2020) 182–189, <https://doi.org/10.1016/j.jtice.2020.11.031>.
- [111] M. Grigatti, E. Boanini, D. Bolzonella, L. Sciubba, S. Mancarella, C. Ciavatta, C. Marzadori, Organic wastes as alternative sources of phosphorus for plant nutrition in a calcareous soil, *Waste Manag.* 93 (2019) 34–46, <https://doi.org/10.1016/j.wasman.2019.05.028>.
- [112] P. Kumararaja, S. Suvana, R. Saraswathy, N. Lalitha, M. Muralidhar, Mitigation of eutrophication through phosphate removal by aluminium pillared bentonite from aquaculture discharge water, *Ocean Coast. Manag.* 182 (2019), 104951, <https://doi.org/10.1016/j.ocecoaman.2019.104951>.
- [113] M.A. Bustamante, F.G. Ceglie, A. Aly, H.T. Mihreteab, C. Ciaccia, F. Tittarelli, Phosphorus availability from rock phosphate: combined effect of green waste composting and sulfur addition, *J. Environ. Manag.* 182 (2016) 557–563, <https://doi.org/10.1016/j.jenvman.2016.08.016>.
- [114] A.M.K. Mbaya, J. Dai, G.H. Chen, Potential benefits and environmental life cycle assessment of equipping buildings in dense cities for struvite production from source-separated human urine, *J. Clean. Prod.* 143 (2017) 288–302, <https://doi.org/10.1016/j.jclepro.2016.12.111>.
- [115] N. Krishnamoorthy, B. Dey, Y. Unpaprom, R. Ramaraj, G.P. Maniam, N. Govindan, S. Jayaraman, T. Arunachalam, B. Paramasivan, Engineering principles and process designs for phosphorus recovery as struvite: a comprehensive review, *J. Environ. Chem. Eng.* 9 (2021), 105579, <https://doi.org/10.1016/j.jece.2021.105579>.
- [116] A. Kunhikrishnan, M.A. Rahman, D. Lamb, N.S. Bolan, S. Saggari, A. Surapaneni, C. Chen, Rare earth elements (REE) for the removal and recovery of phosphorus: a review, *Chemosphere* 286 (2022), 131661, <https://doi.org/10.1016/j.chemosphere.2021.131661>.
- [117] S.P. Munasinghe-Arachchige, P. Cooke, N. Nirmalakhandan, Recovery of nitrogen-fertilizer from centrate of anaerobically digested sewage sludge via gas

- permeable membranes, *J. Water Process Eng.* 38 (2020), 101630, <https://doi.org/10.1016/j.jwpe.2020.101630>.
- [118] J.L. Soler-Cabezas, J.A. Mendoza-Roca, M.C. Vincent-Vela, M.J. Luján-Facundo, L. Pastor-Alcañiz, Simultaneous concentration of nutrients from anaerobically digested sludge centrate and pre-treatment of industrial effluents by forward osmosis, *Sep. Purif. Technol.* 193 (2018) 289–296, <https://doi.org/10.1016/j.seppur.2017.10.058>.
- [119] G. Simoni, B.S. Kirkebaek, C.A. Quist-jensen, M.L. Christensen, A. Ali, A comparison of vacuum and direct contact membrane distillation for phosphorus and ammonia recovery from wastewater, *J. Water Process Eng.* 44 (2021), 102350, <https://doi.org/10.1016/j.jwpe.2021.102350>.
- [120] I.R. Salmón, P. Luis, Process Intensification Membrane crystallization via membrane distillation, *Chem. Eng. Process. Process Intensif.* 123 (2018) 258–271, <https://doi.org/10.1016/j.cep.2017.11.017>.
- [121] M. Sparenberg, I. Ruiz, P. Luis, Economic evaluation of salt recovery from wastewater via membrane, *Sep. Purif. Technol.* 235 (2020), 116075, <https://doi.org/10.1016/j.seppur.2019.116075>.
- [122] K. Sathiasivan, J. Ramaswamy, M. Rajesh, Struvite recovery from human urine in inverse fluidized bed reactor and evaluation of its fertilizing potential on the growth of *Arachis hypogaea*, *J. Environ. Chem. Eng.* 9 (2021), 104965, <https://doi.org/10.1016/j.jece.2020.104965>.
- [123] Y. Leng, A. Soares, The mechanisms of struvite biomineralization in municipal wastewater, *Sci. Total Environ.* 799 (2021), 149261, <https://doi.org/10.1016/j.scitotenv.2021.149261>.
- [124] Y. Leng, A. Soares, Understanding the mechanisms of biological struvite biomineralisation, *Chemosphere* 281 (2021), 130986, <https://doi.org/10.1016/j.chemosphere.2021.130986>.
- [125] F. Pedrero, S.R. Grattan, A. Ben-gal, G.A. Vivaldi, Opportunities for expanding the use of wastewaters for irrigation of olives, *Agric. Water Manag.* 241 (2020), 106333, <https://doi.org/10.1016/j.agwat.2020.106333>.
- [126] M. Farhadkhani, M. Nikaeen, G. Yadegarfar, Effects of irrigation with secondary treated wastewater on physicochemical and microbial properties of soil and produce safety in a semi-arid area, *Water Res.* 144 (2018) 356–364, <https://doi.org/10.1016/j.watres.2018.07.047>.
- [127] S. Ofori, A. Pu, R. Iveta, Treated wastewater reuse for irrigation : pros and cons, *Sci. Total Environ.* 760 (2021), <https://doi.org/10.1016/j.scitotenv.2020.144026>.
- [128] H.K. Shannag, N.K. Al-mefleh, N.M. Freihat, Reuse of wastewaters in irrigation of broad bean and their effect on plant-aphid interaction, *Agric. Water Manag.* 257 (2021), 107156, <https://doi.org/10.1016/j.agwat.2021.107156>.
- [129] K.A. Murrell, P.D. Teehan, F.L. Dorman, Determination of contaminants of emerging concern and their transformation products in treated-wastewater irrigated soil and corn, *Chemosphere* 281 (2021), 130735, <https://doi.org/10.1016/j.chemosphere.2021.130735>.
- [130] E. Ben Mordechay, V. Mordehay, J. Tarchitzky, B. Chefetz, Pharmaceuticals in edible crops irrigated with reclaimed wastewater : evidence from a large survey in Israel, *J. Hazard. Mater.* 416 (2021), 126184, <https://doi.org/10.1016/j.jhazmat.2021.126184>.
- [131] M. Abel-Denee, T. Abbott, C. Eskicioglu, Using mass struvite precipitation to remove recalcitrant nutrients and micropollutants from anaerobic digestion dewatering centrate, *Water Res.* 132 (2018) 292–300, <https://doi.org/10.1016/j.watres.2018.01.004>.
- [132] Z. Frkova, S. Venditti, P. Herr, J. Hansen, Assessment of the production of biodiesel from urban wastewater-derived lipids, *Resour. Conserv. Recycl.* 162 (2020), 105044, <https://doi.org/10.1016/j.resconrec.2020.105044>.

## Annex B



# Effect of salinity on preconcentration of contaminants of emerging concern by nanofiltration: Application of solar photo-Fenton as a tertiary treatment

Dennis Deemter<sup>a</sup>, Isabel Oller<sup>a</sup>, Ana M. Amat<sup>b</sup>, Sixto Malato<sup>a,\*</sup>

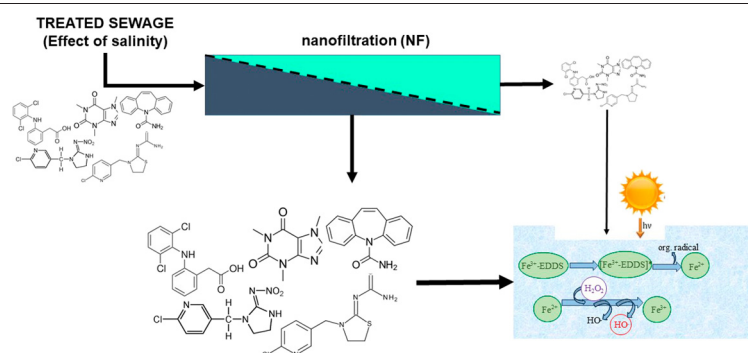
<sup>a</sup> Plataforma Solar de Almería-CIEMAT, Carretera de Senés Km 4, Tabernas, Almería, Spain

<sup>b</sup> Grupo Procesos de Oxidación Avanzada, Campus de Alcoy, Universitat Politècnica de València, Spain

## HIGHLIGHTS

- Microcontaminant permeability order was not influenced by increased salinity.
- Concentration factor is the key factor for permeability order and rate.
- Persulfate and hydrogen peroxide showed different elimination efficiencies.
- Persulfate was found inefficient for the elimination of selected microcontaminants.
- Solar photo-Fenton rapidly eliminated present and residual microcontaminants.

## GRAPHICAL ABSTRACT



## ARTICLE INFO

### Article history:

Received 29 August 2020

Received in revised form 8 October 2020

Accepted 29 October 2020

Available online 17 November 2020

Editor: Dimitra A Lambropoulou

### Keywords:

Microcontaminants

Nanofiltration

Salinity

Tertiary treatment

Solar photo-Fenton

## ABSTRACT

This study focused on the effect of salinity on the performance of a pilot-scale nanofiltration (NF) for preconcentration of microcontaminants (MCs) in combination with solar photo-Fenton or photo-Fenton-like treatment for their elimination from NF permeate and concentrate streams. Photo-Fenton was carried out in a solar simulator at pH of 3 and at natural pH using Ethylenediamine-N, N'-disuccinic acid (EDDS) as an iron complexing agent. Degradation efficacy was tested with MCs commonly found in urban wastewater treatment plant effluents (caffeine, imidacloprid, thiacloprid, carbamazepine and diclofenac). Hydrogen peroxide and persulfate were compared in solar processes. Increase in salinity and pressure had a negligible influence on MC permeability order and NF selectivity. Solar photo-Fenton was able to degrade MCs present in the concentrated stream, and rapidly eliminate any residual MCs that might finally be present in permeate streams. Persulfate used instead of hydrogen peroxide was shown to be inefficient for the selected MCs. Fe(III):EDDS at circumneutral pH was able to remove MCs as quickly as classical photo-Fenton at acid pH, or even faster. This effect supports use of Fe(III):EDDS at natural pH for treating NF concentrates or polishing NF permeates when NF membranes are operated under extreme conditions of salinity.

© 2020 The Authors. Published by Elsevier B.V. This is an open access article under the CC BY-NC-ND license (<http://creativecommons.org/licenses/by-nc-nd/4.0/>).

## 1. Introduction

The worldwide need for clean water is increasing, while its availability rapidly decreases due to the effects of climate change, such as floods and draughts, rising population and widespread pollution by human

\* Corresponding author.

E-mail address: [sixto.malato@psa.es](mailto:sixto.malato@psa.es) (S. Malato).

activity. Therefore, alternative sources of water must be found. Reused wastewater is highly promising as, depending on its final application, very high-quality water can be achieved [Ricart and Rico, 2019; Capocelli et al., 2019]. Growing populations, urbanization and industrialization are demanding higher production of detergents, food and pharmaceuticals [Li et al., 2016], increasing the overall salinity of NF influents [Abdel-Fatah, 2018]. Faster evaporation of water with rising temperatures will also lead to more rapid salination of soil and coastal groundwaters, and therefore, increasing salinity is also expected in UWWs.

Contaminants of Emerging Concern (CECs) are now being recorded for longer times, and microcontaminants (MCs) are increasingly found in urban wastewater (UWW) effluents in ranges from ng/L up to µg/L [Petrović et al., 2003]. Their origins can be found in the use and disposal of a variety of modern-day products, such as pesticides, pharmaceuticals and other organic compounds incorrectly disposed of, or which simply cannot be treated by conventional wastewater treatment plants [Rizzo et al., 2019]. Therefore, new treatment technologies are of the highest priority, while existing methods should be improved, scaled-up and combined to lower UWW treatment costs and prevent contaminants from passing through conventional wastewater treatment systems, resulting in bioaccumulation, chronic toxicity and endocrine disruption [McGinnis et al., 2019; Pico et al., 2019; Rasheed et al., 2019].

Several new perspectives on the problem of MCs passing through conventional wastewater treatments apply nanofiltration membranes (NF). This technology is relatively simple and inexpensive to apply, and consumes less power than current techniques, such as reverse osmosis [Mendret et al., 2019; Voigt et al., 2019]. Two groups of NF membranes, polymeric and ceramic, are widely used commercially. Polymeric NF membranes are used more often due to their lower cost, but have limitations regarding temperature, pH, fouling and cleaning. Although more expensive, ceramic membranes can be applied when the matrix pH is very high or low or temperatures are high, and they are easily cleaned by back-washing and/or incinerating the fouling layer. The main separating mechanism in the membrane technology is size exclusion, but also solution-diffusion and Donnan effect [Silva and Livingston, 2006; Zhang et al., 2019]. However, this can be strongly influenced by a variety of physicochemical mechanisms, such as molecular and surface polarity, pH, salinity and concentration polarization, as well as system parameters such as temperature, flow and pressure [Meschke et al., 2020]. Therefore, the effects of these mechanisms and parameters must be studied for a general understanding of the separation behavior of specific MCs during NF and its products, the concentrate and permeate streams.

In another perspective, Advanced Oxidation Processes (AOPs), which generate highly reactive, nonselective hydroxyl radicals ( $\bullet\text{OH}$ ), are applied to eliminate MCs [Kanakaraju et al., 2018]. One of these processes, photo-Fenton, is based on the catalytic iron cycle ( $\text{Fe}^{2+}/\text{Fe}^{3+}$ ), promoted by hydrogen peroxide ( $\text{H}_2\text{O}_2$ ) and UV-vis light to produce  $\bullet\text{OH}$ . Its main advantage is that it uses simple chemicals and can be powered by solar radiation (renewable energy) with solar compound parabolic collectors already available [Janssens et al., 2019]. This has an important application potential in arid and semi-arid regions, due to their year-round high solar irradiation, where water reuse is also desirable due to its scarcity [UN DESA, 2019].

One of the main drawbacks of photo-Fenton is that it must take place at pH 3 to maintain the iron in solution, which increases operating costs from pH adjustment when urban wastewater is to be treated. The use of a wide variety of iron complexing agents has been studied to avoid this. One of them, Ethylenediamine-N, N'-disuccinic acid (EDDS), makes solar photo-Fenton treatment possible at natural pH (pH = 7) by keeping iron soluble through formation of a stable photoactive complex. In addition, it should be mentioned that EDDS is not only photochemically effective, it is more photoreactive, because it is absorbent in a wider light wavelength which fits better to the solar UV-Vis spectrum, than conventional photo-Fenton [Dong et al., 2019]. Moreover, it is a

biodegradable, environmentally-friendly substance [Tandy et al., 2006]. This information is confirmed by two recent review articles [Clarizia et al., 2017; and of Zhang and Zhou (2019)]. The primary transformation products of EDDS have been recently described [Jaber et al., 2020]. Six different products were identified and described as produced in the initial photo-redox process using lamps simulating solar spectrum. They are oxidized products with a shorter carbon chain than EDDS and aldehyde and/or carboxylic acid functions, proposing the formation of formaldehyde, which is likely to be further oxidized to formic acid. The authors state that these compounds are easily biodegradable and of low toxicity, not inducing them they would entail a greater risk of toxicity for the aquatic environment.

However, the high initial investment and high operating costs (mainly from reagents required) are still a drawback to its practical application. Therefore, solar photo-Fenton efficiency must be mapped over pretreated (UWW) effluents to guarantee its successful and efficient implementation as a tertiary treatment in existing systems, and increase the efficiency of recently developed hybrid systems using both NF and AOPs [Gallego-Schmid et al., 2019]. Focusing on this promising hybrid option, by increasing the MC concentration in the concentrate stream after NF pretreatment of UWW effluents, the total treatment volume could be reduced, significantly lowering reagents and accumulated UV energy required to attain the desired MC elimination percentage.

Thus, there is a pressing need for research on the effect of salinity on separation processes with NF membranes combined with AOPs in different UWW treatment plant (UWWTP) effluents. First the different physicochemical fouling mechanisms of NF membranes when filtering MCs from UWWTP effluents must be mapped. Salinity has already been shown to have an effect on concentration polarization, the formation of a gel-like layer or scaling induced by an accumulation of solutes, such as salts and MCs, near the membrane surface due to the surface polarity of commonly used NF membranes [Bi et al., 2016]. Preferential passage of the solvent through the membrane dramatically decreases the mass transfer coefficient of rejected ions, resulting in local supersaturation, while the bulk concentration in the matrix remains unsaturated [Shi et al., 2014; Song et al., 2018].

Pressure-driven filtration, and more specifically NF for MC removal, has been studied in detail in recent years addressing physicochemical properties of MCs (solute molecular weight/size/geometry, charge, and hydrophobicity), water quality conditions (pH, solute concentration, temperature, background inorganics, and natural organic matter), membrane properties and operating conditions (membrane fouling, membrane pore size, porosity, charge, and pressure) that influence the removal of MCs during membrane filtration [Kim et al., 2018; Patel et al., 2019]. The use of Solar photo-Fenton to treat MCs has been also deeply studied [Kanakaraju et al., 2018], however studies at circumneutral pH are still scarce [Ahile et al., 2020] and even more the use of persulfate as alternative to hydrogen peroxide at circumneutral pH [Wang and Wang, 2018a, 2018b; Ike et al., 2018]. Recently research in AOPs is dominated by the search for cost-effective and sustainable techniques [Miklos et al., 2018] but there is no study about how to combine NF with photo-Fenton at circumneutral pH for treating high salinity NF retentates containing MCs at realistic concentrations. Comparison of different operational variables of solar photo-Fenton process (by using Fe-EDDS) applied to eliminate MCs from both retentate and permeate has not been found in the revised literature. Therefore, this study focused on the effect of salinity on the performance of an NF system for preconcentration of MCs before solar photo-Fenton tertiary treatment for their elimination from natural water. Solar photo-Fenton was carried out at its optimal pH of 3 and at natural pH using EDDS as an iron complexing agent. The degradation efficacy of five MCs commonly found in UWWTP effluents, caffeine (CAF), imidacloprid (IMI), thiacloprid (THI), carbamazepine (CAR) and diclofenac (DIC) were tested in natural water spiked at a concentration of 100 µg/L each. Hydrogen peroxide and persulfate were compared as oxidizing

agents in solar photo-Fenton and photo-Fenton-like processes. Finally, the influence of different Fe:EDDS ratios was also evaluated.

## 2. Materials and methods

### 2.1. Reagents and chemicals

Target MCs (IMI, THI, CAR and DIC) were purchased from Sigma-Aldrich (Germany), except CAF, which was acquired from Fluka. NaCl was from Honeywell-Fluka. HPLC-grade solvents required for monitoring MCs were from Sigma-Aldrich. Iron substances,  $\text{FeSO}_4 \cdot 7\text{H}_2\text{O}$  for Fe (II) and  $\text{Fe}_2(\text{SO}_4)_3 \cdot x\text{H}_2\text{O}$  for Fe(III), as well as Sodium persulfate ( $\text{Na}_2\text{S}_2\text{O}_8$ ) and  $\text{H}_2\text{O}_2$  (35% w/v) were also from Sigma Aldrich.  $\text{H}_2\text{SO}_4$  (95–97%) was from J.T. Baker. The water matrix was natural water (Tabernas, Spain) (see Table SI 1 for composition). Fig. 1 is a schematic overview of the five MCs selected.

### 2.2. Analytical determinations

MC concentrations were measured by ultra-performance liquid chromatography (UPLC) using an Agilent Technologies 1200 series device, with a UV-DAD detector and a Poroshell 120 EC-C18 column ( $3.0 \times 50$  mm). The starting eluent conditions, 95% water with 25 mM Formic acid (mobile phase A) and 5% ACN (mobile phase B) at 1 mL/min, were kept for 5 min. Then, a linear gradient progressed for 10 min to 68% ACN and kept at this concentration for 2 min. The injection volume was 100  $\mu\text{L}$  at a temperature of 30 °C. Samples were prepared by adding 1 mL of ACN to 9 mL of this mixture and then filtered through a hydrophobic PTFE 0.2  $\mu\text{m}$  (Millipore Millex-FG) syringe filter into a 2-mL HPLC vial. Table SI 2 shows the molecular weight, retention time, limit of quantification (LOQ) and maximum absorption wavelength of each target MC. Dissolved organic and inorganic carbon (DOC and IC) were measured with a Shimadzu TOC-VCN analyzer.  $\text{H}_2\text{O}_2$  was determined directly after sampling using Titanium (IV) oxysulfate following DIN 38402H15. Iron was determined after filtering through a 0.45  $\mu\text{m}$  Nylon filter, using 1,10 phenanthroline following ISO 6332. Persulfate determination was adapted from Liang [Liang et al., 2008].

### 2.3. Experimental set-up

#### 2.3.1. NF membrane pilot plant

The NF pilot plant (Fig. 2) consisted of a 400-L feed tank equipped with a recirculation pump to ensure that the concentrate stream was continuously mixed with the tank volume, and the MC concentration increased as the volume was reduced by permeate discharge. The feed tank pump was a single multistage centrifugal pump with a frequency modulator for pressure generation and internal recycling. NF membranes were DOW FILMTEC™ NF90–2540, rolled-sheet polyamide thin-film composite membranes, which work by crossflow filtration. NF membranes have a total surface area of 5.2 m<sup>2</sup> and are operable at up to 45 °C, in pH 2–11, a maximum operating pressure of 41 bars and molecular weight cut-off (MWCO) of 250.0 g/mol. Like most commercial NF membranes, the surface is negatively charged [Zhang et al., 2020]. The system includes three digital flow meters (measuring

permeate, concentrate and recycle flows), two conductivity meters (measuring the conductivity of permeate and concentrate streams in  $\mu\text{S}/\text{cm}$  and  $\text{mS}/\text{cm}$ , respectively), two pressure sensors (before and after the membrane unit; measuring in bars) and a temperature sensor in the recirculation circuit (°C). All values are integrated in a SCADA user interface. The maximum system pressure was set at 10 bars.

#### 2.3.2. Experimental procedure

A stock solution of the MC mixture containing CAF, IMI, THI, CAR and DIC was prepared in methanol to a concentration of 2.5 g/L of each compound, ensuring high solubility and low TOC later, when diluted in water to a  $\mu\text{g}/\text{L}$  range. The desired matrix was prepared in the feed tank to a final concentration of 3, 5 or 7 g/L of NaCl and 100  $\mu\text{g}/\text{L}$  of each MC in order to work close to the actual content usually found in MWWTP effluents. The system was operated at 5, 7 and 10 bars. The first permeate sample (P1) was collected after operating the NF plant for 180 min, the point of concentration polarization, as mentioned in the Introduction. The resulting volume was approximately 100 L of permeate. The second permeate sample (P2) was taken after an additional 660 min of batch operation. The concentrate stream (C1) was collected after attaining a CF of 2.7. All samples (5 L) were stored in separate bottles and kept refrigerated until further use. MC concentrations and main physicochemical parameters of each sample may be found in Table 1.

#### 2.3.3. Solar photo-Fenton treatment

Solar photo-Fenton experiments were performed with a solar simulator (Atlas-SunTest XLS+) with a daylight filter, and a xenon lamp on the chamber ceiling, programed for total radiation of 365  $\text{W}/\text{m}^2$  (300–800 nm) and 30  $\text{W}/\text{m}^2$  of UV radiation (300–400 nm) under continuous ventilation to keep the temperature at 25 °C. A magnetically stirred cylindrical 1-L container (18.5 cm diameter and 4.0 cm deep) was placed in the center inside the solar simulator chamber.

Classic photo-Fenton experiments at pH 3 were carried out with 1 L of sample (P1, P2, C1) acidified with  $\text{H}_2\text{SO}_4$  to pH 3 prior to the addition of  $\text{FeSO}_4 \cdot 7\text{H}_2\text{O}$ . For the experiments at natural pH, carbonates/bicarbonates (known  $\bullet\text{OH}$  radical scavengers) were removed by air stripping after addition of  $\text{H}_2\text{SO}_4$ , lowering the total inorganic carbon to 15 mg/L. The  $\text{Fe}^{3+}$ -EDDS ratio ( $\text{Fe}_2(\text{SO}_4)_3 \cdot 7\text{H}_2\text{O}$  previously dissolved in demineralized water at pH 3, followed by addition of EDDS) was 1:2 for all experiments. The starting iron concentration was 0.10 mM and the  $\text{H}_2\text{O}_2$  concentration was 1.50 mM. In the experiments at natural pH, the EDDS concentration was 0.20 mM. Starting photo-Fenton conditions were selected based on previous results [Klamerth et al., 2010; Miralles-Cuevas et al., 2013]. Further experiments with variations on the parameters given here were also performed: iron concentration doubled to 0.20 mM, EDDS concentration in 0.10 mM halved and persulfate instead of  $\text{H}_2\text{O}_2$  at equal concentrations. For an overview of those experiments see Table SI 3.

## 3. Results and discussion

### 3.1. Effect of salinity on nanofiltration membranes

The differences in influence of the two water matrices (demineralized water and natural water (Tabernas, Spain)), system

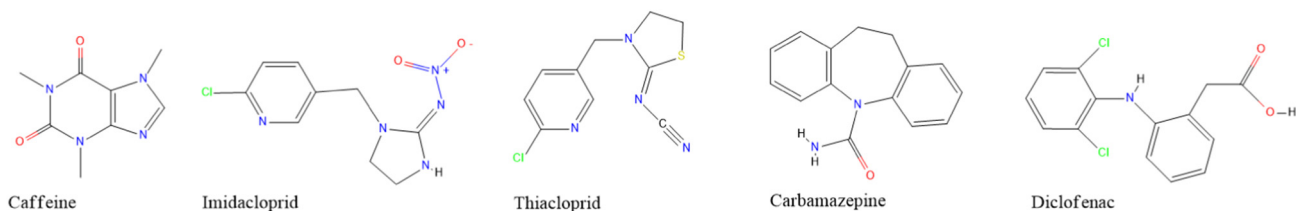
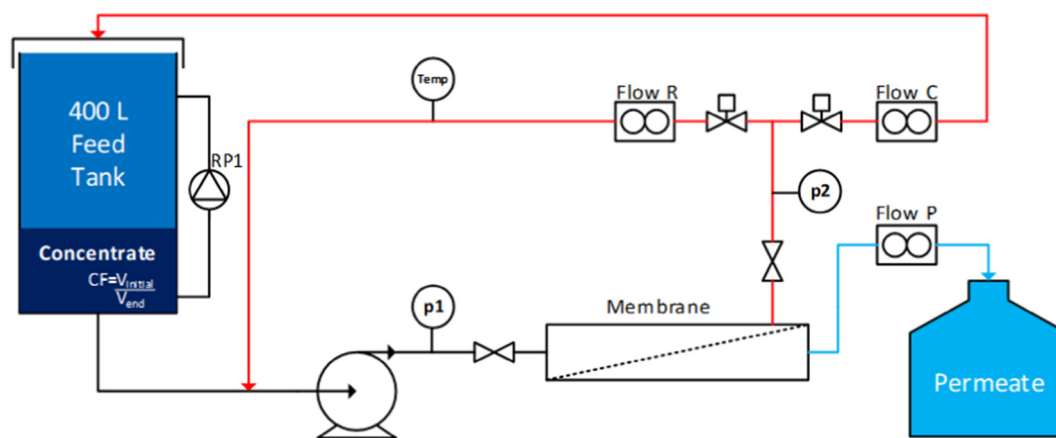


Fig. 1. Schematic overview of the molecular structures of CAF, IMI, THI, CAR and DIC. The molecular charge is shown in red (negative), yellow (moderate negative), blue (positive) or green (neutral).





**Fig. 2.** Schematic overview of the NF pilot plant. 'Temp' is the temperature sensor in the recirculation circuit, 'Flow R, C and P' are the recycle, concentrate and permeate stream digital flow meters, respectively; p1 and p2 are the pressure meters before and after the membrane. The feed tank is equipped with a recirculation pump (RP1). The concentration factor (CF) can be determined by dividing the starting volume ( $V_{start}$ ) by the end volume ( $V_{end}$ ).

pressure (5, 7 and 10 bars), and salinity (3, 5 and 7 g/L of NaCl) were assessed in the NF pilot plant. Water matrices were spiked with target MCs from the stock solution to reach the starting feed tank concentrations of 100  $\mu\text{g/L}$ , each. Total experimental time was set at 360 min when demineralized water was tested, which was the time required to attain the desired maximum concentration factor of 4 ( $CF = 4.0$ ). It should be mentioned that high concentrations of the permeating THI, CAF and CAR were already detected at this stage. During all experiments with the demineralized water matrix, with and without addition of NaCl and at different pressures, permeability of three MCs, THI, CAF and CAR was detected when in operation for over 180 min. This point was therefore set as the membrane surface saturation point time, which is also called the concentration polarization point as described in the Introduction.

In all the experiments, the order of MC membrane permeability was THI, CAF, and CAR with very low concentrations of DIC. This can be explained due to their molecular morphology (see Fig. 1 in Section 2.1), flexibility and weight (252.7, 194.2 and 236.3 g/mol, respectively; DIC 318.1 g/mol; membrane MWCO 250.0 g/mol). Positively charged molecules also significantly promote MC membrane permeability, as the membrane surface is negatively charged (see details in 2.3.1), attracting the positively charged molecules, instead of repelling them. MC increases in the concentrate stream were inversely related to the concentration factor (CF). In addition, as expected, higher NF pilot plant system pressure resulted in higher CFs.

In experiments with addition of 3 g/L of NaCl, the same pressures as in the previous experiments were evaluated. MC permeability through NF membrane showed the same order as without the addition of NaCl. DIC was again not detected in the permeate stream and the rest of MC membrane permeability order remained the same as observed with demineralized water alone (THI, CAF and CAR).

Table 2, shows the time needed to reach 10  $\mu\text{g/L}$  per MC in the permeate stream. Under these conditions, it was possible to obtain a CF of 2.0, 3.0 and 4.0 at 120, 180 and 300 min, respectively, only at 10 bars.

**Table 1**

MC concentration [mg/L] and main physicochemical parameters of each stored sample: Permeate samples (P1 and P2) were collected after NF plant and concentrate stream (C1) was collected after attaining a concentration factor (CF) of 2.7.

	CAF	IMI	THI	CAR	DIC	pH	IC [mg/L]	Conductivity [mS/cm]
P1	0.0091	0.0198	0.0238	0.0050	0.0050	8.3	14.0	2.4
P2	0.0321	0.0505	0.0561	0.0101	0.0079	8.8	25.4	6.5
C1	0.2344	0.1927	0.1692	0.2568	0.2199	8.9	253.8	27.8

At lower pressures, for instance, at 5 bars, a CF of 2.0 was only reached after 420 min. Similarly, salinity (measured as conductivity) increased by a factor of 2.0 in the feed tank at 180, 150 and 90 min, at 5, 7 and 10 bars, respectively.

The system pressure applied was set at 10 bars, because that is the maximum NF pilot plant system pressure, however, higher pressures are more likely to be used in future commercial applications. Especially, at higher salinity, such as with the addition of 5 and 7 g/L of NaCl to the matrix, this low pressure prevented the desired CF of 4 from being reached within the experimental time, which was set at 360 min (data not shown). For instance, with demineralized water and 5 g/L of NaCl at 10 bars, it was only possible to reach a CF of 2.0 and 3.0 at 210 and 360 min, respectively.

Continuing with our objective of assessing the effect of salinity on nanofiltration membranes, the next step was to increase the complexity of the water matrix by using natural water (Tabernas, Spain, physicochemical characterization in Table S1 1). From this point on, IMI was included in the mixture of MCs, as described in Section 2.3.2, because five MCs could provide more variability in NF permeability and retention, enriching the results. Like THI, IMI is one of the neonicotinoids, a group of widely used pesticides that has been showing high persistency in the environment and is increasingly held responsible for the elimination of bees around the world [Kessler et al., 2015; Brandt et al., 2016].

Although the use of natural water as a matrix made the salinity higher than demineralized water, because it also contained salts other than NaCl, no differentiation in MC membrane permeability order, as previously described, was observed after the addition of 3, 5 and 7 g/L NaCl. Total matrix salinity after addition of NaCl was 8200, 11,100 and 14,500  $\mu\text{S/cm}$ , respectively.

Fig. 3 shows the evolution of the total MC concentration in the permeate and concentrate (inset) streams during the full experimental time of 360 min. Final MC increment in the permeate stream was 25.7, 3.2 and 3.8 times higher compared to demineralized water experiments and in the concentrate stream 2.3, 1.7 and 1.4 times higher, with 3, 5 and 7 g/L NaCl added, respectively.

**Table 2**

Time needed to reach 10  $\mu\text{g/L}$  of each MC in the permeate stream in demineralized water with 3 g/L NaCl.

Pressure, bars	5	7	10	
THI	180	150	120	min.
CAF	420	300	210	min.
CAR	-	-	300	min.
DIC	-	-	-	min.

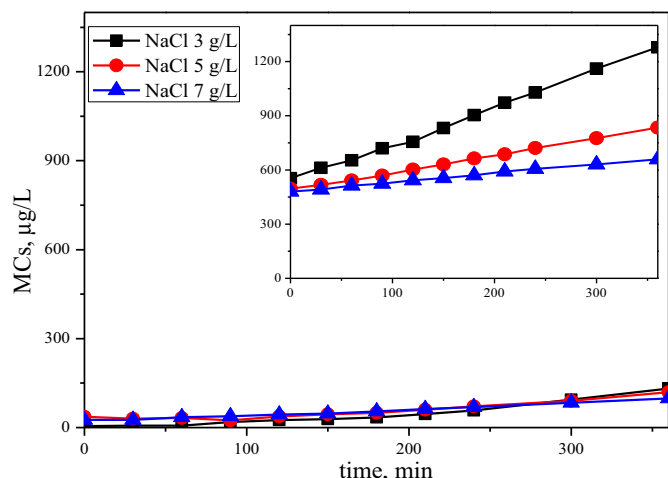


Fig. 3. Concentration over time of the sum of MCs in the permeate and concentrate (inset) streams, after addition of 3, 5 and 7 g/L NaCl to natural water.

When 3 g/L NaCl were added, the permeate and concentrate conductivities at  $t = 0$  min were 430 and 10,500  $\mu\text{S}/\text{cm}$ , respectively, increasing to 2400 and 20,200  $\mu\text{S}/\text{cm}$  at  $t = 360$  min (end of experiment). Thus, after 360 min, salinity had increased by a factor of 5.7 in the permeate stream, 2.3 in the tank and 1.9 in the concentrate stream, and the CF was 3.3. After adding 5 g/L NaCl, permeate and concentrate stream conductivities at  $t = 0$  min were 650 and 13,700  $\mu\text{S}/\text{cm}$ , respectively, increasing to 4300 and 21,400  $\mu\text{S}/\text{cm}$  at  $t = 360$  min. Also after 360 min, salinity in the permeate stream had increased by a factor of 6.5, 1.8 in the tank and 1.6 in the concentrate stream, and the CF was 2.4. Finally, 7 g/L NaCl added to the permeate and concentrate led to conductivities at  $t = 0$  min of 1400 and 17,900  $\mu\text{S}/\text{cm}$ , respectively, increasing to 4600 and 22,700  $\mu\text{S}/\text{cm}$  at  $t = 360$  min. Salinity in the permeate stream increased by a factor of 3.2, 1.5 in the tank and 1.3 in the concentrate. After 360 min, the CF was 1.6, a clearly significant decrease in the concentration capacity of the NF system employed in this study, as a CF near 4 was only attained with addition of 3 g/L NaCl to the natural water which already had a starting conductivity of 2300  $\mu\text{S}/\text{cm}$ .

In all the experiments, the MC membrane permeability order was IMI, THI, CAF and CAR. DIC was not detected in the permeate stream. This is mainly due to the molecular weight of the MCs and their molecular charge as explained above. Growing CF, and thus salinity, was observed with more MCs, and THI and IMI especially increased disproportionately in the permeate stream. It may therefore be concluded that higher salinity resulted in decreased membrane efficiency and MC retention. Based on this conclusion, and for the main objective of simulating the most unfavorable operating conditions, the rest of experiments were carried out with the addition of 7 g/L NaCl at a system pressure of 10 bars. Under these conditions, after 360 min, the total MC concentrations were 104  $\mu\text{g}/\text{L}$  (IMI: 30  $\mu\text{g}/\text{L}$ , THI: 39  $\mu\text{g}/\text{L}$ , CAF: 19  $\mu\text{g}/\text{L}$ , CAR: 11  $\mu\text{g}/\text{L}$  and DIC: 5  $\mu\text{g}/\text{L}$ ) and 659  $\mu\text{g}/\text{L}$  (IMI: 130  $\mu\text{g}/\text{L}$ , THI: 129  $\mu\text{g}/\text{L}$ , CAF: 156  $\mu\text{g}/\text{L}$ , CAR: 162  $\mu\text{g}/\text{L}$  and DIC: 82  $\mu\text{g}/\text{L}$ ) in permeate and concentrate streams, respectively. The final concentration in the feed tank was 659  $\mu\text{g}/\text{L}$ .

After evaluating the effect of salinity on NF system performance, several batches were run to produce enough concentrate and permeate for further tertiary treatment by solar photo-Fenton. Batches were generated at an isobaric system pressure of 10 bars. Natural water (Tabernas, Spain) with a starting concentration of 7 g/L NaCl was used, as it was the highest salinity tested in the previous experiments and high saline effluents from actual UWW are the main target of this combined technology. Furthermore, as NF was proposed to concentrate MCs, it was tested under conditions that were not so mild in order to obtain more conservative (not optimistic) results. For Batch P1, the NF plant was operated

with a starting volume of  $V_0 = 400$  L for 180 min, as permeability of the four MCs IMI, THI, CAF and CAR was detected at over 180 min. The resulting volume after 180 min of Batch P1 was  $V_{P1} = 100$  L of permeate. NF plant operation continued with the remaining 300 L for another 660 min, resulting in Batches P2 and C1 having equal volumes of  $V_{P2} = V_{C1} = 150$  L. This longer operation time than the previous 360 min was selected because a final batch volume ratio close to 4 was desired. These batches (P1 and P2 for permeates with different low concentrations of MCs and C1 for high concentration of MCs) were prepared for later treatment with solar photo-Fenton under different operating conditions. The main objective defined for all the different treatments applied to permeate and concentrate streams was 90% degradation of the sum of MCs. This is an ambitious objective in view of the new regulation in Switzerland (the only country in Europe, for the moment, specifically regulating MCs in UWWTP effluents), which requires 80% of CECs to be eliminated from raw wastewater (Eggen et al., 2014).

## 3.2. Solar photo-Fenton tertiary treatment

### 3.2.1. Conventional solar photo-Fenton treatment at pH 3

The starting conditions for photo-Fenton treatment were selected based on previous results and low initial concentrations of Fe(II) and  $\text{H}_2\text{O}_2$  to reduce the environmental and economic impacts, while still providing high elimination efficiency with a wide range of MCs [Klamerth et al., 2010; Miralles-Cuevas et al., 2013].

Fig. 4 shows the results for samples P1, P2 and C1 with mild experimental parameters for solar photo-Fenton at pH 3 (0.10 mM Fe(II) and 1.50 mM  $\text{H}_2\text{O}_2$ ).

Fig. 4 shows that in sample C1, elimination of CAF, CAR and DIC to below the LOQ (5  $\mu\text{g}/\text{L}$ ) took less than 5 min of treatment. Although IMI and THI showed higher persistence to solar photo-Fenton, more than 70% was eliminated after 30 min.  $\text{H}_2\text{O}_2$  consumption at the end of the experiment was 0.70 mM (around 50% of the starting amount). First order kinetic constant ( $r = kC$ ) were 0.770  $\text{min}^{-1}$ , 0.042  $\text{min}^{-1}$ , 0.041  $\text{min}^{-1}$ , 0.793  $\text{min}^{-1}$ , 0.737  $\text{min}^{-1}$  for CAF, IMI, THI, CAR and DIC, respectively.

In samples P1 and P2, CAF, CAR and DIC were eliminated to LOQ (5  $\mu\text{g}/\text{L}$ ) quite fast within the first 5 min of treatment. Indeed, DIC was degraded by Fenton in the dark ( $t < 0$ ), even before illumination. IMI and THI showed higher persistence in solar photo-Fenton than the other MCs, and only 90% was eliminated from P1 and P2 after 25 and 30 min, respectively. First order kinetic constant for P1 were 0.133  $\text{min}^{-1}$ , 0.060  $\text{min}^{-1}$  and 0.071  $\text{min}^{-1}$ , for CAF, IMI and THI,

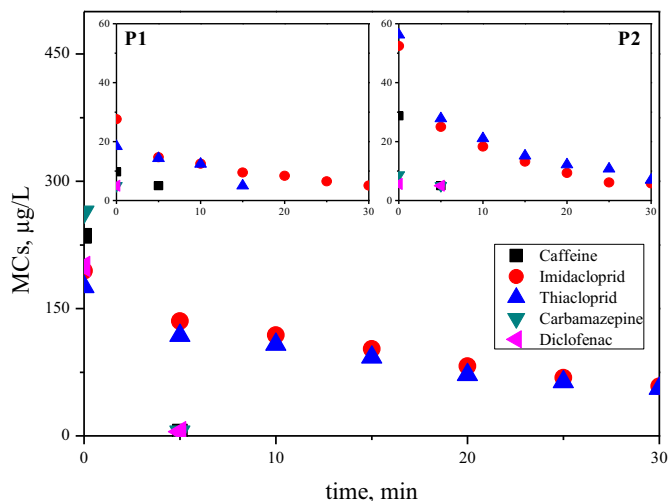


Fig. 4. MC concentrations during solar photo-Fenton treatment at pH 3 of concentrate C1. Insets show results of P1 and P2 tertiary treatments.

respectively. And  $0.350 \text{ min}^{-1}$ ,  $0.083 \text{ min}^{-1}$  and  $0.074 \text{ min}^{-1}$ , for CAF, IMI and THI, respectively, for P2.

$\text{H}_2\text{O}_2$  consumption at the end of the experiments was 0.50 mM and 0.80 mM, respectively. Therefore,  $\text{H}_2\text{O}_2$  consumption was not affected by MC concentration, and was very similar in P1, P2 and C1. Treatment of concentrates was slower but successful as degradation was over 90% of the sum of MCs after 20 min of treatment, and always over 70% for individual MCs after 30 min.

### 3.2.2. Solar photo-Fenton at natural pH using EDDS

Mild solar photo-Fenton at natural pH (0.10 mM Fe(III):EDDS; [1:2] and 1.50 mM  $\text{H}_2\text{O}_2$ ) was also applied to samples P1, P2 and C1 (results shown in Fig. 5). Starting photo-Fenton parameter values were selected based on previous studies with low starting concentrations of Fe(II) and  $\text{H}_2\text{O}_2$  [Miralles-Cuevas et al., 2014].

Elimination of CAF, CAR and DIC to LOQ ( $5 \mu\text{g/L}$ ) was attained in C1 in less than 5 min. More recalcitrant MCs (IMI and THI) were degraded 90% in less than 15 min. The decay of Fe(III):EDDS has been described as parallel to evolution of dissolved Fe, as stated by other studies using Fe(III):EDDS where the complex was evaluated in detail [Soriano-Molina et al., 2018; Costa et al., 2020]. Iron precipitation (when the complex was degraded) started to be detected at just under 20 min, with a total loss of 0.03 mM of dissolved iron after 30 min.  $\text{H}_2\text{O}_2$  consumption was around 1.20 mM after 30 min, but 0.80 mM at 15 min, when 90% degradation was attained. First order kinetic constants were  $0.768 \text{ min}^{-1}$ ,  $0.150 \text{ min}^{-1}$ ,  $0.126 \text{ min}^{-1}$ ,  $0.792 \text{ min}^{-1}$ ,  $0.732 \text{ min}^{-1}$  for CAF, IMI, THI, CAR and DIC, respectively.

As seen in Fig. 5, in samples P1 and P2, elimination of all MCs to LOQ ( $5 \mu\text{g/L}$ ) was rapidly achieved. Within less than 5 min, all MCs were degraded 90%. Iron precipitation due to EDDS degradation began after 10 min and was fully precipitated at 30 min of treatment. Consumption of  $\text{H}_2\text{O}_2$  was 1.20–1.30 mM at the end of the experiment, but as low as 0.60 mM after 5 min. Therefore,  $\text{H}_2\text{O}_2$  consumption was not affected by MC concentration, but naturally decomposed during the treatment time. First order kinetic constant for P1 were  $0.137 \text{ min}^{-1}$ ,  $0.266 \text{ min}^{-1}$  and  $0.304 \text{ min}^{-1}$ , for CAF, IMI and THI, respectively. And  $0.386 \text{ min}^{-1}$ ,  $0.269 \text{ min}^{-1}$  and  $0.192 \text{ min}^{-1}$ , for CAF, IMI and THI, respectively, for P2. Fe(III):EDDS at circumneutral pH was able to rapidly eliminate MCs in the NF samples, at least as efficiently as classic photo-Fenton at acid pH, or even more so, as stated by first order kinetic

constants of the different MCs. IMI and THI were the most recalcitrant MCs in both treatments.

Test were done in water containing high chloride concentration, without any special detrimental effect on the photo degradation of MCs. Lado Ribeiro et al. (2019) reviewed the effects for different AOPs due to the main components present in wastewater, describing the formation of less reactive radicals than hydroxyl ( $\text{Cl}_2^\cdot$ ). Regarding chloride anions at high concentration it was reported (Soriano-Molina et al., 2019) not any effect or slight improvement in the reaction rate due to the intervention of chlorine radicals on MCs degradation.

### 3.2.3. Effect of operating parameters on solar photo-Fenton tertiary treatment at pH 3

Sulfate has previously been reported to decrease photo-Fenton efficiency, as it scavenges hydroxyl and other radicals [De Laat et al., 2004; Zapata et al., 2009; Lado Ribeiro et al., 2019]. When the matrix was acidified to pH 3, the sulfate concentration was almost four times higher than at pH 7. Therefore, the higher reaction rate attained with Fe(III):EDDS at natural pH than with photo-Fenton at pH 3 could be related to hydroxyl radical scavenging by sulfate.

In an attempt to neutralize the negative effect of radical scavenging by sulfate, another 0.60 mM of  $\text{H}_2\text{O}_2$  was added after 15 min (pH 3). Elimination of CAF, CAR and DIC to LOQ ( $5 \mu\text{g/L}$ ) was obtained in less than 5 min, while IMI and THI had still not reached 90% elimination after 30 min. No positive effect of the second addition of  $\text{H}_2\text{O}_2$  on elimination of contaminants was observed, especially in view of the same consumption of  $\text{H}_2\text{O}_2$  (0.70 mM) as in the experimental results shown in Fig. 4.

In a similar attempt to improve solar photo-Fenton at pH 3, a double concentration of iron (0.2 mM) was also tested. Fig. 6 shows elimination to LOQ ( $5 \mu\text{g/L}$ ) of CAF, CAR and DIC in the first 5 min. After 30 min of treatment, 85% and 80% of IMI and THI, respectively, was eliminated. First order kinetic constants were  $0.766 \text{ min}^{-1}$ ,  $0.067 \text{ min}^{-1}$ ,  $0.061 \text{ min}^{-1}$ ,  $0.800 \text{ min}^{-1}$ ,  $0.712 \text{ min}^{-1}$  for CAF, IMI, THI, CAR and DIC, respectively. The positive effects of the increased iron concentration were minimal (compare first order kinetic constants calculated from results in Fig. 4), and  $\text{H}_2\text{O}_2$  consumption was 0.95 mM at 30 min, 20% higher than the basic experimental parameters (Fe 0.10 mM and 1.50 mM  $\text{H}_2\text{O}_2$ ). In addition, after 5 min of treatment,  $\text{H}_2\text{O}_2$  consumption was 0.36 mM, more than double with 0.10 mM Fe(II). Therefore, the

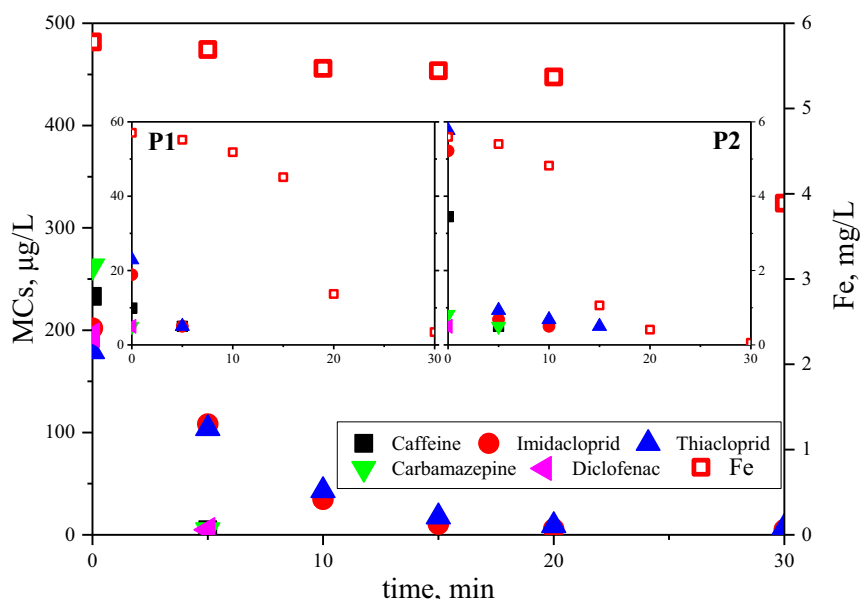
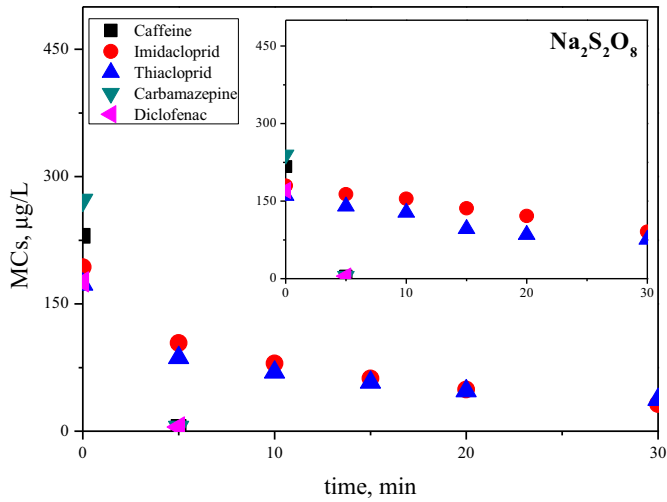


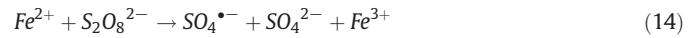
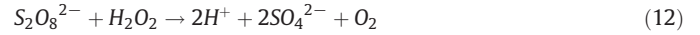
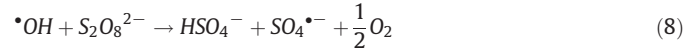
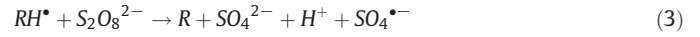
Fig. 5. MC concentrations and dissolved iron evolution during solar photo-Fenton with Fe(III):EDDS [1:2] at natural pH (pH = 7) in concentrate C1. Insets show results with P1 and P2.



**Fig. 6.** MC concentrations during solar photo-Fenton at pH 3 (0.20 mM Fe(II) and 1.50 mM H<sub>2</sub>O<sub>2</sub>) in Concentrate C1. The inset shows the results with persulfate (1.5 mM) as the oxidizing agent.

higher reaction rate with Fe(III):EDDS at natural pH than at pH 3 could not be justified by a lack of oxidizing radicals provoked by a low iron concentration, but could be due to the high concentration of sulfate in C1 which scavenged hydroxyl and other radicals or may be related with the different photoreactivity of iron species formed with Fe(III):EDDS at natural pH or at pH 3.

Finally, persulfate was used as an alternative to H<sub>2</sub>O<sub>2</sub> just to check the possibility of improving traditional solar photo-Fenton treatment of C1 at pH 3. The use of persulfate in photo-Fenton has been described previously elsewhere. [Wang and Wang, 2018a, 2018b; Wang et al., 2019] The added persulfate is activated by a combination of temperature increase, UV-light or transition metals, such as Fe(II) and Fe(III):EDDS (Reactions 13–14 and Figs. 6 and 7). Once activated, it generates the strongly oxidizing sulfate radicals (SO<sub>4</sub><sup>•-</sup>), following the reactions below (Reactions 1–12): [Sánchez-Polo et al., 2013]



These radicals can react with MCs due to their high redox potential, which is similar to <sup>•</sup>OH, but they preferentially work by electron transfer. This preference provides a synergistic effect for MC elimination, while reinforcing the Fenton process by lowering the water pH with sulfuric acid generated by Reaction 12. [Wu et al., 2015; Lian et al., 2017] Therefore, it would be a good alternative to classic photo-Fenton at pH 3, as reaction rates would be higher due to the presence of both hydroxyl and sulfate radicals. However, results of persulfate as an oxidizing agent at pH 3 did not clearly improve the MC degradation rate

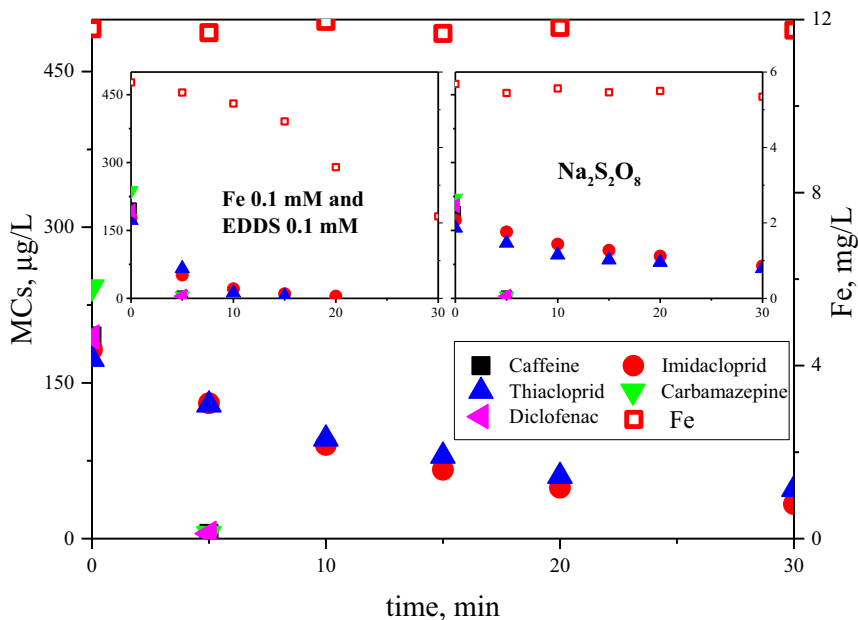


**Fig. 7.** MC concentrations and dissolved iron evolution in C1 during solar photo-Fenton at natural pH (Fe 0.20 mM, EDDS 0.20 mM and 1.50 mM H<sub>2</sub>O<sub>2</sub>). The insets show the results with Fe 0.1 mM and EDDS 0.10 mM and the same ratio with persulfate (1.50 mM) as the oxidizing agent.

(Fig. 6). CAF, CAR and DIC elimination to LOQ (5 µg/L) was attained in less than 5 min. First order kinetic constant were in general lower than classic photo-Fenton at pH 3: 0.753 min<sup>-1</sup>, 0.021 min<sup>-1</sup>, 0.028 min<sup>-1</sup>, 0.774 min<sup>-1</sup>, 0.706 min<sup>-1</sup> for CAF, IMI, THI, CAR and DIC, respectively. Consumption of persulfate was 10% of the starting amount. Only 90% of IMI and THI was eliminated after 30 min of treatment, and although these elimination rates are similar to those with H<sub>2</sub>O<sub>2</sub>, IMI was more persistent with persulfate as the oxidizing agent.

### 3.2.4. Effect of operating parameters on solar photo-Fenton tertiary treatment at natural pH

The effect of operating parameters such as Fe(III):EDDS concentration (0.20 mM iron or half EDDS, 0.10 mM) and persulfate as the oxidizing agent instead of H<sub>2</sub>O<sub>2</sub> was also evaluated in solar photo-Fenton treatment of C1 at natural pH.

When the concentration of iron was doubled (0.20 mM, Fe:EDDS [1:1]), as seen in Fig. 7 and compared to 0.10 mM of iron (Fig. 5, Fe:EDDS [1:2]), CAF, CAR and DIC reached LOQ (5 µg/L) in less than 5 min. Elimination of 80% IMI and 70% THI was also attained after 30 min. First order kinetic constant were 0.732 min<sup>-1</sup>, 0.061 min<sup>-1</sup>, 0.048 min<sup>-1</sup>, 0.776 min<sup>-1</sup>, 0.732 min<sup>-1</sup> for CAF, IMI, THI, CAR and DIC, respectively. Furthermore, no iron precipitation was detected and H<sub>2</sub>O<sub>2</sub> consumption was 1.35 mM after 30 min. The higher concentration of iron resulted in a negative effect on elimination of IMI and THI at natural pH. It may be concluded that increasing the iron concentration to 0.20 mM increased the total concentration of generated •OH. The •OH surplus could then recombine to H<sub>2</sub>O<sub>2</sub> (Reaction 10–11), which at natural pH, promoted the formation of H<sub>2</sub>O and O<sub>2</sub>. Potential competition of EDDS with the MCs for the oxidant, also increasing the dissolved organic carbon, seems to be unlikely, as no iron precipitation was observed, showing that the Fe(III):EDDS complex was stable during the experiment.

As seen in the inset in Fig. 7, with only half of the EDDS concentration (0.10 mM), CAF, CAR and DIC were eliminated to LOQ (5 µg/L) in less than 5 min. Elimination of over 90% of the sum of MCs was achieved after 15 min and H<sub>2</sub>O<sub>2</sub> consumption was 0.70 mM, ending at 1.00 mM after 30 min. First order kinetic constant were 0.737 min<sup>-1</sup>, 0.189 min<sup>-1</sup>, 0.241 min<sup>-1</sup>, 0.772 min<sup>-1</sup>, 0.731 min<sup>-1</sup> for CAF, IMI, THI, CAR and DIC, respectively. Compared to the basic experimental parameters (Fe 0.10 mM, EDDS 0.20 mM and 1.50 mM H<sub>2</sub>O<sub>2</sub>) shown in Fig. 5, the elimination rates were slightly better, however, this time with lower H<sub>2</sub>O<sub>2</sub> consumption. In this case iron precipitation was observed earlier starting after 10 min, with a total loss of 0.02 mM at 15 min and 0.07 mM at 30 min. The loss of iron is well justified, as at the lower concentrations of EDDS, Fe(III) is complexed for shorter times. Thus, the lower EDDS concentration had a positive effect (lower dissolved organic carbon, and therefore less competition with MCs for the oxidants) on MC elimination at natural pH.

Finally, by applying persulfate as the oxidizing agent at natural pH (inset, Fig. 7), CAF, CAR and DIC to LOQ (5.0 µg/L) were eliminated in less than 5 min. The maximum elimination of 60% of the recalcitrant IMI and THI was attained after 30 min. Elimination rates were similar to the curve of the basic experimental parameters using H<sub>2</sub>O<sub>2</sub> at neutral pH as observed in Fig. 5. IMI persistence was similar, although to a lesser extent, to results at pH 3 with persulfate as the oxidizing agent compared to H<sub>2</sub>O<sub>2</sub> at natural pH. First order kinetic constant were 0.729 min<sup>-1</sup>, 0.031 min<sup>-1</sup>, 0.033 min<sup>-1</sup>, 0.758 min<sup>-1</sup>, 0.742 min<sup>-1</sup> for CAF, IMI, THI, CAR and DIC, respectively. Total persulfate consumption was 0.85 mM, which is significantly higher than in the experiment performed at pH 3, but no substantial improvement in MC degradation was observed compared to H<sub>2</sub>O<sub>2</sub> at neutral pH.

The reduction of toxicity of MCs present in water and effluents by solar photo-Fenton has been widely studied in many recent studies, as for example [Miralles-Cuevas et al., 2017; Hong et al., 2020; Gonçalves et al., 2020; Michael et al., 2019], including application of a selected battery of bioassays in vivo (algal growth inhibition test) and in vitro, endocrine disruptors tests (androgenic/glucocorticoid activity and estrogenicity) and cytotoxicity tests [Rivas Ibáñez et al., 2017]. The overall

conclusion was that MCs removal is in concordance with the toxicity reduction shown by many bioanalytical tools. Therefore, in our research we did not delve into this study as there is abundant information regarding the evolution of toxicity during photo-Fenton solar treatment.

## 4. Conclusions

The first increase in salinity and system pressure had a negligible influence on the order of permeability and NF membrane selectivity when natural water was employed as the matrix. Nevertheless, the key factor in such systems for preconcentration before a tertiary treatment is the concentration factor (CF) required, which strongly depends on water matrix salinity and capacity operating pressure.

The higher MC degradation rates in C1 with Fe(III):EDDS at natural pH than at pH 3 could not be justified by a lack of oxidizing radicals caused by low iron concentration, but rather due to the high concentration of sulfate in C1 which scavenged hydroxyl and other radicals.

When persulfate was used instead of hydrogen peroxide, the mediating radicals for oxidation of the MCs, •OH and SO<sub>4</sub><sup>•-</sup>, had different elimination efficiencies. Whereas persulfate was inefficient for the selected MCs, overproduction of radicals lowered the elimination efficiency, perhaps by inducing scavenging and the formation of other (less active) radical species (e.g., chloride radicals) and recombination.

Solar photo-Fenton was demonstrated to be able to degrade, not only MCs present in the concentrate stream of a NF system, but also rapidly eliminate any residual MCs that could be present in the permeate streams after long NF operation. Fe(III):EDDS at circumneutral pH applied to salinized natural water was able to remove MCs from NF streams as quickly as classical photo-Fenton at acid pH, or even faster. This effect reinforces the proposal for using Fe(III):EDDS at natural pH for treating NF concentrates and also for polishing NF permeates when NF membranes are operated under extreme conditions, leaving MCs in the permeate due to increasing salinity in UWWTP effluents.

## CRedit authorship contribution statement

**Dennis Deemter:** Investigation, Writing - original draft. **Isabel Oller:** Conceptualization, Formal analysis, Methodology, Validation, Writing - review & editing, Supervision, Funding acquisition, Project administration. **Ana M. Amat:** Conceptualization, Formal analysis, Methodology, Validation, Supervision, Writing - review & editing, Supervision, Funding acquisition, Project administration. **Sixto Malato:** Writing - review & editing.

## Declaration of competing interest

The authors declare that they have no known competing financial interests or personal relationships that could have appeared to influence the work reported in this paper.

## Acknowledgements

This paper is part of a project that received funding from the European Union's Horizon 2020 Research and Innovation Programme under Marie Skłodowska-Curie Grant Agreement No 765860. Dennis Deemter would like to thank the staff at the Plataforma Solar de Almería. The authors wish to thank the Spanish Ministry of Science, Innovation and Universities (MCIU), AEI and FEDER for funding under the CalypSol Project (Reference: RTI2018-097997-B-C32 and RTI2018-097997-B-C31).

## Appendix A. Supplementary data

Supplementary data to this article can be found online at <https://doi.org/10.1016/j.scitotenv.2020.143593>.

## References

- Abdel-Fatah, M.A., 2018. Nanofiltration systems and applications in wastewater treatment: review article. *Ain Shams Eng J* 9 (4), 3077–3092. <https://doi.org/10.1016/j.asej.2018.08.001>.
- Ahile, U.J., Wuana, R.A., Itodo, A.U., Sha'Ato, R., Dantas, R.F., 2020. A review on the use of chelating agents as an alternative to promote photo-Fenton at neutral pH: current trends, knowledge gap and future studies. *Sci. Total Environ.* 710, 134872. <https://doi.org/10.1016/j.scitotenv.2019.134872>.
- Bi, F., Zhao, H., Zhou, Z., Zhang, L., Chen, H., Gao, C., 2016. Optimal design of nanofiltration system for surface water treatment. *Chin. J. Chem. Eng.* 24 (12), 1674–1679. <https://doi.org/10.1016/j.cjche.2016.05.012>.
- Brandt, A., Gorenflo, A., Siede, R., Meixner, M., Büchler, R., 2016. The neonicotinoids thiacloprid, imidacloprid, and clothianidin affect the immunocompetence of honey bees (*Apis mellifera* L.). *J. Insect Physiol.* 86, 40–47. <https://doi.org/10.1016/j.jinsphys.2016.01.001>.
- Capocelli, M., Prisciandaro, M., Piemonte, V., Barba, D., 2019. A technical-economical approach to promote the water treatment & reuse processes. *J. Clean. Prod.* 207, 85–96. <https://doi.org/10.1016/j.jclepro.2018.09.135>.
- Clarizia, L., Russo, D., Di Somma, I., Marotta, R., Andreozzi, R., 2017. Homogeneous photo-Fenton processes at near neutral pH: a review. *Appl. Catal. B Environ.* 209, 3581. <https://doi.org/10.1016/j.apcatb.2017.03.011>.
- Costa, E.P., Roccamante, M., Amorim, C.C., Oller, I., Sánchez Pérez, J.A., Malato, S., 2020. New trend on open solar photoreactors to treat micropollutants by photo-Fenton at circumneutral pH: increasing optical pathway. *Chem. Eng. J.* 385, 123982. <https://doi.org/10.1016/j.cej.2019.123982>.
- De Laat, J., Truong Le, G., Legube, B., 2004. A comparative study of the effects of chloride, sulfate and nitrate ions on the rates of decomposition of H<sub>2</sub>O<sub>2</sub> and organic compounds by Fe(II)/H<sub>2</sub>O<sub>2</sub> and Fe(III)/H<sub>2</sub>O<sub>2</sub>. *Chemosphere* 55 (5), 715–723. <https://doi.org/10.1016/j.chemosphere.2003.11.021>.
- Dong, W., Sun, S.P., Yang, X., et al., 2019. Enhanced emerging pharmaceuticals removal in wastewater after biotreatment by a low-pressure UVA/FelII-EDDS/H<sub>2</sub>O<sub>2</sub> process under neutral pH conditions. *Chem. Eng. J.* 366, 539–549. <https://doi.org/10.1016/j.cej.2019.02.109>.
- Eggen, R.L.L., Hollender, J., Joss, A., Schärer, M., Stamm, C., 2014. Reducing the discharge of micropollutants in the aquatic environment: the benefits of upgrading wastewater treatment plants. *Environ. Sci. Technol.* 48, 7683–7689. <https://doi.org/10.1021/es500907n>.
- Gallego-Schmid, A., Tarpani, R.R.Z., Miralles-Cuevas, S., Cabrera-Reina, A., Malato, S., Azapagic, A., 2019. Environmental assessment of solar photo-Fenton processes in combination with nanofiltration for the removal of micro-contaminants from real wastewaters. *Sci. Total Environ.* 650, 2210–2220. <https://doi.org/10.1016/j.scitotenv.2018.09.361>.
- Gonçalves, B.R., Guimarães, R.O., Batista, L.L., Ueira-Vieira, C., Starling, M.C.V.M., Trovó, A.G., 2020. Reducing toxicity and antimicrobial activity of a pesticide mixture via photo-Fenton in different aqueous matrices using iron complexes. *Sci. Total Environ.* 740, 140152. <https://doi.org/10.1016/j.scitotenv.2020.140152>.
- Hong, M., Wang, Y., Lu, G., 2020. UV-Fenton degradation of diclofenac, sulpiride, sulfamethoxazole and sulfisomidine: degradation mechanisms, transformation products, toxicity evolution and effect of real water matrix. *Chemosphere* 258, 127351. <https://doi.org/10.1016/j.chemosphere.2020.127351>.
- Ike, I.A., Linden, K.G., Orbell, J.D., Duke, M., 2018. Critical review of the science and sustainability of persulfate advanced oxidation processes. *Chem. Eng. J.* 338, 651–669. <https://doi.org/10.1016/j.cej.2018.01.034>.
- Jaber, S., Lerembouire, M., Thery, V., Delort, A.M., Mailhot, G., 2020. Mechanism of photochemical degradation of Fe(III)-EDDS complex. *J. Photochem. Photobiol. A: Chem.* <https://doi.org/10.1016/j.jphotochem.2020.112646>.
- Janssens, R., Cristovao, M.B., Bronze, M.R., Crespo, J.G., Pereira, V.J., Luis, P., 2019. Coupling of nanofiltration and UV/TiO<sub>2</sub> and UV/H<sub>2</sub>O<sub>2</sub> processes for the removal of anticancer drugs from real secondary wastewater effluent. *J. Environ. Chem. Eng.* 7 (5), 103351. <https://doi.org/10.1016/j.jece.2019.103351>.
- Kanakaraju, D., Glass, B.D., Oelgemöller, M., 2018. Advanced oxidation process-mediated removal of pharmaceuticals from water: a review. *J. Environ. Manag.* 219, 189–207. <https://doi.org/10.1016/j.jenvman.2018.04.103>.
- Kessler, S.C., Tiedeken, E.J., Simcock, K.L., 2015. Bees prefer foods containing neonicotinoid pesticides. *Nature* 521 (7550), 74–76. <https://doi.org/10.1038/nature14414>.
- Kim, S., Chu, K.H., Al-Hamadani, Y.A.J., Park, C.M., Jang, M., Kim, D.-H., Yu, M., Heo, J., Yoon, Y., 2018. Removal of contaminants of emerging concern by membranes in water and wastewater: a review. *Chem. Eng. J.* 335, 896–914. <https://doi.org/10.1016/j.cej.2017.11.044>.
- Klamerth, N., Malato, S., Maldonado, M.I., Agüera, A., Fernández-Alba, A.R., 2010. Application of photo-Fenton as a tertiary treatment of emerging contaminants in municipal wastewater. *Environ. Sci. Technol.* 44, 1792–1798. <https://doi.org/10.1016/j.watres.2012.11.008>.
- Lado Ribeiro, A.R., Moreira, N.F.F., Li Puma, G., Silva, A.M.T., 2019. Impact of water matrix on the removal of micropollutants by advanced oxidation technologies. *Chem. Eng. J.* 363, 155–173. <https://doi.org/10.1016/j.cej.2019.01.080>.
- Li, K., Wang, J., Liu, J., Wei, Y., Chen, M., 2016. Advanced treatment of municipal wastewater by nanofiltration: operational optimization and membrane fouling analysis. *J. Environ. Sci.* 43, 106–117. <https://doi.org/10.1016/j.jes.2015.09.007>.
- Lian, L., Yao, B., Hou, S., Fang, J., Yan, S., Song, W., 2017. Kinetic study of hydroxyl and sulfate radical-mediated oxidation of pharmaceuticals in wastewater effluents. *Environ. Sci. Technol.* 51 (5), 2954–2962. <https://doi.org/10.1021/acs.est.6b05536>.
- Liang, C., Huang, C.F., Mohanty, N., Kurakalva, R.M., 2008. A rapid spectrophotometric determination of persulfate anion in ISCO. *Chemosphere* 73 (9), 1540–1543. <https://doi.org/10.1016/j.chemosphere.2008.08.043>.
- McCinnis, M., Sun, C., Dudley, S., Gan, J., 2019. Effect of low-dose, repeated exposure of contaminants of emerging concern on plant development and hormone homeostasis. *Environ. Pollut.* 252, 706–714. <https://doi.org/10.1016/j.envpol.2019.05.159>.
- Mendret, J., Azais, A., Favier, T., Brosillon, S., 2019. Urban wastewater reuse using a coupling between nanofiltration and ozonation: techno-economic assessment. *Chem. Eng. Res. Des.* 145, 19–28. <https://doi.org/10.1016/j.cherd.2019.02.034>.
- Meschke, K., Hansen, N., Hofmann, R., Haseneder, R., Repke, J.-U., 2020. Influence of process parameters on separation efficiency of strategic elements by polymeric nanofiltration membranes. *Sep. Purif. Technol.* 235, 116186. <https://doi.org/10.1016/j.seppur.2019.116186>.
- Michael, S.G., Michael-Kordatou, I., Beretsou, V.G., Jäger, T., Michael, C., Schwartz, T., Fatta-Kassinos, D., 2019. Solar photo-Fenton oxidation followed by adsorption on activated carbon for the minimisation of antibiotic resistance determinants and toxicity present in urban wastewater. *Appl. Catal. B Environ.* 244, 871–880. <https://doi.org/10.1016/j.apcatb.2018.12.030>.
- Miklos, D.B., Remy, C., Jekel, M., Linden, K.J., Drewes, J.E., Hübner, U., 2018. Evaluation of advanced oxidation processes for water and wastewater treatment – a critical review. *Water Res.* 139, 118–131. <https://doi.org/10.1016/j.watres.2018.03.042>.
- Miralles-Cuevas, S., Arqués, A., Maldonado, M.I., Sánchez-Pérez, J.A., Malato Rodríguez, S., 2013. Combined nanofiltration and photo-Fenton treatment of water containing micropollutants. *Chem. Eng. J.* <https://doi.org/10.1016/j.cej.2012.09.068>.
- Miralles-Cuevas, S., Oller, I., Pérez, J.A.S., Malato, S., 2014. Application of solar photo-Fenton at circumneutral pH to nanofiltration concentrates for removal of pharmaceuticals in MWTP effluents. *Environ. Sci. Pollut. Res.* <https://doi.org/10.1007/s11356-014-2871-2>.
- Miralles-Cuevas, S., Oller, I., Agüera, A., Sánchez Pérez, J.A., Malato, S., 2017. Strategies for reducing cost by using solar photo-Fenton treatment combined with nanofiltration to remove microcontaminants in real municipal effluents: toxicity and economic assessment. *Chem. Eng. J.* 318, 161–170.
- Patel, M., Kumar, R., Kishor, K., Mlsna, T., Pittman, C.U., Mohan, D., 2019. Pharmaceuticals of emerging concern in aquatic systems: chemistry, occurrence, effects, and removal methods. *Chem. Rev.* 119, 3510–3673. <https://doi.org/10.1021/acs.chemrev.8b00299>.
- Petrović, M., Gonzalez, S., Barceló, D., 2003. Analysis and removal of emerging contaminants in wastewater and drinking water. *TrAC Trends Anal. Chem.* 22 (10), 685–696. [https://doi.org/10.1016/S0165-9936\(03\)01105-1](https://doi.org/10.1016/S0165-9936(03)01105-1).
- Pico, Y., Belenguer, V., Corcellas, C., 2019. Contaminants of emerging concern in freshwater fish from four Spanish Rivers. *Sci. Total Environ.* 659, 1186–1198. <https://doi.org/10.1016/j.scitotenv.2018.12.366>.
- Rasheed, T., Bilal, M., Nabeel, F., Adeel, M., Iqbal, H.M.N., 2019. Environmentally-related contaminants of high concern: potential sources and analytical modalities for detection, quantification, and treatment. *Environ. Int.* 122, 52–66. <https://doi.org/10.1016/j.envint.2018.11.038>.
- Ricart, S., Rico, A.M., 2019. Assessing technical and social driving factors of water reuse in agriculture: a review on risks, regulation and the yuck factor. *Agric. Water Manag.* 217, 426–439. <https://doi.org/10.1016/j.agwat.2019.03.017>.
- Rivas Ibáñez, G., Bittner, M., Toušová, Z., Campos-Mañas, M.C., Agüera, A., Casas López, J.L., Sánchez Pérez, J.A., Hilscheroová, K., 2017. Does micropollutant removal by solar photo-Fenton reduce ecotoxicity in municipal wastewater? A comprehensive study at pilot scale open reactors: municipal wastewater toxicity removal by solar photo-Fenton at neutral pH. *J. Chem. Technol. Biotechnol.* 92, 2114–2122. <https://doi.org/10.1002/jctb.5212>.
- Rizzo, L., Malato, S., Antakyali, D., et al., 2019. Consolidated vs new advanced treatment methods for the removal of contaminants of emerging concern from urban wastewater. *Sci. Total Environ.* 655, 986–1008. <https://doi.org/10.1016/j.scitotenv.2018.11.265>.
- Sánchez-Polo, M., Abdel daiem, M.M., Ocampo-Pérez, R., Rivera-Utrilla, J., Mota, A.J., 2013. Comparative study of the photodegradation of bisphenol A by HO, SO<sub>4</sub> and CO<sub>3</sub>/HCO<sub>3</sub> radicals in aqueous phase. *Sci. Total Environ.* 463–464, 423–431. <https://doi.org/10.1016/j.scitotenv.2013.06.012>.
- Shi, X., Tal, G., Hankins, N.P., Gitis, V., 2014. Fouling and cleaning of ultrafiltration membranes: a review. *J. Water Process Eng.* <https://doi.org/10.1016/j.jwpe.2014.04.003>.
- Silva, P., Livingston, A.G., 2006. Effect of solute concentration and mass transfer limitations on transport in organic solvent nanofiltration – partially rejected solute. *Membrane Science* 280, 889–898. <https://doi.org/10.1016/j.memsci.2006.03.008>.
- Song, Y., Qin, W., Li, T., Hu, Q., Gao, C., 2018. The role of nanofiltration membrane surface charge on the scale-prone ions concentration polarization for low or medium saline water softening. *Desalination* 432, 81–88. <https://doi.org/10.1016/j.desal.2018.01.013>.
- Soriano-Molina, P., García Sánchez, J.L., Alfano, O.M., Conte, L.O., Malato, S., Sánchez Pérez, J.A., 2018. Mechanistic modeling of solar photo-Fenton process with Fe<sup>3+</sup>-EDDS at neutral pH. *Appl. Catal. B Environ.* 233, 234–242. <https://doi.org/10.1016/j.apcatb.2018.04.005>.
- Soriano-Molina, P., Plaza-Bolaños, P., Lorenzo, A., Agüera, A., García Sánchez, J.L., Malato, S., Sánchez Pérez, J.A., 2019. Assessment of solar raceway pond reactors for removal of contaminants of emerging concern by photo-Fenton at circumneutral pH from very different municipal wastewater effluents. *Chem. Eng. J.* 366, 141–149. <https://doi.org/10.1016/j.cej.2019.02.074>.
- Tandy, S., Ammann, A., Schulin, R., Nowack, B., 2006. Biodegradation and speciation of residual SS-ethylenediaminedisuccinic acid (EDDS) in soil solution left after soil washing. *Environ. Pollut.* 142 (2), 191–199. <https://doi.org/10.1016/j.envpol.2005.10.013>.
- UN DESA, 2019. *World Population Prospects 2019*.
- Voigt, I., Richter, H., Stahn, M., et al., 2019. Scale-up of ceramic nanofiltration membranes to meet large scale applications. *Sep. Purif. Technol.* 215, 329–334. <https://doi.org/10.1016/j.seppur.2019.01.023>.

- Wang, J., Wang, S., 2018b. Activation of persulfate (PS) and peroxymonosulfate (PMS) and application for the degradation of emerging contaminants. *Chem. Eng. J.* 334, 1502–1517. <https://doi.org/10.1016/j.cej.2017.11.059>.
- Wang, S., Wang, J., 2018a. Trimethoprim degradation by Fenton and Fe(II)-activated persulfate processes. *Chemosphere* 191, 97–105. <https://doi.org/10.1016/j.chemosphere.2017.10.040>.
- Wang, X., Dong, W., Brigante, M., Mailhot, G., 2019. Hydroxyl and sulfate radicals activated by Fe(III)-EDDS/UV: comparison of their degradation efficiencies and influence of critical parameters. *Appl. Catal. B Environ.* 245, 271–278. <https://doi.org/10.1016/j.apcatb.2018.12.052>.
- Wu, Y., Bianco, A., Brigante, M., et al., 2015. Sulfate radical photogeneration using Fe-EDDS: influence of critical parameters and naturally occurring scavengers. *Environ. Sci. Technol.* 49 (24), 14343–14349. <https://doi.org/10.1021/acs.est.5b03316>.
- Zapata, A., Oller, I., Bizani, E., Sánchez-Pérez, J.A., Maldonado, M.I., Malato, S., 2009. Evaluation of operational parameters involved in solar photo-Fenton degradation of a commercial pesticide mixture. *Catal. Today* 144, 94–99. <https://doi.org/10.1016/j.cattod.2008.12.030>.
- Zhang, M., Guan, K., Ji, Y., Liu, G., Jin, W., Xu, N., 2019. Controllable ion transport by surface-charged graphene oxide membrane. *Nat. Commun.* 10, 1253. <https://doi.org/10.1038/s41467-019-09286-8>.
- Zhang, Y., Zhou, M., 2019. A critical review of the application of chelating agents to enable Fenton and Fenton-like reactions at high pH values. *J. Hazard. Mater.* 362, 436–450. <https://doi.org/10.1016/j.jhazmat>.
- Zhang, Y., Wang, L., Sun, W., Hu, Y., Tang, H., 2020. Membrane technologies for Li<sup>+</sup>/Mg<sup>2+</sup> separation from salt-lake brines and seawater: a comprehensive review. *J. Ind. Eng. Chem.* 81, 7–23. <https://doi.org/10.1016/j.jiec.2019.09.002018.09.035>.



## Valorization of UWWTP effluents for ammonium recovery and MC elimination by advanced AOPs

Dennis Deemter<sup>a</sup>, Irene Salmerón<sup>a</sup>, Isabel Oller<sup>a</sup>, Ana M. Amat<sup>b</sup>, Sixto Malato<sup>a,\*</sup>

<sup>a</sup> Plataforma Solar de Almería-CIEMAT, Carretera de Senés Km 4, Tabernas, Almería, Spain

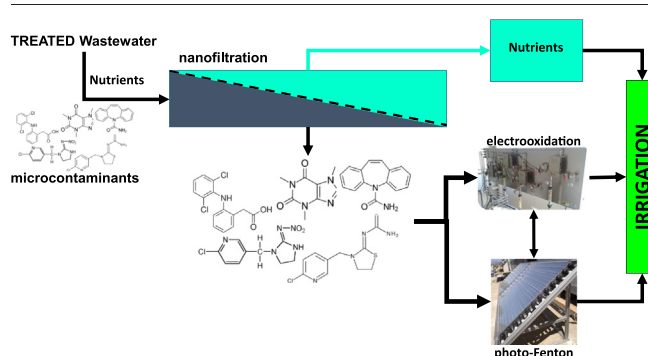
<sup>b</sup> Grupo Procesos de Oxidación Avanzada, Campus de Alcoy, Universitat Politècnica de València, Spain



### HIGHLIGHTS

- Ammonium was successfully recovered from wastewaters with nanofiltration.
- Solar assisted anodic oxidation was the most effective treatment.
- Permeates from concentration factor > 2 were non-suitable for direct irrigation.

### GRAPHICAL ABSTRACT



### ARTICLE INFO

#### Article history:

Received 5 November 2021

Received in revised form 10 January 2022

Accepted 1 February 2022

Available online 6 February 2022

Editor: Dimitra A Lambropoulou

#### Keywords:

Contaminants of emerging concern

Nanofiltration retentate

Solar advanced oxidation processes

Tertiary treatment

Urban wastewater reuse

### ABSTRACT

The main objective of this study was to generate ready-to-use revalorized irrigation water for fertilization from urban wastewater treatment plant (UWWTP) effluents. The focus was on controlled retention of  $\text{NH}_4^+$  and microcontaminants (MC), using nanofiltration. Retentates generated were treated by solar photo-Fenton at circumneutral pH using Ethylenediamine-N, N'-disuccinic acid (EDDS) iron complexing agent. Solar photo-Fenton degradation efficacy was compared with electrooxidation processes as anodic oxidation, solar-assisted anodic oxidation, electro-Fenton and solar photoelectro Fenton. Finally, phytotoxicity and acute toxicity tests were performed to demonstrate the potentially safe reuse of treated wastewater for crop irrigation. Nanofiltration was able to produce a ready-to-use permeate stream containing recovered  $\text{NH}_4^+$  (valuable nutrient). Solar photo-Fenton treatment at circumneutral pH would only be of interest for rapid degradation of contaminants at less than 1 mg/L in nanofiltration retentates. Other alternative tertiary treatments, such as electrooxidation processes, are a promising alternative when a high concentration of MC requires longer process times. Anodic oxidation was demonstrated to be able to eliminate >80% of microcontaminants and solar-assisted anodic oxidation significantly reduced the electricity consumption. Electro-Fenton processes were the least efficient of the processes tested. Phytotoxicity results showed that irrigation with the permeates reduced germination, root development was mainly promoted and shoot development was positive only at low retention rate (concentration factor = 2). Acute and chronic *Daphnia magna* toxicity studies demonstrated that the permeate volumes should be diluted at least 50% before direct reuse for crop irrigation.

### 1. Introduction

The production of synthesized fertilizers is a large global consumer of energy. Life is already endangered by the need for new farmlands due to soil erosion and saturation, by the inappropriate and excessive use of fertilizers and salination by unsuitable irrigation sources (Fernández-Delgado

\* Corresponding author.

E-mail address: [sixto.malato@psa.es](mailto:sixto.malato@psa.es) (S. Malato).



et al., 2020). It is therefore of paramount importance to find alternative ways to produce these fertilizers. Novel processes are already being explored to minimize energy demand on fertilizers production and overall environmental impact. A good example are solar fertilizers (to replace the centralized, fossil-fuel based Haber-Bosch process with a distributed network of modules that would use solar power to pull nitrogen from the atmosphere and also to catalyze the splitting of water molecules to get hydrogen), which aim at alternative, decentralized production of fertilizers with renewable solar energy (Comer et al., 2019; Hargreaves et al., 2020). Another promising way of recovering nutrients for fertilizers comes directly from urine, as it contains the primary macro nutrients: nitrogen, phosphorus and potassium. However, urine collection and effective nutrient recovery are challenging, as single systems are not yet sufficient, and combination and integration of existing systems are still in its early states (Gerardo et al., 2015; Patel et al., 2020; Wei et al., 2018).

The recovery of ammonium from agricultural, industrial, and urban wastewater (UWW) has also a strong potential for reducing the energy necessary to produce synthesized fertilizers, as the streams coming from these sources are generally easy to isolate, highly concentrated or already connected to existing infrastructures (Sakar et al., 2019). In agriculture, this could contribute to treatment of neighboring or nearby surface water bodies using recovery technologies to prevent excessive algae growth or sudden death of microorganisms, and prevent early soil saturation by fertilizers, salts, heavy metals and other contaminants. Thus, reducing pollution and delivering a renewable, sustainable source of revalorized irrigation water would make a synergetic contribution to synthesized fertilizer production, by lowering both the overall economic and environmental footprint (Zeng et al., 2020).

Although the high potential for ammonium recovery from UWW is widely known, such wastewater also contains traces and even high concentrations of pollutants, and therefore, it must be sanitized before its reclamation. Microcontaminants (MCs) in wastewater, known as Contaminants of Emerging Concern (CECs), are in the range of ng/L to µg/L (van Gils et al., 2020). They come from the consumption and disposal of everyday products, such as cosmetics, pesticides, pharmaceuticals and other organic compounds, which are either incorrectly disposed of, or simply cannot be treated by conventional wastewater treatment methods (Farré, 2020; Seibert et al., 2020; Taylor et al., 2020). The resulting bioaccumulation, endocrine disruption, chronic toxicity, irreversible soil pollution and saturation are of “emerging concern”, and demand rapid attention by the combination and/or reinforcement of conventional treatment methods with new technologies (Balogun et al., 2019; Yusuf et al., 2020).

The use of nanofiltration (NF) membranes can be considered an interesting option for tackling the problem of low removal rate of MCs in conventional wastewater treatments. Other membranes of higher pore size (as microfiltration) do not retain MCs. NF is relatively simple and inexpensive, and it could lower treatment costs by (pre)concentrating MCs and reducing the total volume of contaminated streams to be treated, with the subsequent reduction of reagents requirement and plant size (Miralles-Cuevas et al., 2017). Furthermore, NF does not retain ammonium and other needed inorganics, the operation and maintenance costs are lower than reverse osmosis, while organic MC rejection rates remain high (Mendret et al., 2019). The two main types, according to the membrane material, of NF membranes are the cheaper polymeric and the more expensive ceramic membranes. NF membrane selectivity depends on a variety of parameters, which determine the main physicochemical separation mechanisms of size exclusion, solution-diffusion and Donnan effect, such as the molecular and surface charge, concentration, pH, pore size and morphology. Furthermore, system parameters, such as flow rate, pressure and temperature affect process control and optimization (Schäfer and Fane, 2021; Wang and Lin, 2021; Wang et al., 2021). Understanding these mechanisms and parameters for revalorization of wastewater streams is a clear objective of the scientific community (Castro-Muñoz and Fila, 2018; Nath et al., 2018; Suwaileh et al., 2020). In addition, the promising solutions offered by membrane technologies for recovering nutrients, such as ammonium, have recently been gaining attention, especially in remote and emerging

areas, where infrastructures are commonly absent or deficient and fossil fuels are required to transport the nutrients. Recovered nutrients can also dramatically boost agricultural yields, contributing to health and economic development (Chen et al., 2020).

Although NF rejection rates are high and can produce the desired high-quality permeate streams for direct applications, rejection of MCs strongly depends on the abovementioned parameters and varies for every specific compound (Xu et al., 2020). This dependency requires its combination with advanced treatment technologies to prevent MCs being left in the membrane concentrate, which requires further treatment. The most recently studied advanced treatments that offer this versatility are advanced oxidation processes (AOPs).

AOPs generate highly reactive nonselective hydroxyl radicals (HO<sup>•</sup>), which can be deployed for the elimination of MCs. One of these, photo-Fenton, is based on iron catalysis (Fe<sup>2+</sup>/Fe<sup>3+</sup>) under UV-vis light and hydrogen peroxide (H<sub>2</sub>O<sub>2</sub>). The process uses simple chemicals and can be powered by renewable solar radiation using solar compound parabolic collectors (CPC) (Horikoshi and Serpone, 2020; Malato et al., 2009).

Although classic photo-Fenton must be applied at acidic pH to avoid iron precipitation, iron complexing agents, now under study, can maintain iron in solution at circumneutral pH. Ethylenediamine-N, N'-disuccinic acid (EDDS), for example, has shown successful application at pH 6, and even up to pH 9 (Wang et al., 2019). EDDS is biodegradable, and therefore environmentally-friendly (López-Rayo et al., 2019; Temara et al., 2006).

Combinations of different oxidation methods are also currently being promoted to increase MC elimination efficiency. Electrochemical processes, for instance, combine nicely with the Fenton reaction, since they can simultaneously generate different oxidizing agents on the anode surface (mainly HO<sup>•</sup>, ClO<sup>-</sup> and SO<sub>4</sub><sup>-</sup>) depending on the ionic composition of the (UWW) effluent and the nature of the anode (Salmerón et al., 2021). H<sub>2</sub>O<sub>2</sub> generation could be generated requiring a specific set of cathode and air or O<sub>2</sub> bubbling. Then, when iron is added, the Fenton reaction takes place (Brillas et al., 2010; Ganiyu et al., 2020). This is called electro-Fenton (EF). As in photo-Fenton, the Fe<sup>2+</sup> consumed during the reaction can be regenerated by a UV light source such as sunlight, and the process is then known as solar photoelectro-Fenton (SPEF) (Moreira et al., 2017). The principles of this treatment make highly saline effluents very suitable for electrochemical systems because a high concentration of ions in the aqueous solution facilitates the flow of electrons from the anode to the cathode, by lowering ohmic resistance. Therefore, energy consumption required for the elimination of MCs may be lower than in other water matrices. The issue of efficient H<sub>2</sub>O<sub>2</sub> dosage, during the photo-Fenton process, can also be overcome this way due to the onsite generation of this reagent on the cell cathode, during EF by reducing O<sub>2</sub> (Martínez-Huitle and Brillas, 2009).

The main objective and novelty of this study was to generate ready-to-use revalorized irrigation water for fertilization from urban wastewater treatment plant (UWWTP) effluents, based on controlled retention of salts and MCs using NF membranes at several different pH, producing a permeate free of MC, with lower conductivity and rich in NH<sub>4</sub><sup>+</sup>. Retentates generated by NF at different concentration factors (CF) were treated by a set of novel AOPs focusing on the successful integration with NF towards an effective, cost efficient and an environmental friendly reclamation of urban wastewater.

The target was 80% MC elimination, following the Swiss regulation on MCs in UWWTP effluents (elimination of MC to 80% in all Swiss UWWTP), which is the first legislation focusing on MCs elimination (Federal Office for the Environment FOEN Water Division, 2019). First approach experiments were performed under simulated UWWTP effluents. MC commonly found in these effluents were tested in synthetic aqueous solutions that simulate the UWWTP effluents at an initial concentration of 100 µg/L each. MCs elimination by solar photo-Fenton was compared with different electrooxidation (EO) processes as anodic oxidation (AO), solar-assisted anodic oxidation (SAAO), EF and SPEF at circumneutral and alkaline pH, as retentates from NF are good candidates for EO processes due to their high salt content. Phytotoxicity and acute toxicity tests were performed on the permeate, as first approach to assess the potentially safe reuse of treated wastewater for crop irrigation.

## 2. Materials and methods

### 2.1. Reagents and chemicals

The water matrix was natural water (Tabernas, Spain; see Table SI 1 for composition). Salts were purchased from Honeywell-Fluka (NaCl), Labbox Labware S.L. ((NH<sub>4</sub>)<sub>2</sub>SO<sub>4</sub>) and Sigma-Aldrich (Fe<sub>2</sub>(SO<sub>4</sub>)<sub>3</sub>·xH<sub>2</sub>O for Fe(III)), as were the HPLC-grade solvents for MC monitoring. Selected MCs were from Fluka (Caffeine(CAF)) and Sigma-Aldrich (Imidacloprid (IMI), Thiachloprid (THI), Carbamazepine (CAR) and Diclofenac (DIC)). The reagents (H<sub>2</sub>O<sub>2</sub> (35% w/v) and Sodium persulfate (Na<sub>2</sub>S<sub>2</sub>O<sub>8</sub>)) were also purchased from Sigma Aldrich. H<sub>2</sub>SO<sub>4</sub> (95–97%) and NaOH were purchased from J.T. Baker. Table SI 2 shows the molecular structure of the five selected MCs.

### 2.2. Analytical determinations

MC concentrations, dissolved organic carbon (DOC), carbonates, H<sub>2</sub>O<sub>2</sub>, persulfate and iron were determined according to the analytical methods specified in Table SI 3. Quantification limit (LOQ, 5 µg/L), and maximum absorption wavelength of selected MCs evaluated by ultra-performance liquid chromatography can be found in Table SI 4. A TOC (total organic carbon) analyzer was used to measure dissolved organic carbon and inorganic carbon. H<sub>2</sub>O<sub>2</sub> was determined using Titanium (IV) oxysulfate following DIN 38402H15. Iron determination was performed according to ISO 6332.

The ionic composition of the samples was analyzed by ionic chromatography with a Metrohm 850 Professional IC after dilution (1:20, 1:40 and 1:100, v/v), and filtration through a 0.45-µm nylon filter. A Metrosep A Supp 7150/40 column was used for anion determination, thermoregulated at 45 °C with 3.6 mM of sodium carbonate eluent at 0.7 mL/min. A Metrosep C6 150/4.0 column was used for cation determination with 1.7 mM dipicolinic acid eluent solution at 1.2 mL/min.

The concentration of free available chlorine (FAC) was determined by Hach Method 10,069 using N, N-diethyl-*p*-phenylenediamine (DPD) powder pillows and measuring the absorbance with a Thermo Scientific Evolution 220 UV-Visible spectrophotometer at 530 nm.

### 2.3. Experimental setup

#### 2.3.1. Nanofiltration membrane pilot plant

The NF pilot plant is comprised of a 400-L feed tank with a recirculation pump, which continuously mixes the concentrate stream with the tank volume. The MC concentration increased as the volume was reduced by permeate discharge. The NF membrane, a DOW FILMTEC™ NF90–2540, spiral-wound polyamide thin-film composite membrane, works by crossflow filtration. The NF membrane has a total surface area of 2.6 m<sup>2</sup> and is operable from pH 2 to 11. In this study, the maximum system pressure was set at 10 bar. For further details, see (Deemter et al., 2021).

#### 2.3.2. Experimental procedure

A stock solution of the MC mixture containing CAF, IMI, THI, CAR and DIC was prepared in methanol. The resulting concentration was 2.5 g/L of each compound, which ensured high solubility and low DOC when diluted in water to µg/L range. The desired matrix was prepared in the feed tank (400 L) to a final concentration of 5.0 g/L of NaCl, 500.0 mg/L NH<sub>4</sub><sup>+</sup> and 100.0 µg/L of each MC. The system was operated at 10 bar. The main intention, being a first approach study, was to use a simple and reliable analytical method (conventional liquid chromatography) targeting several MCs, since there can be hundreds of those found in actual UWWTP effluents. Therefore, we selected five MCs with easy separation and good detection by UPLC-DAD. Initial concentration was selected low enough but affordable by UPLC-DAD (LOQ, 5 µg / L).

First, the NF pilot plant was operated until 150 L of permeate were collected. This was then stored and designated as P1. The NF process continued until another 50 L of permeate had been accumulated, and this was

**Table 1**

Average MC concentrations [µg/L] and main physicochemical parameters of each effluent. P1, P2, P3, C1 and C2 were defined in the text.

	P1	P2	P3	C1 (CF = 2, V <sub>C</sub> = 200 L)	C2 (CF = 4, V <sub>C</sub> = 100 L)
CAF	5	15	35	150	280
IMI	10	25	55	135	210
THI	15	35	60	130	170
CAR	5	5	10	150	300
DIC	5	5	5	145	255
pH	10	10	10	9	9
NH <sub>4</sub> <sup>+</sup> [mg/L]	140	215	315	705	835
HCO <sub>3</sub> <sup>-</sup> /CO <sub>3</sub> <sup>2-</sup> [mg/L]	25	35	75	300	450
DOC [mg/L]	10	10	10	20	25
Conductivity [µS/cm]	1200	3000	7750	22,000	32,000

labelled as P2. The resulting concentrate volume (V<sub>C</sub>) of about 200 L at CF = 2 was labelled as C1. Another batch was generated by running 400 L in the feed tank but disregarding the first 200 L of permeate. The NF process continued with the remaining 200 L, then another 100 L of permeate was collected and stored, and labelled as P3. The resulting V<sub>C</sub> of about 100 L was labelled C2 (CF = 4). Each effluent generated was stored in a separate vessel and kept refrigerated till further use. Average MC concentrations and main physicochemical parameters of each sample are shown in Table 1. There was a significant increase in MC concentration in permeate as NF proceeded (comparing P1, P2 and P3).

#### 2.3.3. Solar photo-Fenton treatment

Solar photo-Fenton experiments were performed in a solar simulator (Atlas-SunTest XLS+) with a daylight filter, and a xenon lamp on the chamber ceiling, programmed for 365 W/m<sup>2</sup> (300–800 nm) total radiation and 30 W/m<sup>2</sup> UV radiation (300–400 nm) at a controlled temperature of 25 °C. A magnetically stirred 1-L cylindrical container (18.5 cm diameter and 4.0 cm deep) was placed in the center of the solar simulator platform. Further solar photo-Fenton experiments were scaled up to an 80-L CPC photoreactor tilted 37° (Tabernas, Spain). The 4-m<sup>2</sup> CPC irradiated surface is made up of 50-mm outer diameter borosilicate glass tubes. The global UV radiation was measured at one-minute intervals using a Kipp & Zonen CUV 5 pyranometer (280–400 nm), at a sensitivity of 301 µV/W·m<sup>2</sup> and tilted at the same angle as the CPC.

The accumulated UV solar energy needed for kinetic calculations is given by Eq. (1) (Malato et al., 2003).

$$Q_{UV,n} = Q_{UV,n-1} + (t_n - t_{n-1}) * \overline{UV}_{G,n} * A_i / V_t \quad (1)$$

where  $Q_{UV,n}$  [kJ/L] is the accumulated UV energy per unit of volume,  $Q_{UV,n-1}$  [W/m<sup>2</sup>] is the average solar ultraviolet radiation 280–400 [nm] measured over a period of time,  $t_n$  and  $t_{n-1}$ , and  $n$  is the number of samples,  $A_i$  is the irradiated reactor surface and  $V_t$  is the total volume treated.

For the photo-Fenton experiments at circumneutral pH, bicarbonates (known HO· radical scavengers) were removed by air stripping after addition of H<sub>2</sub>SO<sub>4</sub>, lowering HCO<sub>3</sub><sup>-</sup> to around 75 mg/L (final pH at 6.5–7.9). The Fe<sup>3+</sup>:EDDS ratio (Fe<sub>2</sub>(SO<sub>4</sub>)<sub>3</sub>·7H<sub>2</sub>O previously dissolved in demineralized water at pH 3, followed by EDDS addition) was 1:1 for all the experiments and initial H<sub>2</sub>O<sub>2</sub> concentration was 1.50 mM. Operational conditions were selected according to previous process optimisation (Deemter et al., 2021). A summary of the experiments can be found in Table SI 4.

#### 2.3.4. Solar photoelectro-Fenton treatment

The electrooxidation pilot plant consists of commercial Electro MP-Cell plate-and-frame cells (ElectroCell A/S, Denmark). Each cell contained an anode of BDD thin film deposited on a Nb mesh (Nb-BDD) and a carbon-polytetrafluoroethylene GDE as the cathode, both with 100 cm<sup>2</sup> effective area connected to a 100-L feed tank and a 2 m<sup>2</sup> solar CPC photoreactor (23 L total irradiated volume). A constant current density ( $j$ ) of 74

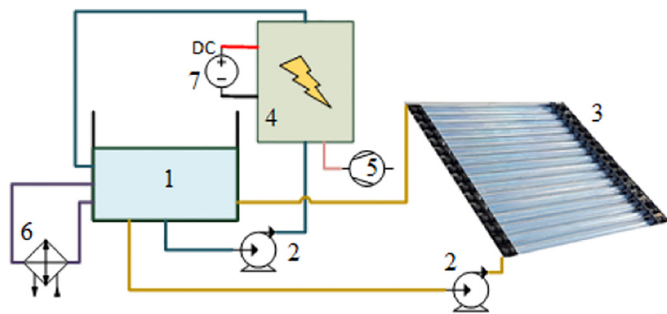


Fig. 1. Schematic view of the electrooxidation pilot plant and main components: 1. Tank, 2. Centrifugal pumps, 3. CPC photoreactor, 4. ElectroCell with BDD anode and carbon-PTFE (gas diffusion electrode) cathode, 5. Air compressor, 6. Heat exchanger and 7. Power supply.

$\text{mA}/\text{cm}^2$  was maintained as optimized by (Salmerón et al., 2019). The electrooxidation current density and other electrooxidation operational parameters were maintained as optimized by (Salmerón et al., 2021). The air pressure to the electrochemical cell was kept at 0.7 bar and air flow rate at 10 L/min. Treated water pressure was 0.5 bar and the flow rate 4 L/min. The air pressure and flow rate to the cell is essential to prevent water flow back into the air circuit. The experimental volume of the electrochemical system was 30 L and when combined with the CPC photoreactor, the total volume was 75 L. The setup includes an automatic cooling system which keeps the temperature at 25 °C to 30 °C (Fig. 1).

### 2.3.5. Toxicity tests

Toxicity tests were performed with commercial kits from MicroBioTests Inc. (Belgium). The PHYTOTOKIT for Liquid Samples was applied to determine phytotoxicity according to ISO Standard 18,763, which assesses the direct effects of chemicals on seed germination and early growth of plants. Moreover, their effects were also evaluated in *Daphnia magna* by recording immobilization (acute 24 and 48 h, and chronic toxicity 72 h) with the DAPHTOXKIT F kit, with a dilution row of 100, 50, 25 and 12.5%.

## 3. Results and discussion

### 3.1. Ammonium recovery by nanofiltration

Permeation of  $\text{NH}_4^+$  through commercial NF membranes was studied in a demineralized water matrix. Fig. 2 shows that  $\text{NH}_4^+$  permeation was minimum at pH 4 and pH 7. At pH 9, there was substantially more permeation from a starting feed tank concentration of 250 mg/L, and higher with 500 mg/L, increasing as CF increased to CF = 4 as pH affects the speciation

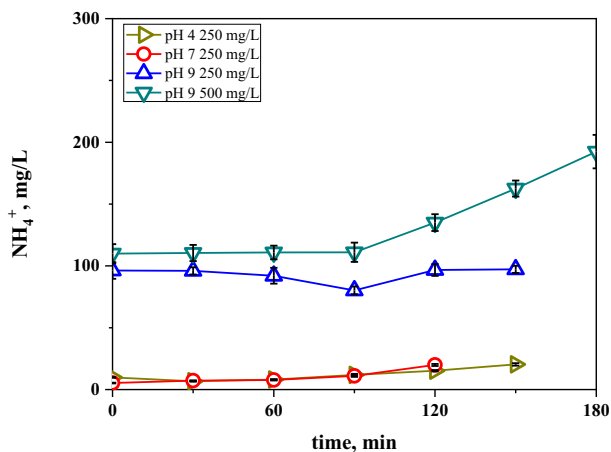


Fig. 2.  $\text{NH}_4^+$  concentrations in mg/L in the permeate stream at different pH and feed tank concentrations. Each experiment was performed until CF = 4.

of the ammonia (at high pH ammonia molecules dominate, whereas at acidic to neutral pH ammonium ions prevail). This means that the non-charge ammonia was rejected at lower pH in comparison to the charged ammonium ions. The increased permeation with time, and consequently CF, was due to the effect of concentration polarization.

The final concentration of  $\text{NH}_4^+$  in the permeate stream, that can be used as revalorized irrigation water, strongly depends on a variety of factors, such as crop, soil pH, soil consistency and type and availability and/or preference for another typical plant nitrogen source, such as  $\text{NO}_3^-$ . A possible negative side effect of  $\text{NH}_4^+$  is that when the plant absorbs the  $\text{NH}_4^+$ ,  $\text{H}^+$  is released, acidifying the soil. Sometimes,  $\text{NH}_4^+$  fertilization is even related to toxicity, making its status contradictory. NF permeates have a high pH (Table 1) and soil types in (semi-)arid areas are usually alkaline, the minor effects of soil acidification and related toxicity must be weighed against the advantages of this renewable and sustainable source of nitrogen in irrigation water for a wide variety of crops [(Britto and Kronzucker, 2002; Conklin, 2005; Hülsmann, 2018).]

To find out whether the selected MCs at a concentration of 100  $\mu\text{g}/\text{L}$  each influence  $\text{NH}_4^+$  permeation, experiments were performed at pH 9 and 500 mg/L  $\text{NH}_4^+$ .  $\text{NH}_4^+$  permeation obtained was similar to Fig. 2.  $\text{NH}_4^+$  permeation was also similar when the same experiments were done with water conductivity increased by adding 5 g/L NaCl. Therefore, neither the MCs in the wastewater nor water conductivity (see Table 1) influenced the permeation of  $\text{NH}_4^+$ . Furthermore,  $\text{NH}_4^+$  recovery was highest at CF = 4, though MC permeation was also higher at that CF. Therefore, if the permeate is to be used directly as revalorized irrigation water, then CF 2, where the concentration of recovered  $\text{NH}_4^+$  is high and MC permeation is low, is to be preferred.

### 3.2. Solar photo-Fenton treatment of NF concentrate stream at lab and pilot scale

Experimental parameters for MC elimination in NF concentrate by solar photo-Fenton were based on previous results with similar saline NF concentrates, ensuring minimal consumables concentration, and thereby, reducing environmental and economic impacts, while keeping elimination efficiency high (Deemter et al., 2021). Therefore, sample C2 (CF = 4) was treated by photo-Fenton in the solar lab-scale simulator using 0.10 mM Fe(III):EDDS; [1:1] and 1.50 mM  $\text{H}_2\text{O}_2$  at pH 9.

High concentrations of bicarbonates from natural water (450 mg/L) were observed at pH 9, making reaction rates very slow (data not shown). Neither did the use of 1.50 mM persulfate as an oxidizing agent provide satisfactory results. Carbonates are well-known ( $\text{HO}^\bullet$ ) scavengers and obstruct solar photo-Fenton performance as reported elsewhere (Lado Ribeiro et al., 2019). Therefore, further experiments were performed at circumneutral pH (between 6.5 and 7.9) after addition of  $\text{H}_2\text{SO}_4$  and air stripping to lower  $\text{HCO}_3^-$  to <75 mg/L.

Fig. 3 shows the elimination of CAR and DIC to LOQ (5  $\mu\text{g}/\text{L}$ ) in 15 and 10 min, respectively. CAF, IMI and THI were more recalcitrant, reaching only 82, 54 and 55%, respectively in 15 min, with almost no degradation from 15 to 30 min, because of the low concentration of iron remaining in solution due to the decomposition of the Fe(III):EDDS complex (Gonçalves et al., 2020; Soriano-Molina et al., 2018). In fact, iron precipitation started immediately, decreasing sharply at 5 to 10 min, and was completely precipitated after 20 min.  $\text{H}_2\text{O}_2$  consumption at the end of the experiment was 0.95 mM with higher consumption during the first 5 min. Blank experiments (photolysis) of CAF, IMI, THI, CAR and DIC did not reveal any substantial degradation after 30 min of illumination.

Using persulfate as an oxidizing agent at circumneutral pH, MC elimination was lower. LOQ (5  $\mu\text{g}/\text{L}$ ) of CAR and DIC was achieved at <5 min and CAF at <15 min. IMI and THI were more persistent, and only 24% and 20%, respectively, were eliminated. Iron concentration decreased gradually from the beginning of the treatment until only 10% was remaining after 30 min. Persulfate consumption was 0.87 mM during the first 5 min of treatment. Sulfate radicals usually show slower reaction rates than  $\text{HO}^\bullet$ , which strongly depends on target MCs, starting iron, and EDDS concentration, as reported previously (Cabrera-Reina et al., 2020; Solís et al., 2020).

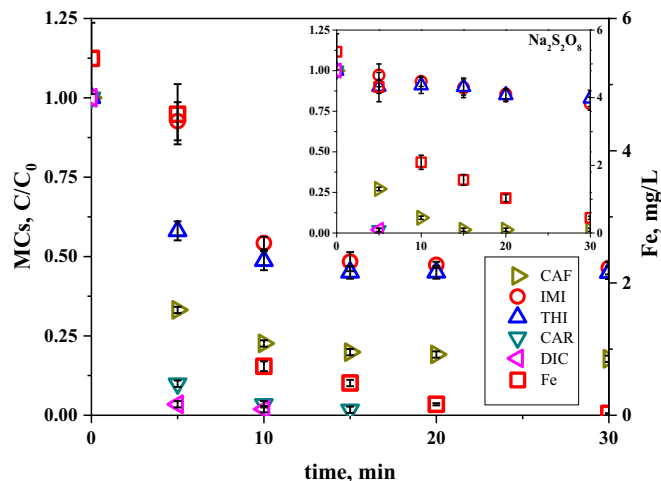


Fig. 3. MC concentrations and dissolved iron evolution (open red square symbol) during photo-Fenton treatment of C2 with Fe 0.10 mM, EDDS 0.10 mM and both H<sub>2</sub>O<sub>2</sub> and persulfate (inserted figure) at 1.5 mM in the solar simulator at circumneutral pH.

Fig. 4 shows solar photo-Fenton treatment of C2 at pilot scale in an 80-L CPC photoreactor, as a function of solar accumulated UV energy (Eq. (1)) collected in the photoreactor after 30 min. Only DIC was eliminated to LOQ (5 µg/L) at <30 min, and 93% CAR was degraded, whereas CAF, IMI and THI, as in the solar simulator, were more recalcitrant, reaching only 70, 49 and 39% elimination at 30 min, respectively. Total MC elimination was 76% with accumulated UV energy of only 1.6 kJ/L. Over 90% of the Fe(III):EDDS complex was degraded in the first 30 min, confirming the inefficient elimination of MCs at circumneutral pH after complex degradation. H<sub>2</sub>O<sub>2</sub> consumption at the end of the experiment was 0.83 mM.

### 3.3. Electrooxidation treatments

Electrooxidation experiments were performed in the SPEF pilot plant with the experimental parameters described in Section 2.3.4. Since the aim of NF is to lower the economic impact by reducing the volume of contaminated streams, the first electrooxidation treatments were performed on C2 (CF = 4), the most concentrated stream, for better comparison with the following electrooxidation treatments. Higher ionic, carbonate and MC concentrations showed increased radical scavenger effects, as mentioned above.

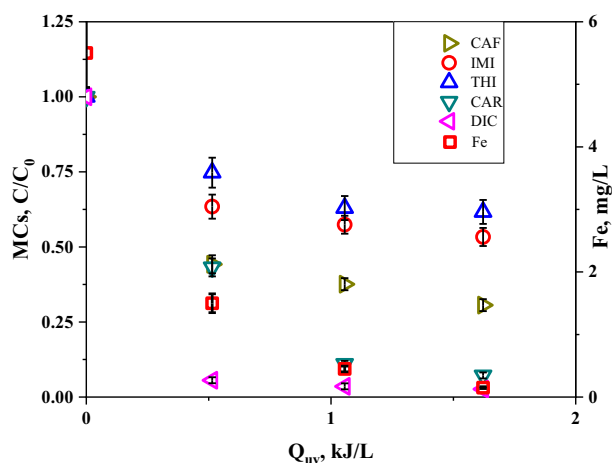


Fig. 4. MC concentrations and dissolved iron during solar photo-Fenton treatment of C2 at circumneutral pH in the pilot plant.

Fig. 5 shows the results with C1 with its natural carbonate concentration and applying AO, SAAO, EF and SPEF oxidation treatments. With AO, MC elimination to LOQ (5 µg/L) was only attained for CAF, THI, CAR and DIC at <150, <180, <45 and < 150 min, respectively. IMI was persistent with only 67% degradation, but the treatment still eliminated 88% of the total MCs. In SAAO, only CAR and DIC were degraded to the LOQ (5 µg/L) at 180 and 45 min, respectively, and CAF was degraded by 84%. The more persistent IMI and THI were degraded 44% and 57%, for a total MC removal of 78% at the end of the treatment. Finally, when SPEF was applied, CAR and DIC were eliminated to LOQ (5 µg/L) at <180 and < 45 min, respectively. CAF, IMI and THI were again more persistent, and were degraded only 82%, 44% and 78%, respectively. Total MC elimination was 80%.

The 80% MC removal target in concentrate C1 was not achieved by EF after 240 min of treatment. Moreover, more consumables were needed than in AO, such as EDDS, which drastically increases DOC and competes with the MCs for the radicals. Furthermore, it consumed over 50% more electricity and produced more free available chlorine (FAC) than AO. Chlorate production was reduced by 15%. Therefore, it was discarded as a suitable treatment for this kind of water as previously reported by (Salmerón et al., 2021).

The target of 80% total MC degradation was reached after 120 min with the AO treatment. Total electricity consumption was 6.1 kWh/m<sup>3</sup> for an experimental volume of 30 L. The final concentration of FAC produced was 3.4 mg/L and chlorate production started to be recorded at 10 min with 20.4 mg/L, increasing linearly to 70.0 mg/L after 240 min.

Both FAC and chlorate are by-products of the EO processes. The by-products are formed from the high concentrations of free dissolved ions in the matrix, in this case chloride. Active chlorine can be generated from free dissolved chloride ions and is widely used in wastewater treatment. Active chlorine species (ACS) are formed from the adsorbed free dissolved ions on the anode surface, resulting in the radical or other oxidizing species of the related ion. Indirect ACS are formed when the oxidizing species, previously generated, acts as an intermediate in the reaction with the MCs in the bulk of the matrix furthest from the anode (Panizza and Cerisola, 2009). ACS, which promotes MC degradation, in what is also called electrochlorination, has the advantage over conventional chlorine treatments of improved performance and absence of potentially dangerous Cl transport and storage (Martínez-Huitle and Brillas, 2009; Mostafa et al., 2018). Chlorates are formed by the reaction of ACS with •OH when a BDD anode is used (Sánchez-Carretero et al., 2011). The original C1 (CF = 2) ionic concentrations are summarized in Table SI 6.

With SAAO, the MC degradation did not quite reach the target of 80%, with only 78% after 240 min, and consumed a total of 3.8 kWh/m<sup>3</sup>

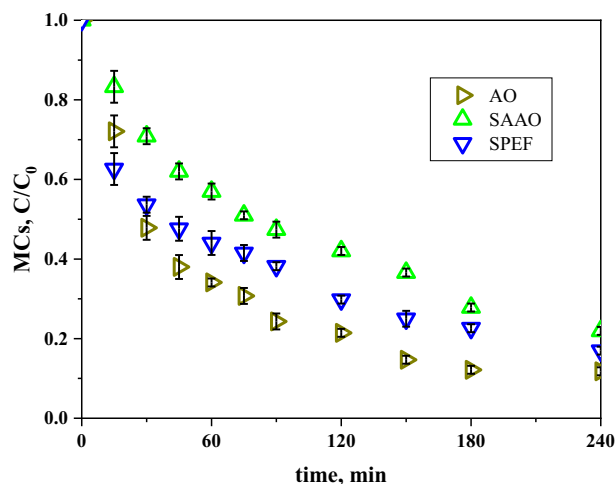


Fig. 5. MC concentrations during AO, SAAO and SPEF treatment at natural pH of C1 (CF = 2).

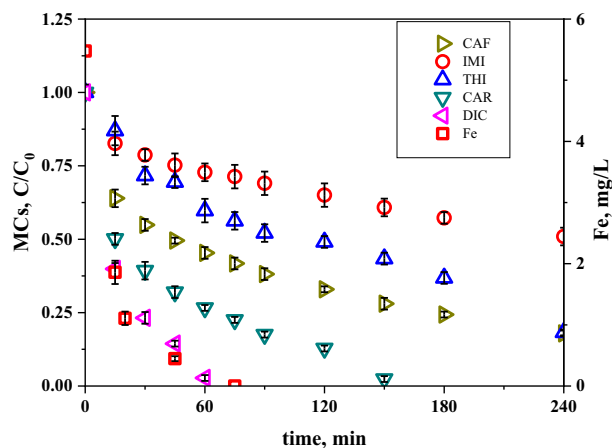


Fig. 6. MC concentrations during pilot-scale SPEF treatment of concentrate C1 (CF = 2) at natural pH and with low carbonate concentration.

electricity, 62% lower than AO alone, and also requiring  $Q_{UV}$  of 13.3 kJ/L for an experimental volume of 75 L. FAC concentration was 4.2 mg/L, along with 33.3 mg/L of chlorate, which is an increase of 23% and 52% respectively from AO.

Finally, 80% degradation was reached at <240 min with the SPEF treatment, which required total electricity consumption of 4.2 kWh/m<sup>3</sup> and  $Q_{UV}$  of 14.2 kJ/L for an experimental volume of 75 L; 11% and 7% higher than SAAO, respectively. MC degradation enhancement by addition of the Fe:EDDS was minimal due to the increase in DOC when EDDS is added. FAC concentration was only 2.1 mg/L at the end of the experiment. Chlorate production was low, with a final concentration of 16.4 mg/L, 50% lower than SAAO, due to the reaction between H<sub>2</sub>O<sub>2</sub> and ACS.

Initial reaction rate ( $r_0$ ) was calculated to compare the different EO processes using mass of MC instead of concentration due to the difference in experimental volume, as shown in Eq. (2).

$$r_0 = \frac{(m_{n+1} - m_n)}{(t_{n+1} - t_n)} \quad (2)$$

where  $m_n$  is the cumulative MC mass at designated time in mg, calculated for the MC concentration and the volume of water treated, 30 L for AO and 75 L for SAAO and SPEF, and  $t_n$  is the time interval in minutes yielding  $r_0$  in mg/min. For AO, SAAO and SPEF  $r_0 = -0.337$ ;  $-0.0696$  and  $-1.305$  mg/min, respectively.

Fig. 6 shows the SPEF treatment results for C1, but with a lower concentration of bicarbonates (76.3 mg/L). The purpose was to find out whether a high concentration of carbonates would be as detrimental as in the photo-Fenton process (Deemter et al., 2021). Only CAR and DIC were eliminated to LOQ (5 µg/L) at 150 and 60 min, respectively. CAF and THI were both

degraded 82%, while IMI was the most persistent with 49% degradation. Total MC elimination was still 82%, demonstrating that the influence of carbonates was negligible in the SPEF treatment, and that the oxidation of MCs occurred mainly through oxidants other than HO<sup>•</sup>. Therefore, analysis of the chlorinated byproducts would be critical for the overall assessment of the system and before the design of the most appropriate treatment.

At the low carbonate concentration, SPEF treatment reached the target degradation of 80% after <220 min with a total electricity consumption of 4.3 kWh/m<sup>3</sup> and a  $Q_{UV}$  of 11.6 kJ/L. FAC production was the highest of all treatments, and over double the experiment with the high carbonate concentration, ending with a concentration of 5.7 mg/L. The final chlorate concentration was 18.2 mg/L, again, similar to treatment with the high carbonate concentration. SPEF at the low carbonate concentration had a  $r_0 = -1.155$  mg/min, 11% lower than with the high carbonate concentration.

### 3.4. Toxicity tests

As one of the main objectives of this study was recovery and reuse of NH<sub>4</sub><sup>+</sup> from the NF permeate stream obtained by pre-concentration of a UWWTP effluent for crop irrigation, phytotoxicity tests were done at two different permeate concentrations at CF = 2 and 4, to evaluate its effects on seed germination, and root and shoot growth. Permeates were tested at pH 7. The CF = 2 and 4 permeates slightly affected *Sorghum saccharatum* reducing germination 10%. CF = 2 also caused 10% less germination in *Sinapis alba*.

In *Sorghum saccharatum*, the CF = 2 permeate promoted 45% more root development than the reference with demineralized water. *S. alba* root development was 17% better with CF = 2. Root development of *Lepidium sativum* was severely affected, showing a 27% and 46% reduction with CF = 2 and 4, respectively.

*Sorghum saccharatum* shoot length was reduced 40% with CF = 4. CF = 2, however, increased it 13%. Shoot growth of *Sinapis alba* was reduced 9% and 39% with CF = 2 and 4, respectively. Finally, *Lepidium sativum* shoot growth was promoted by CF = 2, increasing it by 11%, while CF = 4 decreased it by 17%.

This means that direct application of permeate at CF = 2 was adequate for crop irrigation, in view of both root and shoot growth results. It was not the case for CF = 4, attributed to the higher concentration of MCs contained in permeate, as well as the high salt content (Fig. 7).

The DAPHTOXKIT F test was also applied to determine acute toxicity at 24 and 48 h and chronic toxicity at 72 h. Immobilization of *Daphnia magna* was assessed and compared to a freshwater control. Results are shown in Fig. 8. After 24 h, there was no immobilization at the 12.5, 25 and 50% CF = 2 dilutions. At 100% of CF = 2, only one of the organisms showed some movement. Results were similar in CF = 4, except for the 100% sample, where all organisms were immobilized. After 48 h, samples containing 12.5, 25 and 50% dilutions in CF = 2 showed 0, 2 and 3 out of 5 immobilized organisms, respectively. At 100%, all organisms were



Fig. 7. Photos of phytotoxicity test, from left to right, *Sinapis alba*, *Sorghum saccharatum* and *Lepidium sativum*. All three species showed full germination.

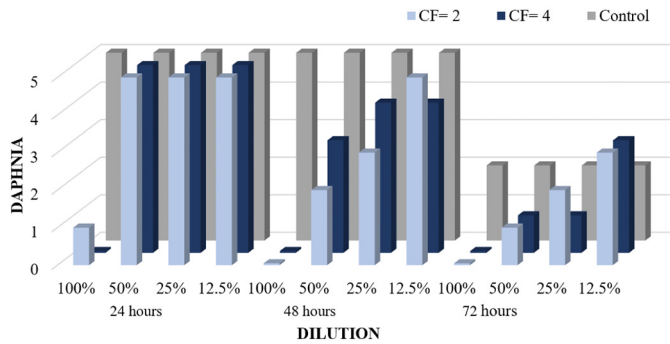


**Fig. 8.** Acute (24 and 48 h) and chronic (72 h) toxicity tests with *Daphnia magna* organisms at different dilutions in freshwater. CF = 2 (front) and CF = 4 (middle) permeates and freshwater control (back).

immobilized. In CF = 4, results were similar. Finally, after 72 h, 3 out of 5 organisms in the control sample were immobilized. CF = 2 showed 2, 3 and 4 immobilized organisms in 12.5, 25 and 50% dilutions, whereas in CF = 4 results were similar. Therefore, both permeate volumes should be diluted at least 50%, to prevent osmotic stress and acute toxicity. At a 25% dilution, only CF = 2 showed chronic toxicity results similar to freshwater.

#### 4. Conclusions

$\text{NH}_4^+$  can effectively be recovered from wastewater using NF at pH 9. NF treatment to a concentration factor of 2 was able to produce a ready-to-use permeate stream with recovered  $\text{NH}_4^+$ . However, despite NF would lead to the elimination of bacteria, in case of antibiotic resistance genes and antibiotic resistant bacteria it is not enough. Therefore, such effect must be checked before crop irrigation.

Persulfate was a less efficient oxidizing agent than  $\text{H}_2\text{O}_2$  by solar photo-Fenton. As dissolved iron quickly disappeared at circumneutral pH, it would only be of interest for rapid degradation of contaminants at less than 1 mg/L in NF retentate. Other alternative tertiary treatments, such as electrooxidation processes, are a promising alternative when a high concentration of MC requires longer treatment times. Analysis of the chlorinated byproducts would be critical for the overall assessment and before the design of the most appropriate treatment.

Solar-assisted anodic oxidation significantly reduced the electricity consumption necessary for degradation and residual FAC and chlorate concentrations were lower than with anodic oxidation. Solar photoelectron-Fenton showed results similar to solar assisted anodic oxidation, but required more consumables. Electro-Fenton was the least efficient of the electro oxidation processes tested.

Phytotoxicity results showed that irrigation with the permeates slightly affected germination. Acute and chronic *Daphnia magna* toxicity studies demonstrated that the permeate volumes should be diluted at least 50% before direct reuse for crop irrigation.

#### CRedit authorship contribution statement

**Dennis Deemter:** Conceptualization, Formal analysis, Methodology, Investigation, Writing – original draft. **Irene Salmerón:** Conceptualization, Formal analysis, Methodology, Investigation, Writing – original draft. **Isabel Oller:** Validation, Writing – review & editing, Supervision, Funding acquisition, Project administration. **Ana M. Amat:** Writing – review & editing. **Sixto Malato:** Supervision, Writing – review & editing, Funding acquisition, Project administration.

#### Declaration of competing interest

The authors declare that they have no known competing financial interests or personal relationships that could have appeared to influence the work reported in this paper.

#### Acknowledgement

This study is part of a project funded by the European Union's Horizon 2020 research and innovation program under Marie Skłodowska-Curie Grant Agreement No 765860. The authors also wish to thank the Spanish Ministry of Science, Innovation and Universities (MCIU), AEI and FEDER for funding under the NAVIA Project (ID2019-110441RB-C32).

#### Appendix A. Supplementary data

Supplementary data to this article can be found online at <https://doi.org/10.1016/j.scitotenv.2022.153693>.

#### References

- Balogun, H.A., Sulaiman, R., Marzouk, S.S., Giwa, A., Hasan, S.W., 2019. 3D printing and surface imprinting technologies for water treatment: a review. *J. Water Process Eng.* 31, 100786. <https://doi.org/10.1016/j.jwpe.2019.100786>.
- Brillas, E., Sirés, I., Cabot, P.L., 2010. Use of both anode and cathode reactions in wastewater treatment. In: Comninellis, C., Chen, G. (Eds.), *Electrochem. Environ.* Springer New York, New York, NY, pp. 515–552. [https://doi.org/10.1007/978-0-387-68318-8\\_19](https://doi.org/10.1007/978-0-387-68318-8_19).
- Britto, D.T., Kronzucker, H.J., 2002.  $\text{NH}_4^+$  toxicity in higher plants: a critical review. *J. Plant Physiol.* 159, 567–584. <https://doi.org/10.1078/0176-1617-0774>.
- Cabrera-Reina, A., Miralles-Cuevas, S., Oller, I., Sánchez-Pérez, J.A., Malato, S., 2020. Modeling persulfate activation by iron and heat for the removal of contaminants of emerging concern using carbamazepine as model pollutant. *Chem. Eng. J.* 389, 124445. <https://doi.org/10.1016/j.cej.2020.124445>.
- Castro-Muñoz, R., Fila, V., 2018. Membrane-based technologies as an emerging tool for separating high-added-value compounds from natural products. *Trends Food Sci. Technol.* 82, 8–20. <https://doi.org/10.1016/j.tifs.2018.09.017>.
- Chen, C., Dong, T., Han, M., Yao, J., Han, L., 2020. Ammonium recovery from wastewater by Donnan Dialysis: a feasibility study. *J. Clean. Prod.* 265, 121838. <https://doi.org/10.1016/j.jclepro.2020.121838>.
- Comer, B.M., Fuentes, P., Dimkpa, C.O., Liu, Y.H., Fernandez, C.A., Arora, P., Realf, M., Singh, U., Hatzell, M.C., Medford, A.J., 2019. Prospects and challenges for solar fertilizers. *Joule.* 3, 1578–1605. <https://doi.org/10.1016/j.joule.2019.05.001>.
- Conklin A.R., *Introduction to Soil Chemistry: Analysis and Instrumentation*, 2005. doi: <https://doi.org/10.1002/0471728225>.
- Deemter, D., Oller, I., Amat, A.M., Malato, S., 2021. Effect of salinity on preconcentration of contaminants of emerging concern by nanofiltration: application of solar photo-Fenton as a tertiary treatment. *Sci. Total Environ.* 756 143593 <https://doi.org/10.1016/j.scitotenv.2020.143593>.
- Farré, M., 2020. Remote and in-situ devices for the assessment of marine contaminants of emerging concern and plastic debris detection. *Curr. Opin. Environ. Sci. Heal.* <https://doi.org/10.1016/j.coesh.2020.10.002>.
- Federal Office for the Environment FOEN Water Division, Reporting for Switzerland under the Protocol on Water and Health, 2019.
- Fernández-Delgado, M., del Amo-Mateos, E., Lucas, S., García-Cubero, M.T., Coca, M., 2020. Recovery of organic carbon from municipal mixed waste compost for the production of fertilizers. *J. Clean. Prod.* 265. <https://doi.org/10.1016/j.jclepro.2020.121805>.
- Ganiyu, S.O., Martínez-Huitle, C.A., Rodrigo, M.A., 2020. Renewable energies driven electrochemical wastewater/soil decontamination technologies: a critical review of fundamental concepts and applications. *Appl. Catal. B Environ.* 270 118857 <https://doi.org/10.1016/j.apcatb.2020.118857>.
- Gerardo, M.L., Aljohani, N.H.M., Oatley-Radcliffe, D.L., Lovitt, R.W., 2015. Moving towards sustainable resources: recovery and fractionation of nutrients from dairy manure digestate using membranes. *Water Res.* 80, 80–89. <https://doi.org/10.1016/j.watres.2015.05.016>.
- Gonçalves, B.R., Guimarães, R.O., Batista, L.L., Ueira-Vieira, C., Starling, M.C.V.M., Trovó, A.G., 2020. Reducing toxicity and antimicrobial activity of a pesticide mixture via photo-Fenton in different aqueous matrices using iron complexes. *Sci. Total Environ.* 740, 140152. <https://doi.org/10.1016/j.scitotenv.2020.140152>.
- Hargreaves, J.S.J., Chung, Y.M., Ahn, W.S., Hisatomi, T., Domen, K., Kung, M.C., Kung, H.H., 2020. Minimizing energy demand and environmental impact for sustainable  $\text{NH}_3$  and  $\text{H}_2\text{O}_2$  production—a perspective on contributions from thermal, electro-, and photocatalysis. *Appl. Catal. A Gen.* 594, 117419. <https://doi.org/10.1016/j.apcata.2020.117419>.
- Horikoshi, S., Serpone, N., 2020. Can the photocatalyst  $\text{TiO}_2$  be incorporated into a wastewater treatment method? Background and prospects. *Catal. Today* 340, 334–346. <https://doi.org/10.1016/j.cattod.2018.10.020>.
- Hülsmann S., Managing water, soil and waste resources to achieve sustainable development goals, 2018. doi: <https://doi.org/10.1007/978-3-319-75163-4>.
- Lado Ribeiro, A.R., Moreira, N.F.F., Li, Puma G., Silva, A.M.T., 2019. Impact of water matrix on the removal of micropollutants by advanced oxidation technologies. *Chem. Eng. J.* 363, 155–173. <https://doi.org/10.1016/j.cej.2019.01.080>.
- López-Rayó, S., Sanchis-Pérez, I., Ferreira, C.M.H., Lucena, J.J., 2019. [S,S]-EDDS/Fe: a new chelate for the environmentally sustainable correction of iron chlorosis in calcareous soil. *Sci. Total Environ.* 647, 1508–1517. <https://doi.org/10.1016/j.scitotenv.2018.08.021>.
- Malato, S., Blanco, J., Campos, A., Cáceres, J., Guillard, C., Herrmann, J.M., Fernández-Alba, A.R., 2003. Effect of operating parameters on the testing of new industrial titania

- catalysts at solar pilot plant scale. *Appl. Catal. B Environ.* 42, 349–357. [https://doi.org/10.1016/S0926-3373\(02\)00270-9](https://doi.org/10.1016/S0926-3373(02)00270-9).
- Malato, S., Fernández-Ibáñez, P., Maldonado, M.I., Blanco, J., Gernjak, W., 2009. Decontamination and disinfection of water by solar photocatalysis: recent overview and trends. *Catal. Today* 147, 1–59. <https://doi.org/10.1016/j.cattod.2009.06.018>.
- Martínez-Huitle, C.A., Brillas, E., 2009. Decontamination of wastewaters containing synthetic organic dyes by electrochemical methods: a general review. *Appl. Catal. B Environ.* 87, 105–145. <https://doi.org/10.1016/j.apcatb.2008.09.017>.
- Mendret, J., Azais, A., Favier, T., Brosillon, S., 2019. Urban wastewater reuse using a coupling between nanofiltration and ozonation: techno-economic assessment. *Chem. Eng. Res. Des.* 145, 19–28. <https://doi.org/10.1016/j.cherd.2019.02.034>.
- Miralles-Cuevas, S., Oller, I., Agüera, A., Sánchez Pérez, J.A., Malato, S., 2017. Strategies for reducing cost by using solar photo-Fenton treatment combined with nanofiltration to remove microcontaminants in real municipal effluents: toxicity and economic assessment. *Chem. Eng. J.* 318, 161–170. <https://doi.org/10.1016/j.cej.2016.06.031>.
- Moreira, F.C., Boaventura, R.A.R., Brillas, E., Vilar, V.J.P., 2017. Electrochemical advanced oxidation processes: a review on their application to synthetic and real wastewaters. *Appl. Catal. B Environ.* 202, 217–261. <https://doi.org/10.1016/j.apcatb.2016.08.037>.
- Mostafa, E., Reinsberg, P., Garcia-Segura, S., Baltruschat, H., 2018. Chlorine species evolution during electrochlorination on boron-doped diamond anodes: in-situ electrogeneration of Cl<sub>2</sub>, ClO<sub>2</sub> and ClO<sub>2</sub>. *Electrochim. Acta* 281, 831–840. <https://doi.org/10.1016/j.electacta.2018.05.099>.
- Nath, K., Dave, H.K., Patel, T.M., 2018. Revisiting the recent applications of nanofiltration in food processing industries: progress and prognosis. *Trends Food Sci. Technol.* 73, 12–24. <https://doi.org/10.1016/j.tifs.2018.01.001>.
- Panizza, M., Cerisola, G., 2009. Direct and mediated anodic oxidation of organic pollutants. *Chem. Rev.* 109, 6541–6569. <https://doi.org/10.1021/cr9001319>.
- Patel, A., Mungray, A.A., Mungray, A.K., 2020. Technologies for the recovery of nutrients, water and energy from human urine: a review. *Chemosphere*. 259, 127372. <https://doi.org/10.1016/j.chemosphere.2020.127372>.
- Sakar, H., Celik, I., Balcik-Canbolat, C., Keskinler, B., Karagunduz, A., 2019. Ammonium removal and recovery from real digestate wastewater by a modified operational method of membrane capacitive deionization unit. *J. Clean. Prod.* 215, 1415–1423. <https://doi.org/10.1016/j.jclepro.2019.01.165>.
- Salmerón, I., Plakas, K.V., Sirés, I., Oller, I., Maldonado, M.I., Karabelas, A.J., Malato, S., 2019. Optimization of electrocatalytic H<sub>2</sub>O<sub>2</sub> production at pilot plant scale for solar-assisted water treatment. *Appl. Catal. B Environ.* 242, 327–336. <https://doi.org/10.1016/j.apcatb.2018.09.045>.
- Salmerón, I., Rivas, G., Oller, I., Martínez-Piarnas, A., Agüera, A., Malato, S., 2021. Nanofiltration retentate treatment from urban wastewater secondary effluent by solar electrochemical oxidation processes. *Sep. Purif. Technol.* 254, 117614. <https://doi.org/10.1016/j.seppur.2020.117614>.
- Sánchez-Carretero, A., Sáez, C., Cañizares, P., Rodrigo, M.A., 2011. Electrochemical production of perchlorates using conductive diamond electrolyses. *Chem. Eng. J.* 166, 710–714. <https://doi.org/10.1016/j.cej.2010.11.037>.
- Schäfer, A.I., Fane, A.G., 2021. *Nanofiltration: Principles, Applications, and New Materials*. John Wiley & Sons.
- Seibert, D., Zorzo, C.F., Borba, F.H., de Souza, R.M., Quesada, H.B., Bergamasco, R., Baptista, A.T., Inticher, J.J., 2020. Occurrence, statutory guideline values and removal of contaminants of emerging concern by electrochemical advanced oxidation processes: a review. *Sci. Total Environ.* 748, 141527. <https://doi.org/10.1016/j.scitotenv.2020.141527>.
- Solís, R.R., Rivas, F.J., Chávez, A.M., Dionysiou, D.D., 2020. Peroxymonosulfate/solar radiation process for the removal of aqueous microcontaminants. Kinetic modeling, influence of variables and matrix constituents. *J. Hazard. Mater.* 400. <https://doi.org/10.1016/j.jhazmat.2020.123118>.
- Soriano-Molina, P., García Sánchez, J.L., Malato, S., Pérez-Estrada, L.A., Sánchez Pérez, J.A., 2018. Effect of volumetric rate of photon absorption on the kinetics of micropollutant removal by solar photo-Fenton with Fe<sup>3+</sup>-EDDS at neutral pH. *Chem. Eng. J.* 331. <https://doi.org/10.1016/j.cej.2017.08.096>.
- Suwaileh, W., Johnson, D., Hilal, N., 2020. Membrane desalination and water re-use for agriculture: state of the art and future outlook. *Desalination*. 491, 114559. <https://doi.org/10.1016/j.desal.2020.114559>.
- Taylor, A.C., Fones, G.R., Mills, G.A., 2020. Trends in the use of passive sampling for monitoring polar pesticides in water. *Trends Environ. Anal. Chem.* 27, e00096. <https://doi.org/10.1016/j.teac.2020.e00096>.
- Temara, A., Bowmer, T., Rottiers, A., Robertson, S., 2006. Germination and seedling growth of the water cress *Rorippa* sp. exposed to the chelant [S,S]-EDDS. *Chemosphere*. 65, 716–720. <https://doi.org/10.1016/j.chemosphere.2006.01.067>.
- van Gils, J., Posthuma, L., Cousins, I.T., Brack, W., Altenburger, R., Baveco, H., Focks, A., Greskowiak, J., Kühne, R., Kutsarova, S., Lindim, C., Markus, A., van de Meent, D., Munthe, J., Schueder, R., Schüürmann, G., Slobodnik, J., de Zwart, D., van Wezel, A., 2020. Computational material flow analysis for thousands of chemicals of emerging concern in European waters. *J. Hazard. Mater.* 397, 122655. <https://doi.org/10.1016/j.jhazmat.2020.122655>.
- Wang, R., Lin, S., 2021. Pore model for nanofiltration: history, theoretical framework, key predictions, limitations, and prospects. *J. Membr. Sci.* 620, 118809. <https://doi.org/10.1016/j.memsci.2020.118809>.
- Wang, X., Dong, W., Brigante, M., Mailhot, G., 2019. Hydroxyl and sulfate radicals activated by Fe(III)-EDDS/UV: comparison of their degradation efficiencies and influence of critical parameters. *Appl. Catal. B Environ.* 245, 271–278. <https://doi.org/10.1016/j.apcatb.2018.12.052>.
- Wang, S., Li, L., Yu, S., Dong, B., Gao, N., Wang, X., 2021. A review of advances in EDCs and PhACs removal by nanofiltration: mechanisms, impact factors and the influence of organic matter. *Chem. Eng. J.* 406, 126722. <https://doi.org/10.1016/j.cej.2020.126722>.
- Wei, S.P., van Rossum, F., van de Pol, G.J., Winkler, M.K.H., 2018. Recovery of phosphorus and nitrogen from human urine by struvite precipitation, air stripping and acid scrubbing: a pilot study. *Chemosphere*. 212, 1030–1037. <https://doi.org/10.1016/j.chemosphere.2018.08.154>.
- Xu, R., Qin, W., Zhang, B., Wang, X., Li, T., Zhang, Y., Wen, X., 2020. Nanofiltration in pilot scale for wastewater reclamation: long-term performance and membrane biofouling characteristics. *Chem. Eng. J.* 395, 125087. <https://doi.org/10.1016/j.cej.2020.125087>.
- Yusuf, A., Sodiq, A., Giwa, A., Eke, J., Pikuda, O., De Luca, G., Di Salvo, J.L., Chakraborty, S., 2020. A review of emerging trends in membrane science and technology for sustainable water treatment. *J. Clean. Prod.* 266, 121867. <https://doi.org/10.1016/j.jclepro.2020.121867>.
- Zeng, X., Zou, D., Wang, A., Zhou, Y., Liu, Y., Li, Z., Liu, F., Wang, H., Zeng, Q., Xiao, Z., 2020. Remediation of cadmium-contaminated soils using *Brassica napus*: effect of nitrogen fertilizers. *J. Environ. Manag.* 255, 109885. <https://doi.org/10.1016/j.jenvman.2019.109885>.

Article

# Assessment of a Novel Photocatalytic TiO<sub>2</sub>-Zirconia Ultrafiltration Membrane and Combination with Solar Photo-Fenton Tertiary Treatment of Urban Wastewater

Dennis Deemter<sup>1</sup>, Fabricio Eduardo Bortot Coelho<sup>2</sup> , Isabel Oller<sup>1</sup>, Sixto Malato<sup>1,\*</sup>  and Ana M. Amat<sup>3</sup>

<sup>1</sup> Plataforma Solar de Almería-CIEMAT, Carretera de Senés Km 4, Tabernas, 04200 Almería, Spain; ddeemter@psa.es (D.D.); isabel.oller@psa.es (I.O.)

<sup>2</sup> Department of Chemistry, University of Turin, Via P. Giuria 7, 10125 Torino, Italy; fabricioeduardo.bortotcoelho@unito.it

<sup>3</sup> Grupo Procesos de Oxidación Avanzada, Campus de Alcoy, Universitat Politècnica de València, 03801 Alcoy, Spain; aamat@txp.upv.es

\* Correspondence: sixto.malato@psa.es

**Abstract:** The objective of this study was to assess the combination of a photocatalytic TiO<sub>2</sub>-coated ZrO<sub>2</sub> UF membrane with solar photo-Fenton treatment at circumneutral pH for the filtration and treatment of urban wastewater treatment plant (UWWTP) effluents. Photocatalytic self-cleaning properties were tested with a UWWTP effluent under irradiation in a solar simulator. Then, both the permeates and retentates from the membrane process were treated using the solar photo-Fenton treatment. The UWWTP effluent was spiked with caffeine (CAF), imidacloprid (IMI), thiacloprid (THI), carbamazepine (CBZ) and diclofenac (DCF) at an initial concentration of 100 µg/L each. Retention on the membrane of *Pseudomonas Aeruginosa* (*P. Aeruginosa*), a Gram-negative bacterial strain, was tested with and without irradiation. It was demonstrated that filtration of a certain volume of UWWTP effluent in the dark is possible, and the original conditions can then be recovered after illumination. The photocatalytic membrane significantly reduces the turbidity of the UWWTP effluent, significantly increasing the degradation efficiency of the subsequent solar photo-Fenton treatment. The results showed that the membrane allowed consistent retention of *P. Aeruginosa* at an order of magnitude of  $1 \times 10^3$ – $1 \times 10^4$  CFU/mL.

**Keywords:** advanced oxidation processes; bacteria retention; photocatalytic membranes; photo-induced super-hydrophilicity; titania; ZrO<sub>2</sub>



**Citation:** Deemter, D.; Coelho, F.E.B.; Oller, I.; Malato, S.; Amat, A.M. Assessment of a Novel Photocatalytic TiO<sub>2</sub>-Zirconia Ultrafiltration Membrane and Combination with Solar Photo-Fenton Tertiary Treatment of Urban Wastewater. *Catalysts* **2022**, *12*, 552. <https://doi.org/10.3390/catal12050552>

Academic Editor: Antonio Eduardo Palomares

Received: 19 April 2022

Accepted: 16 May 2022

Published: 18 May 2022

**Publisher's Note:** MDPI stays neutral with regard to jurisdictional claims in published maps and institutional affiliations.



**Copyright:** © 2022 by the authors. Licensee MDPI, Basel, Switzerland. This article is an open access article distributed under the terms and conditions of the Creative Commons Attribution (CC BY) license (<https://creativecommons.org/licenses/by/4.0/>).

## 1. Introduction

Membranes have proven to be economic, fast and reliable solutions for the world's increasing water contamination problems. These vast and growing problems are due to the increasing use of pesticides and other chemicals known as microcontaminants (MCs), which are usually found in the already limited fresh water supply and agricultural lands, combined with salination [1–3]. MCs are found at trace levels up to significant concentrations, accumulating in wastewater streams and bodies, especially urban wastewater treatment plant (UWWTP) effluent and groundwater. As they are usually within the range of ng/L to µg/L, they often pass through conventional water treatment methods without being treated or recorded. These Contaminants of Emerging Concern (CECs) are found worldwide but are not yet regulated [4,5].

CECs can be removed from UWW with advanced oxidation processes (AOPs), which by generating highly reactive and nonselective hydroxyl radicals ( $\bullet$ OH), can be applied for the elimination of MCs in a wide variety of UWWs, such as ozonation, photo-Fenton or electrooxidation processes [6–8]. On the other hand, other technologies have also been used successfully to remove pharmaceuticals contained in the UWWTP effluents, especially



the membrane system and AOP combination. Membrane systems are known to be very efficient in the retention of microcontaminants due to their physicochemical properties, although a concentrate stream is also generated. Therefore, the management and treatment of the concentrate are likely to be key components for reducing the environmental impacts of wastewater reclamation [9].

The two main categories of membrane materials are polymers and ceramics [10]. They both have distinctive characteristics that control and enable the optimization of overall system parameters, such as the flow rate, pressure and temperature, depending on the treatment being applied to general volumes or specific batches. Polymeric membranes are currently the most widely used in water treatment, but they have major mechanical, thermal, pH and chemical resistance drawbacks. Ceramic membranes, although more expensive, have superior resistance [11–13]. Both types of membrane are subject to fouling and the formation of either inorganic or organic material on the membrane surface. Biofouling involves the deposition of bacteria and other microorganisms that often produce a matrix of extra-cellular polymeric substances on the membrane surface [1,14–16].

Another solution for reducing membrane fouling, as well as for the further treatment of the resulting volumes after filtration, involves the abovementioned AOPs. Photocatalysis via the illumination of semiconductors with light at wavelengths with enough energy to trigger charge ( $e^-$  and  $h^+$ ) separation is a well-known AOP. Photocatalytically active nanoparticles of  $TiO_2$  (titania),  $ZrO_2$ ,  $ZnO$  or  $WO_3$  immobilized on a (membrane) surface can act as photocatalysts in the formation of these  $\bullet OH$ , and have the advantage of not having to be filtered out or separated after the treatment [17]. As the overall efficiency of the supported semiconductors is low, although it might be enough to avoid biofouling, it is not enough for the elimination of MCs present in membrane influent. Therefore, other AOPs have to be applied to treat membrane effluents, as noted before.

In photo-Fenton treatment, a catalytic iron cycle ( $Fe^{2+}/Fe^{3+}$ ) is stimulated by  $H_2O_2$  and UV-Vis light to produce  $\bullet OH$ . This treatment is of special interest as it can be driven by solar irradiation [18–20]. One of the main drawbacks of classic solar photo-Fenton treatment is that its optimal pH is below 3. At higher pH levels, the iron precipitates as ferric hydroxide. A complexing agent, such as ethylenediamine-*N,N'*-disuccinic acid (EDDS), a nontoxic biodegradable complexing agent that is able to keep the iron dissolved at up to pH9, can be used to avoid this [21–23].

Bacteria such as *E. Coli* and *P. Aeruginosa* found in UWWTP effluents can cause severe illness when ingested. Furthermore, effluents containing high concentrations of these bacteria and MCs, when simply discharged in nature or reused for crop irrigation, can become further multidrug-resistant when exposed to other untreated MCs [24–26]. Therefore, effective bacteria removal must be part of any application for its reuse [27]. The proper combination of membrane systems and AOPs could solve biofouling, MC removal and disinfection issues, permitting the consistent reuse of UWWTP effluents.

The objective of this study was to assess the combination of a photocatalytic  $TiO_2$ -coated  $ZrO_2$  UF membrane developed in a previous study [28] with solar photo-Fenton treatment at circumneutral pH for the filtration of UWWTP effluents. Therefore, batches of UWWTP effluents were ultra-filtered using photocatalytic membranes and then treated via solar photo-Fenton treatment. First, the photocatalytic self-cleaning properties were tested with a UWWTP effluent under irradiation in a solar simulator. Then, both the permeates and retentates from membrane process were treated via solar photo-Fenton treatment, using EDDS as an iron complexing agent and hydrogen peroxide or persulfate as oxidants. The aim throughout was a total MC elimination rate of 80%, as per Swiss treatment regulations for UWWTP effluents, which are the first such regulations worldwide [29]. Matrices were spiked with a variety of MCs, caffeine (CAF), imidacloprid (IMI), thiacloprid (THI), carbamazepine (CBZ) and diclofenac (DCF), all frequently found in UWWTP effluents, at an initial concentration of 100  $\mu g/L$  each. Retention on the membrane of *Pseudomonas Aeruginosa* (*P. Aeruginosa*), a Gram-negative, rod-shaped bacterium, was tested with and without irradiation to assess possible future applications for this novel photocatalytic

UF membrane as a (pre)filtration treatment of UWWTP effluents. *P. Aeruginosa* is an opportunistic multidrug-resistant bacterium that is commonly used as a model due to its ability to colonize medical equipment and its association with human diseases. It is able to interact with other bacteria, fungi and viruses; possesses mutational resistance mechanisms; and is known for its biofilm growth, even on inert materials [26,30–32].

## 2. Materials and Methods

### 2.1. Reagents and Chemicals

The UWWTP effluent was taken after secondary treatment in the ‘El Bobar’ UWWTP located in southeast Spain (Almeria) (see Table S1 for physicochemical characterization). Sigma Aldrich supplied  $\text{Fe}_2(\text{SO}_4)_3 \cdot x\text{H}_2\text{O}$  for Fe(III) and the HPLC-grade solvents for MC monitoring. MCs were obtained mainly from Sigma Aldrich (IMI, THI, CBZ and DCF), whereas CAF was supplied by Fluka. The reagents,  $\text{H}_2\text{O}_2$  (35% *w/v*) and sodium persulfate ( $\text{Na}_2\text{S}_2\text{O}_8$ ), were also purchased from Sigma Aldrich. A schematic overview of the five selected MCs is shown in Table S2. UPLC column retention time, LOQ and maximum contaminant absorption data are summarized in Table S3. Type CM0067 Nutrient Broth No. 2 was supplied by OXCID LTD., England, and the *Pseudomonas* Chromogenic Agar by Condalab, Spain, whereas the *Pseudomonas Aeruginosa* was from the Spanish Culture Collection (CECT).

### 2.2. Analytical Determinations

Scanning electron microscopy (SEM) images were taken with a Zeiss Sigma 300 VP Gemini Technology electron microscope at variable pressure. The SEM was equipped for energy-dispersive X-ray spectroscopy (EDX) to determine the chemical composition of the ceramic membrane samples by identifying the elements present, along with their concentration and distribution. Concentrations of selected MCs were determined by ultra-performance liquid chromatography (UPLC) using an Agilent Technologies 1200 series device equipped with a UV-DAD detector and Poroshell 120 EC-C18 column (3.0 × 50 mm). Eluent conditions started from 95% water with 25 mM formic acid (mobile phase A) and 5% acetonitrile (ACN) (mobile phase B) at 1 mL/min for 5 min. This was followed by a 10 min linear gradient to 68% ACN, which was maintained for 2 min. The working temperature was 30 °C and the injection volume was 100 µL. The samples prepared at a 1:9 ACN ratio were mixed and filtered through a hydrophobic PTFE 0.2 µm (Millipore Millex-FG) syringe filter into a 2 mL HPLC vial. Molecular weight, UPLC column retention time, LOQ and maximum contaminant absorption data are given in Table S3. Dissolved organic carbon (DOC) and inorganic carbon values were determined using a Shimadzu TOC-VCN analyzer.  $\text{H}_2\text{O}_2$  values were determined according to DIN 38402H15 with titanium (IV) oxysulfate. Iron values were determined after filtration through a 0.45 µm nylon filter using 1,10 phenanthroline according to ISO 6332. The Liang method [33] was adapted to persulfate determination. Turbidity was measured using a Hach 2100N Turbidimeter. Total suspended solids (TSS) were measured via filtration without binder through a predried and weighed GF 52 090 Glass Microfiber Filter from ALBET LabScience, Germany. The filter paper was then placed in an oven at 105 °C for 60 min. Bacteria were cultured in a Series BD standard incubator at 36 °C.

### 2.3. Experimental Setup

The UWWTP effluent was filtered through a photocatalytic ceramic  $\text{ZrO}_2$  ultrafiltration flat-sheet membrane designed and fabricated in a previous study. The membrane consists of a  $100 \pm 1$ -mm-wide,  $150 \pm 2$ -mm-long, highly porous, multi-channeled SiC support with  $25.2 \times 2$  mm channels and 15 µm pore size supplied by LiqTech Ceramics A/S (Ballerup, Denmark). This is followed by a  $\text{ZrO}_2$ /SiC intermediate layer with 60 nm pores, covered with a wash coating of  $\text{TiO}_2$  particles with a mean size of 10 nm. Membrane function follows the submerged outside-in filtration principle and is able to operate in a pH range of 0–14. Further details are described elsewhere [28]. SEM images of a cut surface can be

seen in Figure 1. Only the irradiated side of the membrane was left open; the remaining sides and bottom of the membrane were covered with a watertight polymer film to ensure that the permeation flow rate was only measured on the 150 cm<sup>2</sup> irradiated surface. The membrane was held in place by a fixture to provide an evenly divided crossflow over both membrane surfaces and was placed on the bottom of a 6 L container. The container was then positioned in a SunTest XLS+ solar simulator, containing a xenon lamp with daylight filter, providing a total light irradiation of 365 W/m<sup>2</sup> (300–800 nm), with a total UV radiation of 30 W/m<sup>2</sup> (300–400 nm), while the temperature was kept at 25 °C. A vacuum was created in the membrane support with a Watson Marlow 520 S peristaltic pump through a MARPRENE 902.0048.016 #25 tube at 20 rpm to obtain the permeate volume (see Figure 2 for a schematic view). The MC mixture containing CAF, IMI, THI, CBZ and DCF in methanol had previously been prepared as a stock solution. Each compound had a final concentration of 2.5 g/L to ensure solubility and low DOC. The UWWTP effluent was spiked with this stock solution to a final concentration of 100 µg/L per MC.

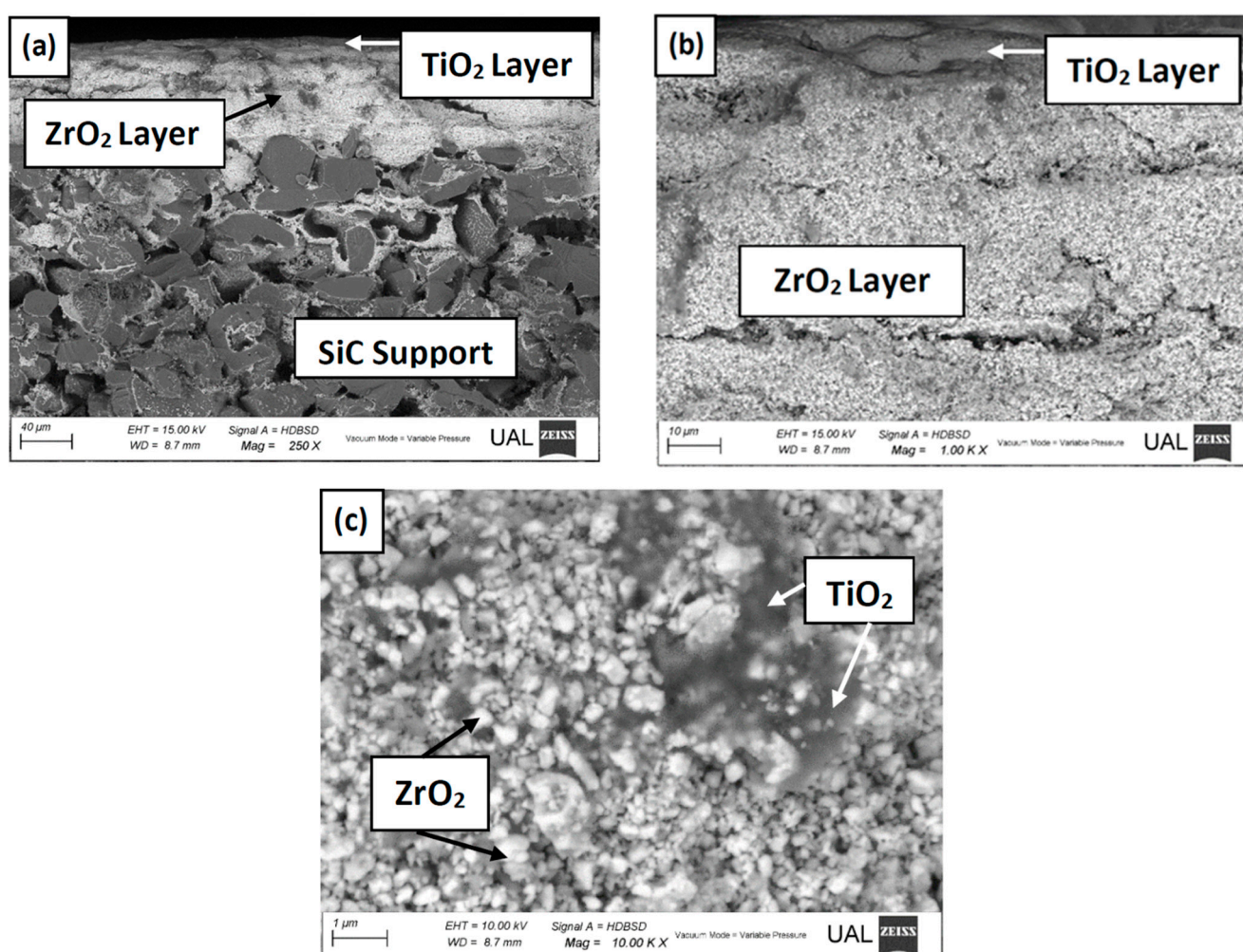


**Figure 1.** SEM images of a cross-section of the membrane: (a) the triple-layer membrane construction, showing the SiC support in grey, followed by the ZrO<sub>2</sub> intermediate UF membrane layer, while the grey shadows on top are the TiO<sub>2</sub> wash coating; (b) side view and (c) top view, showing the intermediate ZrO<sub>2</sub> UF membrane layer covered by the TiO<sub>2</sub> wash coating. The presence of the ZrO<sub>2</sub> and the TiO<sub>2</sub> wash coating was confirmed by EDX.

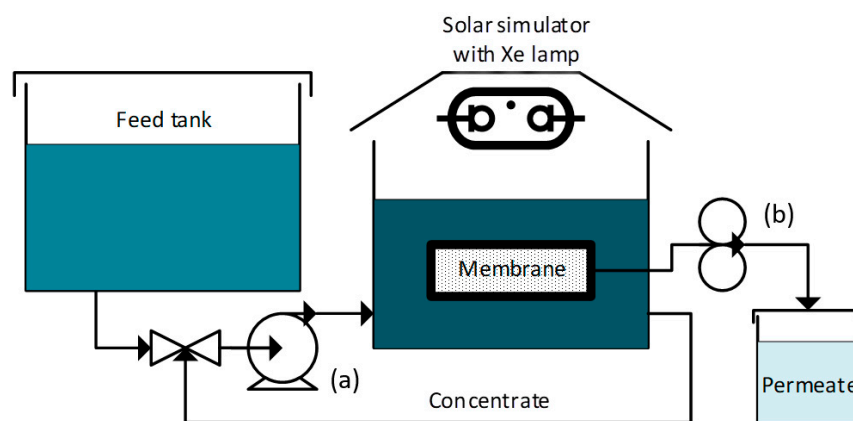


**Figure 2.** Schematic overview of the experimental set-up, with a recirculating pump (a) and a peristaltic pump (b), creating a vacuum in the membrane support to generate flow.

### 2.3.1. Solar Photo-Fenton Treatment

Solar photo-Fenton experiments were performed in the solar simulator described above, using a cylindrical 1 L container as the reactor (18.5 cm diameter and 4.0 cm depth), which was held in place and stirred magnetically in the center of the solar simulator. In selected experiments, the bicarbonates, known to be  $\bullet\text{OH}$  radical scavenger, naturally present in UWWTP effluents, were air-stripped from the experimental volumes before starting the solar photo-Fenton treatments by adding  $\text{H}_2\text{SO}_4$  to lower the concentration of  $\text{HCO}_3^-$  to 75 mg/L. The  $\text{Fe}^{3+}$ :EDDS complex was formed by predissolving  $\text{Fe}_2(\text{SO}_4)_3 \cdot 7\text{H}_2\text{O}$  in demineralized water at pH 3, followed by the addition of EDDS. A ratio of 1:1 was maintained during all experiments and the starting reagent concentration was 1.50 mM for both  $\text{H}_2\text{O}_2$  and persulfate. Table S4 summarizes the experiments.

### 2.3.2. Retention of *P. Aeruginosa*

The membrane was placed in the container as described above, and the system was sterilized with  $\text{H}_2\text{O}_2$  to ensure that there were no living bacteria in it. In this case, the water matrix was 5 L of natural water (Tabernas, southeast Spain). The *P. Aeruginosa* inoculum was prepared 20 h prior to the start of experiment and added to the reactor at a concentration of  $1 \times 10^6$  CFU/mL, which is known for its predominant bacterial growth and is commonly used as a standard inoculum concentration to be followed by bacterial inactivation [34–36]. Petri dishes with bovine agar were prepared for sampling by applying a 10-fold serial dilution with sample volumes of 50  $\mu\text{L}$  each for the concentrate and a total sample volume of 500  $\mu\text{L}$  for the permeate. Samples of the membrane surface were taken with a swab before the experiment and after 90 min and applied on the agar for cultivation. Further samples were taken from the reactor (concentrate) at 0, 30, 60 and 90 min, and afterwards from the peristaltic pump (permeate). Permeate volumes were measured separately every 30 min, showing a constant flow. The Petri dishes with the samples were stored in an incubator at 36 °C for 48 h.

## 3. Results and Discussion

### 3.1. Fouling and Self-Cleaning Properties

Several batches of UWWTP effluents were filtered through the  $\text{TiO}_2$ - $\text{ZrO}_2$  UF membrane. The turbidity varied from 8.7 to 21.3 NTU. During filtration to a concentration factor (CF) of 2, the pH of the concentrate slightly increased. The resulting permeate turbidity range, measured periodically from the start of the experiment to CF = 2, was 0.4 to 0.6 NTU. The TSS values of the different permeate volumes varied from 0.6 to 1.3 mg/L.

The membrane's self-cleaning capabilities were determined by continuously filtering the UWWTP effluents for 6 h (Figure 3a). The severely fouled membrane was then placed in a beaker under simulated sunlight with demineralized water and stirred lightly. The beaker was placed in the center of the solar simulator at the above irradiation settings

for 1 h to remove the fouling (Figure 3b). Irradiation continued for 2 h (Figure 3c) and 3 h (Figure 3d), showing continuous cleaning of the membrane, although not reaching its original condition, as shown in Figure 3e.

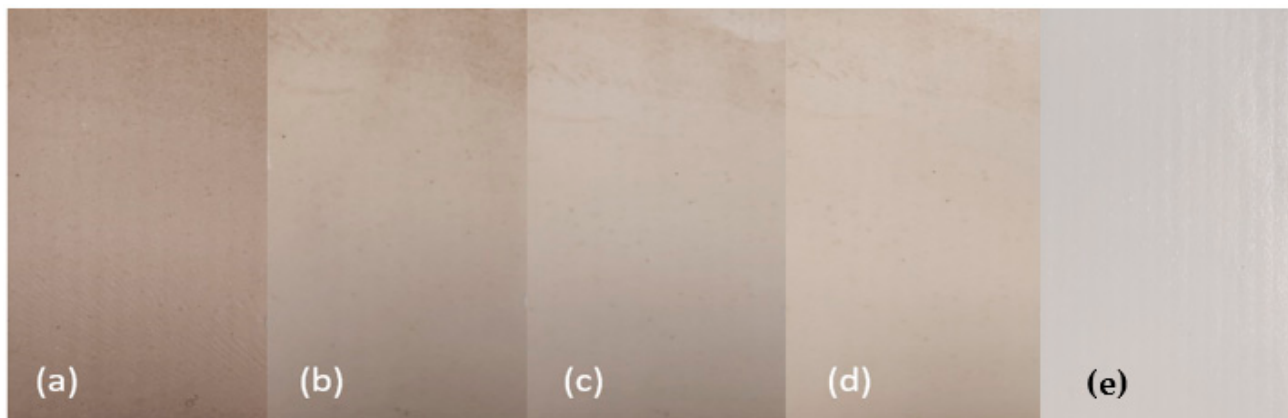


**Figure 3.** Membrane surface cleaning in demineralized water in the solar simulator. Pictures taken by conventional photography of the surface: (a) fouling color after 6 h of UWWTP effluent filtration, (b) after 1 h, (c) 2 h and (d) 3 h of irradiation, and (e) fresh membrane surface.

A clear difference from the originally severely fouled state can be observed after three 1 h irradiation periods. As a control test, another fouled membrane sample was first rinsed and placed in demineralized water but without illumination, then lightly stirred for three hours. Even after manual cleaning, membrane fouling could not be removed, demonstrating the self-cleaning effects of the photocatalytic membrane surface under irradiation. Both the original state of the fouled membrane (Figure 4a) and the membrane after 3 h of self-cleaning under simulated solar irradiation were further assessed by SEM (Figure 4b). Figure 4a is dark gray due to the presence of organic material and fouling. The presence of organic material was confirmed by EDX as having an atomic percentage of carbon of over 90%. Figure 4b shows the membrane surface with a dark spot of residual fouling in the middle. The surrounding area is the  $\text{TiO}_2$  layer. The light-white area in the upper left corner is a minor defect of the  $\text{TiO}_2$  layer due to previous manual cleaning.

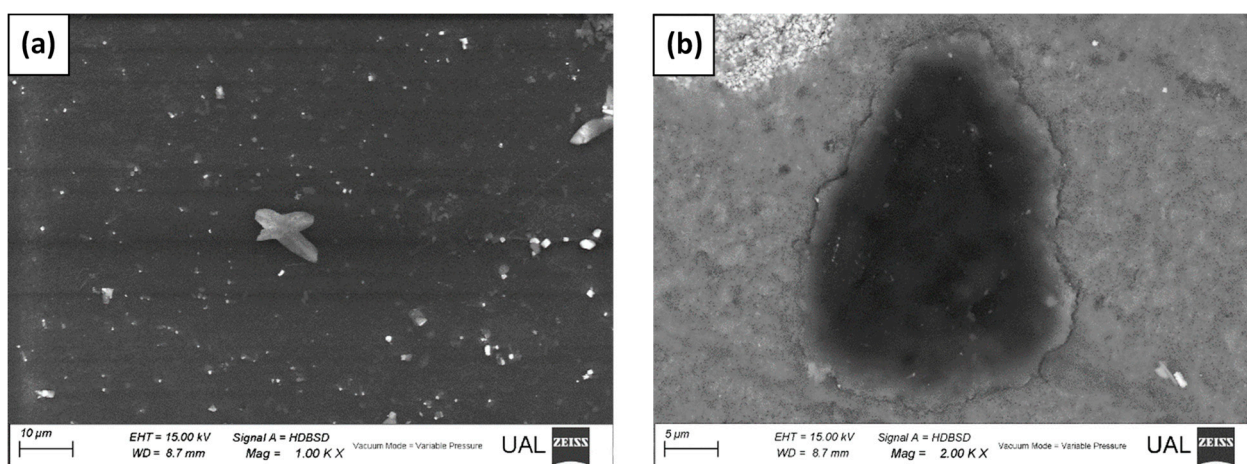


**Figure 4.** SEM images of the membrane after 6 h of filtration (a) and after cleaning for 3 h under simulated solar irradiation (b).

After observing a clear visual difference in the state of fouling, its physical removal—that is, recovery of most of the membrane porosity and not just a change in color—was confirmed in filtration experiments. Here, 250 mL filtered samples were taken, and the

time necessary to obtain this amount was recorded to determine whether the time needed to filter a certain volume could be affected by cleaning and whether the original filtration capability could be reached (see Figure 5). The normalized flow is shown in Figure 5 to demonstrate change in flow rate based on the original flow and how it slows down for the reasons stated below. In both cases, a clear difference in flow rate can be seen between the membrane kept in the dark and under light during filtration. This again demonstrates the self-cleaning capabilities of the photocatalytic membrane when filtering UWWTP effluents.

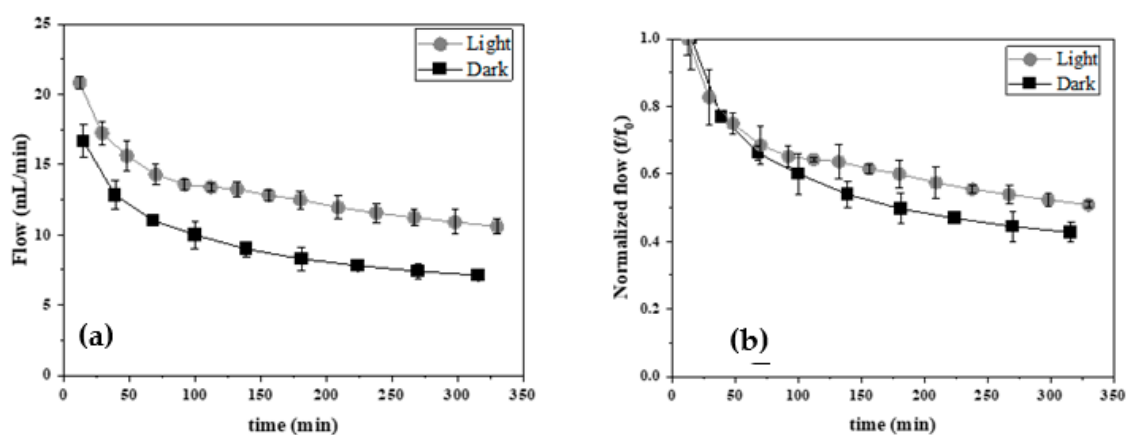


**Figure 5.** Filtration experiments with UWWTP effluent: (a) flow rates (mL/min) in the dark and in the light; (b) normalized flow rates ( $f/f_0$ ) in the dark and in the light.

The original flow rate of 21 mL/min through the membrane in the light can be observed to be higher than the 17 mL/min rate in the dark. This can be attributed to irradiation of the membrane inhibiting attachment of suspended matter in the UWWTP effluent on the photocatalytic membrane surface. Another phenomenon is photo-induced super-hydrophilicity (PSH) of  $\text{TiO}_2$ , resulting in higher flow rates and less fouling, as also previously observed [28] and reported elsewhere [37,38]. Strong decreases in flow rate can be observed up to around 60 min, both in the light and in the dark, as fouling builds up inside the membrane pores where irradiated light cannot reach. From 60 to 120 min, a clear difference can be observed in the curve of the normalized flow rate in the light (Figure 5b), strongly suggesting that there is no photodegradation of fouling on the outer membrane surface in the dark experiment. After 120 min, the curve of filtration under radiation follows the same trend as the curve of filtration in the dark, suggesting that both membranes follow a similar trend in internal fouling, while the outer surface of the illuminated membrane is kept clean. Here, 1 L of permeate is generated in 120 min of operation in the dark.

The next step involved the observation of the effects of self-cleaning on the fouled membrane after 60 of minutes irradiation, which is considered the necessary filtration time, because this is when the curve of the normalized flow in the light deviates from the normalized flow in the dark. Furthermore, over this time, the UWWTP effluent was also spiked with 100  $\mu\text{g/L}$  of each of the target MCs, namely CAF, IMI, THI, CBZ and DCF.

Figure 6 shows the flow rate during the first filtration of 1 L of UWWTP effluent in the dark. Then, the membrane was cleaned for 60 min without filtration under illumination. The second period began after this, with further filtration of 2 L of UWWTP effluent in the dark, followed by cleaning again using the same procedure followed by a third filtration. It was demonstrated that filtration of a certain volume of UWWTP effluent in the dark is possible only up to a certain amount of fouling, although the original conditions can then be recovered after illumination. However, after filtering a larger volume of UWWTP effluent, fouling could become irreversible, emphasizing the need for the definition and optimization of operating variables when using photocatalytic membranes to maintain their self-cleaning capability. There was no retention of MCs due to the high porosity of

the photocatalytic membrane, and there was no difference in the operation of membranes with UWWTP effluent, with or without MCs, as most of the fouling was eliminated by self-cleaning.

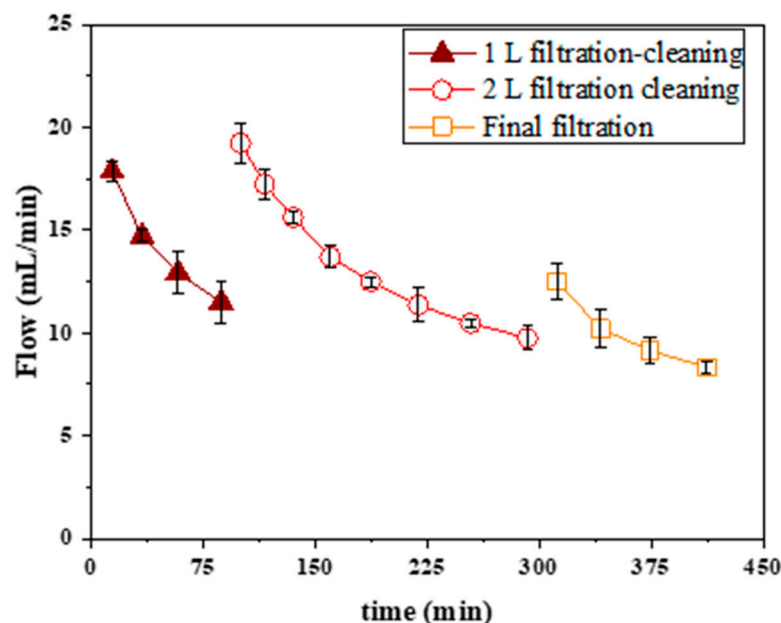


**Figure 6.** Filtration in the dark with self-cleaning under illumination series of UWWTP effluent spiked with 100 g/L of each MC. Note: ▲, filtration of 1 L, followed by cleaning (60 min); ○, after cleaning, filtration of 2 L, followed by cleaning (60 min); ‘□’ after cleaning, filtration again.

The self-cleaning mechanisms of the  $\text{TiO}_2\text{-ZrO}_2$  UF membrane are not only based on the previously mentioned super-hydrophilicity. Other mechanisms that prevent fouling of different compounds on the membrane surface can be assigned to the formation of different radical species ( $\cdot\text{OH}$  and other) when the photocatalytic surface material is irradiated with a photon energy equal or higher than the band gap energy of the semiconductor. The produced radical species react with organics and eliminate biofouling [39]. The specific band gaps of the UF membrane lie at 2.5 and 3.1 eV, due to the mixture of  $\text{TiO}_2\text{-ZrO}_2$ , as described in previous work [28].

### 3.2. Solar Photo-Fenton Treatment of Membrane Streams

The effect of UWWTP effluent filtration with the photocatalytic membrane was also evaluated in later photo-Fenton treatment of both the concentrate and permeate volumes, which still contained the initial concentration of MCs, as they were not retained by the membrane. The advantage of the photocatalytic membrane lies in pretreatment of UWWTP effluents because it significantly lowers the turbidity and particle concentration, thereby improving the availability of photons for the solar photo-Fenton process. Experiments were carried out using 0.1 mM Fe:EDDS 1:1 and 1.5 mM  $\text{H}_2\text{O}_2$  as the oxidizing agents (Figure 7). These had been found to be the optimal settings for solar photo-Fenton testing in a previous study [40].

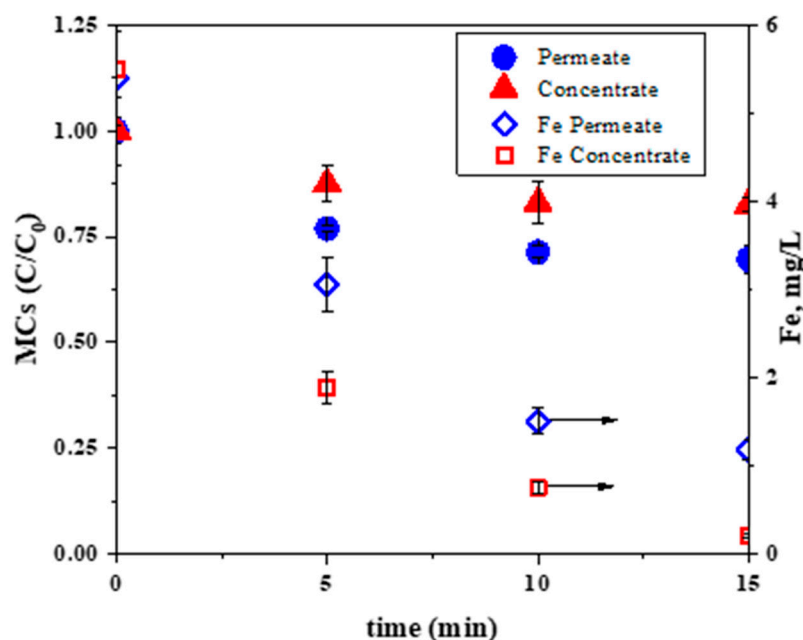


**Figure 7.** MC concentration (●: permeate; ▲: concentrate) in the UWWTP effluent during solar photo-Fenton treatment and the evolution of dissolved iron (◇: permeate; □: concentrate) in the solar simulator, with 0.1 mM Fe:EDDS 1:1 and 1.5 mM H<sub>2</sub>O<sub>2</sub>.

When the solar photo-Fenton treatment was applied to the concentrate at its natural bicarbonate concentration (720 mg/L), 16% CAF, 12% IMI, 9% THI and 27% CBZ were eliminated. DCF was already degraded by photolysis during the filtration step, or at least to below the detection limit. A total MC elimination rate of 17% was recorded, along with an H<sub>2</sub>O<sub>2</sub> consumption rate of 12.5 mg/L. All dissolved iron had precipitated within 15 min, as it is well-known that the Fe-EDDS complex degrades more rapidly in the presence of particulate organic matter. The same process applied to the permeate-volume-produced MC elimination of 32% CAF, 22% IMI, 19% THI, 42% CBZ and 81% DCF, resulting in a total MC elimination rate of 32%. In this case, H<sub>2</sub>O<sub>2</sub> consumption equaled 18 mg/L at the end of the experiment. The dissolved iron concentration at 15 min was higher during treatment of the permeate volume, with 22% remaining, as the Fe-EDDS complex was degraded less rapidly due to the presence of less particulate organic matter, which was removed by the self-cleaning membrane. This demonstrated that lowering the turbidity and particle concentration during filtration using self-cleaning membranes had a beneficial effect on the following photo-oxidation treatment. However, the elimination of MCs was low in both cases.

As bicarbonates are well known radical scavengers, the solar photo-Fenton process was prevented from attaining its full potential when they were present at high concentrations in the concentrate and permeate volumes, explaining the low MC elimination rates observed. This has also been observed in other studies in the literature [41,42]. Therefore, experiments were performed on the same concentrate and permeate volumes as in Figure 7, but this time after removing bicarbonates (see Figure 8). The concentrate and permeate volumes were air-stripped using H<sub>2</sub>SO<sub>4</sub> to lower their initial bicarbonate concentration of 720 mg/L to 75 mg/L. During this process, the pH dropped from pH 8 to circumneutral.



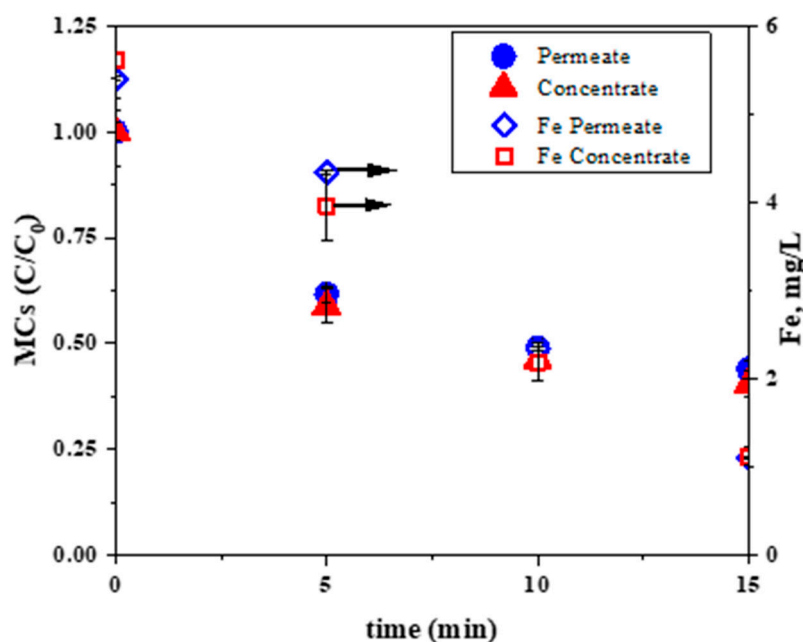
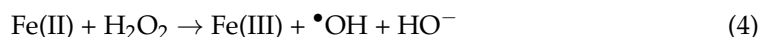


**Figure 8.** Evolution of MC concentration (●: permeate; ▲: concentrate) and dissolved iron (◇: permeate; □: concentrate) rates during solar photo-Fenton treatment in the solar simulator, with UWWTP effluents containing a low concentration of bicarbonates (75 mg/L) with 0.1 mM Fe:EDDS 1:1 and 1.5 mM H<sub>2</sub>O<sub>2</sub>.

This time the concentrate degradation efficiency was much higher, showing MC degradation of 66% CAF, 52% IMI, 45% THI and 83% CBZ. Meanwhile, DCF, as previously, was degraded by photolysis during the filtration step, or at least below the detection limit. The total MC elimination rate was 64%, more than three times higher than with the natural concentration of bicarbonates. In addition, the H<sub>2</sub>O<sub>2</sub> consumption was higher (30 mg/L), showing that dissolved iron disappeared more slowly (better stability of the Fe-EDDS complex), with 80% of iron consumed after 15 min, which was similar to the permeate volume treatment, containing its natural concentration of bicarbonates. Lower bicarbonate concentrations trigger fewer •OH radical scavenging effects as part of the solar photo-Fenton cycle at circumneutral pH (Equations (1)–(3)) [43]. This interrupts these cycles less and regenerates the Fe(III)-EDDS complex from Fe(II)-EDDS, which is formed after quick photo degradation of the Fe(III)-EDDS complex in the first few minutes of the experiment after reacting with H<sub>2</sub>O<sub>2</sub>, whereas the Fe(II) also reacts with H<sub>2</sub>O<sub>2</sub> to form Fe(III) and •OH (Equation (4)) [44], explaining the higher H<sub>2</sub>O<sub>2</sub> consumption rates.



The degradation efficiency was also higher in the permeate volume, eliminating 60% CAF, 46% IMI, 39% THI, 78% CBZ and 78% DCF in 15 min. Total elimination was 59%, double that in the treatment with the natural bicarbonate concentration. This time the H<sub>2</sub>O<sub>2</sub> consumption was almost three times lower, at 12.7 mg/L, attaining an iron concentration similar to the concentrate volume in 15 min, with 20% left. The lower H<sub>2</sub>O<sub>2</sub> consumption can be attributed to the lower concentration of (natural) organic matter present, mainly due the lower turbidity (Section 3.1) and MC concentration profiles. Although both concentrate and permeate volumes had similar total concentrations of MCs (450 mg/L), their relative concentrations were very different, e.g., the presence and absence of DCF. Along with

differences in the type, size and morphology of the organic matter, less  $\text{H}_2\text{O}_2$  reacted with this particulate matter, instead of being mainly consumed by the solar photo-Fenton reaction, producing  $\bullet\text{OH}$  without the interference of the effects of radical scavenging by bicarbonates, as the concentration was equal in both concentrate and permeate volumes. The significantly lower  $\text{H}_2\text{O}_2$  consumption at a similar MC degradation rate shows the economic advantages of a pretreatment with the photocatalytic UF membrane. An attempt was also made to use persulfate [45] as an oxidizing agent instead of  $\text{H}_2\text{O}_2$ , at the same molar concentration, although it was found to be ineffective for the degradation of the selected MCs in the UWWTP effluent. Only 19.6% of the MCs were degraded (results not shown) compared to 64% under conventional solar photo-Fenton treatment.

### 3.3. Retention of *P. Aeruginosa*

The retention of *P. Aeruginosa* was also tested to assess future applications of the  $\text{TiO}_2$ - $\text{ZrO}_2$  UF membrane. Figure 9 shows the results of filtering natural water (from Tabernas, Spain; see Table S5 for physicochemical characterization) with a starting concentration of  $1 \times 10^6$  CFU/mL. The membrane showed a stable flow rate of 31 mL/min over a  $150 \text{ cm}^2$  surface. Samples were taken and prepared, as described in Section 2.3.2, and *P. Aeruginosa* CFU values were counted and calculated after 48 h of cultivation at  $36 \text{ }^\circ\text{C}$ . Samples of the permeate volume at  $t = 0 \text{ min}$  contained no *P. Aeruginosa*, or at least it was under the detection limit. Two replicates, Rep1 and Rep2, were run.

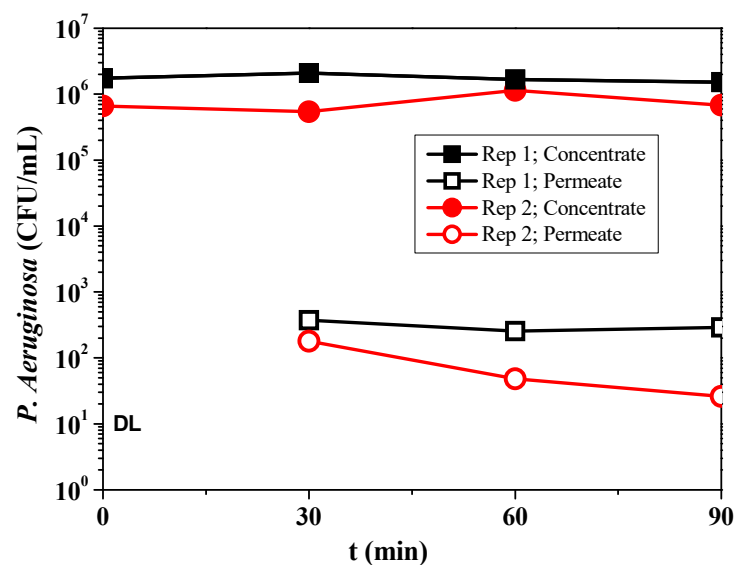


**Figure 9.** Retention of *P. Aeruginosa* in self-cleaning photocatalytic membranes with an initial concentration of  $1 \times 10^6$  CFU/mL in natural water (Tabernas, Spain). Detection limit (DL) =  $10^1$ .

The results in Figure 9 show that the membrane allowed the consistent retention of *P. Aeruginosa* of an order of magnitude of  $1 \times 10^3$ – $1 \times 10^4$  CFU/mL within 90 min of filtration during Rep1 (permeate). Although the concentration of *P. Aeruginosa* in the permeate volume significantly decreased compared to the concentrate volume, lower values were expected as a function of the photocatalytic UF membrane pore size, the zirconia intermediate layer (60 nm) and the size of the rod-like *P. Aeruginosa*, which has nominal size range of 500–800 nm by 1500–3000 nm [28,46,47]. The lower-than-expected retention rate of *P. Aeruginosa* may have been due to minor damages in the photocatalytic  $\text{TiO}_2$  membrane surface due to previous manual cleaning, as can also be observed in Figure 4b, and minor defects in the intermediate zirconia layer, making it possible for *P. Aeruginosa* to permeate the intermediate zirconia layer. However, the decreasing trend in Rep2 (permeate) in Figure 9 shows the effects (irreversible) of fouling at these sites with minor damage. A continuous fouling mechanism that can also be seen in Figure 6 resulted in a satisfactory *P. Aeruginosa* concentration in the permeate volume when operating for

more than 180 min. Certain controlled fouling mechanisms are commonly applied in ceramic membrane production and industry as a pretreatment for similar reasons.

An irradiated membrane surface would prevent the adhesion of bacteria through the abovementioned hydrophilicity, as well as degradation of any preliminary extracellular polymeric substances (EPS) produced by the bacteria to bind themselves to surfaces and for cohesion promoting protection from unfavorable conditions. Thus, the membrane would show less fouling and longer operating times. These substances can normally be observed as a slime-like biofilm layer [48].

#### 4. Conclusions

The TiO<sub>2</sub>-ZrO<sub>2</sub> ultrafiltration membrane proved to have self-cleaning capabilities when irradiated by simulated solar light after UWWTP effluents were filtered. This reduced the turbidity in the permeate by a factor of 20–50 NTU. It has been demonstrated that filtration of a certain volume of effluent in the dark is possible only up to a certain amount of fouling, then the original conditions can be recovered after illumination. However, after filtering a larger volume of effluent, fouling could become irreversible. Furthermore, the irradiated membrane showed lower fouling rates during the filtration of UWWTP effluents when irradiated. This was mainly attributed to the properties of irradiated TiO<sub>2</sub>, including the formation of •OH, which is able to degrade microorganisms as well as microcontaminants. The TiO<sub>2</sub>-ZrO<sub>2</sub> membrane significantly reduces the turbidity of the UWWTP effluent, which in turn significantly increases the degradation efficiency of the subsequent solar photo-Fenton treatment. Lowering the bicarbonate concentrations in both the concentrate and permeate resulted in higher efficiency of the solar photo-Fenton process.

The membrane shows retention of *P. Aeruginosa* to an order of magnitude of  $1 \times 10^3$ – $1 \times 10^4$  CFU/mL. The positive effects on retention of fouling of the larger pores and minor defects can be seen when repeating short term filtration experiments. Longer filtration with the TiO<sub>2</sub>-Zirconia ultrafiltration membrane could have positive effects on the retention of microorganisms, which would then be reversible after illumination.

**Supplementary Materials:** The following supporting information can be downloaded at: <https://www.mdpi.com/article/10.3390/catal12050552/s1>, Table S1: Composition of Urban Wastewater Treatment Plant Effluent; Table S2: Schematic overview of molecular structures of selected MCs; Table S3: Molecular weight, UPLC column retention time, LOQ and maximum contaminant absorption; Table S4: Overview of oxidation treatments and their parameters; Table S5: Composition of natural water (Tabernas, Spain).

**Author Contributions:** Conceptualization, D.D., I.O. and S.M.; methodology, D.D.; investigation, D.D. and F.E.B.C.; data curation, D.D. and F.E.B.C.; writing—original draft preparation, D.D. and F.E.B.C.; writing—review and editing, D.D., I.O., S.M. and A.M.A.; supervision, S.M. and A.M.A.; project administration, I.O.; funding acquisition, I.O., S.M. and A.M.A. All authors have read and agreed to the published version of the manuscript.

**Funding:** This paper is part of a project funded by the European Union's Horizon 2020 Research and Innovation Programme under Marie Skłodowska-Curie Grant Agreement No. 765860. The authors wish to thank the Spanish Ministry of Science, Innovation and Universities (MCIU), AEI and FEDER for funding under the CalypSol Project (Ref: RTI2018-097997-B-C32 and RTI2018-097997-B-C31).

**Data Availability Statement:** Not Applicable.

**Acknowledgments:** Dennis Deemter would like to thank the staff at the Plataforma Solar de Almería.

**Conflicts of Interest:** The authors declare no conflict of interest.

## Abbreviations

AMR	Antimicrobial resistance
AOPs	Advanced oxidation processes
CAF	Caffeine
CBZ	Carbamazepine
CF	Concentration factor
CPC	Compound parabolic collector
DCF	Diclofenac
EDDS	Ethylenediamine- <i>N</i> : <i>N'</i> -disuccinic acid
EDX	Energy-dispersive X-ray spectroscopy
EPS	Extracellular polymeric substances
IC	Inorganic carbon
IMI	Imidacloprid
LOQ	Limit of quantification
MCs	micro contaminants
NF	Nanofiltration
PSH	Photo-induced super-hydrophilicity
RO	Reverse osmosis
SEM	Scanning electron microscopy
THI	thiacloprid
TOC	Total organic carbon
TSS	Total suspended solids
UF	Ultrafiltration
UWW	Urban wastewater
UWWTP	Urban wastewater treatment plant

## References

- Messaoudi, M.; Douma, M.; Tijani, N.; Messaoudi, L. Study of the permeability of tubular mineral membranes: Application to wastewater treatment. *Heliyon* **2021**, *7*, e06837. [[CrossRef](#)] [[PubMed](#)]
- Gao, Y.; Zhang, Y.; Dudek, M.; Qin, J.; Gisle, Ø.; Stein, W.Ø. A multivariate study of backpulsing for membrane fouling mitigation in produced water treatment. *J. Environ. Chem. Eng.* **2021**, *9*, 104839. [[CrossRef](#)]
- Alawad, S.M.; Khalifa, A.E. Case Studies in Thermal Engineering Development of an efficient compact multistage membrane distillation module for water desalination. *Case Stud. Therm. Eng.* **2021**, *25*, 100979. [[CrossRef](#)]
- Comas, J.; Corominas, L. Balancing environmental quality standards and infrastructure upgrade costs for the reduction of microcontaminant loads in rivers. *Wat. Res.* **2018**, *143*, 632–641. [[CrossRef](#)]
- de Santiago-martín, A.; Meffe, R.; Teijón, G.; Martínez, V.; López-heras, I.; Alonso, C.; Arenas, M.; de Bustamante, I. Pharmaceuticals and trace metals in the surface water used for crop irrigation: Risk to health or natural attenuation? *Sci. Total Environ.* **2020**, *705*, 135825. [[CrossRef](#)]
- Asgar, A.; Lutze, H.V.; Tuerk, J.; Schmidt, T.C. Influence of water matrix on the degradation of organic micropollutants by ozone based processes: A review on oxidant scavenging mechanism. *J. Hazard. Mater.* **2022**, *429*, 128189. [[CrossRef](#)]
- Ribeiro, J.P.; Nunes, M.I. Recent trends and developments in Fenton processes for industrial wastewater treatment—A critical review. *Environ. Res.* **2021**, *197*, 110957. [[CrossRef](#)]
- Du, X.; Oturan, M.A.; Zhou, M.; Belkessa, N.; Su, P.; Cai, J.; Trellu, C.; Mousset, E. Nanostructured electrodes for electrocatalytic advanced oxidation processes: From materials preparation to mechanisms understanding and wastewater treatment applications. *Appl. Catal. B Environ.* **2021**, *296*, 120332. [[CrossRef](#)]
- Rizzo, L.; Malato, S.; Antakyali, D.; Beretsou, V.G.; Đolić, M.B.; Gernjak, W.; Heath, E.; Ivancev-Tumbas, I.; Karaolia, P.; Ribeiro, A.R.L.; et al. Consolidated vs new advanced treatment methods for the removal of contaminants of emerging concern from urban wastewater. *Sci. Total Environ.* **2019**, *655*, 986–1008. [[CrossRef](#)]
- Bouzerara, F.; Guvenc, C.M.; Demir, M.M. Fabrication and properties of novel porous ceramic membrane supports from the (Sig) diatomite and alumina mixtures. *Bol. Soc. Esp. Cerám. Vidr.* **2021**; *1–10*, in press. [[CrossRef](#)]
- Zsirai, T.; Qiblawey, H.; Ahmed, A.; Bach, S.; Watson, S.; Judd, S. Ceramic membrane filtration of produced water: Impact of membrane module. *Sep. Purif. Technol.* **2016**, *165*, 214–221. [[CrossRef](#)]
- da Silva Biron, D.; Dos Santos, V.; Zeni, M. *Ceramic Membranes Applied in Separation Processes*; Springer: Berlin/Heidelberg, Germany, 2017. [[CrossRef](#)]
- Gitis, V.; Rothenberg, G. *Ceramic Membranes: Ceramic Membranes: New Opportunities and Practical Applications*; John Wiley & Sons: Hoboken, NJ, USA, 2016. [[CrossRef](#)]

14. Zhang, L.; Xu, L.; Graham, N.; Yu, W. Unraveling membrane fouling induced by chlorinated water versus surface water: Biofouling properties and microbiological investigation. *Engineering*, 2021; *in press*. [CrossRef]
15. Hoslett, J.; Maria, T.; Malamis, S.; Ahmad, D.; van den Boogaert, I.; Katsou, E.; Ahmad, B.; Ghazal, H.; Simons, S.; Wrobel, L.; et al. Science of the Total Environment Surface water filtration using granular media and membranes: A review. *Sci. Total Environ.* **2018**, *639*, 1268–1282. [CrossRef] [PubMed]
16. Czuba, K.; Bastrzyk, A.; Rogowska, A.; Janiak, K.; Pacyna, K.; Kossi, N.; Podstawczyk, D. Towards the circular economy—A pilot-scale membrane technology for the recovery of water and nutrients from secondary effluent. *Sci. Total Environ.* **2021**, *791*, 148266. [CrossRef] [PubMed]
17. Kolesnyk, I.; Kujawa, J.; Bubela, H.; Konovalova, V.; Burban, A. Separation and Purification Technology Photocatalytic properties of PVDF membranes modified with g-C<sub>3</sub>N<sub>4</sub> in the process of Rhodamines decomposition. *Sep. Purif. Technol.* **2020**, *250*, 117231. [CrossRef]
18. Della-Flora, A.; Wilde, M.L.; Thue, P.S.; Lima, D.; Lima, E.C.; Sirtori, C. Combination of solar photo-Fenton and adsorption process for removal of the anticancer drug Flutamide and its transformation products from hospital wastewater. *J. Hazard. Mater.* **2020**, *396*, 122699. [CrossRef]
19. Foteinis, S.; Monteagudo, J.M.; Durán, A.; Chatzisyneon, E. Environmental sustainability of the solar photo-Fenton process for wastewater treatment and pharmaceuticals mineralization at semi-industrial scale. *Sci. Total Environ.* **2018**, *612*, 605–612. [CrossRef]
20. Li, Y.; Cheng, H. Chemical kinetic modeling of organic pollutant degradation in Fenton and solar photo-Fenton processes. *J. Taiwan Inst. Chem. Eng.* **2021**, *123*, 175–184. [CrossRef]
21. Norén, A.; Fedje, K.K.; Strömvall, A.-M.; Rauch, S.; Andersson-Sköld, Y. Low impact leaching agents as remediation media for organotin and metal contaminated sediments. *J. Environ. Manag.* **2021**, *282*, 111906. [CrossRef]
22. Vandevivere, P.C.; Saveyn, H.; Verstraete, W.; Feijtel, T.C.J.; Schowanek, D.R. Biodegradation of metal-[S,S]-EDDS complexes. *Environ. Sci. Technol.* **2001**, *35*, 1765–1770. [CrossRef]
23. Clarizia, L.; Russo, D.; di Somma, I.; Marotta, R.; Andreozzi, R. Homogeneous photo-Fenton processes at near neutral pH: A review. *Appl. Catal. B Environ.* **2017**, *209*, 358–371. [CrossRef]
24. Vineyard, D.; Hicks, A.; Karthikeyan, K.G.; Barak, P. Economic analysis of electro dialysis, denitrification, and anammox for nitrogen removal in municipal wastewater treatment. *J. Clean. Prod.* **2020**, *262*, 121145. [CrossRef]
25. Igere, B.E.; Okoh, A.I.; Nwodo, U.U. Wastewater treatment plants and release: The case of Odunsi for emerging bacterial contaminants, resistance and determinant of environmental wellness. *Emerg. Contam.* **2020**, *6*, 212–224. [CrossRef]
26. del Mar Cendra, M.; Torrents, E. *Pseudomonas aeruginosa* biofilms and their partners in crime. *Biotechnol. Adv.* **2021**, *49*, 107734. [CrossRef] [PubMed]
27. Rizzo, L.; Gernjak, W.; Krzeminski, P.; Malato, S.; McArdell, C.S.; Perez, J.A.S.; Schaar, H.; Fatta-Kassinos, D. Best available technologies and treatment trains to address current challenges in urban wastewater reuse for irrigation of crops in EU countries. *Sci. Total Environ.* **2020**, *710*, 136312. [CrossRef] [PubMed]
28. Coelho, F.E.B.; Deemter, D.; Candelario, V.M.; Boffa, V.; Malato, S.; Magnacca, G. Development of a Photocatalytic Zirconia-Titania Ultrafiltration Membrane with Anti-fouling and Self-cleaning Properties. *J. Environ. Chem. Eng.* **2021**, *9*, 106671. [CrossRef]
29. Federal Office for the Environment FOEN Water Division. *Reporting for Switzerland under the Protocol on Water and Health*. 2019. Available online: [https://unece.org/DAM/env/water/Protocol\\_reports/reports\\_pdf\\_web/Switzerland\\_summary\\_report\\_en.pdf](https://unece.org/DAM/env/water/Protocol_reports/reports_pdf_web/Switzerland_summary_report_en.pdf) (accessed on 12 May 2022).
30. Hosseinkhan, N.; Allahverdi, A.; Abdolmaleki, F. The novel potential multidrug-resistance biomarkers for *Pseudomonas aeruginosa* lung infections using transcriptomics data analysis. *Informatics Med. Unlocked.* **2021**, *22*, 100509. [CrossRef]
31. Horna, G.; Ruiz, J. Type 3 secretion system of *Pseudomonas aeruginosa*. *Microbiol. Res.* **2021**, *246*, 126719. [CrossRef]
32. Shaker, M.M.; Al-Hadrawi, H.A.N. Measuring the effectiveness of antibiotics against *Pseudomonas aeruginosa* and *Escherichia coli* that isolated from urinary tract infection patients in Al-Najaf city in Iraq. *Mater. Today Proc. in press* **2021**, 10–13. [CrossRef]
33. Liang, C.; Huang, C.F.; Mohanty, N.; Kurakalva, R.M. A rapid spectrophotometric determination of persulfate anion in ISCO. *Chemosphere* **2008**, *73*, 1540–1543. [CrossRef]
34. Lozano, C.; López, M.; Rojo-Bezares, B.; Sáenz, Y. Antimicrobial susceptibility testing in *Pseudomonas aeruginosa* biofilms: One step closer to a standardized method. *Antibiotics* **2020**, *9*, 880. [CrossRef]
35. Díez-Aguilar, M.; Martínez-García, L.; Cantón, R.; Morosini, M.I. Is a new standard needed for diffusion methods for in vitro susceptibility testing of fosfomycin against *Pseudomonas aeruginosa*? *Antimicrob. Agents Chemother.* **2016**, *60*, 1158–1161. [CrossRef]
36. Mizunaga, S.; Kamiyama, T.; Fukuda, Y.; Takahata, M.; Mitsuyama, J. Influence of inoculum size of *Staphylococcus aureus* and *Pseudomonas aeruginosa* on in vitro activities and in vivo efficacy of fluoroquinolones and carbapenems. *J. Antimicrob. Chemother.* **2005**, *56*, 91–96. [CrossRef]
37. Kim, S.M.; In, I.; Park, S.Y. Study of photo-induced hydrophilicity and self-cleaning property of glass surfaces immobilized with TiO<sub>2</sub> nanoparticles using catechol chemistry. *Surf. Coatings Technol.* **2016**, *294*, 75–82. [CrossRef]
38. Saini, A.; Arora, I.; Ratan, J.K. Photo-induced hydrophilicity of microsized-TiO<sub>2</sub> based self-cleaning cement. *Mater. Lett.* **2020**, *260*, 26888. [CrossRef]

39. Rani, C.N.; Karthikeyan, S.; Arockia, S.P. Photocatalytic ultrafiltration membrane reactors in water and wastewater treatment—A review. *Chem. Eng. Process. Process Intensif.* **2021**, *165*, 108445. [[CrossRef](#)]
40. Deemter, D.; Oller, I.; Amat, A.M.; Malato, S. Effect of salinity on preconcentration of contaminants of emerging concern by nanofiltration: Application of solar photo-Fenton as a tertiary treatment. *Sci. Total Environ.* **2020**, *756*, 143593. [[CrossRef](#)]
41. Rommozzi, E.; Giannakis, S.; Giovannetti, R.; Vione, D.; Pulgarin, C. Detrimental vs. beneficial influence of ions during solar (SODIS) and photo-Fenton disinfection of *E. coli* in water: (Bi)carbonate, chloride, nitrate and nitrite effects. *Appl. Catal. B Environ.* **2020**, *270*, 118877. [[CrossRef](#)]
42. Gonçalves, B.R.; Guimarães, R.O.; Batista, L.L.; Ueira-Vieira, C.; Starling, M.C.V.M.; Trovó, A.G. Reducing toxicity and antimicrobial activity of a pesticide mixture via photo-Fenton in different aqueous matrices using iron complexes. *Sci. Total Environ.* **2020**, *740*, 140152. [[CrossRef](#)] [[PubMed](#)]
43. Soriano-Molina, P.; Sánchez, J.L.G.; Malato, S.; Pérez-Estrada, L.A.; Pérez, J.A.S. Effect of volumetric rate of photon absorption on the kinetics of micropollutant removal by solar photo-Fenton with Fe<sup>3+</sup>-EDDS at neutral pH. *Chem. Eng. J.* **2018**, *331*, 84–92. [[CrossRef](#)]
44. Li, J.; Mailhot, G.; Wu, F.; Deng, N. Journal of Photochemistry and Photobiology A: Chemistry Photochemical efficiency of Fe (III)-EDDS complex: OH radical production. *J. Photochem. Photobiol. A Chem.* **2010**, *212*, 1–7. [[CrossRef](#)]
45. Kanafin, Y.N.; Makhatova, A.; Zarikas, V.; Arkhangelsky, E.; Pouloupoulos, S.G. Photo-Fenton-Like Treatment of Municipal Wastewater. *Catalysts* **2021**, *11*, 1206. [[CrossRef](#)]
46. Iglewski, B. *Pseudomonas*. In *Medical Microbiology*, 4th ed.; Baron, S., Ed.; The University of Texas: Galveston, TX, USA, 1996. Available online: <https://www.ncbi.nlm.nih.gov/books/NBK8326/%0A> (accessed on 12 May 2022).
47. Formosa, C.; Grare, M.; Duval, R.E.; Dague, E. Nanoscale effects of antibiotics on *P. aeruginosa*. *Nanomed. Nanotechnol. Biol. Med.* **2012**, *8*, 12–16. [[CrossRef](#)] [[PubMed](#)]
48. Harimawan, A.; Ting, Y. Colloids and Surfaces B: Biointerfaces Investigation of extracellular polymeric substances (EPS) properties of *P. aeruginosa* and *B. subtilis* and their role in bacterial adhesion. *Colloids Surf. B Biointerfaces* **2016**, *146*, 459–467. [[CrossRef](#)] [[PubMed](#)]